ACADEMIC REPORT

2023-2024

शैक्षणिक प्रतिवेदन 2023-2024

होमी भाभा राष्ट्रीय संस्थान
HOMI BHABHA NATIONAL INSTITUTE

(परमाणु ऊर्जा विभाग की एक सहायता प्राप्त संस्था एवं यूजीसी अधिनियम 1956 की धारा 3 के तहत एक मानद विश्वविद्यालय है)

(A Deemed to be University u/s 3 of UGC Act 1956 and a Grant-in-Aid Institute of the Department of Atomic Energy, Govt. of India)

Location of HBNI Central Office, Constituent Institutions & Off Campus Centres


HRI, Prayagraj


HBCH & MPMMCC
Varanasi


VECC, Kolkata


RRCAT, Indore


SINP, Kolkata


IPR, Gandhinagar


NISER, Bhubaneswar


BARC, Mumbai


IoP, Bhubaneswar


TMC, Mumbai

IMSc, Chennai


HBNI Central Office


IGCAR, Kalpakkam

Academic Report
2023-2024

CONTENTS

From the Vice Chancellor's Desk

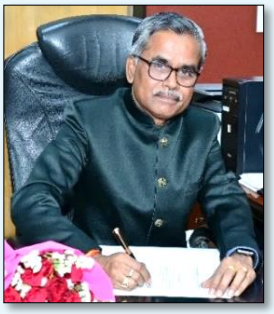

I take pleasure in presenting the academic report of HBNI for the year 2023-24. Over the past nineteen years of its existence, HBNI has grown in stature and today it is recognized as one of the best research universities offering challenging research opportunities in frontier areas of science, engineering, technology, and mathematics. HBNI is also one of the universities which is offering academic programs that contribute to skill development of its students. The courses in Oncology, Clinical Research and Nursing are making effective contributions to the country's human resource base in these important areas of Medical & Health Sciences. During the academic year (August 1, 2023-July 31, 2024) HBNI offered 44 academic programmes and awarded 318 Ph.D., 89 M.Tech., 304 M.Sc./Integrated M.Sc. degrees in various science disciplines, and 63 post graduate & super specialty medical degrees. Till July 31, 2024, total degrees awarded include 2669 Ph.D., 735 M.D., 220 D.M., 259 M.Ch., and 1600 M.Tech. degrees. During this period, Homi Bhabha Cancer Hospital & Mahamana Pandit Madan Mohan Malaviya Cancer Centre, Varanasi, became second Off-Campus Centre of HBNI with the approval of Ministry of Education, and HBNI is presently affiliating 12 institutions of DAE for their academic programmes.

In the MoE's National Institute Ranking Framework exercise for the academic year 2023-24, HBNI received 6th rank in Research Institution Category, 16th rank in University Category and 27th rank in the Overall Category. Based on high-quality publications in 82 high impact selected journals, the Nature Index 2024 has placed HBNI in the third position, among all academic institutions in India and in the first position regarding publications in the discipline of physical sciences for the period during the academic year. These results are testimonials to the remarkable efforts our faculty members and students have put in their research work. The research output presented in the report as the theses highlights clearly shows that the efforts of HBNI towards broadening the base and the nature of research, making it interdisciplinary and socially useful are bearing the fruits. It gives me immense pleasure to note that our faculty

members and students have been recognized for their research efforts and received several awards, academic honors, and fellowships during the academic year.

The New Education Policy 2020 reflects the shift in vision regarding education from the creation of a resource pool to a path of holistic development of the person. HBNI has implemented several guidelines for HEIs as per NEP-2020 to provide a holistic education to the future generation, like setting up of the Industry Linkage Centre, R & D Cell, Alumni and Placement Cell, Institution Innovation Council, introduction of Academic Break, Uniform Credit System, Student Transfer etc., for the benefit of its students. Efforts are on to implement the remaining guidelines in a phased manner in the coming academic year.

I take this opportunity to extend my gratitude to Prof. A. K. Mohanty, Chairman, Council of Management, HBNI for his guidance and support in all ventures of HBNI. I express my sincere thanks to Prof. Anil Kakodkar, Chancellor, HBNI for providing valuable inputs to the growth of HBNI. I also thank all the members of Council of Management, Academic Council and Planning and Monitoring Board, of HBNI for their valuable inputs and support to the programmes of HBNI. Thanks are due to the Board of Study members, Deans (Academic), Deans (Student Affairs), nodal officers at our CIs/OCC, and HBNI colleagues and staff for their devoted efforts towards making HBNI a word class centre of advanced scientific research and academic excellence.

U Kamachi Mudali

(U. Kamachi Mudali)

Section I
(Overview)

Academic Programmes of the Institute

The Homi Bhabha National Institute (HBNI) brings together the academic and research programmes conducted by the following twelve premier institutions of DAE, as its Constituent Institutions (CIs)/ Off Campus Centres (OCCs):

1. Bhabha Atomic Research Centre (BARC), Mumbai
2. Indira Gandhi Centre for Atomic Research (IGCAR), Kalpakkam
3. Raja Ramanna Centre for Advanced Technology (RRCAT), Indore
4. Variable Energy Cyclotron Centre (VECC), Kolkata
5. Saha Institute of Nuclear Physics (SINP), Kolkata
6. Institute for Plasma Research (IPR), Gandhinagar
7. Institute of Physics (IoP), Bhubaneswar
8. Harish-Chandra Research Institute (HRI), Allahabad
9. Institute of Mathematical Sciences (IMSc), Chennai
10. Tata Memorial Centre (TMC), Mumbai
11. National Institute of Science Education and Research (NISER), Bhubaneswar
12. Homi Bhabha Cancer Hospital & Mahamana Pandit Madan Mohan Malaviya Cancer Centre (HBCH & MPMMCC), Varanasi

The HBNI offers a range of academic programmes in Chemical Sciences, Engineering Sciences, Medical & Health sciences, Life sciences, Mathematical Sciences and Physical Sciences. It also has a program in Applied Systems Analysis. All institutions, except NISER, conduct programmes at post-graduate level. NISER admits Higher Secondary passed students for its five years Integrated M.Sc. program.

❖ **Disciplines in which HBNI Offers Ph.D.:**

- ✓ Applied System Analysis
- ✓ Chemical Sciences
- ✓ Computer Science
- ✓ Computational Biology
- ✓ Earth & Planetary Science
- ✓ Engineering Sciences
- ✓ Humanities & Social Sciences
- ✓ Life Sciences
- ✓ Mathematical Sciences
- ✓ Medical & Health Sciences

- ✓ Physical Sciences
- ✓ Theoretical Computer Science

Most of the Ph.D. programmes are multi-disciplinary in nature having guides and co-guides from different branches of science and engineering.

- ❖ **Disciplines in which HBNI Offers Integrated Ph.D.**

- ✓ Applied System Analysis
- ✓ Chemical Sciences
- ✓ Computational Biology
- ✓ Engineering Sciences
- ✓ Life Sciences
- ✓ Mathematical Sciences
- ✓ Physical Sciences

- ❖ **M.Tech.** in Engineering Sciences consists of one year of course work and one year of project work. The course work is offered at all the campuses of BARC Training School and IPR Training School. Project work is offered at BARC, IGCAR, RRCAT, VECC, IPR and other units of DAE. Those who are not able to pursue or not interested in pursuing the project/research work, have the option to get a post graduate diploma in lieu of M.Tech. BARC training school also offers post graduate diploma in Life Sciences after one year of course work.

- ❖ **M.Sc. (Engg.)** program emphasizes on research project work extending up to one and a half years after one year of course work. This program is offered at BARC, IGCAR, VECC, RRCAT and IPR.

- ❖ **Integrated M.Sc.** of five-year duration in Physical Sciences, Chemical Sciences, Mathematical Sciences and Life Sciences is offered at NISER. M.Sc. in Physical Sciences of two-year duration is offered at HRI. M.Sc. in Medical & Radiological Physics of two-year duration is offered at NISER.

Super Specialty Courses in Medical & Health Sciences offered at TMC are listed below:

- ❖ **Doctor of Medicine (D.M.)** in Medical Oncology, Pediatric Oncology, Gastroenterology, Critical Care, Oncopathology, and Interventional Radiology.

- ❖ **Master of Chirurgiae (M.Ch.)** in Surgical Oncology, Gynaecological Oncology, Plastic Surgery & Reconstructive Surgery, Head & Neck Oncology.

Two years Certified Fellowship Programmes in Medical & Health Sciences offered at TMC are listed below:

Post-MD two years Certified Fellowship Program is offered with specialization in Orthopaedic Oncology, Breast Oncology, Thoracic Oncology, Uro Oncology, Interventional Oncology, Surgical Pathology, Haemato Pathology, Dental & Prosthetic Surgery, Preventive Oncology, Infectious Diseases & HIV Medicine, Gastrointestinal Oncology, Pulmonary Oncology, Molecular Haemato Oncology, Oral Oncology with Reconstructive Surgery.

Post Graduate Courses in Medical & Health Sciences at TMC include:

- **MD** (Pathology, Anaesthesia, Radio-diagnosis, Radiation Oncology, Microbiology, Nuclear Medicine, Palliative Medicine, Immuno-Hematology & Transfusion Medicine and in Nuclear Medicine).
- **M.Sc.** (Nursing), **M.Sc. (**Clinical research), **M.Sc**. (Public Health in Epidemiology) and **M.Sc**. (Occupational Therapy in Oncology) programmes are offered at TMC.
- **M.Sc.** (Nuclear Medicine and Molecular Imaging Technology)

Post Graduate Courses in Medical & Health Sciences offered at RMC-BARC:

- **M.D. (Nuclear Medicine)**
- **M.Sc. (Nuclear Medicine and Molecular Imaging Technology)**
- **M.Sc. (Hospital Radio Pharmacy)**

PG Diploma Course offered at TMC:

- **Fusion Imaging Technology (PGDFIT)**

PG Diploma Courses offered at BARC:

- **Diploma in Radiological Physics (DipRP)**
- **Diploma in Medical Radio Isotope Techniques (DMRIT)**
- **Diploma in Nuclear Science and Engineering (DipNSE)**

Management of HBNI

The **Council of Management** chaired by Secretary, DAE is the apex body for the management of HBNI. **Academic Council** chaired by Vice Chancellor, HBNI manages the academic issues and functioning of the institute on the advice of the **Board of Studies,** which has been constituted for each major discipline, and has representatives from all CIs and OCC as well as experts from other reputed Indian institutes. To manage the affairs of the HBNI, each CI has one or more **Deans (Academic)**. **Standing Committee of Deans** chaired by VC, HBNI and comprising of Dean, HBNI, Associate Deans at HBNI, Deans (Academic) from all the institutions, ensures harmony in the processes. CIs and OCCs have also established a robust framework of admission to different academic programmes approved by **Standing Academic Committee** constituted at each CI/OCC.

The Council of Management is the prime body for the management of the Institute.

Council of Management (CoM)
(As on July 31, 2024)

Prof. A. K. Mohanty, Secretary DAE & Chairman, AEC	**Chairman**
Prof. U. Kamachi Mudali, Vice Chancellor	Member
Shri Vivek Bhasin, Director, BARC	Member
Smt. Seema S. Jain, Member (Finance), AEC	Member
Shri Shankar V. Nakhe, Director, RRCAT	Member
Dr. Sudeep Gupta, Director, TMC	Member
Prof. Gautam Bhattacharyya, Director, SINP	Member
Prof. V. Ravindran, Director, IMSc	Member
Prof. Mustansir Barma, Professor Emeritus, TIFR Centre for Inter-Disciplinary Sciences, Hyderabad	Member
Prof. Surendra Prasad, Former Director, IIT Delhi	Member
Prof. A. K. Tyagi, Dean, HBNI	Member
Dr. P. C. Selvin, Registrar, HBNI	Non-member Secretary

Academic Council
(As on July 31, 2024)

Prof. U. Kamachi Mudali, Vice Chancellor, HBNI	Chairperson
Prof. A. K. Tyagi, Dean, HBNI	Member
Shri Vivek Bhasin, Director, BARC	Member
Shri C. G. Karhadkar, Director, IGCAR	Member
Shri S. V. Nakhe, Director, RRCAT	Member
Prof. Sumit Som, Director, VECC	Member
Prof. Gautam Bhattacharyya, Director, SINP	Member
Prof. Shashank Chaturvedi, Director, IPR	Member
Prof. Karuna Kar Nanda, Director, IoP	Member
Prof. V. Ravindran, Director, IMSc	Member
Prof. Dileep Jatkar, Director (acting), HRI	Member
Dr. Sudeep Gupta, Director, TMC	Member
Prof. H. N. Ghosh, Director, NISER	Member
Prof. Siva Umapathy, IISc, Bengaluru	Member
Prof. Manoj K Tiwari, IIM Mumbai	Member
Prof. Devang Khakhar, IIT Bombay	Member
Prof. S. M. Yusuf, BARC	Member
Dr. Pankaj Chaturvedi, TMC, Mumbai	Member
Prof. A. Srinivasan, NISER	Member
Prof. Pranay Swain, Convenor, BoS (Applied Systems Analysis)	Member
Prof. Bedangadas Mohanty, Convenor, BoS (Physical Sciences)	Member
Prof. R. Tewari, Convenor, BoS (Engineering Sciences)	Member
Prof. Partha Saha, Convenor, BoS (Life Sciences)	Member
Prof. Meena Mahajan, Convenor, BoS (Mathematical Sciences)	Member
Prof. S. D. Banavali, Convenor, BoS (Medical & Health Sciences)	Member
Prof. P. K. Mohapatra, Convenor, BoS (Chemical Sciences)	Member
Prof. C. Gunanathan, Convenor, BoS (Integrated Masters Programme)	Member
Dr. P. C. Selvin, Registrar, HBNI	Secretary

Advisory Committee

Secretary, DAE and Chairman, AEC	**Chairman**
Vice Chancellor, HBNI	Member
Director, BARC	Member
Director, IGCAR	Member
Director, RRCAT	Member
Director, VECC	Member
Director, IPR	Member
Director, SINP	Member
Director, TMC	Member
Director, IMSc	Member
Director, TIFR	Member
Director, NISER	Member
Director, HRI	Member
Director, IoP	Member
Dean, HBNI	Member-Secretary

Officers of the Institute

(As on July 31, 2024)

Academic		Administrative	
Prof. U. Kamachi Mudali	Vice Chancellor	Dr. P. C. Selvin	Registrar
Prof. A. K. Tyagi	Dean	Shri S. Jakhotia	Finance Officer
Prof. D. K. Maity	Associate Dean		
Prof. D. Dutta	Associate Dean		
Prof. Naveen Kumar	Associate Dean		
Prof. B. K. Nayak	Associate Dean		
Prof. H. Pal	Associate Dean		

Board of Studies of HBNI

(As on July 31, 2024)

❖ BoS (Chemical Sciences)
1. Prof. P. K. Mohapatra, BARC - Convener
2. Prof. V. Sudarsan, BARC - Co-Convener
3. Prof. A. Dutta, IIT, Bombay
4. Prof. Tapas Das, BARC
5. Prof. D. K. Maity, HBNI
6. Prof. K. A. Venkatesan, IGCAR
7. Prof. A. Srinivasan, NISER
8. Prof. H. S. Biswal, NISER
9. Prof. Deepa Khushalani, TIFR
10. Prof. Avinash Kumbhar, SPPU
Balancing Members:
1. Prof. B. S. Patro
2. Prof. Dipanwita Dutta, HBNI
❖ BoS (Engineering Sciences)
1. Prof. R. Tewari, BARC-Convener
2. Prof. J. Chattopadhyay, BARC Co-Convener
3. Prof. G. Sugilal, BARC
4. Prof. V. H. Patankar, BARC
5. Prof. V. G. Gaikar, ICT
6. Prof. C. P. Paul, RRCAT
7. Prof. P. Y. Nabhiraj, VECC
8. Prof. C. P. Paul, RRCAT
9. Prof. B. Dikshit, BARC
10. Prof. S. K. Pathak, IPR
11. Prof. Anish Kumar, IGCAR
Balancing Members:
1. Prof. Gopika Vinod, VECC
2. Prof. A. K. Dureja, BARC
❖ BoS (Medical & Health Sciences)
1. Prof. S. D. Banavali, TMC – Convener
2. Prof. Sandeep Basu, RMC-Co-Convener
3. Prof. Sudeep Gupta, Director ACTREC, TMC
4. Dr. Nithya Gogtay, KEM Hospital, Mumbai
5. Dr. Ashutoshnath Agarwal, PGIMER, Chandigarh
6. Dr. Manisha Pawar, TMH
7. Prof. Siddhartha Laskar, TMC
8. Dr. Ajay Puri, TMC
9. Dr. J. P. Agarwal, TMC
10. Dr. Suyash Kulkarni, TMC
Balancing Members:
1. Dr. Rajesh Kinhikar, TMC
2. Prof. D. K. Maity, HBNI
❖ BoS (Life Sciences)
1. Prof. Partha Saha, SINP - Convener
2. Prof. S. Gautam, BARC - Co-Convener
3. Prof. Praful Singru, SBS, NISER
4. Prof. Rahul Siddharthan, IMSc
5. Prof. Sorab Dalal, ACTREC
6. Prof. Harapriya Mohaptra, NISER
7. Prof. B. S. Patro, BARC
8. Prof. B. N. Pandey, BARC
9. Prof. Y. V. Nancharaiah, IGCAR
10. Prof. Sharmila Bapat, NCCS, Pune
Balancing Members:
1. Prof. Shovan Majumder, RRCAT
2. Prof. Sunil K. Ghosh, HBNI
3. Prof. D. K. Maity, HBNI
❖ BoS (Mathematical Sciences)
1. Prof. Meena Mahajan, IMSc - Convener
2. Prof. D. Surya Ramana, HRI Co-Convener
3. Prof. Anish Ghosh, TIFR, Mumbai
4. Prof. K. Sandeep, TIFR, Bengaluru
5. Prof. Jugal K. Verma, IIT Bombay
6. Prof. B. Sury, ISI, Bengaluru
7. Prof. K. N. Raghavan, IMSc
8. Prof. K. V. Subrahmanyam, CMI-Chennai
9. Prof. Brundaban Sahu, NISER
Balancing Members:
1. Prof. B. K. Nayak, HBNI
2. Prof. D. Dutta, HBNI
❖ BoS (Physical Sciences)
1. Prof. B. Mohanty, NISER -Convener
2. Prof. V. K. Aswal, BARC -Co-Convener

3. Prof. Anushuman Maharana, HRI
4. Prof. Awadesh Mani, IGCAR
5. Prof. D. Indumathi, IMSc
6. Prof. Biju Raja Sekhar, IoP
7. Prof. Sudip Sengupta, IPR
8. Prof. Shovan Majumder, RRCAT
9. Prof. Gopal Mukherjee, VECC
10. Prof. Kumar Sankar Gupta, SINP
Balancing Members:
1. Prof. B. K. Nayak, HBNI
2. Prof. D. Dutta, HBNI
❖ **BoS (Applied Systems Analysis)**
1. Prof. Pranay Swain, NISER - Convener
2. Prof. Karuna Jain, IIT Bombay
3. Prof. A. K. Dureja, BARC
4. Prof. Surinder Jaswal, TISS
5. Prof. Amit Garg, IIM Ahmedabad
6. Prof. P. K. Mohapatra, BARC
7. Prof. A. K. Nayak, NCPW
8. Prof. Garima Sharma, NCPW

❖ **BoS (Integrated Masters Programme)**
1. Prof. C. Gunanathan, NISER - Convener
2. Prof. Pranay Swain, NISER Co-Convener
3. Chair, School of Life Sciences, NISER (Ex-Officio)
4. Chair, School of Chemical Sciences, NISER (Ex-Officio)
5. Chair, School of Mathematics, NISER (Ex-Officio)
6. Chair, School of Physical Sciences, NISER (Ex-Officio)
7. Chair, School of Undergraduate Studies Committee, NISER (Ex-Officio)
8. Prof. Anirban Basu, HRI
9. Prof. B. R. Sekhar, IoP
10. Prof. Sujit Roy, IIT Bhubaneswar
Balancing Members:
1. Prof. D. Dutta, HBNI
2. Prof. Meena Mahajan, IMSc
3. Prof. Partha Saha, SINP

Deans (Academic) at Constituent Institutions (CIs)/Off-Campus Centres (OCCs)

(As on July 31, 2024)

S. No.	Name of the CI/Off-Campus Centre	Discipline	Name of the Dean Academic
1.	Bhabha Atomic Research Centre	Life Sciences	Prof. B. S. Patro
		Chemical Sciences	Prof. C. N. Patra
		Physical & Mathematical Sciences	Prof. Dinesh Udupa
		Engineering Sciences Stream-I	Prof. Sulekha Mukhopadhyay
		Engineering Sciences Stream-II	Prof. Gopika Vinod
		Medical & Health Sciences	Prof. Sandip Basu
2.	Indira Gandhi Centre for Atomic Research	Chemical Sciences	Prof. C. V. S. B. Rao
		Physical Sciences	Prof. Awadesh Mani
		Engineering Sciences	Prof. A. Nagesha
3.	Raja Ramanna Centre for Advanced Technology	All Disciplines	Prof. Shoven K. Majumder
4.	Variable Energy Cyclotron Centre	Physical Sciences	Prof. Parnika Das
		Engineering Sciences	Prof. P. Y. Nabhiraj
5.	Saha Institute of Nuclear Physics	Chemical & Life Sciences	Prof. Partha Saha
		Physical Sciences	Prof. Harvendra Singh
6.	Institute for Plasma Research	All Disciplines	Prof. Mainak Bandopadhyay
7.	Institute of Physics	Physical Sciences	Prof. Arijit Saha
8.	Institute of Mathematical Sciences	Mathematical Sciences	Prof. K. Srinivas
		Physical Sciences	Prof. R. Rajesh
		Life Sciences	Prof. Sitabhra Sinha
9.	Harish-Chandra Research Institute	All Disciplines	Prof. Ujjwal Sen
10.	Tata Memorial Centre	All Disciplines	Prof. Shripad Banavali
11.	National Institute of Science Education and Research	All Disciplines	Prof. Pranay Swain
12.	Mahamana Pandit Madan Mohan Malaviya Cancer Centre & Homi Bhabha Cancer Hospital, Varanasi	Medical & Health Sciences	Dr. Shashikant C. U. Patne

List of Faculty Members

(As on July 31, 2024)

HBNI	
1.	Prof. U. Kamachi Mudali
2.	Prof. A. K. Tyagi
3.	Prof. Dilip K. Maity
4.	Prof. Haridas Pal
5.	Prof. B. K. Nayak
6.	Prof. D. Dutta
7.	Prof. Naveen Kumar
8.	Dr. Anshu Singhal
9.	Dr. Rachna Agarwal
BARC	
❖ **Chemical Sciences**	
10.	Prof. A. C. Bhasikuttan
11.	Prof. Arya Ashok Kumar
12.	Prof. Awadhesh Kumar
13.	Prof. C. P. Kaushik
14.	Prof. Chandra Nath Patra
15.	Prof. A. L. Rufus
16.	Prof. Chiranjib Majumder
17.	Prof. Dhruva Kumar Singh
18.	Prof. Hari Prasad Upadhyaya
19.	Prof. P. A. Hassan
20.	Prof. Hirendra Nath Ghosh
21.	Prof. Jyotirmayee Mohanty
22.	Prof. K. Dash
23.	Prof. Kallola Kumar Swain
24.	Prof. M. C. Rath
25.	Prof. Madhava B Mallia
26.	Prof. Mrinal R. Pai
27.	Prof. Niharendu Choudhury
28.	Prof. Puspalata Rajesh
29.	Prof. R. Mishra
30.	Prof. Raghunath Acharya
31.	Prof. Rajesh V. Pai
32.	Prof. S. Jeyakumar
33.	Prof. S. K. Jha
34.	Prof. S. N. Achary
35.	Prof. Salil Verma
36.	Prof. Sangita D. Kumar
37.	Prof. Sanjukta A. Kumar
38.	Prof. Shilpa N. Sawant
39.	Prof. Soumyakanti Adhikari
40.	Prof. Subir Kumar Ghosh
41.	Prof. Sudarsan V.
42.	Prof. Sukhendu Nath
43.	Prof. Suparna Sodaye
44.	Prof. Suresh C. Parida
45.	Prof. Tapas Das
46.	Prof. Vandana Pulhani
47.	Prof. Vinita Grover Gupta
48.	Prof. Virendra Kumar
49.	Prof. Y. K. Bhardwaj
50.	Dr. A Jahur Mondal
51.	Dr. Adya Prasad Mishra
52.	Dr. Ajay K. Singh
53.	Dr. Amit Kunwar
54.	Dr. Ankita Rao
55.	Dr. Anupkumar B.
56.	Dr. Arunasis Bhattacharyya
57.	Dr. Arup Kumar Pathak
58.	Dr. Ashis Kumar Satpati
59.	Dr. Asim Kumar Ghosh
60.	Dr. Atanu Barik
61.	Dr. Balaji Prasad Mandal
62.	Dr. Dayamoy Banerjee
63.	Dr. Dhandeep Dutta
64.	Dr. Dimple Dutta
65.	Dr. Drishty Satpati
66.	Dr. Gunjan Verma
67.	Dr. Hemant Shivram Sodaye
68.	Dr. Jayshree Ramkumar
69.	Dr. Jyoti Prakash
70.	Dr. Kaustava Bhattacharyya
71.	Dr. Kedarnath G.
72.	Dr. Kumar Abhinav Dubey
73.	Dr. Madhumita Goswami
74.	Dr. Mainak Roy
75.	Dr. Manidipa Basu
76.	Dr. Manoj Kumbhakar
77.	Dr. Manoj Mohapatra

78.	Dr. Musharaf Ali S. K.
79.	Dr. N. N. Meeravli
80.	Dr. Naina Raje
81.	Dr. Nandita Maiti
82.	Dr. Neetika Rawat
83.	Dr. P. S. Ramanjaneyulu
84.	Dr. P. Mathi
85.	Dr. Prabhat Kumar Singh
86.	Dr. Pradeep Kumar
87.	Dr. Pramod Sharma
88.	Dr. R. Ganguly
89.	Dr. Rahul Tripathi
90.	Dr. Ritesh Ruhela
91.	Dr. Ritu M Srivastava
92.	Dr. Rubel Chakravarty
93.	Dr. Sandeep Nigam
94.	Dr. Sandeep Kumar Sharma
95.	Dr. Sandip Dey
96.	Dr. Sangita D Lenka
97.	Dr. Sharmishtha Dutta Choudhury
98.	Dr. Sipra Choudhury
99.	Dr. Soumaditya Mulla
100.	Dr. Suchandra Chatterjee
101.	Dr. Suchismita Mishra
102.	Dr. Sudarshan Kathi
103.	Dr. Sumit Kumar
104.	Dr. Tirumalesh Keesari
105.	Dr. Usha Pandey
106.	Dr. Veena Subramanian
107.	Dr. Adish Tyagi
108.	Dr. Aditi Chakrabarty Patra
109.	Dr. Aishwarya Soumitra Kar
110.	Dr. Ajish Kumar K. S.
111.	Dr. Ankur Saha
112.	Dr. Apurav Guleria
113.	Dr. Arijit Sengupta
114.	Dr. Arnab Sarkar
115.	Dr. Atindra Banerjee
116.	Dr. Bal Govind Vats
117.	Dr. Beena G. Singh
118.	Dr. Bholanath Mahanty
119.	Dr. Biswajit Sadhu
120.	Dr. Brindaban Modak
121.	Dr. Chhavi Agarwal

122.	Dr. Debasis Banerjee
123.	Dr. Dibakar Goswami
124.	Dr. Hirakendu Basu
125.	Dr. J. Selvakumar
126.	Dr. Jayashree Biswal
127.	Dr. K. C. Barick
128.	Dr. K. R. S. Chandrakumar
129.	Dr. Kaushik Sanyal
130.	Dr. Mahesh Sundararajan
131.	Dr. Mahesh Tiwari
132.	Dr. Malaya Kumar Nayak
133.	Dr. Manjulata Sahu
134.	Dr. Manoj Kumar Sharma
135.	Dr. Mhejabeen Sayed
136.	Dr. Mohini Guleria
137.	Dr. Nilanjal Misra
138.	Dr. Nilotoal Barooah
139.	Dr. Nimai Pathak
140.	Dr. N. R. Singh
141.	Dr. P. Chandramohan
142.	Dr. Pallavi Singhal
143.	Dr. Pankaj Kumar Patro
144.	Dr. Parveen Kumar Verma
145.	Dr. Prasad Padmakar Phadnis
146.	Dr. Priya Maheshwari
147.	Dr. Raghunath Chowdhury
148.	Dr. Rajib Ghosh
149.	Dr. Remya Devi P S
150.	Dr. Rimpi Dawar
151.	Dr. Ruma Gupta
152.	Dr. Sabyasachhi Patra
153.	Dr. Sabyasachhi Rout
154.	Dr. Sajeev Y.
155.	Dr. Sanhita Chaudhury
156.	Dr. Sanjay Kumar
157.	Dr. Santosh Kumar Gupta
158.	Dr. Saurav Kumar Guin
159.	Dr. Seemita Banerjee
160.	Dr. Seraj Ahmad Ansari
161.	Dr. Srinivasu Kancharlapalli
162.	Dr. Sumana Sengupta
163.	Dr. Surajit Panja
164.	Dr. Tijo Joseph V.
165.	Dr. V Kusum Vats

❖ Engineering Sciences	
166.	Prof. A. Vinod Kumar
167.	Prof. Alok Awasthi
168.	Prof. Archana Sharma
169.	Prof. Arun Kumar Nayak
170.	Prof. D. C. Kar
171.	Prof. Deb Mukhopadhyay
172.	Prof. Gopal Joshi
173.	Prof. Gopalakrishnan Sugilal
174.	Prof. Jayanta Chattopadhyay
175.	Prof. Raghvendra Tewari
176.	Prof. Ram Nivas Singh
177.	Prof. A. K. Dureja
178.	Prof. Amit Sinha
179.	Prof. Aniruddha Biswas
180.	Prof. Arijit Laik
181.	Prof. Betty C. A.
182.	Prof. Biswaranjan Dikshit
183.	Prof. Deep Prakash
184.	Prof. Dinesh Kumar Chandraker
185.	Prof. Geogy Jiju Abraham
186.	Prof. Gopika Vinod
187.	Prof. Joydipta Banerjee
188.	Prof. Jung Bahadur Singh
189.	Prof. K. Anand Rao
190.	Prof. Kapilesh Bhargava
191.	Prof. Kinshuk Dasgupta
192.	Prof. Kulwant Singh
193.	Porf. M. K. Samal
194.	Prof. Paritosh Prabhakar Nanekar.
195.	Prof. R. Karthikeyan
196.	Prof. Rajeev Kapoor
197.	Prof. S. K. Satpati
198.	Prof. S. R. Shimijith
199.	Prof. Samiran Sengupta
200.	Prof. Sanjib Majumdar
201.	Prof. Sudipta Chakraborty
202.	Prof. Sujay Bhattacharya
203.	Prof. Sulekha Mukhopadhyay
204.	Prof. Suneel Kumar Gupta
205.	Prof. Supratik Roychowdhury
206.	Prof. Tarasankar Mahata
207.	Prof. Tessy Vincent
208.	Prof. V. H. Patankar
209.	Prof. Yogita Parulekar
210.	Dr. Abhijeet Mohan Vaidya
211.	Dr. Abhishek Mukherjee
212.	Dr. Anil Kumar Tiwari
213.	Dr. Anindya Chakravarty
214.	Dr. Chiradeep C Gupta
215.	Dr. Debanik Roy
216.	Dr. Gaurav Bhutani
217.	Dr. Imran Ali Khan
218.	Dr. K. K. Singh
219.	Dr. Kamal Sharma
220.	Dr. Kamlesh Chandra
221.	Dr. Maha Nand Jha
222.	Dr. Mahendra Prasad
223.	Dr. Manoj Kumar
224.	Dr. Mithilesh Kumar
225.	Dr. Noble Jacob
226.	Dr. Pranesh Sengupta
227.	Dr. Praveen Kumar
228.	Dr. Ranjan Kumar
229.	Dr. Rishi Verma
230.	Dr. Soumitra Kar
231.	Dr. Suman Neogy
232.	Dr. Surender Kumar Sharma
233.	Dr. T. Sree Rama Chandra Murthy
234.	Dr. Abhijit Raha
235.	Dr. Bhaskar Paul
236.	Dr. Nirvik Sen
237.	Dr. Onkar Suresh Gokhale
238.	Dr. Poulami Chakraborty Srivastava
239.	Dr. Prabhat Ranjan
240.	Dr. Punit Arora
241.	Dr. Sabyasachi Mitra
242.	Dr. Sangeeta Pal
243.	Dr. Vishwanadh Bathula
❖ Life Sciences	
244.	Prof. Anand Ballal
245.	Prof. Anand M Badigannavar
246.	Prof. Anu Ghosh
247.	Prof. B. N. Pandey
248.	Prof. Bhavani S. Shankar
249.	Prof. Briija Sankar Patro
250.	Prof. Deepak Sharma
251.	Prof. Hema Rajaram

252.	Prof. Joy G. Manjeya
253.	Prof. Mahesh Subramanian
254.	Prof. Ravindra D. Makde
255.	Prof. S. N. Jamdar
256.	Prof. Sandur Santosh Kumar
257.	Prof. Satyendra Gautam
258.	Prof. Y. V. Nancharaiah
259.	Dr. Ajay Saini
260.	Dr. Amit Das
261.	Dr. Archana Mukherjee
262.	Dr. Archana Joshi Saha
263.	Dr. Aruna Jyothi Kora
264.	Dr. Ashish Kumar Srivastava
265.	Dr. B. K. Das
266.	Dr. Bhakti Basu
267.	Dr. Bhaskar Sanyal
268.	Dr. B. B. Mishra
269.	Dr. Celin Acharya
270.	Dr. Dharmendra Kumar Maurya
271.	Dr. Gagan Deep Gupta
272.	Dr. Himanshi N. Mishra
273.	Dr. J. Souframanien
274.	Dr. Jitendra Kumar
275.	Dr. Nagesh Bhat
276.	Dr. R. Shashidhar
277.	Dr. Rahul Checker
278.	Dr. Rajani Kant Chittela
279.	Dr. Rajesh Kumar
280.	Dr. Ramesh Hire
281.	Dr. Rath Devashish
282.	Dr. S. P. Chawla
283.	Dr. S. N. Hajare
284.	Dr. Sheetal Uppal
285.	Dr. S. C. Bihani
286.	Dr. Sudhir Singh
287.	Dr. Suvendu Mondal
288.	Dr. Sweetie R. Kanatt
289.	Dr. Vishal Prashar
290.	Dr. Vishwas M Kulkarni
291.	Dr. Yogendra Singh Rajpurohit
292.	Dr. Amit Kumar
293.	Dr. Ananganti Narasimha
294.	Dr. Archana N. Rai
295.	Dr. Avik Chakraborty

296.	Dr. Chandan Kumar
297.	Dr. Hiren Joshi
298.	Dr. Jayakumar Sundarraj
399.	Dr. Jyoti Tripathi
300.	Dr. Manisha Banerjee
301.	Dr. Murali M S Balla
302.	Dr. P Sriyutha Murthy
303.	Dr. Promod Kumar Gupta
304.	Dr. Raghvendra S. Patwardhan
305.	Dr. S. T. Mehetre
306.	Dr. Shraddha Singh
307.	Dr. Sonia Chadha
308.	Dr. Sudhir Kumar Gupta
309.	Dr. Sudhir Kumar Shukla
310.	Dr. Suman Bakshi
311.	Dr. Sumit Gupta
312.	Dr. Swathi Kota
313.	Dr. Vandan Nagar
314.	Dr. Vinay Jain
❖ **Medical & Health Sciences**	
315.	Prof. Basant L Malpani
316.	Prof. Gaurav Malhotra
317.	Prof. Rahul Vithalrao Parghane
318.	Prof. Sandip Basu
319.	Prof. Sunil Dutta Sharma
320.	Dr. Ashwini Kalshetty
321.	Dr. J. G. Kalbhande
322.	Dr. Priyanka Verma
323.	Dr. Satish C. Mishra
324.	Dr. Sunita Nitin Sonavane
❖ **Physical Sciences**	
325.	Prof. B. K. Sapra
326.	Prof. Dinesh Kumar Aswal
327.	Prof. S. M. Yusuf
328.	Prof. Satyaranjan Santra
329.	Prof. V. K. Aswal
330.	Prof. A. K. Gupta
331.	Prof. Abhas Kumar Mitra
332.	Prof. Aditi Ray
333.	Prof. Ajay Singh
334.	Prof. Alka B. Garg
335.	Prof. Anil Kumar Chauhan
336.	Prof. Anurag Gupta
337.	Prof. Aradhana Shrivastava

338.	Prof. Debasis Sen
339.	Prof. Dibyendu Bhattacharyya
340.	Prof. Dinesh Venkatesh Udupa
341.	Prof. J. Padma Nilaya
342.	Prof. Jagannath
343.	Prof. K. K. Yadav
344.	Prof. Keshaw D. Joshi
345.	Prof. Kripamay Mahata
346.	Prof. Lalit Mohan Pant
347.	Prof. M. V. Suryanarayana
348.	Prof. Mala N Rao
349.	Prof. Manoj Kumar Warrier
350.	Prof. Mukesh Kumar
351.	Prof. N. Padma
352.	Prof. Nandini Garg
353.	Prof. P U Sastry
354.	Prof. Prashant Shukla
355.	Prof. R. C. Rannot
356.	Prof. Ranjan Mittal
357.	Prof. Rekha Rao
358.	Prof. Sakuntala T
359.	Prof. Srikumar Ghorui
360.	Prof. Subhankur Mitra
361.	Prof. Sukanta Karmakar
362.	Prof. T Palani Selvam
363.	Prof. Tej Singh
364.	Prof. Usha Pal
365.	Prof. V. Jha
366.	Dr. Ajay Kumar Mishra
367.	Dr. Amit Kumar
368.	Dr. Amitava Roy
369.	Dr. Aparna Shastri
370.	Dr. Arup Biswas
371.	Dr. Asavari Santosh Dhavale
372.	Dr. Asawari D Rath
373.	Dr. Ashok Kumar Bakshi
374.	Dr. Ashok Kumar Verma
375.	Dr. Babita Tiwari
376.	Dr. Bhushan Dhabekar
377.	Dr. Biplab Ghosh
378.	Dr. Brahmananda Chakraborty
379.	Dr. C. D. Sijoy
380.	Dr. Chitra Murli
381.	Dr. D. R. Mishra

382.	Dr. Debarati Bhattacharya
383.	Dr. G. Laxmi Narasimha Reddy
384.	Dr. G. Sridhar
385.	Dr. Himal Bhatt
386.	Dr. Himanshu Kumar Poswal
387.	Dr. Jayanta Mondal
388.	Dr. Jitendra Bahadur
389.	Dr. Keka R. Chakraborty
390.	Dr. Krishan Kumar Pandey
391.	Dr. Mayank Shukla
392.	Dr. Munish Kumar
393.	Dr. Narender Singh Rawat
394.	Dr. Paritosh Modak
395.	Dr. Partha Sarathi Sarkar
396.	Dr. Prakash Chandra Rout
397.	Dr. Pratap Baburao Wagh
398.	Dr. Priyamvada M. Dighe
399.	Dr. Raghwendra Kumar
400.	Dr. Rajeev Kumar
401.	Dr. Rajul Ranjan Choudhury
402.	Dr. Ramesh Chandra Das
403.	Dr. Renju George Thomas
404.	Dr. Rohit Shukla
405.	Dr. S. Anand
406.	Dr. Sanjay Kumar Sahu
407.	Dr. Santanu Bera
408.	Dr. Shashwati Sen Yeram
409.	Dr. Soumen Bhattacharyya
410.	Dr. Subir Bhattacharyya
411.	Dr. Surendra Singh
412.	Dr. Swapan Das
413.	Dr. Swarupananda Pradhan
414.	Dr. T. Jayasekharan
415.	Dr. Veerendra Kumar Sharma
416.	Dr. Venkata Ramana Ikkurthi
417.	Dr. Vibha Saxena
418.	Dr. Vinod Singh Rawat
419.	Dr. Vir Krishen Dhar
420.	Dr. Yogesh K. Gupta
421.	Dr. Yogesh Kashyap
422.	Dr. Amit P Srivastava
423.	Dr. Anil Jain
424.	Dr. Anup Kumar Bera
425.	Dr. Apu Sarkar

426.	Dr. Ashish Kumar Agrawal
427.	Dr. Ashok Kumar Yadav
428.	Dr. Asim Pal
429.	Dr. B. Sunder Sahayanathan
430.	Dr. Chandrani Nayak
431.	Dr. Debdutta Lahiri
432.	Dr. Debjani Karmakar
433.	Dr. Dipak Kumar Mishra
434.	Dr. Gayatri Mohanto
435.	Dr. Giri Dhari Patra
436.	Dr. Goutam Dev Mukherjee
437.	Dr. H. Kumawat
438.	Dr. Jose V Mathew
439.	Dr. Kiran R. M.
440.	Dr. Krishna Kumar Singh
441.	Dr. Manmeet Kaur
442.	Dr. Mayanak Kumar Gupta
443.	Dr. Mohit Tyagi
444.	Dr. Niranjan Suryakant Ramgir
445.	Dr. Nishant Chaudhary
446.	Dr. Param Jeet Singh
447.	Dr. Parasmani Rajput
448.	Dr. Partha Sarathi Ghosh
449.	Dr. Pramod Bhatt
450.	Dr. Purnananda Nandi
451.	Dr. Purushottam Jha
452.	Dr. R. B. Tokas
453.	Dr. Rajib Kar
454.	Dr. Ranita Basu
455.	Dr. Ranu Bhatt
456.	Dr. Rosaline Mishra
457.	Dr. S. K. Pandit
458.	Dr. S. P. Behera
459.	Dr. S. P. Tripathy
460.	Dr. Sabyasachi Paul
461.	Dr. Sanjay Kumar Mishra
462.	Dr. Shankar Prasad Koiry
463.	Dr. Shilpa Tripathi
464.	Dr. Shiv Govind Singh
465.	Dr. Shivanand Chaurasia
466.	Dr. Shovit Bhattacharya
467.	Dr. Shuvendu Jena
468.	Dr. Sk Maidul Haque
469.	Dr. Sohrab Abbas
470.	Dr. Somsundar Mukhopadhyay
471.	Dr. Sugam Kumar
472.	Dr. Suhail Ahmad Khan
473.	Dr. Sunit Kedia
474.	Dr. V. V. Parkar
475.	Dr. Vinayak Mishra
476.	Dr. Vineet Kumar
477.	Dr. Aniruddha Kumar BARCTS(NPCIL), Tarapur

IGCAR

❖ Chemical Sciences

478.	Prof. A. Suresh
479.	Prof. C. V. S. Brahmmananda Rao
480.	Prof. Hrudananda Jena
481.	Prof. K. A. Venkatesan
482.	Prof. R. Kumar
483.	Prof. Rajesh Ganesan
484.	Prof. V. Jayaraman
485.	Dr. K. Sundararajan
486.	Dr. K. I. Gnanasekar
487.	Dr. N. Ramanathan
488.	Dr. Sublime Ningshen
489.	Dr. A. Sree Rama Murthy
490.	Dr. Arindam Das
491.	Dr. Ashish Jain
492.	Dr. B. Anandkumar
493.	Dr. B. Sreenivasulu
494.	Dr. Chowdari Jagadeeswara Rao
495.	Dr. G. Gopakumar
496.	Dr. Pavan Kumar Narayanam
497.	Dr. R. Kumaresan
498.	Dr. R Venkata Krishnan
499.	Dr. Satendra Kumar

❖ Engineering Sciences

500.	Prof. A. Nagesha
501.	Prof. A. John Arul
502.	Prof. Aniruddha Moitra
503.	Prof. Anish Kumar
504.	Prof. M. Vasudevan
505.	Prof. Mahadevan S
506.	Prof. R Suresh Kumar
507.	Prof. V. Karthik
508.	Dr. A. Jasmin Sudha
509.	Dr. C. Sudha

510.	Dr. Chitta Ranjan Das
511.	Dr. G V Prasad reddy
512.	Dr. P Mangarjuna Rao
513.	Dr. R. Mythili
514.	Dr. Vani Shankar
515.	Dr. A. Ravi Shankar
516.	Dr. B. Arivazhagan
517.	Dr. David Vijayanand V
518.	Dr. Diptimayee Samantaray
❖ **Physical Sciences**	
519.	Prof. Ramachandran Divakar
520.	Prof. Sandip Kumar Dhara
521.	Prof. Arup Dasgupta
522.	Prof. Awadhesh Mani
523.	Prof. C. Venkata Srinivas
524.	Prof. Christopher David
525.	Prof. N. Subramanian
526.	Prof. R. Govindaraj
527.	Prof. S. Ganesamoorthy
528.	Dr. B. Sundaravel
529.	Dr. Nithya Ravindran
530.	Dr. O. Annalakshmi
531.	Dr. R. Ramaseshan
532.	Dr. S. Amirthapandian
533.	Dr. S. Tripura Sundari
534.	Dr. Sharat Chandra
535.	Dr. V. Sivasubramanian
536.	Dr. Amit Kumar
537.	Dr. Anees P.
538.	Dr. Arun K. Prasad
539.	Dr. Barid Baran Lahiri
540.	Dr. Chanchal Ghosh
541.	Dr. Dipak Kumar Baisnab
542.	Dr. Edward Prabu Amaladass
543.	Dr. Haraprasanna Tripathy
544.	Dr. K. Ganesan
545.	Dr. K. Prabhakar
546.	Dr. N. R. Sanjay Kumar
547.	Dr. Rajendra Ganpat Joshi
548.	Dr. Ramanathaswamy Pandian
549.	Dr. Ravi Chinnappan
550.	Dr. S. Abhaya
551.	Dr. S. C. Vanithakumari
552.	Dr. Sainath G.
553.	Dr. Syamalarao Polaki
554.	Dr. T. Sathyanarayana Annam
555.	Dr. Vinod K.
RRCAT	
❖ **Chemical Sciences**	
556.	Dr. Dipankar Nanda
❖ **Engineering Sciences**	
557.	Prof. Christ Prakash Paul
558.	Prof. Mangesh Balkrishna Borage
559.	Prof. Ajit Upadhyay
560.	Dr. Prabhat Kumar Gupta
561.	Dr. Vikas Kumar Jain
562.	Dr. Rahul Shukla
❖ **Life Sciences**	
563.	Prof. Alok Dube
564.	Dr.Khageshwar Sahu
565.	Dr. Rashmi Shrivastava
❖ **Physical Sciences**	
566.	Prof. Anand Moorti
567.	Prof. Aparna Chakrabarti
568.	Prof. Arup Banerjee
569.	Prof. Gurvinderjit Singh
570.	Prof. Indranil Bhaumik
571.	Prof. J. A. Chakera
572.	Prof. Manoranjan Prasad Singh
573.	Prof. Maulindu Kumar Chattopadhyay
574.	Prof. Mohammed Hussein Modi
575.	Prof. Om Prakash
576.	Prof. Sanjay Kumar Rai
577.	Prof. Satya Ram Mishra
578.	Prof. Shovan K Majumder
579.	Prof. Sudhir Kumar Dixit
580.	Prof. Suni Verma
581.	Prof. Tapas Ganguli
582.	Prof. Tarun Kumar Sharma
583.	Prof. Vibhuti Bhushan Tiwari
584.	Prof. Vinit Kumar
585.	Dr. Arvind Kumar Srivastava
586.	Dr. Avnish K Sharma
587.	Dr. Brahma Nand Upadhyaya
588.	Dr. Chandrachur Mukherjee
589.	Dr. Haranath Ghosh
590.	Dr. Himanshu Singhal
591.	Dr. J. Jayabalan

592.	Dr. Maheswar Nayak
593.	Dr. Manoj Kumar Tiwari
594.	Dr. P K Mukhopadhyay
595.	Dr. Pankaj Misra
596.	Dr. Rajeev Bhatt
597.	Dr. Raktim Dasgupta
598.	Dr. Ramakanta Biswal
599.	Dr. Sanyasi Rao Bobbili
600.	Dr. Shreyashkar Dev Singh
601.	Dr. Srinibas Satapathy
602.	Dr. Surya Mohan Gupta
603.	Dr. Vijay Kumar Dixit
604.	Dr. Yogesh Verma
605.	Dr. Archana Sagdeo
606.	Dr. Arun Kumar Rai
607.	Dr. C. Kamal
608.	Dr. Chandra Pal Singh
609.	Dr. Himanshu Srivastava
610.	Dr. Jitendra Kumar
611.	Dr. L. S. Sharath Chandra
612.	Dr. Manoj Kumar Singh
613.	Dr. Pooja Gupta
614.	Dr. Pragya Tiwari
615.	Dr. Ravindra Jangir
616.	Dr. Sachin Kumar Srivastava
617.	Dr. Salahuddin Khan
618.	Dr. Shailesh Kumar Khamari
619.	Dr. Shankar Lal
620.	Dr. Soma Banik
621.	Dr. Suman Bagchi
622.	Dr. Suparna Pal
623.	Dr. Uday Chakravarty
624.	Dr. Vishnu Kumar Sharma
VECC	
❖ Engineering Sciences	
625.	Prof. P. Y. Nabhiraj
626.	Prof. Paramita Mukherjee
627.	Prof. Sandip Pal
628.	Prof. Sarbajit Pal
629.	Dr. Hemendra Kumar Pandey
630.	Dr. Tapatee Kundu Roy
❖ Physical Sciences	
631.	Prof. Arup Bandyopadhyay
632.	Prof. Parnika Das

633.	Prof. Sarmishtha Bhattacharyya
634.	Prof. Sourav Sarkar
635.	Dr. Anand Kumar Dubey
636.	Dr. Animesh Goswami
637.	Dr. Deepak Pandit
638.	Dr. Gargi Chaudhri
639.	Dr. Gayathri N. Banerjee
640.	Dr. Gopal Mukherjee
641.	Dr. Jedidiah Pradhan
642.	Dr. Jhilam Sadhukhan
643.	Dr. Kaushik Banerjee
644.	Dr. Partha Pratim Bhaduri
645.	Dr. Prasanta Karmakar
646.	Dr. Samir Kundu
647.	Dr. Sanyal Dirtha
648.	Dr. Siddhartha Dechoudhury
649.	Dr. Tapan Kumar Rana
650.	Dr. Tilak Kumar Ghosh
651.	Dr. Tumpa Bhattacharjee
652.	Dr. Uttam Bhunia
653.	Dr. Vaishali Naik
654.	Dr. Zubayer Ahammed
655.	Dr. Ajay Kumar Himanshu
656.	Dr. Arindam Kumar Sikdar
657.	Dr. Ayan Ray
658.	Dr. Debasis Mondal
659.	Dr. Pratap Roy
660.	Dr. Rupa Chatterjee
661.	Dr. Sanjib Muhuri
662.	Dr. Shashi C Srivastava
663.	Dr. Supriya Mukhopadhyay
HRI	
❖ Mathematical Sciences	
664.	Prof. Manoj kumar
665.	Prof. P. K. Ratnakumar
666.	Prof. Punita Batra
667.	Prof. R. Thangadurai
668.	Prof. Surya D. Ramana
669.	Dr. Amrita Ghosh
670.	Dr. Aprameyo Pal
671.	Dr. Bhamidi Sai Somanjana Sreedhar
672.	Dr. Gyan Prakash
673.	Dr. Hemangi Madhusudan Shah
674.	Dr. Jishnu Ray

675.	Dr. Tuhin Ghosh
676.	Dr. Umeshkumar V. Dubey
❖ **Physical Sciences**	
677.	Prof. Aditi Sen De
678.	Prof. Asesh Krishna Datta
679.	Prof. Dileep Prabhakar Jatkar
680.	Prof. Prasenjit Sen
681.	Prof. Ujiwal Sen
682.	Dr. Anirban Basu
683.	Dr. Anshuman Maharana
684.	Dr. Santosh Kumar Rai
685.	Dr. T. P. Pareek
686.	Dr. Tapas Kumar Das
687.	Dr. Debraj Rakshit
688.	Dr. Sayan Choudhury
689.	Dr. Sudip Chakraborty
690.	Dr. Tathagata Ghosh
IMSc	
❖ **Life Sciences**	
691.	Dr. Areejit Samal
692.	Dr. Rahul Siddharthan
693.	Dr. Sandeep Choubey
❖ **Mathematical Sciences**	
694.	Prof. Amritanshu Prasad
695.	Prof. Jaya N. Iyer
696.	Prof. Meena Bhaskar Mahajan
697.	Prof. Saket Saurabh
698.	Prof. Sankaran Viswanath
699.	Prof. Sanoli Gun
700.	Prof. Srinivas Kotyada
701.	Prof. Vijay Kodiyalam
702.	Dr. Anirban Mukhopadhyay
703.	Dr. Dishant Mayurbhai Pancholi
704.	Dr. Pralay Chatterjee
705.	Dr. Vikram Sharma
706.	Dr. Anup Biswanath Dixit
707.	Dr. C. Ramya
708.	Dr. Indrava Roy
709.	Dr. Prakash Saivsan
710.	Dr. Rahul Gupta
711.	Dr. S. Sundar
712.	Dr. Sushmita Gupta
713.	Dr. Sushmita Venugopal
❖ **Physical Sciences**	
714.	Prof. V. Ravindran
715.	Prof. Raghib Hassan Syed
716.	Prof. Rajesh R.
717.	Prof. Satyavani Vemparala
718.	Prof. Sibasish Ghosh
719.	Prof. Sitabhra Sinha
720.	Dr. Gopalakrishna Shrihari
721.	Dr. Manjari Bagchi
722.	Dr. Mukul S. Laad
723.	Dr. Partha Mukhopadhyay
724.	Dr. Pinaki Chaudhuri
725.	Dr. Ronojoy Adhikari
726.	Dr. Sanatan Digal
727.	Dr. Sujay K. Ashok
728.	Dr. V. S. Nemani
729.	Dr. Ajit Coimbatore Balram
730.	Dr. Arnab Pal
731.	Dr. Chandrashekar C. M.
732.	Dr. Debayan Chakraborty
733.	Dr. Dhiraj Kumar Hazra
734.	Dr. Ganesh Ramchadran
735.	Dr. Padmanath Madanagopalan
736.	Dr. Roji Pius
737.	Dr. Sayantan Sharma
IOP	
❖ **Physical Sciences**	
738.	Prof. Karuna Kar Nanda
739.	Prof. B K Panigrahi
740.	Prof. Biju Raja Sekhar
741.	Prof. Pradip Kumar Sahu
742.	Prof. Som Tapobrata
743.	Prof. Sudipta Mukherji
744.	Prof. Sanjib Kumar Agarwalla
745.	Dr. Arijit Saha
746.	Dr. Aruna Kumar Nayak

747. Dr. Debasish Chaudhuri
748. Dr. Debottam Das
749. Dr. Dinesh Topwal
750. Dr. Goutam Tripathy
751. Dr. Kirtiman Ghosh
752. Dr. Manimala Mitra
753. Dr. Samal Debakanta
754. Dr. Saptarshi Mandal
755. Dr. Satyaprakash Sahoo

IPR

❖ Chemical Sciences

756. Prof. Sudhir Kumar Nema

❖Engineering Sciences

757. Prof. Paritosh Chaudhuri
758. Prof. Surya Kumar Pathak
759. Prof. Vipulkumar L. Tanna
760. Dr. Alphonsa Joseph
761. Dr. Manoj Kumar Gupta
762. Dr. Nirav I. Jamnapara
763. Dr. Rajesh Kumar
764. Dr. Ritesh Sugandhi
765. Dr. Suryakant B. Gupta
766. Dr. Rana Pratap Yadav

❖ Physical Sciences

767. Prof. Anitha V P
768. Prof. Jana Mukti Ranjan
769. Prof. Lalit Mohan Awasthi
770. Prof. Mahendrajit Singh
771. Prof. Mainak Bandopadhyay
772. Prof. Pramod Kumar Sharma
773. Prof. Raju Daniel
774. Prof. Subrata Pradhan
775. Prof. Sudip Sengupta
776. Dr. Debasis Chandra
777. Dr. Ganesh Rajaraman
778. Dr. Hiteshkumar B Pandya
779. Dr. Indranil Bandyopadhyay
780. Dr. Joydeep Ghosh
781. Dr. Malay Bikas Chowdhuri
782. Dr. Mrityunjay Kundu
783. Dr. Mukesh Ranjan
784. Dr. Nirmal Kumar Bisai
785. Dr. Rajendraprasad Bhattacharyay
786. Dr. Ravi G
787. Dr. Saikia Bipul
788. Dr. Samir Khirwadkar
789. Dr. Sanjeev Kumar Sharma
790. Dr. Sanjeev Kumar Varshney
791. Dr. Shantanu Kumar Karkari
792. Dr. Ziauddh Khan
793. Dr. Amreen Ara Hussain
794. Dr. Amulya Kumar Sanyasi
795. Dr. C. Balasubramanian
796. Dr. Devendra Sharma
797. Dr. Gourab Bansal
798. Dr. Harshita Raj
799. Dr. Jinto Thomas
800. Dr. Jugal Chowdhury
801. Dr. Jyoti Shankar Mishra
802. Dr. Kishore Kanti Mishra
803. Dr. N Ramasubramanian
804. Dr. Ngangom Aomoa
805. Dr. Pintu Bandyopadhyay
806. Dr. Pratipalsinh A Rayjada
807. Dr. Rakesh Moulick
808. Dr. Ramkrishna Rane
809. Dr. Sarveshwar Sharma
810. Dr. Sejal Shah
811. Dr. Shekar Goud Thatipamula
812. Dr. Shishir Purohit
813. Dr. Smruti R. Mohanty
814. Dr. Subhash P. V.

NISER

❖ Applied Systems Analysis

815. Dr. Amarendra Das
816. Dr. Amarjeet Nayak

817. Dr. Debashis Pattanaik
818. Dr. Joe Varghese Yeldho
819. Dr. Pranaya Kumar Swain
820. Dr. Rooplekha Khuntia
❖ **Chemical Sciences**
821. Prof. Alagar Srinivasan
822. Dr. Bhargava B. L.
823. Dr. Chandra Shekhar Purohit
824. Dr. Chidambaram Gunanathan
825. Dr. Himansu Sekhar Biswal
826. Dr. Jogendra Nath Behera
827. Dr. Moloy Sarkar
828. Dr. Nagendra Kumar Sharma
829. Dr. Nembenna Sharanappa
830. Dr. P. C. Ravikumar
831. Dr. Prasenjit Mal
832. Dr. Sanjib Kar
833. Dr. Saravanan Peruncheralathan
834. Dr. Subhadip Ghosh
835. Dr. Sudip Barman
836. Dr. Upakarasamy Lourderaj
837. Dr. Venkatasubbaiah Krishnan
838. Dr. Arindam Ghosh
839. Dr. Bidraha Bagh
840. Dr. Bishnu Prasad Biswal
841. Dr. Dipak Samanta
❖ **Engineering Sciences**
842. Dr. Anup Kumar Bhattacharya
843. Dr. Sabyasachi Karati
❖ **Life Sciences**
844. Dr. Chandan Goswami
845. Dr. Debasmita Pankaj Alone
846. Dr. Harapriya Mohapatra
847. Dr. K. Chandrasekhar Panigrahi
848. Dr. Manjusha Dixit
849. Dr. Palok Aich
850. Dr. Pankaj Vidyadhar Alone
851. Dr. Praful S. Singru

852. Dr. Subhasis Chattopadhyay
853. Dr. Anirudhha Datta Roy
854. Dr. Himabindu Vasuki Kilambi
855. Dr. K. Venkatsai Badireenath
856. Dr. Mohammed Saleem
857. Dr. Renjith Mathew
858. Dr. Rudresh Acharya
859. Dr. Srinivasan Ramanujam
860. Dr. Swagata Ghatak
861. Dr. Tirumala Kumar Chowdary
❖ **Mathematical Sciences**
862. Dr. Anil Kumar Karn
863. Dr. Binod kumar Sahoo
864. Dr. Brundaban Sahu
865. Dr. Anisur Rahaman Molla
866. Dr. Anupam Pal Chowdhary
867. Dr. Aritra Banik
868. Dr. Chitrabhanu Chaudhury
869. Dr. Deepak Kumar Dalai
870. Dr. Dinesh Kumar Keshari
871. Dr. Kamal Lochan Patra
872. Dr. Kaushik Majumder
873. Dr. Krishanu Dan
874. Dr. Manas Ranjan Sahoo
875. Dr. Manoj Mishra
876. Dr. Meher Jaban
877. Dr. Nabin Kumar Jana
878. Dr. Panchugopal Bikram
879. Dr. Ramesh Manna
880. Dr. Rishiraj Bhattacharyya
881. Dr. Ritwik Mukherjee
882. Dr. Roy Sutanu
883. Dr. Sanjay Parui
884. Dr. Senthil Kumar K.
885. Dr. Subhankar Mishra
886. Dr. Sudhir Kumar Pujahari
887. Dr. Sumana Hatui
888. Dr. Tushar Kanta Naik

❖ Physical Sciences	
889.	Prof. Bedangadas Mohanty
890.	Dr. Ashok Kumar Mohapatra
891.	Dr. Colin Benjamin
892.	Dr. Prasanjit Samal
893.	Dr. Pratap Kumar Sahoo
894.	Dr. Ritwick Das
895.	Dr. Sanjay Kumar Swain
896.	Dr. Shamik Banerjee
897.	Dr. Subhankar Bedanta
898.	Dr. A.V. Anil Kumar
899.	Dr. Abdur Rahman
900.	Dr. Ajaya Kumar Nayak
901.	Dr. Amaresh Kumar Jaiswal
902.	Dr. Anamitra Mukherjee
903.	Dr. Ashis Kumar Nady
904.	Dr. Chethan N. Gowdigere
905.	Dr. Guneshwar Thangjam
906.	Dr. Jaya Khanna
907.	Dr. Jayesh M Goyal
908.	Dr. Joydeep Bhattacharjee
909.	Dr. Kartikeswar Senapati
910.	Dr. Kush Saha
911.	Dr. Liton Majumdar
912.	Dr. Luke Chamandy
913.	Dr. Najmal Haque
914.	Dr. Narayan Rana
915.	Dr. Nishikanta Khandai
916.	Dr. Pathikrit Bhattacharya
917.	Dr. Priyadarshi Chowdhury
918.	Dr. Prolay Kumar Mal
919.	Dr. Sayantani Bhattacharyya
920.	Dr. Shovan Pal
921.	Dr. Subhasish Basak
922.	Dr. Sumedha
923.	Dr. Surya Snata Rout
924.	Dr. Tapan Mishra
925.	Dr. Tuhin Ghosh
926.	Dr. V. Ravi Chandra
927.	Dr. Victor Roy
928.	Dr. Yogesh Kumar Srivastava
SINP	
❖ Chemical Sciences	
929.	Dr. Dulal Senapati
930.	Dr. Montu K. Hazra
931.	Dr. Padmaja Prasad Mishra
❖ Life Sciences	
932.	Prof. Debashis Mukhopadhyay
933.	Prof. Partha Saha
934.	Dr. Chandrima Das
935.	Dr. Gautam Garai
936.	Dr. Oishee Chakrabarti
937.	Dr. Rahul Banerjee
938.	Dr. Sampa Biswas
939.	Dr. Udayaditya Sen
940.	Dr. H. Raghuraman
941.	Dr. Kaushik Sengupta
942.	Dr. Sangram Bagh
943.	Dr. Soumen Kanti Manna
944.	Dr. Subhabrata Majumder
945.	Dr. Subhendu Roy
946.	Dr. Tofayel Ahmed
❖ Physical Sciences	
947.	Prof. Gautam Bhattacharyya
948.	Prof. Abhik Basu
949.	Prof. Bijay Kumar Agrawal
950.	Prof. Chandan Mazumder
951.	Prof. Harvendra Singh
952.	Prof. Indranil Das
953.	Prof. Krishanakumar S. R. Menon
954.	Prof. Pradip Kumar Roy
955.	Prof. Satyajit Hazra
956.	Prof. Ushasi Datta
957.	Dr. Amit Ghosh
958.	Dr. Anjali Mukherjee
959.	Dr. Arti Garg
960.	Dr. Chinmay Basu
961.	Dr. Maitreyee Nandy
962.	Dr. Nayana Majumdar
963.	Dr. Satyaban Bhunia
964.	Dr. Satyaki Bhattacharya

965.	Dr. Subir Sarkar
966.	Dr. Suchandra Dutta
967.	Dr. Supratic Chakraborty
968.	Dr. Tinku Sinha Sarkar
969.	Dr. Akashrup Banerjee
970.	Dr. Arnab Kundu
971.	Dr. Arunava Mukherjee
972.	Dr. Augustine Kshetrimayum
973.	Dr. Biswajit Karmakar
974.	Dr. Biswarup Satpati
975.	Dr. Debasish Banerjee
976.	Dr. Debasish Das
977.	Dr. Kalpataru Pradhan
978.	Dr. Krishanu Roychowdhury
979.	Dr. Mala Das
980.	Dr. M. K. Mukhopadhyay
981.	Dr. Pratik Majumdar
982.	Dr. Samik Duttagupta
983.	Dr. Sankar De
984.	Dr. Sudipto Chakrabarti
TMC	
❖ Life Sciences	
985.	Prof. Arvind D Ingle
986.	Prof. Manoj Balkrishna Mahimkar
987.	Prof. Sorab Nariman Dalal
988.	Dr. Abhijt De
989.	Dr. Amit Dutt
990.	Dr. Ashok Varma
991.	Dr. Chilakapati Murali Krishna
992.	Dr. Joyti Anand Kode
993.	Dr. Kakoli Bose
994.	Dr. Pritha Ray
995.	Dr. Sanjay Gupta
996.	Dr. Venkatraman Prasanna
997.	Dr. Vikram Suryaprakash Gota
998.	Dr. Dibyendu Bhattacharyya
999.	Dr. Khizer Hasan Syed
1000.	Dr. Nandini Verma
1001.	Dr. Rohan Jayant Khadilkar
1002.	Dr. Sanjeev Waghmare
1003.	Dr. Sejal Patwardhan
1004.	Dr. Sharath Chandra Arandkar
1005.	Dr. Shilpee Dutt
1006.	Dr. Sonam Mehrotra
1007.	Dr. Subir Biswas
1008.	Dr. Sunil S. Kumar Shetty
❖ Medical & Health Sciences	
1009.	Prof. Ajay Puri
1010.	Prof. Aliasgar V Moiyadi
1011.	Prof. Amit Prakashchandra Joshi
1012.	Prof. Amita Maheswari
1013.	Prof. Amol Trymbakrao Kothekar
1014.	Prof. Anant Gokarn
1015.	Prof. Anant Ramaswamy
1016.	Prof. Aparna Sanjay Chatterjee
1017.	Prof. Archi Ramesh Agrawal
1018.	Prof. Ashwin Luis Desouza
1019.	Prof. Ashwini Narsingrao Budrukkar
1020.	Prof. Atul M. Budukh
1021.	Prof. Atul Prabhakar Kulkarni
1022.	Prof. Avanish Parmesh Saklani
1023.	Prof. Ayushi Sahay
1024.	Prof. Bharat Rekhi
1025.	Prof. Bhausaheb Pandurang Bagal
1026.	Prof. Conjeevaram S. Parmesh
1027.	Prof. Deepa Ravindranathan Nair
1028.	Prof. Dushyant Jaiswal
1029.	Prof. Gagan Prakash
1030.	Prof. Gaurav Narula
1031.	Prof. Gauravi Ashish Mishra
1032.	Prof. Girish Chinnaswamy
1033.	Prof. Goda Jayant Sastri
1034.	Prof. Gouri Himalaya Pantvaidya
1035.	Prof. Gulia Seema
1036.	Prof. Hasmukh Kantilal Jain
1037.	Prof. Jaya Ghosh
1038.	Prof. Jayita Kedar Deodhar
1039.	Prof. Jeson Rajan Doctor
1040.	Prof. Jigeeshu Vasishtha Divatia
1041.	Prof. Jyoti Bajpai
1042.	Prof. Kedar Kamalakar Deodhar
1043.	Prof. Madhavi G. Shetmahajan
1044.	Prof. Mahendra Pal
1045.	Prof. Mahesh Goel
1046.	Prof. Malini Premkumar Joshi
1047.	Prof. Manish Suresh Bhandare
1048.	Prof. Manisha Nandkumar Pawar
1049.	Prof. Manju Sengar

1050.	Prof. Maya Prasad
1051.	Prof. Mukta Ravindra Ramdwar
1052.	Prof. Munita Meenu Bal
1053.	Prof. Murthy Vedang
1054.	Prof. Navin Khattry
1055.	Prof. Nayana Shekar Amin
1056.	Prof. Neha Mittal
1057.	Prof. Nehal Rishi Khanna
1058.	Prof. Nikhil Vijay Patkar
1059.	Prof. Nilendu C. Purandare
1060.	Prof. Nilesh Pandurang Sable
1061.	Prof. Nitin Sudhakar Shetty
1062.	Prof. Pankaj Chaturvedi
1063.	Prof. Papagudi G. Subramanian
1064.	Prof. Poonam K. Panjwani
1065.	Prof. Prabhash Kumar
1066.	Prof. Prachi Sunil Patil
1067.	Prof. Prakash Shetty
1068.	Prof. Prashant Ramesh Tembhare
1069.	Prof. Priti Dhansukhbhai Desai
1070.	Prof. Priya Ranganathan
1071.	Prof. Raghu Sudarshan Thota
1072.	Prof. Rajiv Kumar
1073.	Prof. Reena Zarir Engineer
1074.	Prof. Reshma Ambulkar
1075.	Prof. Sabita Shambhulal Jiwnani
1076.	Prof. Sachin Punatar
1077.	Prof. Sajid Shafique Quresh
1078.	Prof. Sandeep Vivek Gurav
1079.	Prof. Sangeeta Bhikaji Desai
1080.	Prof. Sanjay Biswas
1081.	Prof. Santosh Menon
1082.	Prof. Sarbani Ghosh Laskar
1083.	Prof. Sarin Rajeev
1084.	Prof. Shaesta Abdulaziz Mehta
1085.	Prof. Shailesh Vinayak Shrikhande
1086.	Prof. Shalaka Prakash Joshi
1087.	Prof. Sharmila Anil Pimple
1088.	Prof. Shashank Ojha
1089.	Prof. Sheela Prashant Sawant
1090.	Prof. Sheila Nainan Myatra
1091.	Prof. Shilpushp Jagannath Bhosale
1092.	Prof. Shraddha Patkar
1093.	Prof. Shripad Dinanath Banavali
1094.	Prof. Siddhartha Sankar Laskar
1095.	Prof. Sneha Shah
1096.	Prof. Sohan Lal Solanki
1097.	Prof. Sridhar Epari
1098.	Prof. Subhash Chotelal Yadav
1099.	Prof. Sudeep Gupta
1100.	Prof. Sudhir Vasudevan Nair R.
1101.	Prof. Sumeet Gujral
1102.	Prof. Sumitra Ganesh Bakshi
1103.	Prof. Supriya Jayant Sastri
1104.	Prof. Suyash Sureshchandra Kulkarni
1105.	Prof. Swapnil Ulhas Rane
1106.	Prof. Swapnil Yeshwant Parab
1107.	Prof. Tabassum Abdulwahid Wadasadawala
1108.	Prof. Tanuja Manjanath Shet
1109.	Prof. Tejpal Gupta
1110.	Prof. Vandana Agarwal
1111.	Prof. Vanita Maria Noronha
1112.	Prof. Venkatesh Rangarajan
1113.	Prof. Vijay Maruti Patil
1114.	Prof. Vijaya Prakash Patil
1115.	Prof. Vikas Sureshchand Ostwal
1116.	Prof. Vikram Anil Chaudhari
1117.	Prof. Vinay Kant Shankhdhar
1118.	Prof. Vivek Gajanan Bhat
1119.	Dr. Abhishek Chatterjee
1120.	Dr. Aekta Shah
1121.	Dr. Akshay Dwarkadas Baheti
1122.	Dr. Ameya Dattatraya Puranik
1123.	Dr. Amrita Guha
1124.	Dr. Anjana S Wajekar
1125.	Dr. Anuja Dhananjay Deshmukh
1126.	Dr. Arpita Sahu
1127.	Dr. Asawari Jingonda Patil
1128.	Dr. Bhakti Dushyant Trivedi
1129.	Dr. Chetan Anil Dhamne
1130.	Dr. Gaurav Vijay Salunke
1131.	Dr. Gauri Rohan Deshpande
1132.	Dr. Janu Amit Kumar
1133.	Dr. Katha Nikhil Rabade
1134.	Dr. Kinjalka Ghosh
1135.	Dr. Kunal B Gala
1136.	Dr. Lingaraj Nayak

1137. Dr. Madhavi Dattatraya Desai	1167. Dr. Atanu Bhattacharjee
1138. Dr. Manish Pruthi	1168. Dr. Avinash Rameshrao Pagdhune
1139. Dr. Nandini Sharrel Menon	1169. Dr. Badira Cheriyalinkal Parambil
1140. Dr. Naveen Mummudi	1170. Dr. Dhanlaxmi L. Shetty
1141. Dr. Palak Bhavesh Popat	1171. Dr. Gauri Raman Gangakhedkar
1142. Dr. Poonam Joshi	1172. Dr. Gurukaran Preet Singh
1143. Dr. Prabht Bhargava	1173. Dr. Indraja Devidas Dev
1144. Dr. Pradip Ramdas Chaudhari	1174. Dr. Jifmi Jose Manjali
1145. Dr. Prakash R Nayak	1175. Dr. Kajari Bhattacharya
1146. Dr. Rahul Krishnatry	1176. Dr. Meenakshi Singh
1147. Dr. S. Valpapuram Jamema	1177. Dr. Nivedita Chakrabarty
1148. Dr. Sheetal Vidyadhar Gaikwad	1178. Dr. Nupur Suresh Kenkre
1149. Dr. Shiva Kumar Thiagarajan	1179. Dr. Omshree Shetty
1150. Dr. Sukhada D. Savarkar	1180. Dr. Parthiban K Velayutham
1151. Dr. Sumathi S Hiregoudar	1181. Dr. Prachi Mittal
1152. Dr. Sushmita Rath	1182. Dr. Pratik Chandrani
1153. Dr. Trupti Pai	1183. Dr. Revathy Krishnamurthy
1154. Dr. Uma M Sakhadeo	1184. Dr. Ritu Raj Upreti
1155. Dr. Vasundhara Patil	1185. Dr. Sangeeta Kakoti
1156. Dr. Vidisha Vipin Tuljapurkar	1186. Dr. Shamali Poojary
1157. Dr. Vikas Singh	1187. Dr. Shivakumar Gudi
1158. Dr. Akanksha Chichra	1188. Dr. Shrikant C Raut
1159. Dr. Amandeep Manjit Singh Arora	1189. Dr. Shruti Gairola
1160. Dr. Ameya Rajan Bindu	1190. Dr. Shwetabh Sinha
1161. Dr. Amit Kumar Jayant Choudhari	1191. Dr. Shyam Srinivasan
1162. Dr. Anisha A Navkudkar	1192. Dr. Suchismita Ghosh
1163. Dr. Anuprita Dilip Daddi	1193. Dr. Sudivya Prashast Sharma
1164. Dr. Aparna Katdare	1194. Dr. Sujata Lall
1165. Dr. Archya Dasgupta	1195. Dr. Sumeet Prakash Mirgh
1166. Dr. Ashwini D Rane	1196. Dr. Suryatapa Saha

HBNI at a Glance

During the last academic year (August 1, 2023-July 31, 202) HBNI has awarded 318 Ph.D. degrees. The total number of Ph.D. degrees awarded by HBNI till July 31, 2023 stands at 2351. HBNI also awarded 89 M.Tech., 147 M.Sc., and 157 Integrated M.Sc. degrees in various science disciplines, 63 post graduate & super specialty medical degrees, and 24 diplomas in Radiological Physics (DipRP) during this period. 1039 students have been admitted to different academic programmes during 2023-24, out of which 349 students are for Ph.D. program.

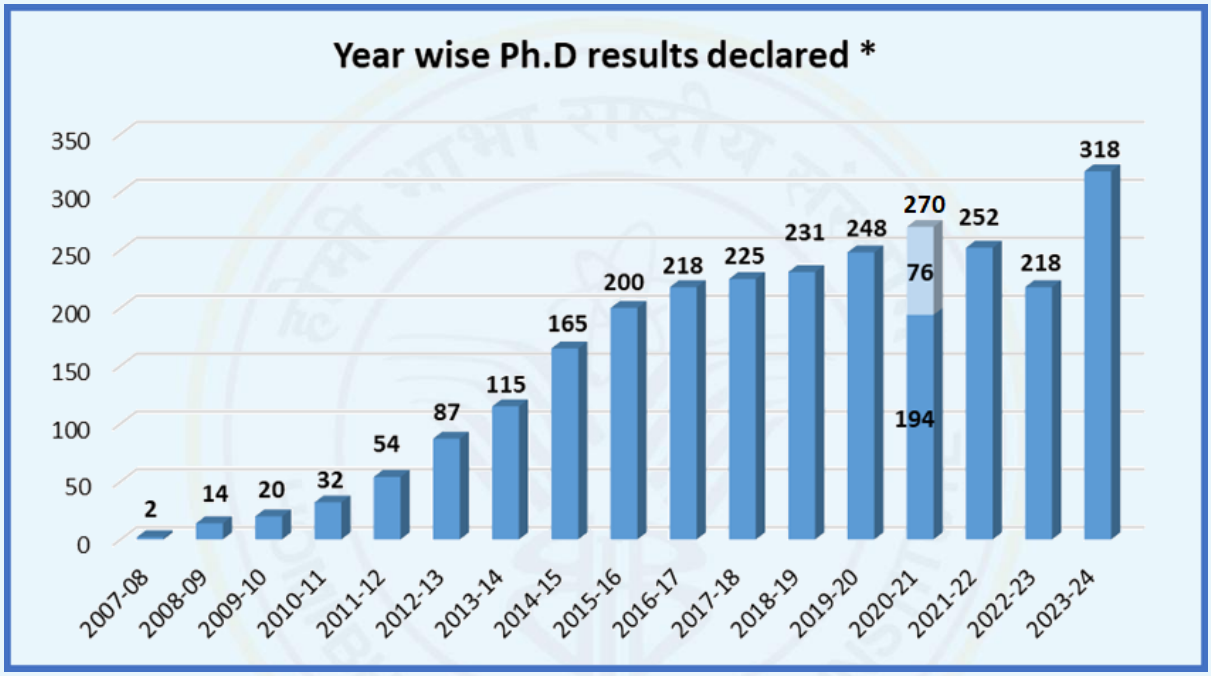

*The data from 2007-08 to 2019-20 is for the period April 1 of preceding year to March 31 of the ending year. The data for 2020-21 is for the period April 1, 2020 to July 31, 2021. Dark blue area (194) gives the data from April 1, 2020 to March 31,2021, light blue area (76) gives the data from April 1, 2021 to July 31, 2021. The data for 2021-22 and 2022-23 is for the period August 1 of the preceding year to July 31 of the ending year.

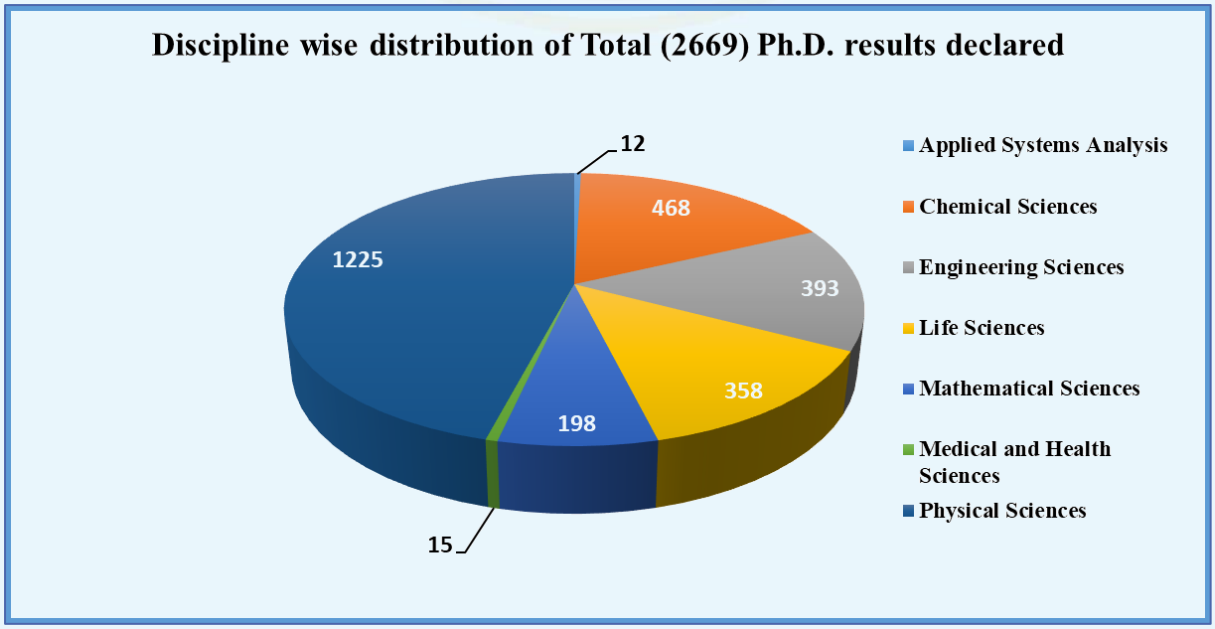

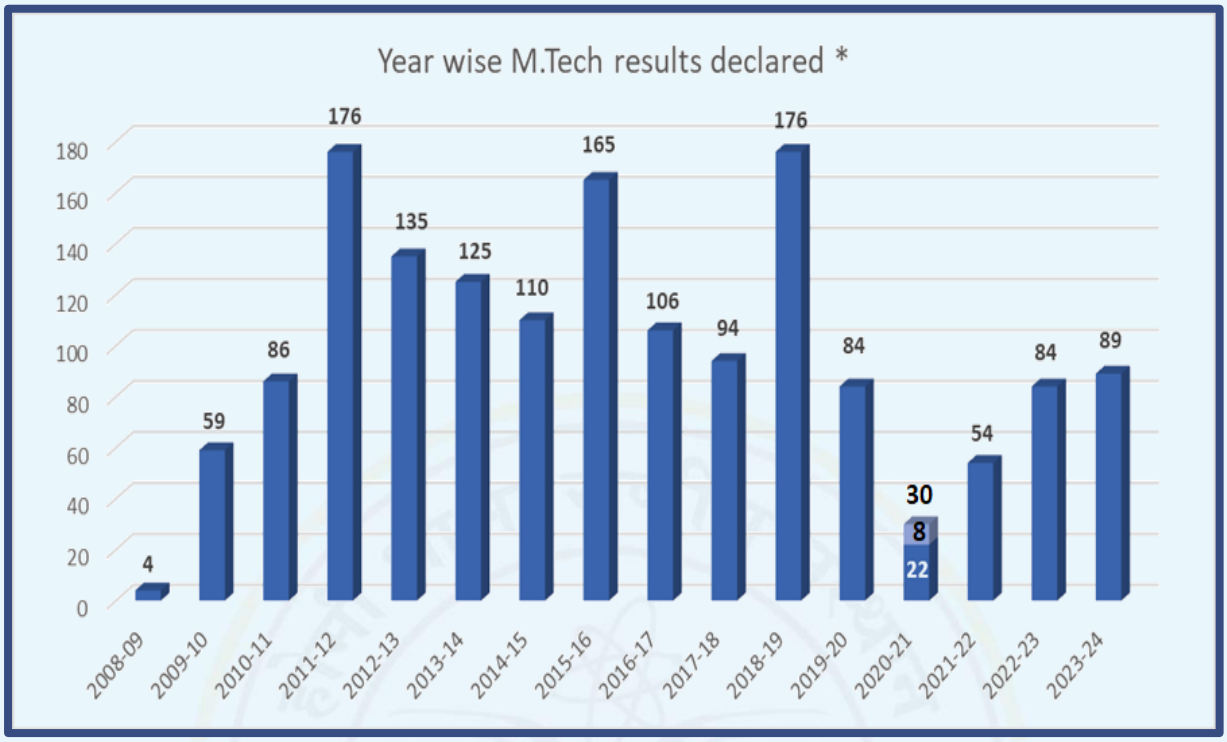

*The data from 2008-09 to 2019-20 is for the period April 1 of the preceding year to March 31 of the ending year. The data for 2020-21 is for the period April 1, 2020 to July 31, 2021. Dark blue area (22) gives the data from April 1, 2020 to March 31, 2021, light blue area (8) gives the data from April 1, 2021 to July 31, 2021. The data for 2021-22, 2022-23 and 2023-24 is for the period August 1 of the preceding year to July 31 of the ending year.

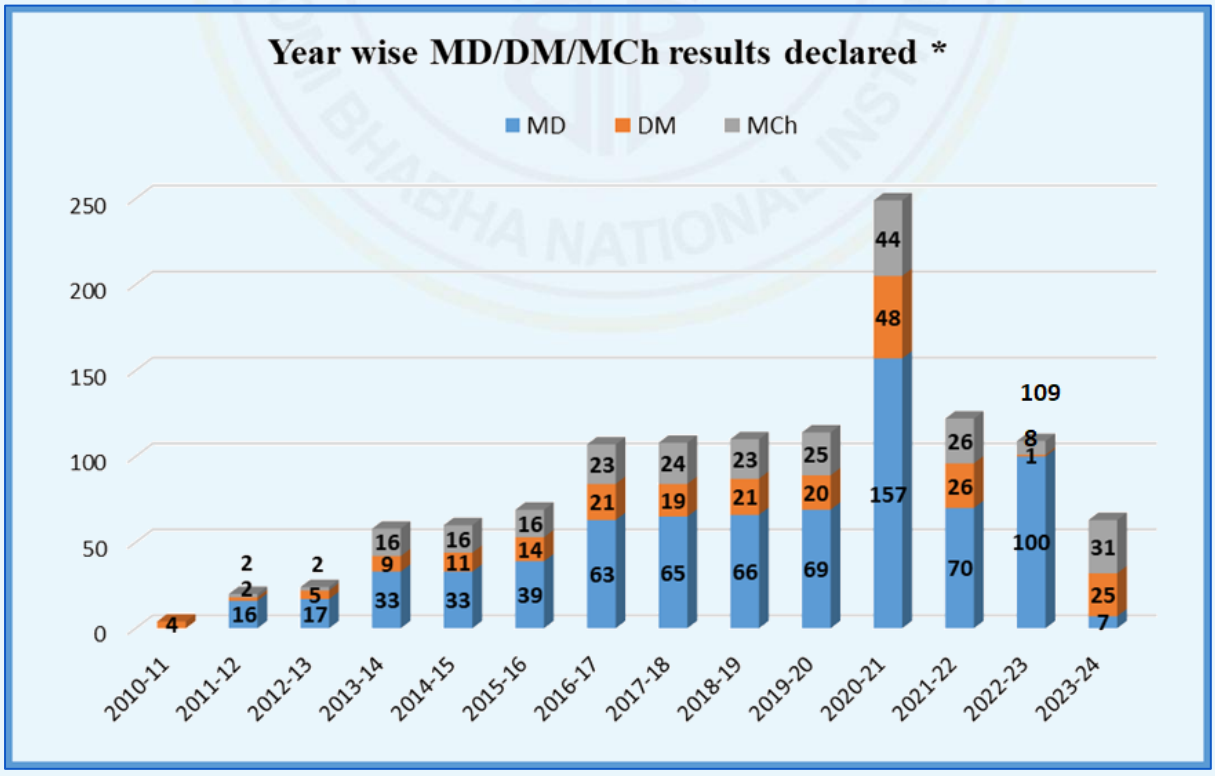

*The data from 2010-11 to 2019-20 is for the period April 1 of preceding year to March 31 of the ending year. The data for 2020-21 is for the period April 1, 2020 to July 31, 2021. The data for 2021-22, 2022-23 and 2023-24 is for the period August 1 of the preceding year to July 31 of the ending year.

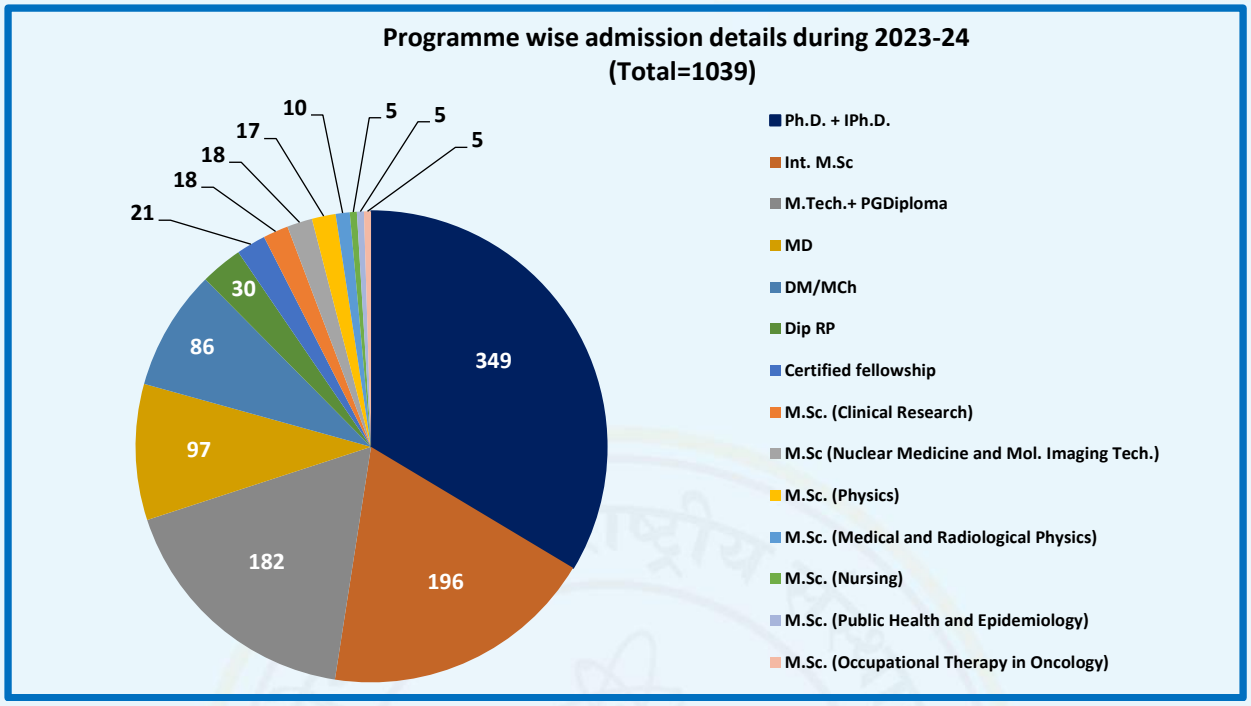

Number of students admitted to different academic programmes of CIs/OCC during August 1, 2023 – July 31, 2024

Academic Programme	BARC	IGCAR	RRCAT	VECC	SINP	IPR	TMC	IoP	IMSc	HRI	NISER	Total
Ph.D. + Integrated Ph.D	57	35	8	7	22	27	47	09	15	20	102	**349**
M.Tech + PG Diploma	154	20	….	….	….	8	….	….	….	….	….	**182**
M.D.	06	….	….	….	….	….	91	….	….	….	….	**97**
Dip RP	30	….	….	….	….	….	….	….	….	….	….	**30**
D.M./M.Ch	….	….	….	….	….	….	86	….	….	….	….	**86**
M.Sc. (Physics)	….	….	….	….	….	….	….	….	….	17		**17**
Integrated M.Sc.											196	**196**
M.Sc. (Nursing)	….	….	….	….	….	….	5	….	….	….	….	**5**
M.Sc (Nuclear Medicine and Molecular Imaging Technology)	6	….	….	….	….	….	12	….	….	….	….	**18**
M.Sc. (Medical and Radiological Physics)	….	….	….	….	….	….	….	….	….	….	10	**10**
M.Sc. (Public Health and Epidemiology)	….	….	….	….	….	….	5	….	….	….	….	**5**
M.Sc. Clinical Research							18					**18**
M.Sc. (Occupational Therapy in Oncology)	….	….	….	….	….	….	5	….	….	….	….	**5**
Certified fellowship	….	….	….	….	….	….	21	….	….	….	….	**21**
Total	**253**	**55**	**8**	**7**	**22**	**35**	**290**	**09**	**15**	**37**	**308**	**1039**

Section II
(Theses at a Glance)

1. Applied System Analysis

During the period of the report, seven doctoral students received Ph.D. degree in Applied System Analysis in the subject Humanities and Social Sciences from Homi Bhabha National Institute. Thesis highlights of some of the selected theses are given below.

1.1 National Institute of Science Education and Research

1.1.1 Sociological Aspects of Sex Reassignment Surgery: An Empirical Study of Lived Experiences of Transgender People in Odisha

The thesis deals with sociological aspects of sex reassignment surgery based on an empirical study of lived experiences of transgender people in Odisha. Among the many socio-economic and psychological challenges, transgender individuals face gender dysphoria. This condition arises when a person's gender identity conflicts with the biological sex assigned at birth, leading to a struggle with gender identity disorder and nonconformity to traditional gender norms. Sex reassignment surgery (SRS) is crucial in alleviating gender dysphoria and achieving gender transition, providing much-needed socio-psychological comfort. The findings of the study described in the thesis highlights the sociological, psychological, and economic issues associated with gender identity disorder. Non-acceptance, exclusion, harassment, and discrimination pervade almost every aspect of their lives, as reported by all study participants. These issues call for a more inclusive and empathetic understanding of the challenges faced by this significant yet small population segment. The study emphasizes the need for a new paradigm focused on harmony rather than control, domination, and fragmented pleasure. The findings reveal that social marginalization and discrimination are major factors influencing transgender individuals to opt for SRS in hopes of greater societal acceptance. The study underscores several policy implications, highlighting the multifaceted discrimination and limited livelihood options faced by this vulnerable population segment.

1.1.2 Esports as a New Age Profession and its Socio-Cultural Appeal in India: A Systemic Inquiry into the New Normative Practice in Operational Working Hours

The thesis talks about Esports which is a billion-dollar industry projected to reach a spectatorship of 640 million by 2025, making it a popular career choice among teens and young adults. Despite having the world’s largest youth population and the fifth largest economy (both promising grounds for esports), India’s esports industry is underdeveloped. Forty-one Indian professional gamers (pro-gamers) were interviewed to determine what factors are holding back the growth of esports in the country. Theoretically, pro-gamers can be positioned as liminal agents working in the confluence of work and leisure in the esports platform, expending immaterial labour in today’s neoliberal-digitized economy. They are

knowledge workers, innovative rebels, set on an unconventional career path who redefine work & life in contemporary times. Respondent narratives illuminate the difficulties of pursuing an esports career in India rooted in techno-economic, sociocultural-political, and psychological challenges. The best way for India to establish itself in the esports industry would be to learn from other nations' successes and implement a localized approach uniquely suited to India's demographic and cultural makeup.

1.1.3 Social Contexts of Solid Waste in Urban Households: Uncovering the Practices of Waste Segregation and Littering in Bhubaneswar

The thesis attempts to study the social aspect of municipal solid waste in urban space and uncover the linkages, conflicts, and power relations between economic, political, and social components of the solid waste management issue in Bhubaneswar, India. The study explored household level waste segregation, association of socio-demographic factors with nature and volume of waste generation, factors influencing littering and to deep-dive into the existing policies on waste management through the lens of political ecology and actor-network theories. Relevant data obtained through household survey, semi-structured interview with key informants, observation: participant and non- participant, and ethnography were analyzed appropriately to generate meaningful insights pertaining to solid waste management issues in the Indian city of Bhubaneswar. The study found an association of socio-demographic factors with the nature and volume of waste generated across households. Lack of availability of dustbins, laziness, and habits were primary factors of littering. Swachh Bharat Abhiyan, as a policy, has not been adequate to reduce household littering because of non-acknowledgment of the responsibility for waste generated and the political benefits involved.

2. Chemical Sciences

During the period of the present report, 55 research fellows have received their Ph.D. degrees in Chemical Sciences from Homi Bhabha National Institute (HBNI). Quite diverse areas of research work have been carried out in these Ph.D. theses, as have been the case in every year since the inception of this Institute. The highlights of some of the selected Ph.D. theses in Chemical Sciences are given below.

2.1 Bhabha Atomic Research Centre, Mumbai

2.1.1 Design, Synthesis and Characterization of Molecular Precursors for Metal Chalcogenide Materials and their Energy Applications

Metal chalcogenides constitute an important class of semiconductor materials. Among these, the Cu, Ag, In and Sn based binary chalcogenide are the emerging members of this family of the materials, due to their earth abundant, low cost and environmental benign characteristics. These chalcogenides offer a wide range of unique chemical and physical properties, which have been exploited for diverse applications such as photovoltaics, thermoelectric devices, Li-ion batteries, photocatalysis, etc. Accordingly, various methods have been used for the preparation of the respective metal chalcogenide nanomaterials. However, the advantages of the metal-organic precursor route over other methods and its limited exploration in case of these chalcogenides prompted us to design novel precursors and investigate their utility for the preparation of the metal chalcogenide nanostructures.

The present research work deals with the synthesis and characterization of novel air stable complexes of Cu, Ag, In and Sn, with various internally functionalized chalcogenolate ligands. Molecular structures of the complexes have been unambiguously established by SCXRD and hetero nuclei NMR spectroscopy. TGA have also been used to study their decomposition pathways. The complexes have been explored as molecular precursors for the preparation of binary metal chalcogenides. The facile cleavage of C-E bond in these complexes makes them as the versatile precursors for the preparation of nanostructured metal chalcogenides. The phase purity, morphology, composition, and band gap of the prepared nanostructures have been investigated by p-XRD, electron microscopic (SEM, TEM and EDX) and spectroscopic (Raman and DRS) techniques. Utilization of these precursors presents a robust synthetic route, demonstrating a control over the composition, phase characteristics and band gap of the chalcogenide nanostructures synthesized thereby through the introduction of subtle variations in the precursor structures, reaction temperature, growth duration and proper choice of high boiling solvent. Application of these nanomaterials in PEC solar cells and as the anodes in the Li-ion battery results in the nice electrochemical performance. The knowledge from the present thesis can be used for the large-scale preparation of technologically

important metal chalcogenide nanomaterials without involving toxic and sensitive chemicals for practical applications, especially as the materials in solar cells.

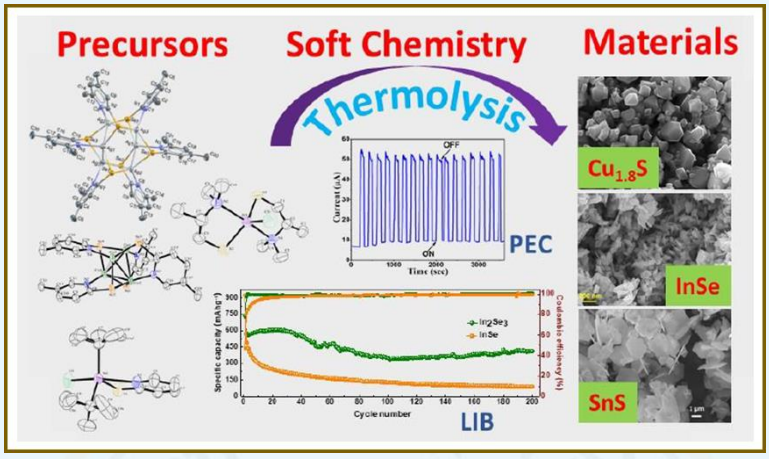

Schematic representation of utility of molecular precursor in the preparation of nanostructures for solar cell and battery

2.1.2 Electrochemical Determination and Recovery of Uranium and Plutonium in Aqueous Medium

For the safe and long-term operation of nuclear reactors, the fissile content [Uranium (U) + Plutonium (Pu)] in the fuel must be maintained at a fixed level. For this purpose, accurate and precise analytical techniques are required. Many destructive and nondestructive analytical techniques are available to the analysts for determination of U and Pu in nuclear fuel samples. Among these, the redox titrimetry is more favored on account of operational simplicity, less analysis time, low-cost equipment and high accuracy and precision. This technique is routinely employed for nuclear sample analysis. Despite several advantages of redox titrimetry, the method generates laboratory analytical waste solutions having impurities such as iron (Fe), chromium (Cr), silver (Ag), and titanium (Ti), which are added during titration and makes the recovery of U and Pu cumbersome. The aim of the research work was to develop a simple voltammetric method for simultaneous determination of U and Pu in nuclear samples for routine analysis. The present technique produces analytical waste that is free from metallic impurities. However, coupled chemical reactions of U(IV) and Pu(IV) at the electrode surface cause inconsistency in the U(VI) reduction current and makes voltammetry unsuitable for simultaneous determination of U and Pu. Hence, developing a voltammetric technique for the simultaneous determination of U and Pu for nuclear samples is a challenging task. Besides, the redox titrimetry employed for determination of U and Pu lead to both unanalyzed waste (U and Pu) and analyzed waste (U, Pu, Fe, Cr, Ag, Ti) in acidic medium. Because of the strategic importance of Pu and the hazardous and toxic nature of Pu and U, they must be recovered completely from these analytical waste solutions before their final disposal. Conventional method for Pu recovery (precipitation/ion exchange) involves complicated steps, generates large volume of secondary waste, and leads to radiation dose to the working personnel. Therefore, the aim of the thesis was to develop a simplified electrochemical method to

recover U and Pu separately as UO_2/U_3O_8 and PuO_2, respectively, just by varying the electrode potential and thus to substitute the routinely employed precipitation or ion exchange method. On this ground, a few electrochemical strategies were developed for simultaneous electrochemical determination and recovery of U and Pu in aqueous medium containing 1 M H_2SO_4 using PEDOT-PSS/GC electrode for FBTR fuel samples. This method is selective for FBTR samples only for which [Pu]/[U] >2. For nuclear samples having [Pu]/[U] < 2, the above method was modified and observed that the coupled chemical reactions of U(IV) and Pu(IV) were ceased at 5 M H_2SO_4. Hence, the simultaneous voltametric determination of U and Pu was possible on PEDOT-PSS/GC, irrespective of the [Pu]/[U] ratio. It was also observed that low acidity of nitric acid helps to detect very low levels of U on a PEDOT-PSS/GC electrode. A new electrochemical approach was demonstrated for selective electrochemical recovery of U in the presence of interfering lanthanide ions in aqueous medium on PEDOT-PSS/Pt electrode. A two-step approach to recover Pu from real carbonate waste containing different fission products and radiolytic and hydrolytic degradation products of TBP was demonstrated. A simple two step electrochemical method was also demonstrated for the recovery of Pu and U as potassium plutonium(III) sulfate and potassium uranium(IV) sulfate solid from real aqueous acidic waste solutions generated in the chemical quality control labs in a nuclear facility.

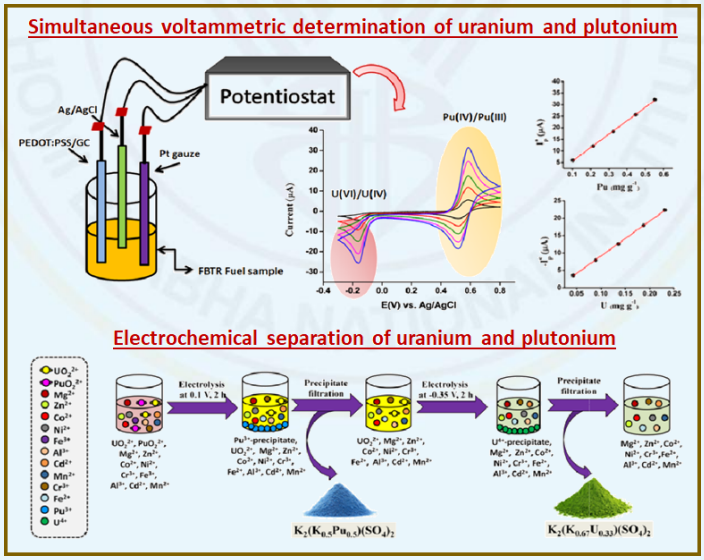

Electrochemical determination and recovery of uranium and plutonium in aqueous medium

2.1.3 Physicochemical and Biological Evaluation of Organic–Inorganic Nanostructures for Cancer Therapy

One of the challenges in cancer chemotherapy is the low target to non-target ratio of therapeutic agents which incur severe adverse effect on the healthy tissues. In this regard, nanomaterials have tremendous potential for impacting cancer therapy by altering the toxicity profile of the drug. Some of the striking advantages provided by the nanocarrier mediated targeted drug delivery are, relatively high build-up of drug concentration at the

tumor site, improved drug content in the formulation and enhanced colloidal stability. The thesis deals with the development of new surface functionalized nanostructured materials for advanced cancer therapeutics and diagnostics. A series of soft nano-assemblies such as PEGylated vesicles, magnetic nanoparticles and organic-inorganic hybrid nanostructures were demonstrated for specific applications in the area of targeted therapy and diagnostics. All the developed formulations were well characterized using DLS, zeta, XRD, TEM, Cryo-TEM, SANS, SAXS, FTIR, VSM, TGA measurements. The in-house developed cost effective PEGylated liposomal doxorubicin nanoparticles have shown tremendous potential in both in-vitro as well as in-vivo studies in both syngeneic and xenograft model. The curcumin loaded PEGylated lipid nanoparticles have shown selective induction of apoptosis to lung cancer cell lines with minimal normal tissue toxicity. The tartaric acid coated particles (TMNCs) were designed to act as a single platform theranostic platform for obtaining chelator free bimodal (MRI/SPECT-CT) imaging with combinatorial chemo-thermal therapeutic efficiency in human breast carcinoma. It has shown a very high T2 (r2=171 $mM^{-1}s^{-1}$) contrasting ability than the FDA approved ferumoxides (r2=120 $mM^{-1}s^{-1}$) and ferumoxtran (r2=65 $mM^{-1}s^{-1}$) as MRI contrast agents.

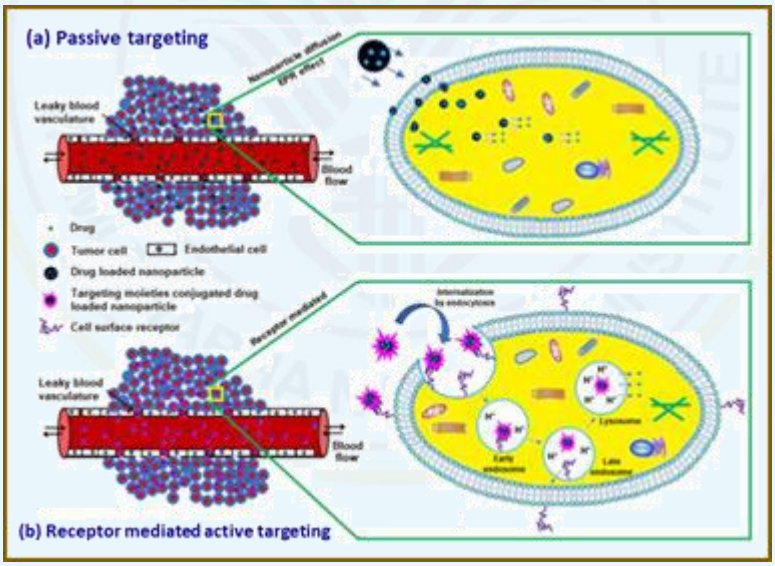

Schematic showing (a) passive targeting through EPR effect and (b) receptor mediated active targeting

Three sets of Fe_3O_4 based nano-formulations were also developed with dual drug loading capacity (Curcumin & Doxorubicin, Doxorubicin & Methotrexate and Doxorubicin and Nitric oxide) with enhanced cancer cell killing efficacy with reduction in multidrug resistance. Novel methodology has been devised to impart shape selectivity during the formation Fe_3O_4 nanoparticles (Cubic shape). A highly stable micellar based nano-formulation of curcumin was also designed to load as high as 50 mg/mL of curcumin for nasal drop application (which is still stable even after 5 years of preparation). So far, this nano-formulation has been transferred to three companies as technology transfer document. Thus, the reported work in

the present thesis highlights the application of organic-inorganic nanocarriers for the affordable treatment of cancer.

2.1.4 Preparation, Characterization and Efficacy Evaluation of Protein Nano-Carrier/Gel-based Drug Delivery Systems for Therapeutic Applications

The thesis demonstrates a green method of thermal denaturation involving pluronic and a modified chemical cross-linking method involving dithiothreitol (DTT) for the synthesis of protein nanoparticles in the size range of 25-250 nm with spherical morphology. The nanoparticles were characterized employing all the relevant photophysical and biochemical techniques and studied for their interaction with anticancer drugs like curcumin, DOX and IRI. After optimizing the loading of anti-cancer drugs within protein nanoparticles, the formulation was evaluated for drug delivery parameters by monitoring release kinetics, cellular uptake, *in vitro* cytotoxicity and *in vivo* pharmacokinetics and efficiency. The results established that the particle size of ~125 nm and hydrophilic lipophilic balance of ~22 is optimal to achieve maximum intracellular delivery of payload through albumin and gelatin based nanocarriers. The formulation designed for passive targeting of DOX exhibited a higher availability of the drug in plasma as compared to that in the nonspecific organs and showed better efficacy as compared to plain drug in murine fibrosarcoma tumor model. IRI-GNP-F, the folic acid conjugated active formulation of IRI demonstrated significantly higher efficacy in the folate receptor (FR) positive-cancer cell line (HeLa). Lastly, curcumin loaded gelatin-F127-lipid nanogel exhibited accelerated wound healing in animal studies due to the release of curcumin in the form of vesicles. The data presented in this thesis has addressed some of the fundamental problems related to drug delivery applications, such as understanding the role of size, hydrophobicity, and presence of homing ligand in controlling the cellular uptake of drug loaded protein nanoparticles at the target sites.

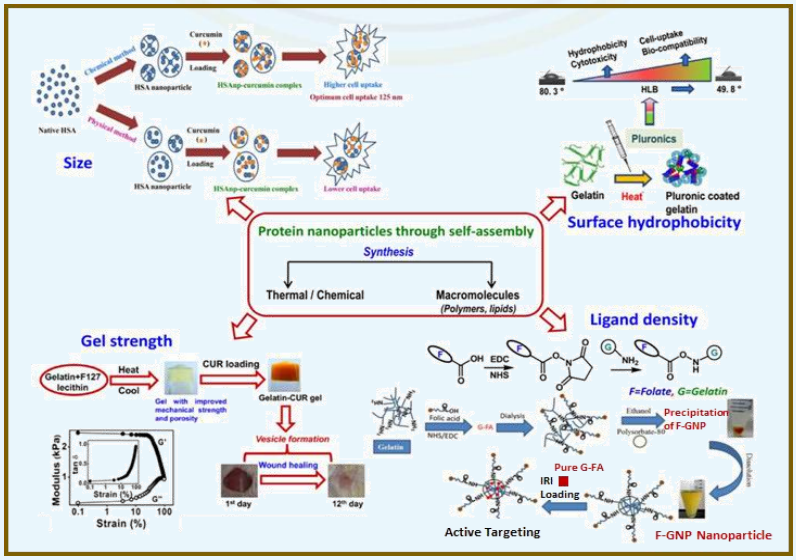

Schematics of the protein nanoparticle synthesis through self-assembly, their characterization

2.1.5 Development of Radiolabeled Peptides and Peptide-Drug Conjugates for Diagnostic Imaging and Targeted Radiotherapy of Cancerous Lesions

Breast cancer has the highest global incidence amongst all the cancer types. Early detection of breast cancer is the key for timely intervention and proper treatment planning. Human epidermal growth factor receptors (HER2) are over-expressed in breast cancers and are associated with poor prognosis and aggressively metastatic disease. The present thesis focused on development of HER2-targeting ligands for breast cancer detection and therapy. Towards this, peptides exhibiting attractive advantages of high target affinity, specificity, favorable pharmacokinetics, and ease of synthesis were chosen as suitable ligands. A HER2-targeting A9 peptide was subjected to several modifications (PEGylation, cyclization, D-amino acid incorporation, retro variant) to overcome the challenges of in vivo enzymatic degradation. The peptides were synthesized by solid phase synthesis methodology manually and purified and characterized. Peptides were then radiolabeled with theranostic radionuclide, $^{177}LuCl_3$. Lu-labeled original A9 peptide exhibited rapid blood clearance resulting in low tumor uptake. It also underwent high metabolic degradation. The pegylated variant, [^{177}Lu]Lu-DOTA-PEG4-A9 demonstrated improved metabolic stability, tumor uptake and retention. Further the peptide was cyclized on resin by copper (I)-catalyzed azide-alkyne cycloaddition (CuAAC) 'click reaction.' The cyclic variant [^{177}Lu]Lu-DOTA-c[Tz]-A9 exhibited increased binding affinity towards HER2-positive cells, high metabolic stability and tumor uptake. To introduce changes in the backbone all the L-amino acids were replaced by D-amino acids and thus inverso- and retro-inverso A9 peptides were synthesized. These peptides had enormously enhanced metabolic stability, tumor uptake/retention was observed to be higher for the retro-inverso variant. Another analogue studied was the retro-variant where the C- and N-terminal were swapped and the amino acids were arranged in reverse manner. The retro variant showed most promising results with highest tumor uptake amongst the six investigated A9 analogs.

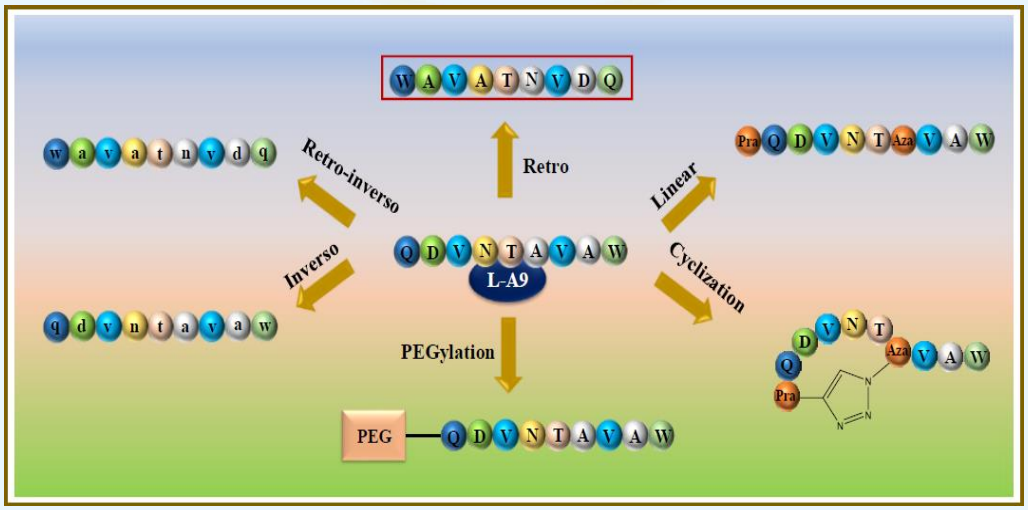

Different A9 peptide analogs investigated in this thesis.
Best analog, Retro A9, is indicated in the box

2.2 Indira Gandhi Centre for Atomic Research, Kalpakkam

2.2.1 Rational Design of Non-Precious Metal and Carbon Based Electrocatalysts for Oxygen Reduction Reaction

A fuel cell (FC) can be a safer alternative among the existing approaches towards the hydrogen management/mitigation issues associated with the nuclear industry. Current fuel cell (FC) technology relies on the precious metal (Pt) based electrocatalysts for hydrogen oxidation (HOR) and oxygen reduction reactions (ORR), taking place at the anode and cathode, respectively. Pt based electrocatalysts limit the wide commercialization of the technology, especially owing to the high cost and scarcity of this precious metal. The ORR being over 10^6 times slower than that of HOR, the design of the active and stable non-precious metal based electrocatalysts is very essential.

In the present work, developments and evaluation of various non-precious metal based electrocatalysts have been presented. The electrocatalysts thus developed include Y single-atom catalyst (SAC), Co SAC, Mn SAC, and the ionic liquid modified Co-encapsulated N-doped carbon nanofiber (Co@NNCNF-IL) based catalysts. These catalysts were synthesized from low-cost chemicals through easy synthetic routes. Developed catalysts were characterized by various techniques to decode their structure-function relationship and their ORR performance in alkaline and acidic medium, to demonstrate the potential catalytic performances of these developed materials. In summary, the development of low-cost alternatives to commercial Pt/C electrode were expected to contribute to the goal of wide implementation of fuel cell technology.

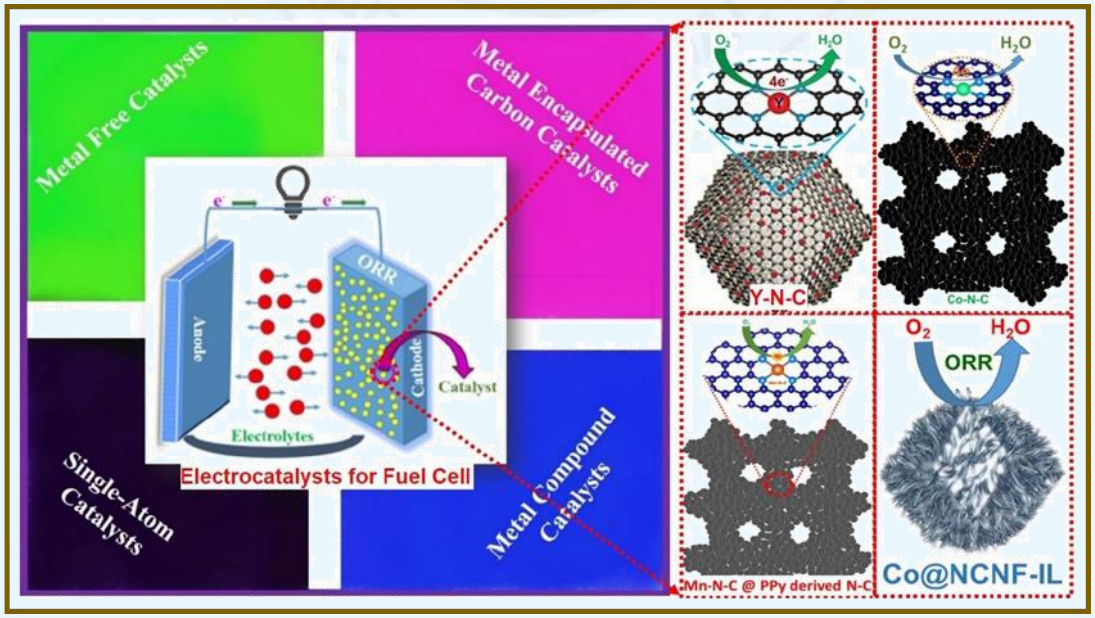

Design of non-precious metal and carbon based electrocatalysts for oxygen reduction reaction

2.2.2 Experimental Investigation of Phase Equilibria, Phase Stability and Thermo-Physical Properties of Zr & U-based Alloys

The principal objective of the present investigation is to generate experimental data in support of the development of fuel and structural materials for future Indian fast reactors. In-depth knowledge of phase equilibria, phase stability, phase transformation, crystal structure, micro-structural evolution, and thermo-physical properties of fuel and clad materials serve as useful inputs in the design of the fuel elements as well as in predicting their performance under normal and off-normal reactor operating conditions. The solidus, liquidus, and invariant equilibria serve as the useful inputs for optimizing their phase diagrams by using the CALPHAD method. Zr-based alloys find extensive applications in the development of such materials because of their desirable high-temperature mechanical properties, combined with their low absorption cross-section for thermal neutrons. Al-U plate-type fuel with Al clad is being used in research reactors all over the world. U-based Cr-U alloy is extremely important from the view point of fuel-clad chemical interaction (FCCI).

The research work in the thesis presents the results of the detailed investigations carried out on the phase equilibria, phase stability, and thermo-physical properties of the Zr- and U-based binary systems, namely, Al-Zr, Sn-Zr, Fe-Zr, Cr-Zr, Cr-U & Al-U. A variety of experimental techniques, namely, differential thermal analysis (DTA), differential scanning calorimetry (DSC), the spot technique (thermo-optometry), X-ray diffraction (XRD), high temperature X-ray diffraction (HTXRD), scanning electron microscope (SEM), and EDX have been used in the present investigation. In addition, the thermal expansivity and heat capacity of some of the alloys have also been investigated. An attempt has been made to interpret the thermo-physical data with a suitable model. DSC has been used as the major experimental technique to study the high-temperature phase stability and thermal properties of the studied alloys.

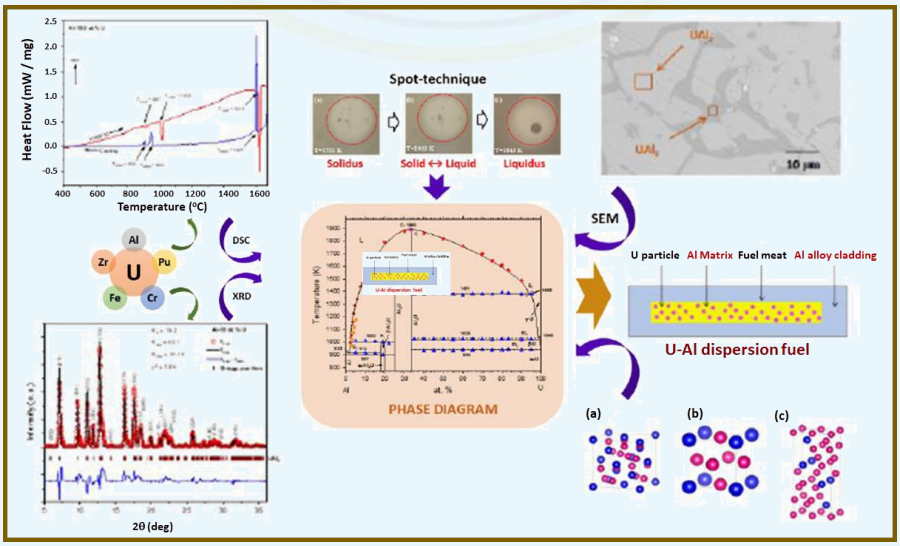

Phase equilibria, phase stability, and thermo-physical properties of Zr and U-based binary systems

2.2.3 Luminescence Properties of Lanthanides and Uranium doped Borophosphate Glasses

The work presented in the thesis emphasizes the development of borophosphate and lanthanide loaded analogues of borophosphate glasses (BPG) for the immobilization of radionuclides. The thesis extensively focuses on the spectroscopic characterization and photoluminescence (PL) studies of RE^{3+} (RE = Ce, Gd, Dy, Eu, Nd, and Pr) and uranyl ion in the studied BPG. These glasses support high solubility of lanthanides and uranium ion, indicating their potential for efficient waste immobilization. Additionally, the studied BPGs demonstrate excellent thermal stability and glass-forming ability, making them suitable for long-term storage of waste materials. Moreover, the low-temperature process required for vitrification and the minimal volatilization of the dopants during the vitrification process contribute to the reduced secondary waste generation. the thermal and chemical stabilities observed with the prepared BPGs further support their suitability for nuclear waste immobilization. The BPGs that are devoid of the crystalline phases were investigated to find out their PL properties, keeping in mind the spectroscopy-based characterization of the waste-loaded glass matrices in actual practices/applications, using such a nondestructive characterization technique. The low phonon energy of these matrices enables the high-intensity emission even at low dopant concentrations (0.1 mol%), which is beneficial for qualitative assessment of the vitrified materials. The luminescence properties provide valuable insights towards the site symmetry and the local environments of the dopant ions. The PL studies contributed in understanding the stability of the hexavalent uranium ion within the glass matrices. Furthermore, the analysis of the excitation, emission, and PL lifetime allows to achieve a comprehensive understanding of the energy transfer mechanism between the dopant ions.

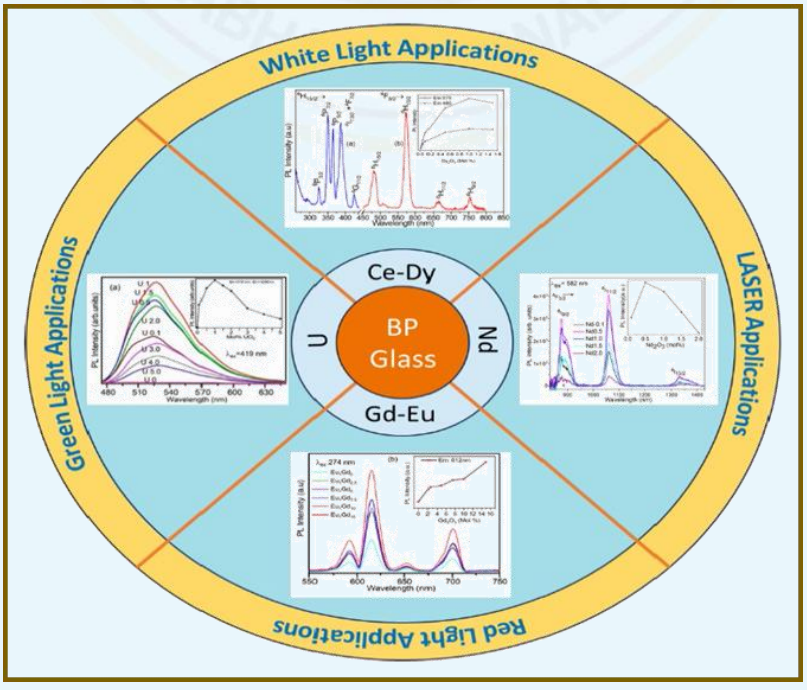

Luminescence properties of lanthanide and uranium doped BP glasses and their applications

This insight enhances our knowledge of the interaction and dynamics within the glass systems. Collectively, these findings highlight the suitability of the prepared glasses for various applications, such as qualitative assessment of vitrified matrices, understanding the stability of uranium ion in the matrices, and elucidating the energy transfer mechanisms between dopant ions. The study contributes to the broader understanding of the optical and luminescent properties of these BPG materials, supporting their potential uses in a range of optical and photonic applications.

2.2.4 Studies Pertaining to Direct Electrochemical De-oxidation of Solid Metal Oxides in Molten $CaCl_2$

Molten salt electrolysis is one of the most widely used electrometallurgical methods for metal production. The direct oxide electrochemical reduction (DOER) process is a novel molten salt-based electrolytic method for directly converting solid metal oxides to metals and alloys. The metal oxide, configured as cathode, is reduced to the respective metal in the solid state either by electron, popularly known as the Fray-Farthing-Chen (FFC) Cambridge process (electro-deoxidation) or by in situ electro-generated reductant metal, e.g., Ca, which is also called the Ono-Suzuki (OS) process (electro-calciothermic reduction) under the application of a suitable potential between the cathode and a graphite anode in $CaCl_2$ based melts. In the present study, experiments were conducted to understand the mechanistic aspects of the influence of moisture and hydrolysis products like $Ca(OH)_2$ on the electrochemical behavior of $CaCl_2$ melt, which is highly hygroscopic, using transient electroanalytical techniques, viz., cyclic voltammetry (CV), semi-integral voltammetry, and electrochemical impedance spectroscopy (EIS) at 900 °C. Direct electrochemical reduction of solid ThO_2, a highly thermodynamically stable and electrically non-conducting oxide, to Th metal in $CaCl_2$ and $CaCl_2$-CaO (0.5 wt.%) melts at 900 °C was demonstrated for the first time in this study. Electro-calciothermic reduction experiments conducted with NiO and ThO_2 pellet cathodes and platinum coil anode in $CaCl_2$–CaO (1 wt.%) melt at 900 °C, exhibited the feasibility of metallization without any product contamination. The electro-deoxidation of mixed ThO_2- NiO (7:3 molar ratio) and ThO_2-Fe_2O_3 (7:1.5 molar ratio) to Th_7Ni_3 and Th_7Fe_3 intermetallic compounds, respectively, was demonstrated for the first time in $CaCl_2$ melt at 900 °C.

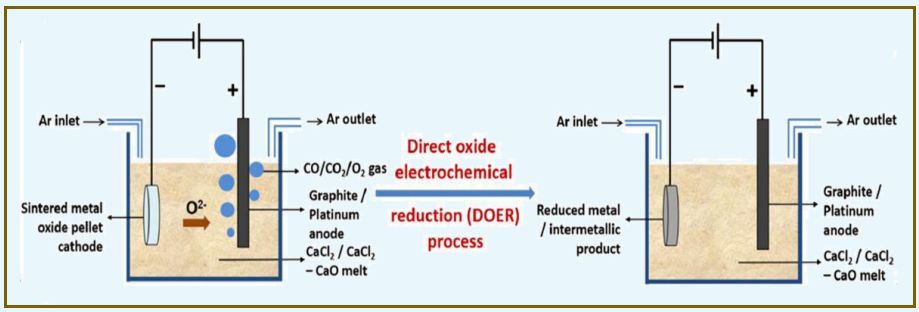

Direct oxide electrochemical reduction (DOER) process for metal/intermetallic compound preparation in molten $CaCl_2$ based electrolytes

2.2.5 $AlCl_3$ Assisted Conversion of Uranium and Lanthanide (Sm, Nd, Pr, Ce and La) Oxides to their Corresponding Chlorides in Molten LiCl-KCl Eutectic for Pyrochemical Reprocessing

In electrorefining step of pyrochemical reprocessing of metallic fuel, LiCl-KCl-UCl_3 (6 wt.%) is used as the electrolyte. Spent fuel is dissolved in molten LiCl-KCl salt with addition of $CdCl_2$ at 773 K. Moisture and oxygen impurities convert chlorides of actinides and fission products present in LiCl-KCl melt to their respective oxides and oxychlorides, which decrease the efficiency of the electrorefining process. Thus, conversion of actinide oxides to their corresponding chlorides is an important step for pyrochemical reprocessing. The research work presented in this thesis aims to convert a representative of actinide oxides, i.e., UO_2 to UCl_3 in LiCl-KCl melt at 773 K. Conversion reactions were carried out with Sm_2O_3 as the representative of lanthanide oxides in LiCl-KCl melt. Further, investigations were also carried out to study the influence of lanthanide (Nd, Pr, Ce and La) oxides on the conversion efficiency of UO_2. $AlCl_3$ and Al metal were used in the conversion of UO_2 to UCl_3 in LiCl-KCl melt at 773 K. $AlCl_3$ was also used to convert lanthanide oxides to their respective chlorides.

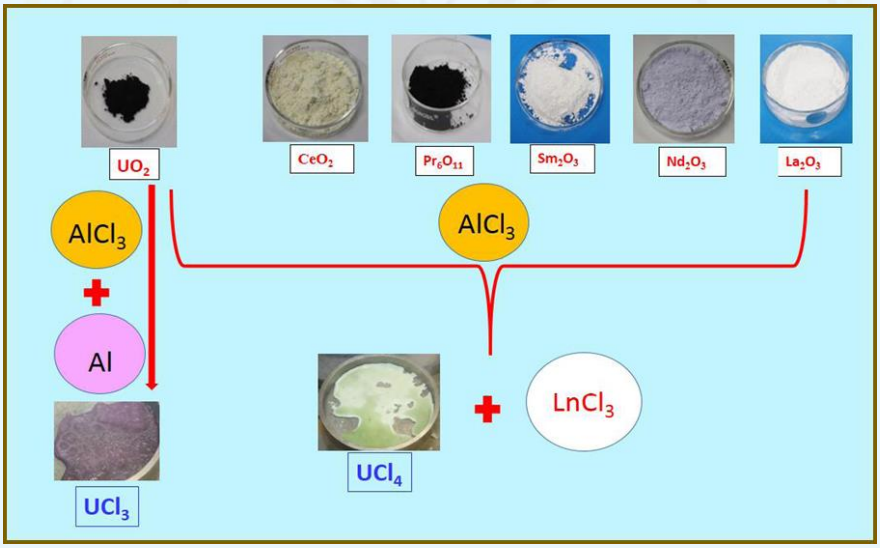

Conversion of UO_2 and lanthanide oxides to their corresponding chlorides using $AlCl_3$ and Al metal in the LiCl-KCl melt at 773 K

2.3 National Institute of Science Education and Research (NISER), Bhubaneswar

2.3.1 Thioketone and Pyrazole based Luminescent Boron Compounds: Synthesis, Characterization and Photophysical Properties of Poly(indazaboles)

The present thesis deals with the synthesis, characterization, and applications of new S,O-chelated and N,O-chelated boron compounds, and also those of the N,N fused boron polymers. A series of S,O-chelated thioketone-based tetra-coordinated boron compounds

were synthesized and their optical, electrochemical properties, and DFT studies were carried out systematically. These compounds showed potential applications as the semi-conductors (electron mobility of 0.003 cm2V-1S-1), single component photo-detector (responsivity up to ≈ 6 mAW-1), non-linear optical materials, TADF emitters and reversible ON/OFF sensors in the detection of cyanide ions. Similarly, a series of N,O-chelated pyrazole-based tetra-coordinated boron compounds were synthesized and their usages as the chemo-sensor for the detection of picric acid. The propeller structure of these molecules showed good aggregation-induced emission properties useful for practical applications. In the present thesis work, indazole-based organo-boron main chain polymers were synthesized and characterized, and their optical properties and thermal stability were investigated aiming their potential applications.

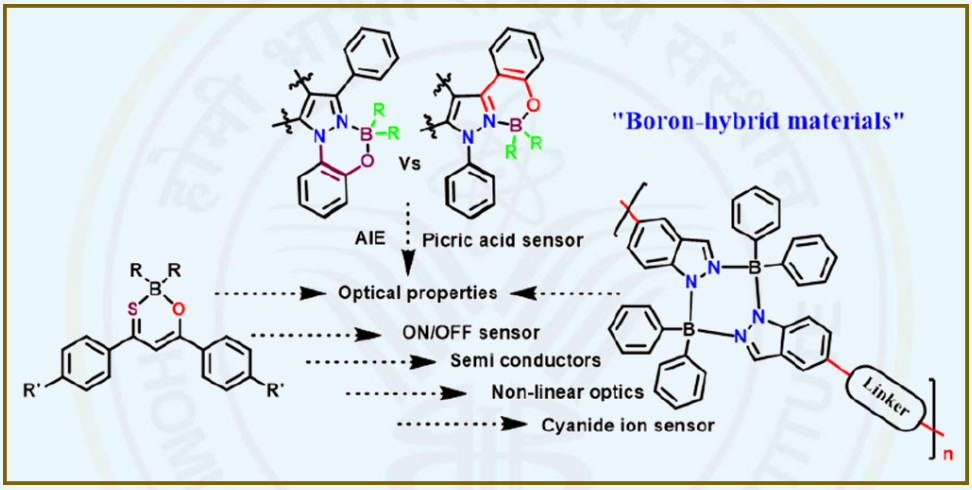

Thioketone and pyrazole based luminescent boron compounds investigated in the thesis

2.3.2 Molecular Zinc(I) Dimers, Zinc (II) Hydrides, and Cations: Synthesis, and Catalytic Applications with Mechanistic Insights

Zinc is a less expensive, nontoxic, and abundant element on the earth's crust than other precious transition or lanthanide elements. Thus, zinc-based systems have attracted immense interests for their uses as the catalysts in different chemical reactions. Present thesis reports the synthesis of conjugated bis-guanidinate (CBG)-stabilized zinc-based complexes and evaluates their applications in catalysis processes. Detailed mechanistic insights have been investigated by isolating the key intermediates of these CBG-stabilized zinc-based complexes. At first, CBG supported Zn(I) dimers, Zn(II) hydrides, and the corresponding cations were isolated and thoroughly characterized. Subsequently, Zn(I) dimers were employed as the pre-catalysts for the C-H borylation of terminal alkynes. Additionally, the CBG zinc(II) hydride complex was used for the hydro-functionalization of ketones and the chemo-selective hydroboration of isocyanates. Moreover, the chemo-selective reduction of nitriles and isonitriles and 1,2-regioselective hydro-functionalization of N-heteroarenes were also demonstrated by using the zinc hydride species as the catalysts. Further, neutral, and cationic

CBG-stabilized zinc alkyls, halides, and hydride complexes were employed as the catalytically active species in the cyanosilylation reactions. Furthermore, various stoichiometric experiments were also performed, and the key intermediates were isolated to propose/substantiate the most probable catalytic cycles/mechanisms. Overall, the thesis provides an excellent guideline for the designing of effective zinc-based catalysts, achieving the difficult organic transformations, and understanding the details of the reaction mechanisms.

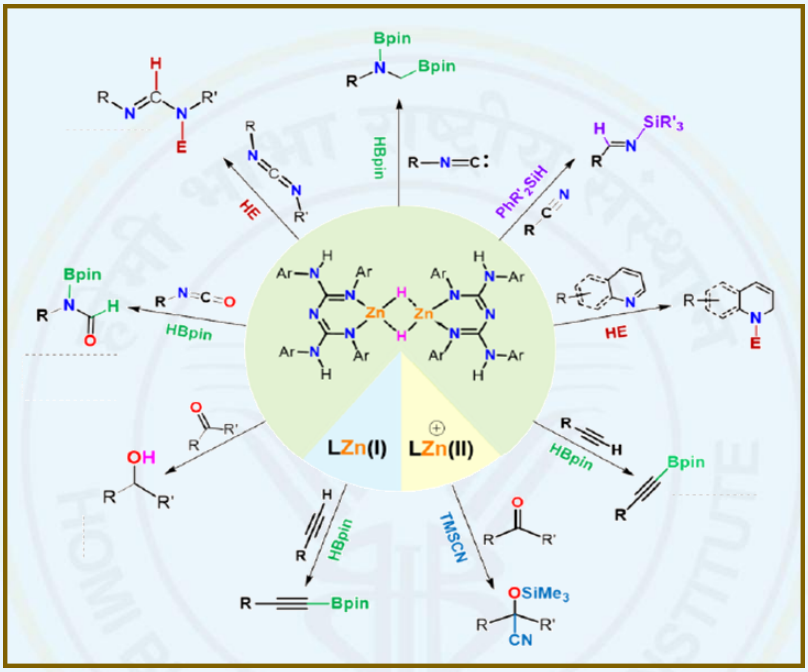

Zinc catalyzed reduction of unsaturated organic functionalities

2.3.3 Weak Chelation Assisted C-H Bond Activation via Cobaltacycles: A Sustainable Approach towards the Synthesis and Functionalization of N-heterocycles

The transition metal-catalyzed C-H bond functionalization strategy has opened a wide range of opportunities to develop organic transformations in a step and atom-economical manner. Earth-abundant 3d transition metals further translate these transformations into a cost-effective and ecofriendly approach. The selective C-H bond activation could be achieved by utilizing the proximal directing group present in a molecule. In this regard, strongly chelating N-directing groups (8-aminoquinoline, pyrimidine, pyridine) are well explored. However, readily available, and weakly coordinating O-directing groups (aldehyde, ketone, ester substituted amide) are underdeveloped. Thus, synthetic transformations utilizing earth abundant 3d transition metal catalysts and easily available weakly coordinating directing groups are sustainable methods for C-H functionalization.

In the present research work, several synthesis methodologies have been developed using cobalt(III)-catalyst in combination with weak chelation, where various sp^2 C-H bonds have been functionalized to synthesize useful organic molecules, as are shown in the scheme below. Also, the Passible mechanisms for each of these transformations have also been investigated, as are supported by several mechanistic studies and control experiments.

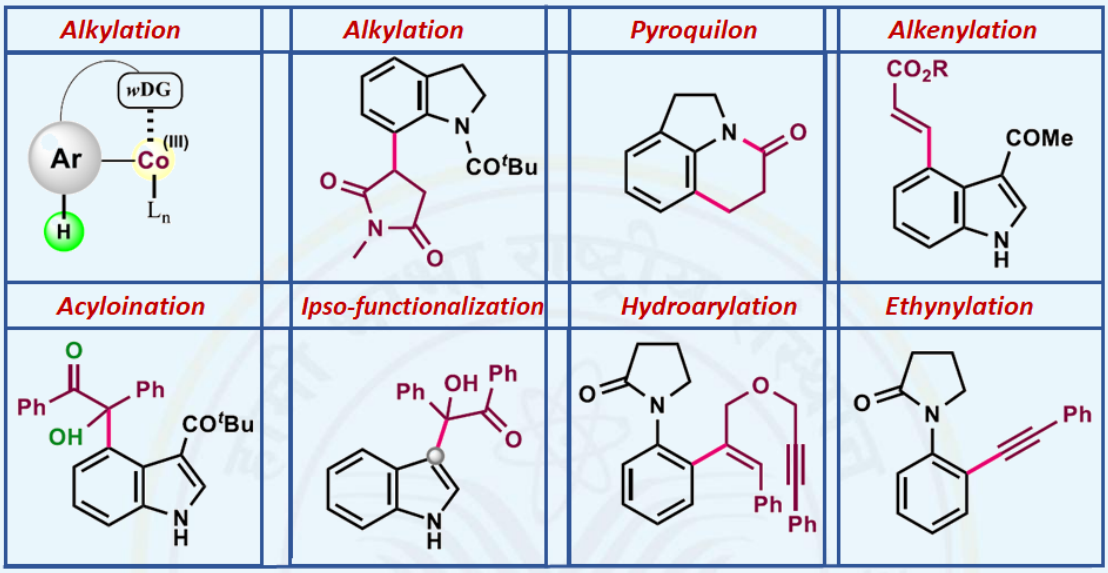

Luminescent coinage metal nanoclusters and their interactions with target analytes

2.3.4 Understanding the Interactions of Luminescent Coinage Metal Nanoclusters with Target Analytes Using Various Spectroscopic and Microscopic Techniques

Research related to nanomaterials has emerged as one of the most cutting-edge and modish areas of scientific exploration in recent years. Among these nanomaterials, metal nanoclusters (MNCs) have garnered significant attention due to their ultrasmall size (<2 nm), low toxicity, advantageous optical properties, and excellent water solubility. It has been revealed in the literature that while substantial research has been directed towards probing the interactions of larger sized nanomaterials with various target analytes, studies on the interactions of MNCs with important analytes are still in their infancy. As a result, understanding on how MNCs communicate with target analytes is rather limited. Therefore, to fill this knowledge gap, further investigations on the said aspects are very essential. Understanding the behavior of MNCs, both in the absence and presence of different analytes, is expected to provide valuable information, not only on the fundamentals behind their actions, but also to acquire knowledge on various MNCs mediated applications, such as bio-analysis, bioimaging, nanomedicine, sensing, optoelectronics, catalysis, energy harvesting, etc. The primary objective of the present thesis was to address the aforementioned issues.

The thesis provides a requisite introduction on the inorganic nanoparticles, with special attention on metal nanoclusters. It also covers the instrumentation and research

methodologies employed in the present research work. Investigations conducted in this thesis aimed to explore the interaction mechanism of bovine serum albumin (BSA) with three distinct types of copper nanoclusters (CuNCs) possessing chemically different surface ligands, namely, tannic acid (TA), chitosan, and cysteine (Cys). The potential of these CuNCs as the effective enzyme inhibitors on the activity modulation of α-Chymotrypsin and the associated interaction mechanisms have been investigated. The development of a nanoscale fluorescence sensory system based on chitosan capped CuNCs based materials for the selective and sensitive detection of highly reactive oxidative species (hROS) and antioxidants within a single chemical entity is also a part of the present study. Present thesis also investigates the impact of surface ligands of CuNCs in catalyzing the $NaBH_4$ mediated reduction of 4-nitrophenol to 4-aminophenol, and thereby explores some issues related to the concerned reaction mechanism. Various aspects of the electronic interactions between non-plasmonic fluorescence bimetallic silver-capped gold (F-AgAu) nanoparticles and plasmonic gold nanoparticles (AuNPs) have also been explored in the present thesis.

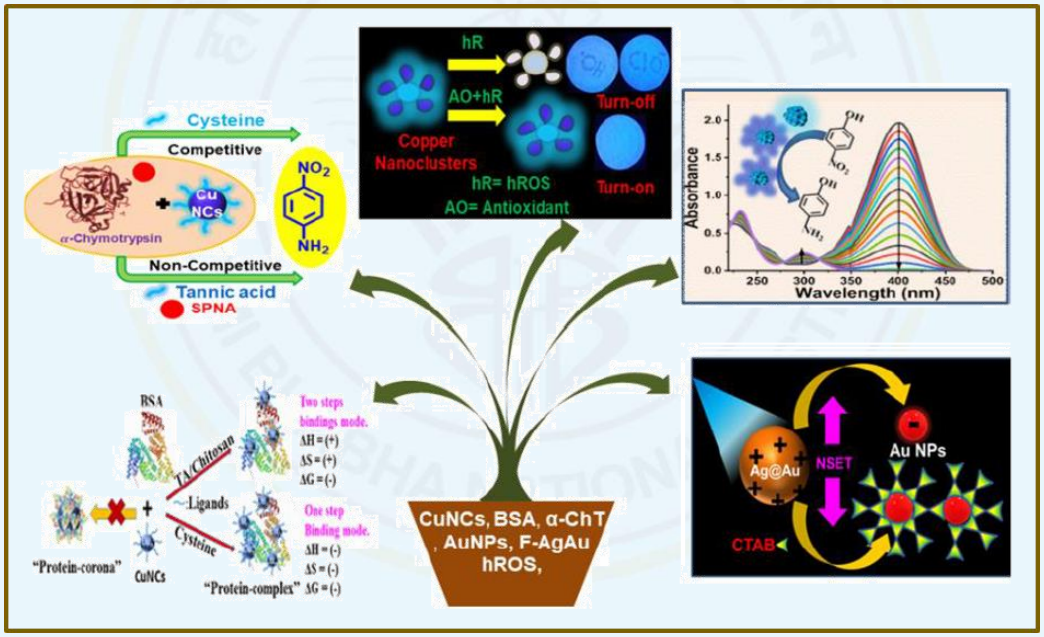

Luminescent coinage metal nanoclusters and their interactions with target analytes

2.3.5 MOF derived Metal Chalcogenide Nanostructured Materials as Electrocatalysts for Water Splitting in Electrochemical Energy Conversion

The notable potential of metal chalcogenides in advancing energy conversion techniques is highlighted in the present thesis, illustrating that these materials exhibit remarkable electrochemical characteristics toward the production of hydrogen and oxygen, including reduced overpotential values, faster kinetics, high conductivity, and extended durability under harsh electrolytic conditions. The results obtained in the present research demonstrate that the MOF derived metal chalcogenides are attractive choice of the materials for their

utilizations in the next-generation energy conversion electrodes. This is due to numerous benefits of these materials that include high abundance, low cost, and a range of morphologies. The remarkable abilities of these materials in the electrochemical processes involving the evolution of hydrogen and oxygen have opened the door for the creation of durable and efficient energy conversion technologies, which will contribute to the growing demand for renewable energy sources. The study also highlights the critical importance of temperature and reaction time in achieving optimal catalytic performance for the materials derived from MOF systems. Taking everything into consideration, present thesis provides very informative data about electrochemical energy conversion using a range of electroactive materials, establishing the required groundwork for the future achievements in the creation and application of the advanced energy conversion technology.

The findings of the research have the potential to contribute to the energy sector, paving the way for the development of more efficient, sustainable, and environmentally friendly materials for energy conversion techniques.

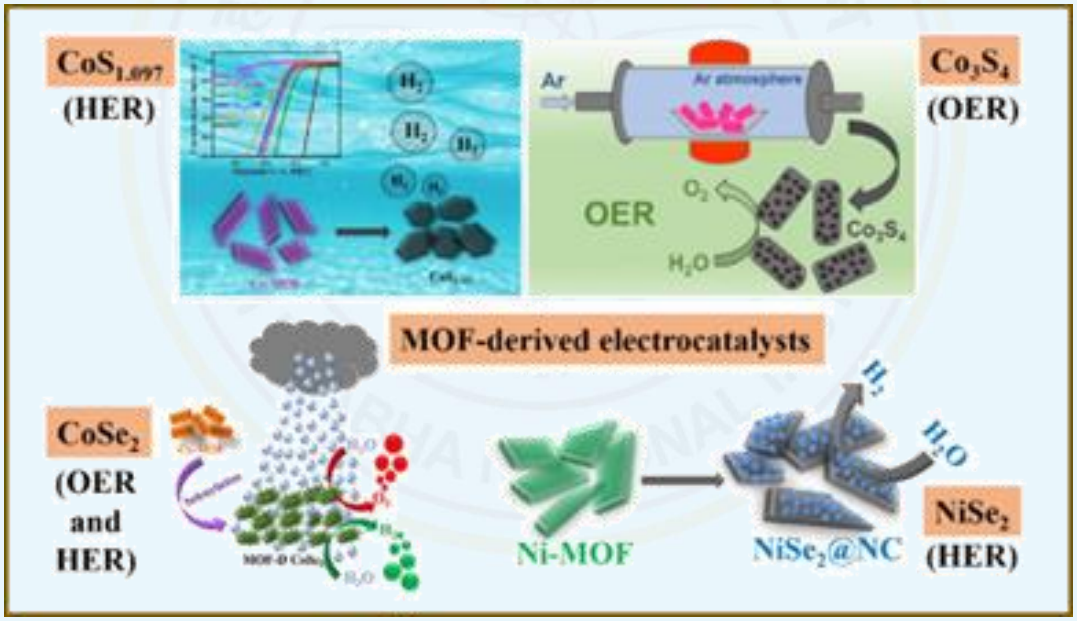

MOF-derived electrocatalysts useful for the electrochemical water splitting

2.3.6 Synthesis and Functionalization of N-Heterocycles via Bismuth Catalyzed S_EAr Reaction and Nickel Catalyzed C-H/C-N Bond Activation

N-heterocycles are found to be the core structure of many biologically active compounds and pharmaceuticals. Hence, functionalization of heterocycles is an important aspect of the medicinal chemistry, wherein substituents can help in increasing the affinity of these compounds for a certain biological target. In this regard, classical synthesis as well as transition metal catalyzed C-H and C-N bond activation techniques has proved to be a highly efficient method to construct C-C bonds on a heterocyclic moiety. In this context, in the

present thesis several methodologies have been developed based on Lewis acid (Bi(III)) and 3d transition metal (Ni) catalysts to achieve the selective C-H bond activation as well as C-N bond functionalization to obtain the the targeted molecules. The electrophilic aromatic substitution (S_EAr) strategy enables the remote functionalization of the tetrahydroquinoline and indoline using isatin and trichloroacetimidate as the electrophiles. In C-H bond activation strategy, sequential C-H bond activation of indoline, indole, and pyridylpyridones was achieved in the presence of a nickel catalyst. Additionally, the nickel catalyst facilitated the aryl-aryl bridging through C-N bond activation of 2-Pyridylpyridones and 6-Purinylpyridones, yielding the corresponding biaryl compounds. These approaches contribute novel pathways for the tailored molecular synthesis, opening their potential biological applications.

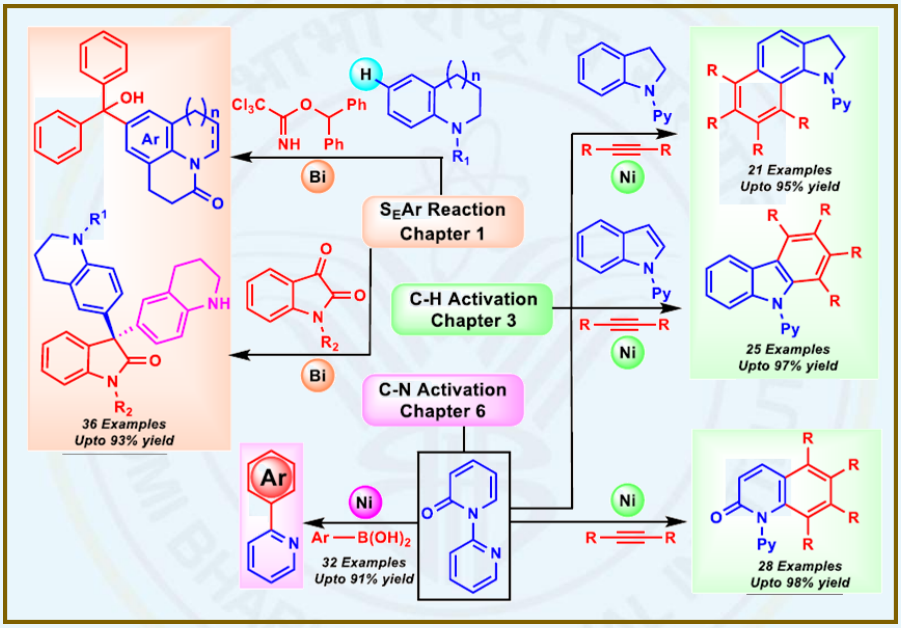

Representative molecular system synthesized via C-H and C-N bond activation strategies

2.3.7 Selective C–N, C–S and C–C Bond Formation of Substituted Thioamides and Nitriles

The present thesis has elucidated the double N-heteroannulation strategy from the acyclic precursors to prepare tetracyclic norneocryptolepine analogues. These tetracyclic molecules contain α-carboline core and is a natural product isolated from the leaves of Justicia Betonica. The photophysical properties of the selected indolofused quinoline have been investigated in the present thesis. Further, the present thesis has also reported a one pot two step synthesis of indolofused quinolines from the acyclic precursors. Moreover, conversion of the derivative of indolofused quinoline to neocryptolepine have also been demonstrated. A series of control experiments have also been conducted in order to confirm that the N-arylation proceeds through S_NAr pathway. The chemoselective Ullmann coupling of thioamides to yield 2-iminobenzothiolanes in good to excellent yields with broad substrate scope have also been demonstrated in the present thesis.

The chiral induction on the substrate has also been examine in the present work using optically pure isothiocyanate. Unfortunately, however, no chiral induction was observed in the obtained product. Hydrolysis of the substituted 2-iminobenzothiolanes to yield 2-oxobenzothiolanes has also been investigated in the present thesis. Accordingly, S-analogue of 2-oxindole having quaternary center at C-3 position has been synthesized. Control experiments were performed to conclude that the S-arylation proceeded through the Ullmann coupling process. Chemoselective N-arylation of thioamides through base mediated pathway has been demonstrated in the present study. N-arylation of α-oxo ketene S,N-acetals has also been reported. It has been envisioned that it is possible to improvise the substrate so that both the S-center and the N-center can be made available for cyclization reaction. Thus, thioamides were suitably subjected to the cyclization reaction. Exclusively N-arylated products were obtained over S-arylated products. Mechanistic studies revealed that the base mediated N-arylation occurs through a radical pathway. It has been shown that the selective monoarylation of disubstituted malononitriles occurs through nickel mediated pathway. The research work carried out is the first report for the selective functionalization of disubstituted malononitriles using 3d transition metal catalyst. The reason for the selection of nickel-based catalysts was due to its high reactivity towards insertion reactions. Broad substrate scope has been investigated in the present research work. From the mechanistic studies it has been concluded that the reaction proceeds through the formation of organonickel complex formation, aryl group transfer, imine formation and finally hydrolysis of the intermediate to give the ß-ketonitrile compounds. In summary, present thesis has developed quite efficient methodologies for the synthesis of heterocycles and b-ketonitrile compounds.

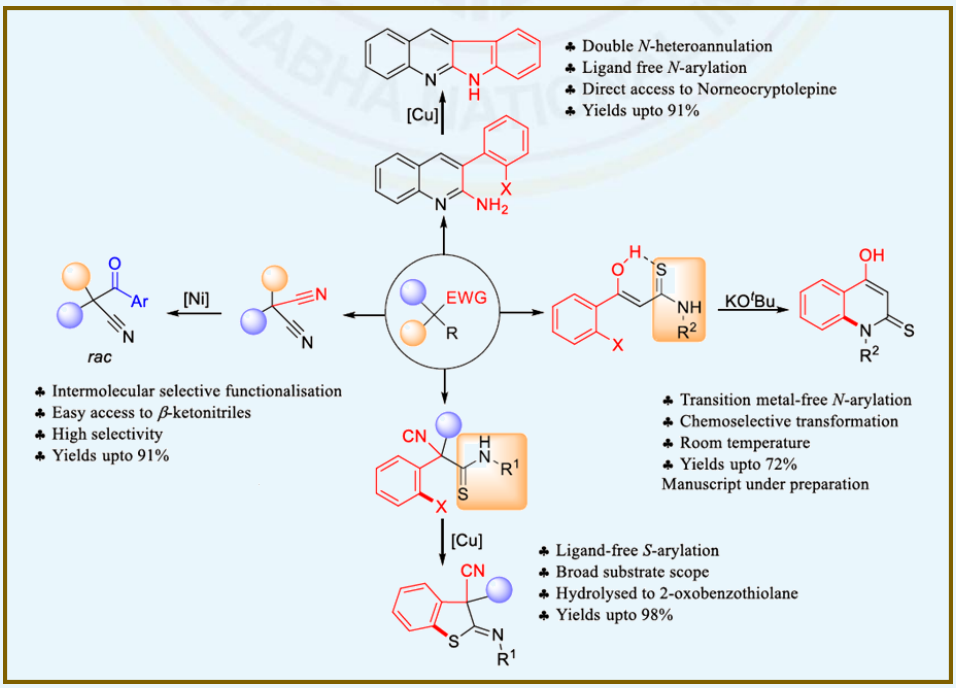

Various selective C–N, C–S and C–C bond formations explored in the thesis

2.3.8 Machine Learning Representation of Potential Energy Surfaces and Energy Transfer in Gas-Surface Scattering

Understanding reactions using computational methods gives atomistic details of the reaction and reveals the often overlooked, dynamical picture. This requires knowledge of the potential energy surface (PES) which is traditionally represented in an analytical form using energy data obtained from quantum chemistry calculations. However, this becomes a bottleneck for systems with more than three degrees of freedom. To this end, a part of the work reports the use of machine learning (ML) methods to represent PESs. Two ML methods - gaussian processes for regression and artificial neural networks were used to represent the PESs for two 4-dimensional systems, $HeH^+ + H_2$ and $C_5N^- + H_2$, and the 5-dimensional $C_2^- + H_2$ system. Further, ML representation of the PES for high dimensional systems requires a large amount of data. On the contrary, ab initio classical trajectories have been used in dynamical simulations for higher dimensional systems but are CPU intensive. Here, a new scheme is proposed that combines ML and "on-the-fly" dynamics to represent the PES using data generated during ab initio classical trajectories. The second part of the thesis deals with the study of energy transfer processes in gas-surface scattering. Recent quantum state resolved molecular beam experiments have revealed that formaldehyde upon scattering from Au(111) surface, exhibits rotational rainbow for a specific axis. Classical trajectory simulations have been used to model and study the dynamics of this system. It was found that the rotational rainbow is dictated by the minimum energy surface of the interaction potential resulting in orientational steering. Further, the scattering of formaldehyde on a single layer graphene (SLG) surface has been studied. It was found that the trapping probability of formaldehyde on SLG decreases with increasing collision energy, however it is much greater than that from gold surface. The results indicate that the average rotational energy of the direct-scattered molecules from graphene surface are similar. However, the rotational rainbow in this system is dependent on the collision energy of formaldehyde.

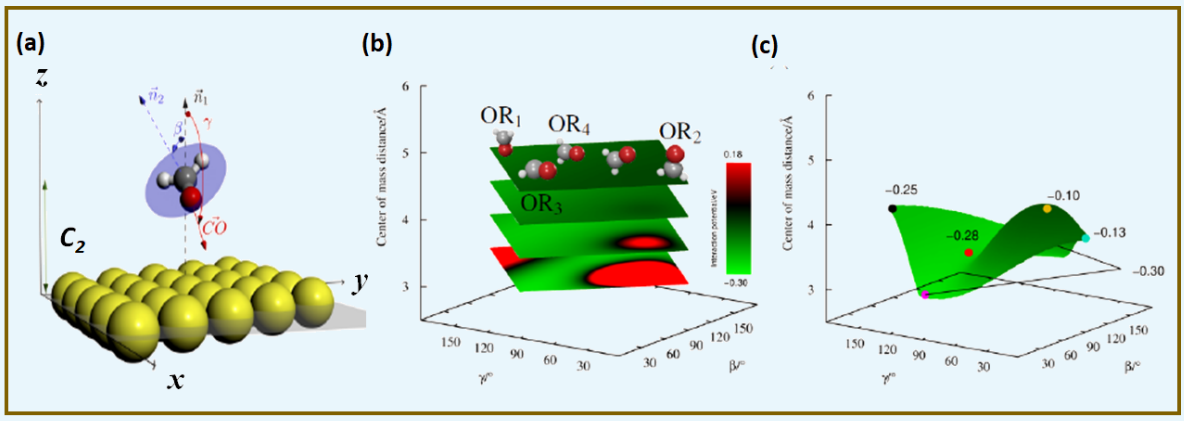

(a) Coordinate system, (b) interaction potential, and (c) minimum energy surface for gold-formaldehyde system

3. Engineering Sciences

During the period of the present report, 50 research fellows have received their Ph.D. degrees in Engineering Sciences from Homi Bhabha National Institute. Following are the highlights of some selected theses in Engineering Sciences.

3.1 Bhabha Atomic Research Centre, Mumbai

3.1.1 A Study on Sonochemical Decontamination of Graphite Substrate

Graphite constitutes a major waste stream in the nuclear industry. Chemical dissolution in acid fails to dislodge the entire radioactive material from the pores. Most process intensification techniques enhance mass transfer from the surface to bulk, though the mass transfer from the pores remain the rate limiting step. Use of the mechanochemical effects of cavitation is an effective intensification method to decontaminate porous substrates. Cavitation bubbles are used to access the pores and dislodge embedded materials by the impact of their implosion. This mechanism has been used in this doctoral work to demonstrate decontamination of waste graphite substrates from fuel fabrication facilities. The novelty of the work lies in the kinetic studies of decontamination of three different contaminants on graphite. The recovery of uranium, yttria and ceria from graphite showed a doubling of reaction rate, due to sonication over silent recovery under similar conditions. Implosion of cavitation bubbles on the surface and the pores of the graphite substrate leads to its erosion and wear. The effect of erosion of graphite at different operating frequencies of ultrasound was studied to determine the erosion rate and thereby determine the recyclability of the graphite substrate. Based on the pore size, the pore diffusion-controlled kinetics governs the decontamination rate of each of the contaminants, sitting inside the pores.

The effect of temperature and the concentration of the acid used, power density of the ultrasound, addition of oxidant/ reducing agent in the leachate on the decontamination kinetics were studied to arrive at the best conditions of operation. This would ensure faster decontamination rate and better recyclability of the graphite substrate. A study on graphite recyclability based on its (a) compressive strength; (b) electrical conductivity; (c) porosity, after the non-destructive decontamination using ultrasound showed <5% change in the respective properties after 10 cycles of decontamination. A novel erosion minimization pathway using ionic liquid for graphite under sonication was demonstrated. A similar decontamination study was also extended to other uranium loaded sorbents (silica nanoparticles and a porous biohybrid). Therefore, the doctoral work presents a complete decontamination strategy for graphite, including its erosion under ultrasound, its prevention strategies, and its recyclability. With the immense surge in demand of graphite, sustainable

consumption and reuse of nuclear graphite wastes is the need of the hour. This research is an initial attempt in that direction.

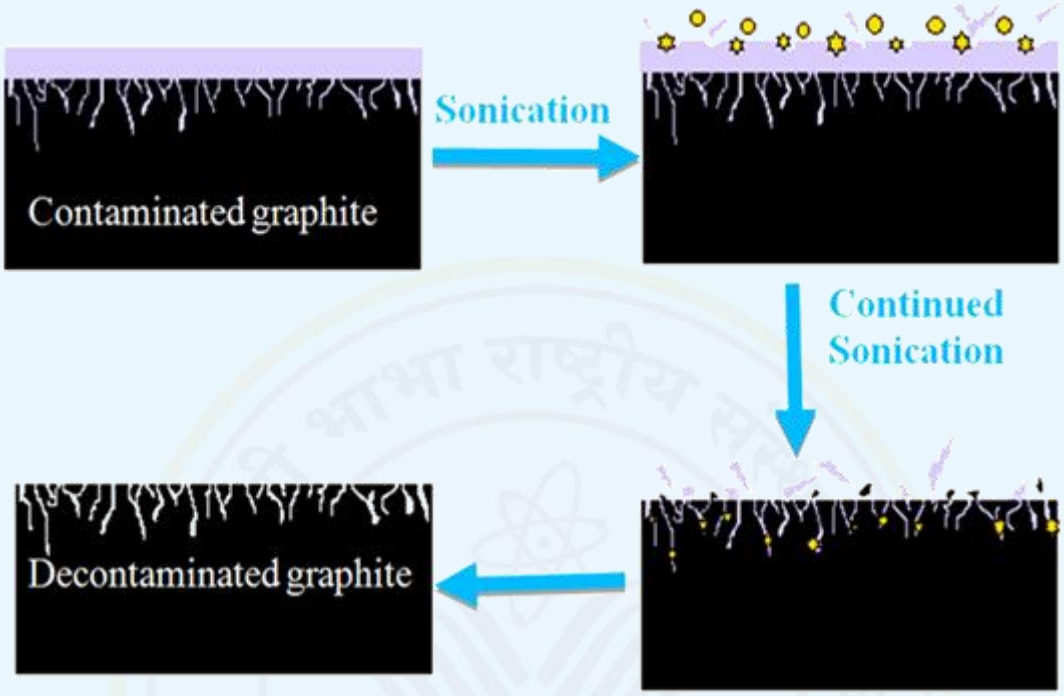

Sonochemical decontamination process of Graphite

3.1.2 Study of High Voltage Discharge and Optimization of Electrical Parameters in Copper Vapor Laser

The CVL is a widely used efficient laser known for its high power. It is used in several applications such as laser isotope separation, material processing, high-speed photography, and communication. This research links CVL's phantom current to electrode geometry, aiming to boost laser performance. By altering electrode pin configurations, phantom current is reduced, enhancing output power, beam profile, and pulse duration. In the past, only chemicals reduced phantom current in KE-CVL lasers, and this research compares the results with KE-CVL. It shows a 71% to 57% phantom current drop when changing from an 8-pin to 0-pin configuration. In the plane-plane resonator, optical power increased from 27.7 W to 36.6 W, and the pulse duration extended from 35 ns to 75 ns switching from 8 pins to 0 pins. Electrode geometry's impact on discharge stability and performance is rarely studied. The thesis finds that the eight-pin electrode, with high electric field enhancement, can initiate thermal instability at higher laser pressure compared to 0 and 36-pin configurations. The research also examines radiated and conducted EMI in high-power, high-repetition-rate electrically excited CVL, showing that impedance mismatch causes EMI via load reflection. Changing the electrode pin configuration from 8 pins to 0 pins reduced conducted EMI by 2 dBµV. The thesis presents a new method for calculating laser discharge electrical parameters,

emphasizing the benefits of the 0-pin electrode configuration. It also covers jitter in CVL's pulsed power supply, demonstrating how to reduce jitter from 47 ns to 18 ns by dissipating residual voltage on the capacitor before the next charging pulse.

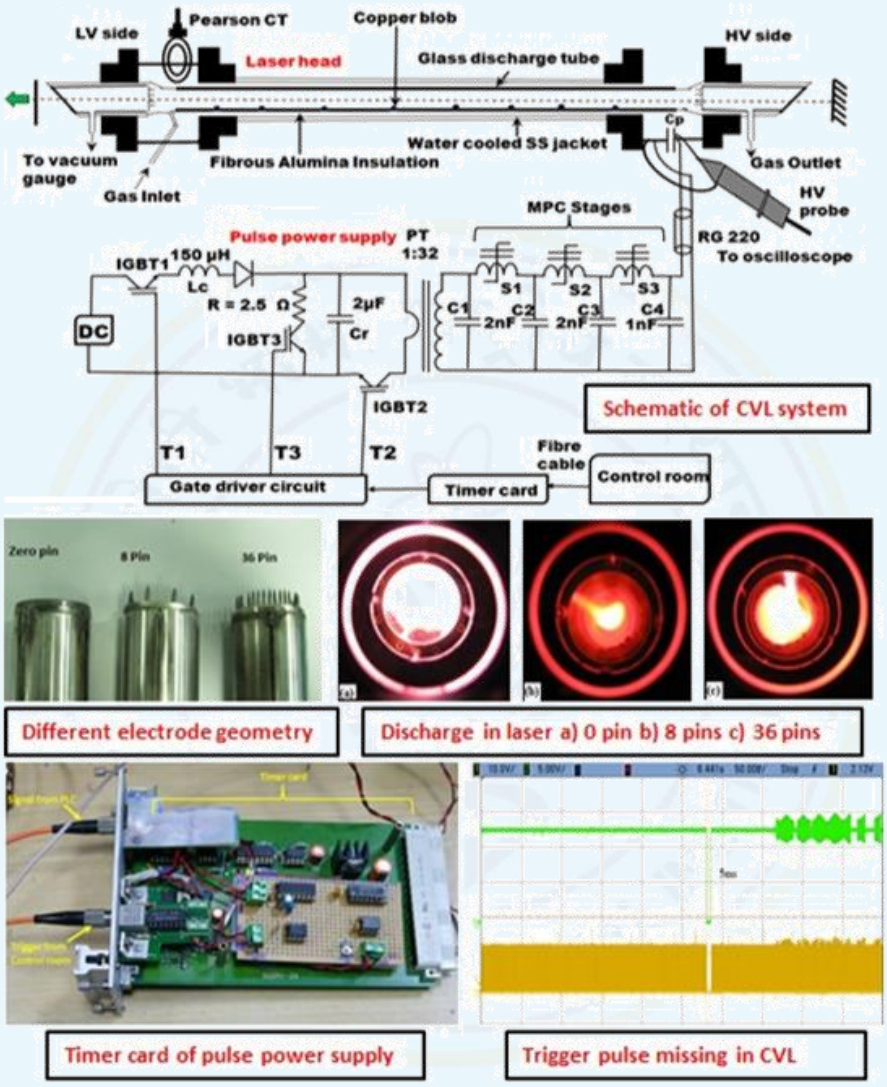

Schematic of complete CVL system, different electrode geometry fitted in the laser head, high Voltage discharge at cathode end in laser, timer card and trigger pulse missing for impedance stabilization

3.1.3 Experimental and CFD Simulations of Coolability and Ablation Behaviour of Sacrificial Material by Molten Corium in the Core Catcher of an Advanced Nuclear Reactor

India is designing the advanced nuclear reactors apart from the Pressurised Heavy Water Reactors (PHWRs), which include the Pressurised Water Reactors (PWRs). During a severe accident, corium is formed in the core, which is a complex mixture containing molten nuclear fuel, clad, structural material, control rods, etc. Corium is formed at very high temperatures

at around 2727 °C. To strengthen the safety and mitigate the consequences of core melt accidents, a core catcher device is designed to retain and cool the molten corium for a prolonged period. The concern for coolability of corium grows when water comes into the picture. There exists a potential threat of steam explosion due to interaction of molten corium with water. In addition, if propagation of the molten core is not arrested, it will lead to ablation of the basemat thus causing the groundwater contamination and release of radioactivity into the environment. Hence, retention and cooling of such reactive materials pose a complex technological and scientific challenge. The proposed core catcher for an Indian advanced reactor is an ex-vessel V-shaped carbon steel vessel partially filled with special refractory sacrificial material (mixture of fusible oxides) along with strategic cooling by side cooling and subsequent delayed top flooding (Schematic shown below). The ablation of sacrificial material due to interaction with the molten corium is important to lower the volumetric enthalpy of the melt pool, i.e., mixture of molten corium and sacrificial material. Once the temperature of the melt pool is reduced below 1227 °C, it is possible to cool it. In addition, the mixing of the sacrificial material with molten corium aids in melt inversion, which allows oxidised components, majorly sacrificial material mixed with molten corium, to relocate to the top layer of the core catcher over the metallic components, mainly structural and clad materials, due to density differences. This reduces the extent of metal water reactions when the core catcher is flooded with water from the top. This also ensures the entrapment of the radioactivity inside the core catcher vessel. The time of the top cooling is an important factor which is decided by the time required for the completion of melt inversion, and formation of a stable solid crust around the melt pool, which prevents the water ingression into the bottom of the melt pool thereby avoiding metal water reactions. Ablation characteristics of sacrificial material used in this core catcher with corium is complex because of involvement of different materials at high temperatures. The sacrificial material used here is very specific and exclusively developed for the core catcher for the Indian advanced reactor. The literature lacks the studies on the above aspects with the sacrificial material used here. In view of the above, one of the objectives of the thesis is to study the ablation characteristics of the sacrificial material used in this core catcher and its propagation. Cooling of the core catcher to remove the stored heat as well as the decay heat from the molten corium is one of the important steps to arrest the progression of the severe accident. Different cooling strategies (indirect cooling by water from side of the core catcher and subsequently flooding the core catcher at the top after a time delay) affect the corium coolability and the crust formation rates inside the core catcher vessel. The crust formation at the top of the melt pool and its adhesion to the core catcher vessel wall restricts the water ingression into the melt pool, which prevents the exothermic metal water interaction thus preventing generation of highly combustible hydrogen gas. In view of the above, the second objective of the thesis is to study the heat transfer characteristics of the decay heat generating molten corium by different cooling strategies.

Since, performing full-scale prototypic experiment is extremely challenging and prohibitory due to involvement of very high temperature and presence of radioactive materials, a CFD based model capable to simulate the ablation characteristics and coolability with the prototypic cooling strategy of the melt pool is important to develop. The CFD models has never been assessed for the ablation behaviour of the sacrificial material by the corium and the heat transfer from the molten pool when flooded with water at the top, in addition to cooling on the inclined side walls, as in the proposed design. This requires an integrated study involving material ablation, natural convection inside the heat generating melt pool, natural convection heat transfer from the side wall and from the top of the melt pool with melting and solidification inside the melt pool. As a result, the third objective of the thesis is to develop a CFD based model for ablation and coolability within the core catcher and to validate it using simulated tests.

The following are the main insights and major conclusions obtained in this thesis:

a. Both experiments and the CFD simulations of the ablation phenomena of the sacrificial material by corium show that the high temperature melt preferentially ablates the corners of the sacrificial material, and complete ablation after a time period of 500 s.
b. Immediate flooding of the core catcher for cooling, leads to water ingression into the bottom of melt pool through the gap created between core catcher vessel wall and crust formed. This causes melt eruptions and creation of several new channels in the melt pool making it porous. In addition, during the immediate flooding, there is excessive instantaneous steam generation due to direct interaction of melt pool with water. While with delayed flooding, a stable crust without melt eruptions was observed with adhesion of crust to the simulated vessel wall thus restricting the water ingression into the melt pool. Hence, melt eruption and water ingression in the melt pool and metal water interaction can be prevented by flooding of the core catcher after this time delay.
c. Coolability and the heat transfer behaviour of the melt pool show that it is beneficial to submerge the core catcher vessel into the water for side indirect cooling until the delay in top flooding. This ensures that the vessel outer temperature is below 100 °C, even though the melt is at 2500 °C. In addition, the cooling strategy of side cooling followed by delayed top flooding is an effective way of cooling and stabilizing the molten pool in case of ex-vessel severe accident scenario.
d. Material characterization of the solidified melt pool confirm the migration of the light oxidic components of the melt pool to the top layer over the heavier metallic components. Thus, the stratification of the metallic component (steel) at the bottom layer of the core catcher, ensures that there is no metal water interaction upon flooding the core catcher vessel for cooling.
e. The CFD simulation results show that the combination of solidification and melting model with SST k-ω turbulence model are capable of simulation of the ablation of

sacrificial material and the melt front progression along with coolability in the core catcher within accuracy under 8.8 %.

f. Though the velocity vectors show the complex eddy formation due to local convective currents in the melt pool, the impact of the local convective currents is not significant on the temperature of the melt pool as the magnitude of the velocity is very low.

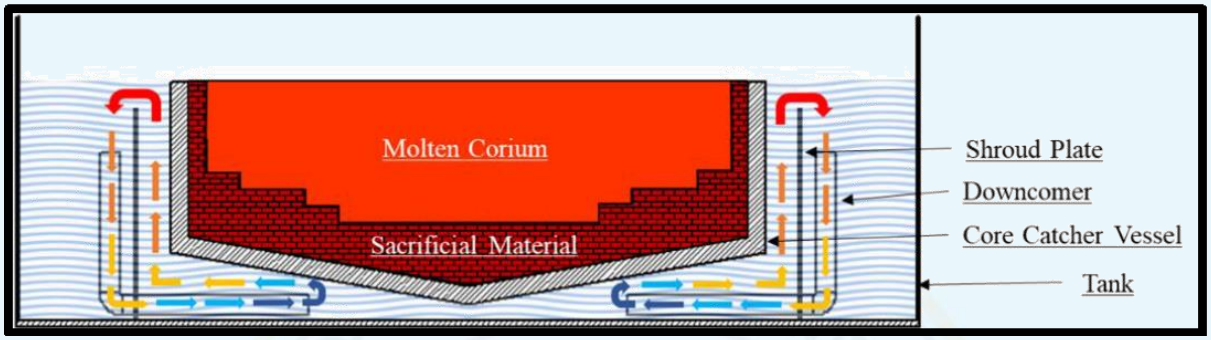

Schematic showing proposed core catcher vessel model

3.1.4 Catalytic Decomposition of Sulphuric Acid in Integrated Reactor: Experimental Study, Modeling & Optimization

The decomposition of sulphuric acid (H_2SO_4), is a three-step and energy intensive process in sulphur-based water splitting processes (Iodine-Sulfur (IS) and Hybrid sulphur (HyS) cycles) for hydrogen production. Decomposition of sulphur trioxide (SO_3) is the overall rate-controlling reaction/step in the entire three-step decomposition process. The overall decomposition rate (and conversion) of SO_3, in heterogeneous catalytic system is controlled by transport (heat and mass transfer) resistances in the catalyst bed (macro-scale) and catalyst particles (micro-scale), together with intrinsic reaction rate. The present research work is on investigation of transport resistances in catalytic decomposition of SO_3 in Packed Bed Reactors (PBRs) using Chromium doped iron oxide (Cr-Fe_2O_3) catalyst, through multi-scale modeling and experimentation, and to maximize SO_3 conversion.

Initially, activation energy, ~74 kJ mol-1 and frequency factor,*k*' 183 m^3 $kg^{-1}s^{-1}$ and effectiveness factor, (η) of Cr-Fe_2O_3 catalysts (pellet~0.12 and foam~ 0.26) are obtained through kinetic experimental studies. Further, transport resistances in the catalyst bed and particles, together with intrinsic reaction rate are investigated through 1-Dimensional (1-D) model and a multi-scale model, Double Porosity Model (DPM) and the models are validated with experimental studies in PBRs. A lower transport resistance has been observed in foam type catalyst than that of pellet type catalyst (Schematic shown below). Model parameters in DPM are then tuned for maximizing the SO3 conversion in PBR.

Non-isothermal η estimated using DPM (pellet ~ 0.147 and foam ~ 0.249) is in good agreement with experimental data and Weisz derived model (pellet ~ 0.165 and foam ~

0.252). Significant temperature drop is observed in foam type catalyst (ΔT~12K) than pellet type catalyst. Optimum porosity required for maximum non-isothermal η (η ~0.32) is found to be ~0.6. The present work and developed models are useful for the design, rating, and optimization study of industry scale PBR for the catalytic-decomposition of SO_3.

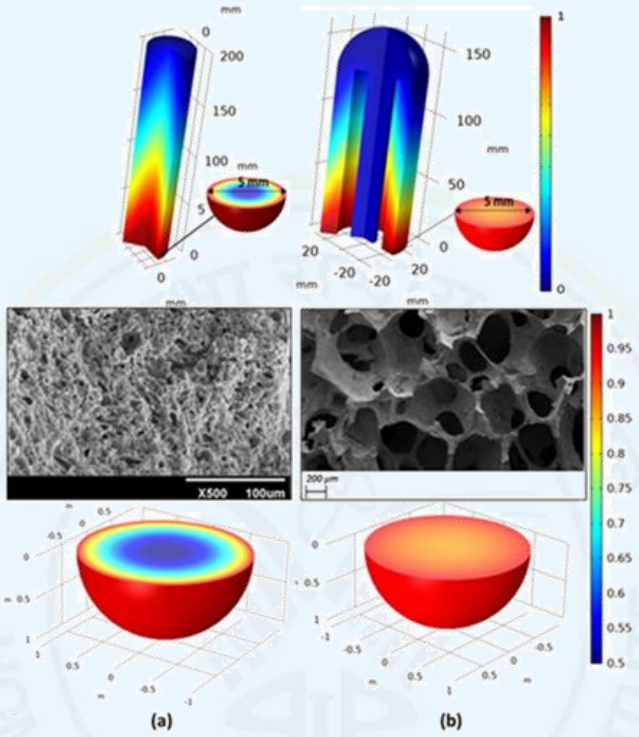

Schematic showing Concentration profile of SO_3 in PBRs and Cr-Fe_2O_3 catalyst generated using DPM (a) pellet type catalyst with SEM image of pellet and (b) foam type catalyst with SEM image of foam, at the inlet and near the high temperature wall of PBR

3.1.5 Study, Simulation and Experimentation for Ultrasonic Imaging and Gauging of Thin-Walled Tubes and Pipes

Ultrasonic gauging and imaging of metallic tubes and pipes is a multi- disciplinary task which involves the understanding of acoustic physics of the transducer, the acoustic properties of the propagating medium and analog front-end electronics for generating and receiving ultrasonic signals, as it must be performed in-situ and come across several challenges due to curvature, limited access and corroded/ eroded surface roughness occur due to harsh operating conditions. The main objective of the thesis work was to elaborate the understanding of ultrasonic testing and measurement process in thin-walled tubes and pipes using simulation studies, using modern finite element technology software, and validating the results by experimentation, using water-immersible ultrasonic equipment. Simulation studies were carried out to study the ultrasonic wave propagation and testing for SS, Aluminium, and Zircaloy tubes and SS and CS pipes using focused and unfocused piezoelectric longitudinal

wave immersion transducers. By utilizing the in-house developed 4- Channel ultrasonic inspection system and inspection-head assembly, experimentation was carried out for the measurement of sag and dimensions for thin-walled tubes and pipes and accuracy of sag and dimensions was within ±2%. Li-ion Battery-operated, water-immersible IP-67-grade ultrasonic 2-Channel ultrasonic equipment was mounted inside the inspection head assembly and the entire assembly was placed inside the pipe filled-with water, for gauging, imaging and profilometry and more than 200 MB gauging and B-Scan imaging data was acquired, over a duration of five hours. Extensive testing was carried out for the measurement of wall thicknesses, for measurement of 10% to 60% loss in wall thickness for 300mm Nominal Bore, 12mm wall thickness (WT) CS pipes and to locate as well as visualize standard volumetric and planar flaws in pipes, in the presence of 100 LPM flow of water and the test setup is shown in schematic below. The simulation results for the metallic pipes were found in good agreement with the experimental data, providing an ultrasonic Pipe inspection and gauging (UPIG) tool for the accurate and quantitative assessment of WT for thin-walled tubes and pipes, in the presence of flow of water.

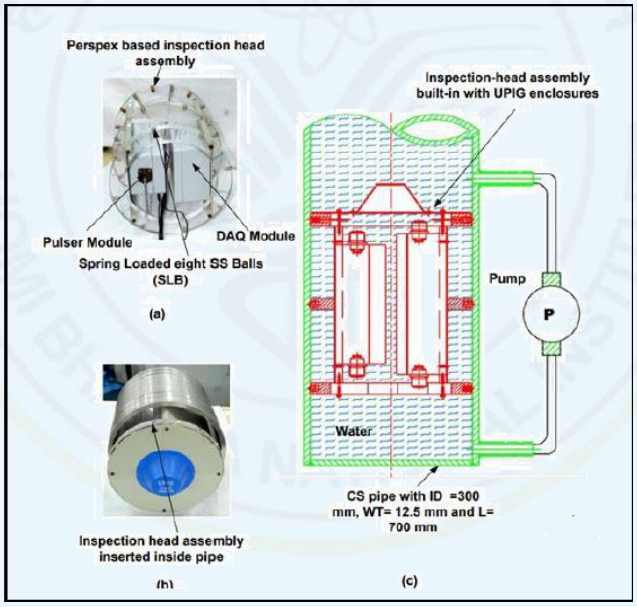

Schematic showing (a) inspection-head assembly mounted with 2-Ch ultrasonic instrumentation, (b) sample pipe inserted with inspection-head and ultrasonic instrumentation assembly, (c) diagram for test setup of inspection of CS pipe inserted with inspection head assembly, and in the presence of 100 LPM flow of water through pipe

3.1.6 Study and Characterization of 60 kW Indirectly Heated Cathode-based Strip Electron Gun

Linear electron guns are increasingly being used in various fields such as large area coating, surface treatment, laser isotope purification, material processing applications, etc. The thesis reports the study and characterization of Indirectly Heated Cathode-based Strip Electron Gun (IHCEG). An improved design of electron gun was developed to reduce high voltage

breakdown issue during high-power operation as shown in Schematic (a) and (b). For this, new conical frustum shield electrode geometry was designed, fabricated, and installed in IHCEG setup for controlling high voltage surface flashover through reduction in electric field intensification at triple junctions, over insulator surface and by providing more uniform potential gradient. Optimized parameters were (d_T, d_B) = (30, 35) mm, (D_T, DB) = (45, 50) mm, l = 50 mm, r = 7 mm and (u_T, u_B) = (28, 24) mm, (S_T, S_B) = (30, 28) mm, h = 1.25 mm, and s = 0.75 for 60 kV and 1.5 kV insulators respectively. % reduction in electric field strength with respect to no shield electrode was 98.4% each at TJ 'A' and 'P,' and 96.6% at 'Q.' Experimental validation by monitoring breakdown signal was done which settled 73% faster and 38% reduction in power spectrum was observed with respect to no shield electrode. New 3-D cost function formulation and implementation using JUPYTER notebook for low-power DHEG optimization has been done, which was further developed for high-power IHCEG to achieve desired 2700 -bent electron beam at target plane as shown in schematic (c) and (d). Effect of copper and aluminum as target materials at different electron beam currents was studied by evaluating electron beam-generated plasma properties for electron gun characterization. Optimal spatial parameters of atmospheric pressure plasma jet were achieved by optimizing the input gas flow rate and microwave power by using COMSOL Multiphysics simulation tool and experimental validation. CST Studio-particle tracking module simulation tool was used for performing 3-D electron gun modelling, design, electrostatic, electromagnetic, and 3-D particle tracking simulations. For IHCEG, simulation and experimental result of electron beam cross-section was (76 x 16.5 mm^2) and (77 x 18 mm^2) respectively at the target plane.

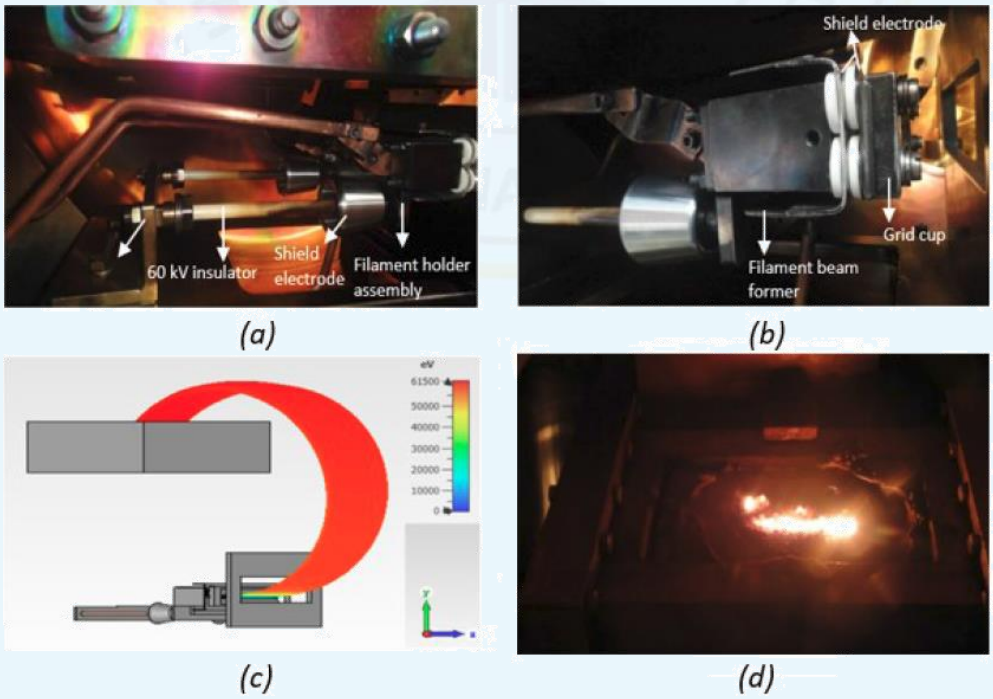

Schematic showing (a) Assembly of conical frustum shield electrodes in the experimental setup at 60 kV insulator (b) 1.5 kV insulator (c) 270^0-bent electron beam (d) Experimentally obtained electron beam

3.2 Indira Gandhi Centre for Atomic Research, Kalpakkam

3.2.1 Development of Ceramic Coatings for FBR Applications Involving High Temperature Sodium Environment

Air Plasma Sprayed (APS) ceramic coatings are currently being investigated for use in avant-grade sodium-cooled Fast Breeder Reactors (FBRs) involving liquid-sodium environments. In particular, applications such as chemical, electrical, and thermal barriers, wear and tribology, environmental barriers, and sacrificial ceramic coatings for core catcher linings, are areas of concern. However, ceramics are reported to be susceptible to liquid-metal corrosion in aggressive liquid-sodium environments. Therefore, it is essential to investigate the APS coating/liquid-sodium interaction and expand the processing space of APS coatings to various candidate ceramics. Subsequently, several APS coating materials/systems that can perform well in FBR environments are to be identified. Towards this, the present study adopted several candidate APS materials, viz. YSZ, Al_2O_3, Y_2O_3, $MgAl_2O_4$, TiSZ, $Y_4Al_2O_9$, and $La_2Zr_2O_7$ for investigations based on the available literature. Different APS coatings (topcoat) on SS 316LN substrate with a NiCrAlY (bondcoat) interlayer were subjected to liquid-sodium at 400 °C (core inlet temperature of typical FBR operation) for different durations (Schematic a).

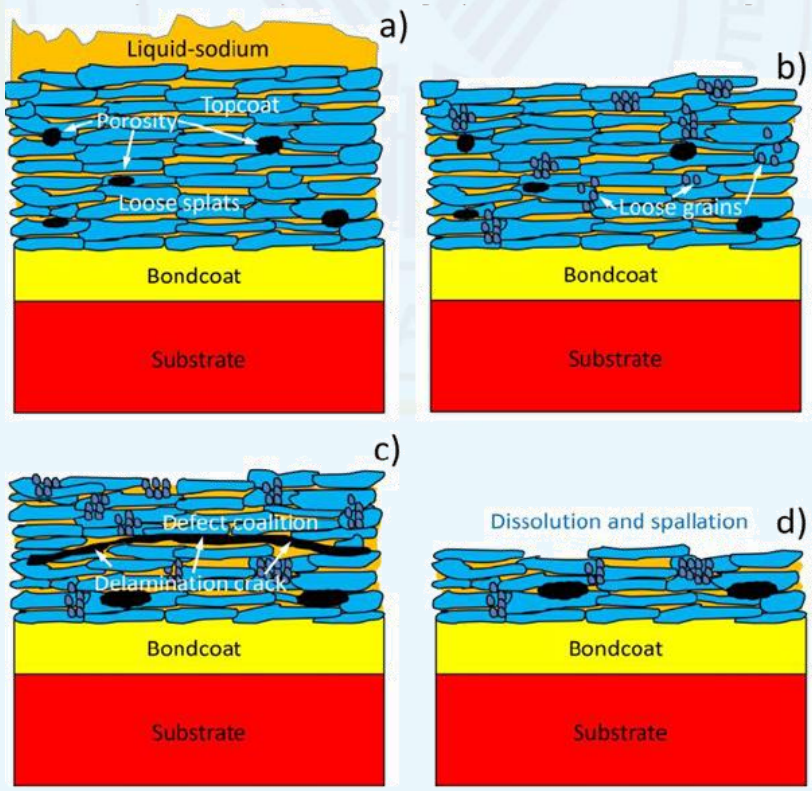

Graphical representation of the general degradation characteristics of APS coatings in liquid-sodium

APS coatings that performed satisfactorily in liquid-sodium were further ranked based on their long-term compatibility and corrosion performance. In contrast, those degraded in

liquid-sodium were analyzed to review their corrosion and interaction mechanisms. Additionally, the performance of selected APS coatings during their interaction with the Ultra-High Temperature (UHT) simulant corium melt (~2500 °C) was also studied. Another significant aspect of the study was modifying the APS topcoat architecture by microstructure re-engineering using Laser Surface Remelting (LSR) to attenuate the liquidsodium infiltration into the coating. From the experimental results, the APS coatings may be ranked from good to worse for their performance in liquid-sodium as follows: $Y_4Al_2O_9/MgAl_2O_4$ >Alumina >Y_2O_3>$La_2Zr_2O_7$> TiSZ > YSZ. The deterioration of APS coatings in liquid-sodium (Schematic b-d) can be due to factors such as dissolution, increment in defect density, defect coalition, delamination, and chemical reaction. The characteristic lamellar morphology of the APS layers and the weakening of cohesive bonding between the splats also play a crucial role in the degradation due to liquid-sodium infiltration. The study outcomes indicated that LSR is an efficient technique to improve the performance of APS coatings in liquid-sodium.

3.2.2 Numerical Simulation and Experimental Validation of Fusion Welding of 316LN Stainless Steel

Conventional welding methods such as shielded metal arc welding (SMAW) or tungsten inert gas (TIG) welding cause significant issues like distortion, residual stresses, and microstructural inhomogeneity. This study explores advanced techniques like A-TIG, laser and Hybrid laser-MIG welding (HLMW) for welding of 316LN SS used for critical components in fast reactor nuclear power plants. The final weld metal microstructure is influenced by the welding thermal cycle, affecting the mechanical and corrosion properties of the joint. Mechanical strength relies on weld attributes, composition, and properties determined by weld pool hydrodynamics during welding. Experimental studies on the weld pool face challenges due to small dimensions, molten pool opacity and high temperatures. CFD modeling quantitatively describes thermal and flow patterns during weld pool formation in advanced welding processes addressing challenges. The numerical model predicts temperature, weld pool evolution, and final weld bead geometry. In the A-TIG simulation study, the numerical approach enhanced the understanding of the oxygen content's influence on weld pool development, crucial for controlling and achieving desired weld bead dimensions. The CFD study estimated that a minimum oxygen content of 335 ppm is required to cause reversal of Marangoni convection and enhance the penetration capability in 10 mm thick 316 LN SS plate at 300 A current. The laser welding modeling focused on finding a suitable heat source model to capture the laser keyhole and studying the impact of laser power on weld penetration. The results showed that the hybrid heat source could accurately simulate the weld bead shape, size, and keyhole dynamics in laser welding. The modelling framework on HLMW proposes the suitability of different hybrid heat source models appropriate for the welding of 316 LN SS. The study demonstrated the double-ellipsoidal rotary Gaussian heat source as the appropriate model for HLMW and it illustrated that the synergy effect between the laser and MIG heat sources based on their separation distance on the depth of penetration was

demonstrated using the proposed model. The developed numerical models provide a valuable tool for accurately simulating and predicting weld pool dynamics aiding engineers in selecting and optimizing welding processes. Validation through experiments including weld bead shape, size and temperature values showed good agreement with the simulation results, as depicted in Schematic below.

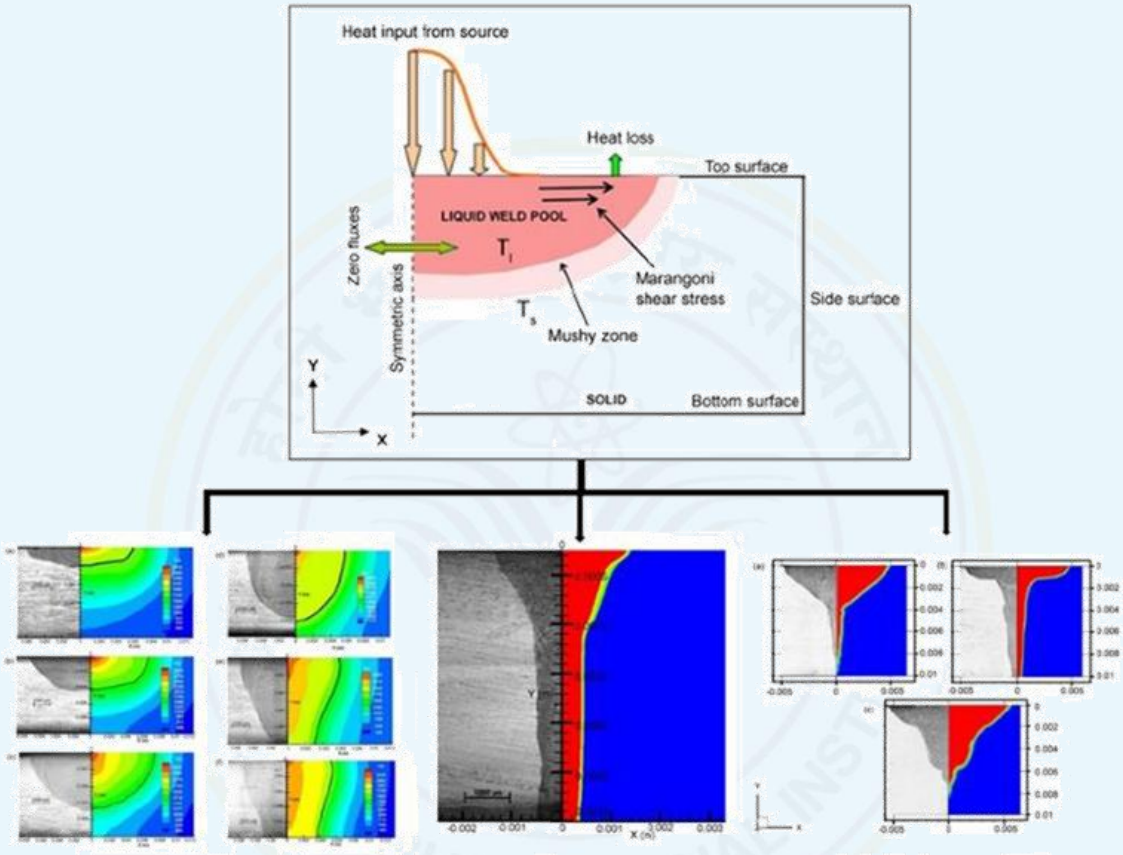

Schematic showing the computational boundary conditions and weld bead comparison for A-TIG, Laser and HLMW

3.3 Institute for Plasma Research, Gandhinagar

3.3.1 Guided and Leaky Modes Characteristics of Dielectric Loaded Helix Structure

The electromagnetic characteristics of helical structure owing to its skewed boundary condition, which supports hybrid modes as well as circular rotation of the field, finds various applications starting from microwaves to optical communications. The guided and leaky mode characteristics for planar as well circular rod type dielectric structures are relatively well known. However, the investigation to the leaky mode characteristics coupled with guided modes for a dielectric loaded Helix structure is not explored at all despite the fact that helix structure exhibits unique characteristics. The present thesis work addresses these critical issues both analytically and experimentally. A generalized analytical and computational

numerical theory, for both the guided and leaky modes, has been developed to investigate the dispersion and radiation properties of dielectric loaded helix with and without radial thickness. In the first work, propagation, and radiation characteristics of Dielectric Loaded Helical Antenna (DLHA) have been investigated theoretically, computationally and experimentally. In the second part, we have investigated the complex mode EM wave dispersive characteristics of Dielectric Loaded Radially thick Helix (DLRTH), which shows leaky wave modes characteristics. The two distinguish characteristics and applications of the proposed DLRTH structure are found. The first one is that it supports slow wave propagation having phase velocity ten times less than the velocity of light, which finds potential application in SW (phase delay) devices and phase filters. The second feature is that it supports a wide leaky mode region, which can be controlled by pitch angle, which finds application in beam steering-based leaky wave antennas system. Based on the theory, a leaky wave dielectric loaded helix is designed using CST Microwave Computational software. In last part of the work, a wideband circularly polarized two-layer concentric cylindrical dielectric resonator antenna (CDRA) is designed and simulated for C-band applications.

3.3.2 Analysis, Design and Characterization of Metasurfaces for RCS Reduction

In recent years, Metasurfaces have gained significant attention for radar cross section (RCS) reduction in RADAR stealth applications. Their unique properties address the major limitations of conventional radar absorbing materials (RAM) in terms of various electromagnetic (EM) characteristics such as reflection coefficients and polarization independence over a wider bandwidth and for wider angle of incidence as well as having light weight, especially in microwave frequencies. This has been accomplished by using the benefits of loading different geometrical shapes of constituent unit cells in periodic array as a Metasurface which exhibits wide bandwidth, wide incidence, and polarization independent absorption characteristics. Further, it is exceptionally light weight with much reduced thickness and hence can be easily wrapped over any geometrical shape. Most of the reported designs, based on Metasurfaces, present a 10dB reduction in reflection, which is not sufficient for extremely sensitive defence application. Only a few reported studies proposed a computational design of 20 dB reflection reduction value, however, their experimental characterization has not been reported. In addition, the potential targets in defence application have planar as well as non-planar surfaces, therefore it is necessary to study the performance of the developed Metasurface absorber on conformal surfaces, as well. All the previously reported works have limitation in terms of reflection reduction value, fractional bandwidth, and different geometrical shapes of conformal Metasurface. The thesis addresses these issues by designing, development and characterization of broadband, polarization-insensitive Metasurface absorbers (MA), having different unit cell geometry, which exhibits 20 dB reflection reduction. Additionally, RCS reduction capabilities of different geometrical shapes of conformal Metasurfaces (planar, cylindrically bent and 90° dihedral surfaces) have also been characterized numerically and experimentally. A thorough Electromagnetic

analysis, design and experimental characterization are reported. The major contribution of this thesis is 20 dB reflection reduction value as well as development and experimental validation of conformal Metasurfaces for real world RADAR stealth application.

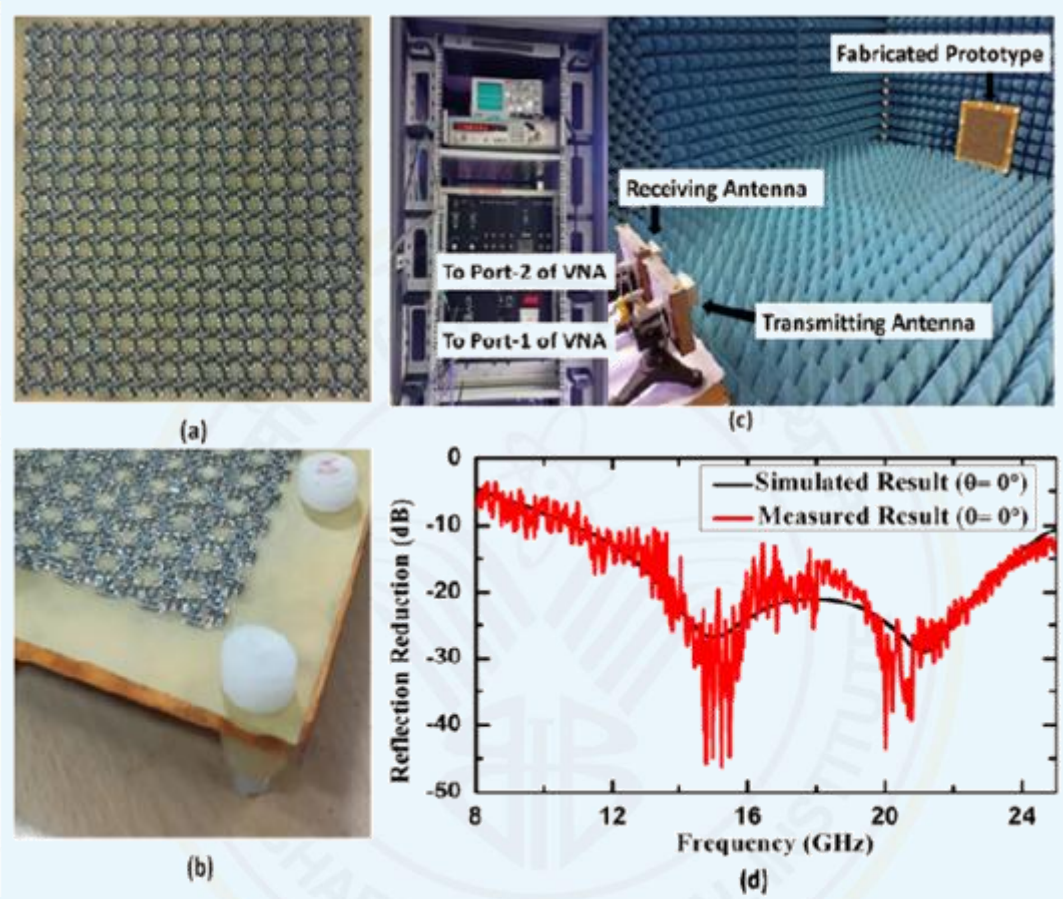

Highlights of the resistive arm based planar and conformal Metasurfaces for RCS reduction (a) Top view, (b) 3D view of fabricated prototype, (c) experimental setup, and (d) simulated and measured refection reduction characteristic of the developed planar Metasurface absorber under normal incidence

3.3.3 Development of Pulsed Supersonic Beam System for Tokamak Edge Diagnostics and other Applications

The thesis discusses the development of a Supersonic Molecular Beam Injection (SMBI) system for edge plasma diagnostics of tokamak. Edge plasma diagnostics with SMBI involves injecting a supersonic neutral beam of helium atoms into the plasma, and record spectroscopic emissions of helium to estimate the plasma electron temperature and density using CR modeling. The SMBI system plays a crucial role in edge plasma diagnostics. To have high particle density for the beam without significantly disturbing the vacuum the injector need to be operated in pulse mode. A high beam density and low divergence for the SMBI ensures optimal spatial and temporal resolutions. Optimizing the performance of the SMBI requires charecterization of jet, from where the molecular beam is extacted. In this work a

number of innovative diagnostic techniques were conceptualized and implemented to measure flow parameters and quantify transient behavior of the jet. The experimental charecterization of the jet is further verified with appropriate simulations and theoritical models. A prototype SMBI system is developed and demonstrated to generate a pulsed supersonic molecular beam.

The effect of the dynamic background on the jet boundary is investigated using pressure transducers. A novel time-of-flight probe, designed and developed to study the flow velocity of a pulsed supersonic jet is ued to measure the velocity of He and N_2 gas and is verified with DSMC simulations. The axial density of the jet is estimated using the Pitot probe technique with flow rate correction to accommodate internal boundary layer and sudden constriction effects. A novel supersonic nozzle profile is proposed to generate directed flow for rarefied jets, and the effectiveness of such a nozzle is experimentally demonstrated using an additive manufactured nozzle. The results are verified with simulations as well. Transient effects within the jet are investigated using the Rayleigh scattering technique with atomic clusters as tracers. With meticulous alignment and calibrations, the sensitivity of this setup is increased by an order of magnitude, enabling the visualization of complete spatial and temporal profiles of the jet including the growth at the barrel shock boundaries, and disintegration at the normal shock boundaries.

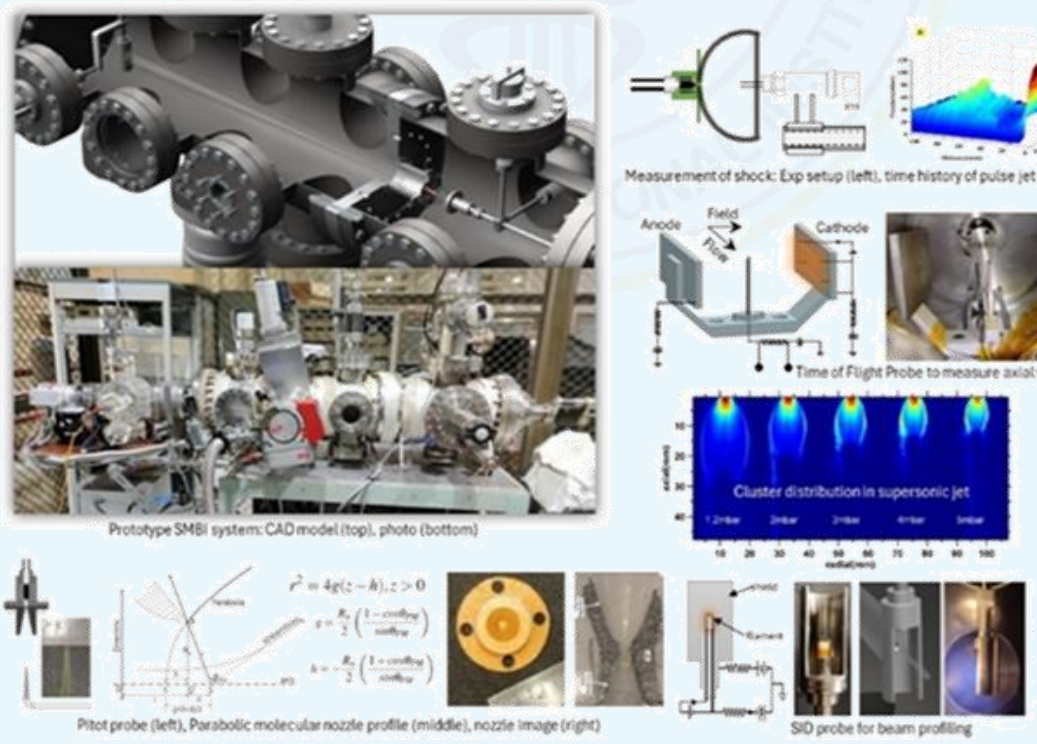

Developed Supersonic Molecular beam injection (SMBI)

Finally, an experimental system is devised to produce a supersonic molecular beam. Conditions for generating the molecular beam are identified using the Knudson curve estimated from experimentally measured jet parameters. A novel shielded ionization discharge (SID) probe is developed to validate the operating region and optimized the skimmer position to achieve high beam density and low divergence. Lastly, the study discusses a prototype SMBI system and delineates future upgrades and potential integration into tokamaks, while also highlighting the applications for both basic and applied science.

3.4 Raja Ramanna Centre for Advanced Technology, Indore

3.4.1 Investigation on Shape Control Methodologies of Piezoactuator-based X-ray Deformable Mirror, its Fabrication and Characterization for Adaptive Optics

High brightness x-rays at synchrotron radiation (SR) beamlines require adaptive focusing optics which can deliver aberration-free, adjustable micron-size focal spots of high energy SR and providing flexibility to accommodate different experimental geometries for a wide range of applications. Piezoactuated x-ray deformable mirrors (PXDMs) have capability of providing a beam profile of variable focal length and capable of correcting wavefront distortion introduced by other imperfect optics of beamline. The objective of the present work is to design and develop a PXDM to achieve the target aspheric and arbitrary shape for focusing of SR beam in sub-micron size at the experimental station of beamlines of Indus-2 SR source.

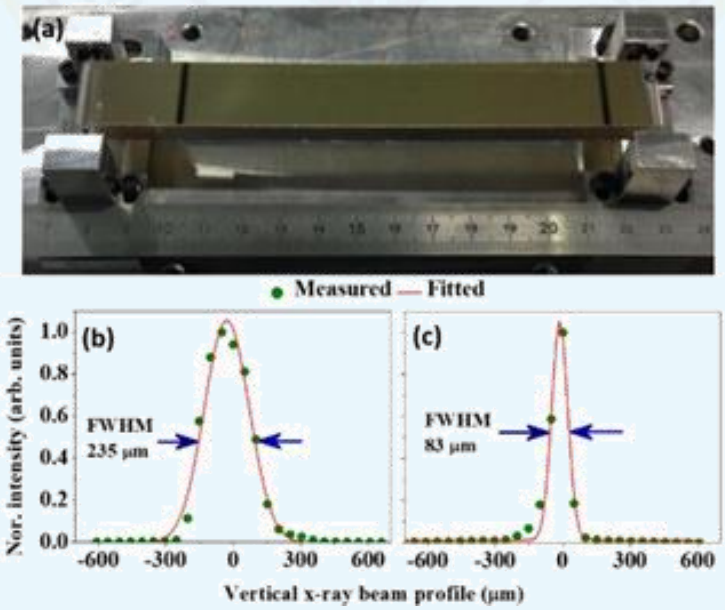

Schematic showing (a) Fabricated PXDM of zerodur mounted in the designed fixture. Measured vertical x-ray beam profile (b) without PXDM (direct beam) and (c) with PXDM of zerodur

In the present thesis work, the models and methodologies required to generate the desired shape using piezoactuators are analyzed. Initially, direct finite element- and piezo response function (PRF)-based optimization for shape control of smart structures are examined. Four global optimization techniques, namely genetic algorithm, simulated annealing, particle swarm optimization and teacher learning-based optimization are compared to develop a robust and fully reproducible method for the shape control of PXDMs and smart structures. Additionally, the response of piezoceramic actuator under high electric field (≥ 0.1 kV/mm) in bending mode is analyzed due to its necessity for generating sufficient deflection in PXDMs. The nonlinear analysis thus established is used for the development of iterative piezo response function (iPRF)-based optimization, a metaheuristic approach, for solving similar shape control problems using nonlinear piezoactuator.

A PXDM of zerodur is fabricated (as shown in Schematic (a)) and characterized to ensure it's focusing capability for high energy x-rays. The voltages of nine actuators of PXDM are optimized by the iPRF-based optimization technique to achieve the target parabolic profile. The ex-situ characterization of PXDM at optimum voltage has given the RMSE of 42 nm between the targeted and the achieved parabolic profile. The in-situ characterization of PXDM is done at BL-12, ADXRD beamline of Indus-2. The PXDM has focused the high energy x-ray beam in vertical direction from 235 µm FWHM to 83 µm FWHM (Schematic (b) and (c)) and, proved the robustness and reliability of the shape control methodology, fabrication, and characterization process to achieve the target profile of PXDMs for focusing and wavefront correction of high energy x-ray in beamlines.

3.5 Variable Energy Cyclotron Centre, Kolkata

3.5.1 Experimental Evaluation of the Thermodynamic Processes for Helium Liquefaction/ Refrigeration Systems Operated in Mixed Mode

Helium liquefiers and refrigerators are highly energy-intensive due to a very low operational temperature range of 4.5K – 20K. It is observed that most of the the liquid helium plants, regardless of whether they are designed as a liquefier or a refrigerator, operate in off-design mixed-modes when integrated with large superconducting systems. The performance of the liquid helium plants during mixed-mode operation depends on the operating condition and the off-design condition deteriorates its performance efficacy. The dissertation has examined the performance of helium liquefier and refrigerator under various mixed modes by investigating via simulation and validating through experimentation on three operating liquid helium plants. The evaluation of each off-design process assessment has been done through exergy analysis tool. The different mixed-modes presented here are liquefaction–isothermal refrigeration, and liquefaction-variable temperature refrigeration. The efficiency of the last heat exchanger or heat exchangers, which are typically operating near or below the temperature of 20K, will largely determine the output of a liquefaction/refrigeration cycle.

Due to this, the behavior of heat exchangers operating in this temperature range has also been a subject of this inquiry. It was shown that the effectiveness of these heat exchangers might drop to 70%. A built-in helium purifier has been identified as one of the most energy-intensive auxiliary equipment that has not been investigated from the perspective of energy destruction. An analytical and experimental investigation of two different popular helium-nitrogen separation processes, namely a cryo-condensation type integrated with helium liquefier and a cryosorption type, by varying nitrogen concentration of feed impure helium, has been carried out in order to address the technological gaps in the helium separation process. The current work may serve as a reference for designing and operating mixed modes in liquefier/refrigerators for optimum performance because little literature addresses the thermodynamic assessment of the liquefier/refrigerator, including its important components, utilizing comprehensive experimentation followed by exergy analysis.

4. Life Sciences

During the period of the present report, 51 research fellows received their Ph.D. degrees in Life Sciences from Homi Bhabha National Institute (HBNI). Following are the highlights of some of the selected Ph.D. theses in Life Sciences.

4.1 Bhabha Atomic Research Centre, Mumbai

4.1.1 Enhancement of Post-harvest Quality of Fishery Products through Hurdle Technology

Fish is highly perishable muscle food commodity due to its high nutritional content and biological composition. The most preferred fish consumption is in fresh or chilled stored form. However, chilled fish have a very low shelf life. Hence, different treatments or hurdles are also required to delay the spoilage of fish under chilled condition. Fish has higher demand globally due to its taste and nutritional content. High production leads to generation of high amount of waste also across the world. The fish processing is an important step prior to its marketing. This results in huge amount (approx. 20-80%) of waste generation depending upon processing such as gutting, scaling or filleting and fish species. This waste creates negative impact on environment. Hence, effective utilization of fish waste is an important step. Present thesis describes the research work towards enhancing the quality of three fishes namely rohu, seer and basa. The shelf-life enhancement of two fish (rohu and seer) steaks using hurdles such as spice extract (ajwain) and γ - irradiation under chilled storage.

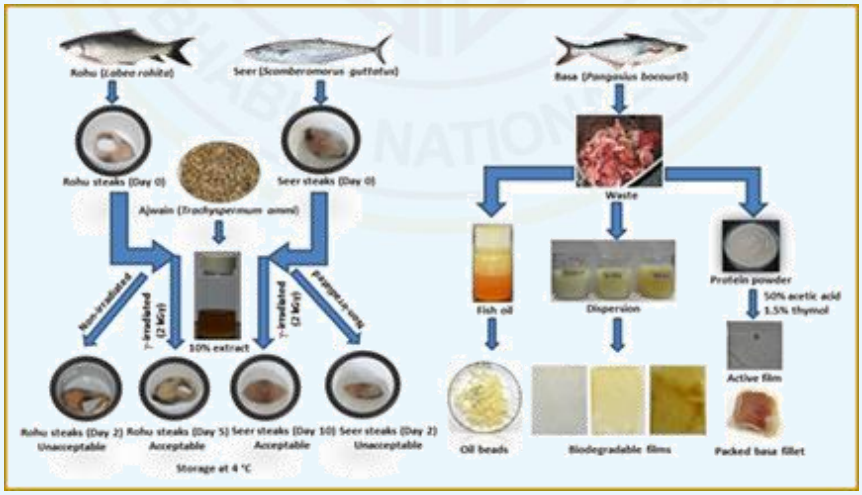

Development of value-added products from different fish

The efficient utilization of waste generated from other fish (basa) to produce encapsulated fish oil, biodegradable film and active film using thymol. The shelf-life of rohu and seer fish steaks were found to be 5 and 10 days respectively when treated with 10% ajwain extract and 2 kGy γ - irradiation at 4 °C storage. However, all non-irradiated samples (untreated or treated with extract) were spoiled on day 2. Hence, synergistic effect of extract and irradiation treatments were found in fish steaks shelf-life enhancement. The waste obtained from basa

was used to develop different products. (i) Extraction of oil from waste followed by encapsulation using sodium alginate.

The encapsulated fish oil had higher shelf-life of 12 days as compared to non-encapsulated fish oil with shelf-life lower than 4 days when stored at 25 °C under dark condition. (ii) Dispersion from waste was treated with 0, 10 and 25 kGy γ -irradiation followed by drying at 50 °C to obtain biodegradable films. The film obtained from dispersion treated with 10 kGy had higher quality such as high tensile strength and low water solubility as compared to other films. (iii) Protein powder obtained from waste was used to develop active film by adding thymol as an active ingredient. Active film was developed using 0.75% protein powder, 0.075% glycerol and 1.5% thymol in 50% acetic acid solution followed by drying at 25 °C. Basa fillets packed in this film gave the shelf life of 6 and 10 days when treated with 1 and 2 kGy -irradiation respectively at 4 °C storage. However, fillets packed in active film without irradiation treatment spoiled on day 2. Hence, synergistic effect of active film and irradiation was found in fillet shelf-life enhancement.

4.1.2 Molecular Investigations into the Process of *Plasmodial* Protein-Mediated Hemozoin Production and its Inhibition by Chloroquine

The thesis explores the critical challenge posed by malaria parasites, a pervasive global health concern affecting millions worldwide. With a staggering 247 million cases reported annually across 82 endemic countries, the urgency for effective treatments intensifies, particularly considering the growing resistance to frontline antimalarial drugs. At the heart of our investigation lies the physiological bottleneck of malaria parasites—the process of hemozoin production. This intricate mechanism involves the sequestration of cytotoxic free heme, generated during the digestion of host hemoglobin, into inert hemozoin crystals. While various theories abound regarding hemozoin formation, evidence suggests a pivotal role for protein-mediated conversion, notably involving heme detoxification protein (HDP). Yet, despite its significance, our understanding of both HDP and antimalarial drugs, particularly those of the quinolone family, remains incomplete.

To bridge these knowledge gaps, the work in the present thesis introduces the pyridine hemochrome assay, an advanced method surpassing its predecessors in accuracy and precision, ideal for studying HDP-mediated heme crystallization into hemozoin. Enabled by this assay, the substrate and the time kinetic experiments have been conducted in this thesis, validating the HDP's pivotal role in hemozoin crystallization and enhancing future antimalarial screening. The in-vitro study unveiled the new insights into chloroquine's mechanism, revealing its nuanced impact on hemozoin production by perturbing crystal nuclei formation and stability. Despite challenges in expressing soluble HDP, it could be managed to express a truncated version of HDP in soluble phase and underscore the importance of N-terminal residues in heme binding and transformation. Furthermore, the

conventional notion of HDP's isolated function has been challenged, proposing its interaction with detergents may influence hemozoin formation. These findings deepen the overall understanding of the malaria pathogenesis and prompt a re-evaluation of protein-detergent interactions, opening new research avenues. In summary, this thesis marks a significant advancement in combating malaria, offering valuable insights, and guiding future discoveries in the field.

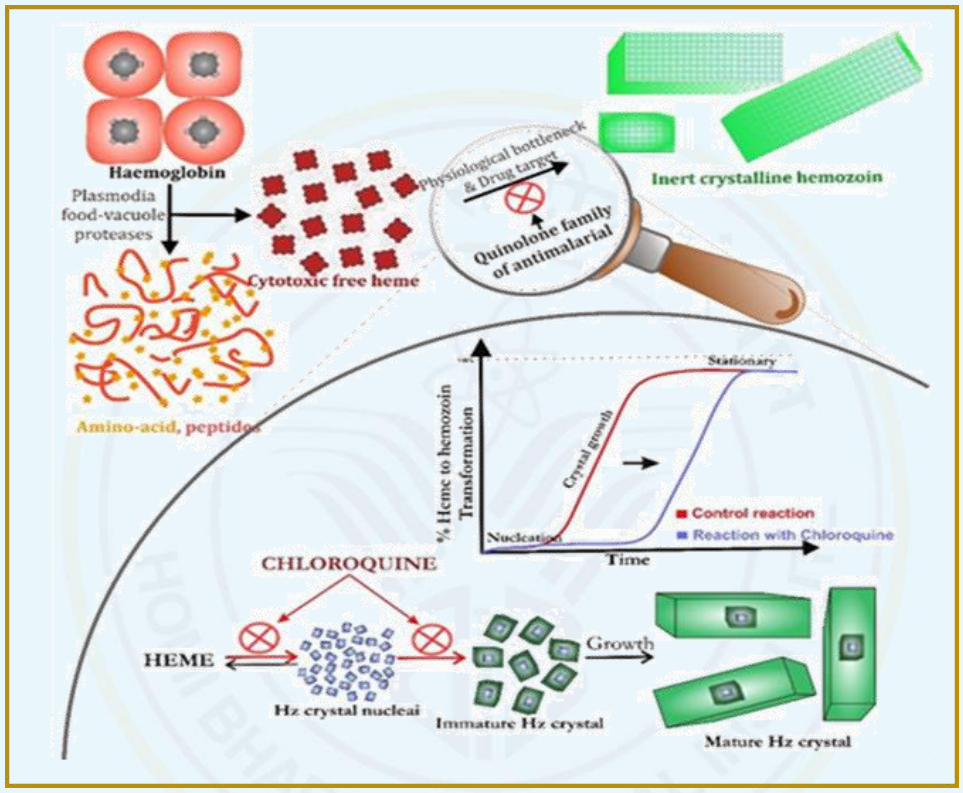

Schematic representation of chloroquine's mechanism of action, perturbing nucleation events during heme-to-hemozoin transformation

4.2 Institute of Mathematical Sciences, Chennai

4.2.1 Elucidating and Leveraging Design Principles towards Realistic Reconstruction of Boolean Models of Gene Regulatory Networks

GRNs may be modelled as a Boolean network (BN) in which nodes and directed edges represent genes or proteins and their interactions respectively. In BNs, a gene assumes a binary state and its temporal dynamics is governed by the state of its regulators via a regulatory logic rule (or Boolean function (BF)). The dynamics of BNs under synchronous update (in which all nodes are updated simultaneously) lead to fixed point attractors (which correspond to cellular phenotypes) or cyclic attractors. Advances in experimental techniques including omics approaches have fostered the reconstruction of real Boolean GRNs for several

cellular processes in a wide range of species. It is now imperative to understand whether the regulatory logic rules in such models are just random or possess distinct features.

In the present thesis, the nature of regulatory logic rules has been systematically investigated by first compiling a dataset of 2687 logic rules from 88 reconstructed discrete models, and then examining in that dataset, the preponderance of various known types of biologically meaningful BFs. Two types that were particularly preponderant in the dataset were read-once functions (RoFs) and nested canalyzing functions (NCFs). This was explained by showing that RoFs and NCFs have the minimum complexity at a given number of inputs (k) and given bias (P) in terms of the Boolean complexity and the average sensitivity respectively. Furthermore, the abundance and biological plausibility of more recently published types of logic rules namely, link operator functions (LOFs) and composition structures, respectively, were also explored. Even if the network structure of a GRN was kept fixed, there was generally a very large number of combinations of BFs (across all nodes) that can recover the same set of biological fixed points (or cellular phenotypes), and it was usually unclear how a certain model or subset of models were chosen as the biologically relevant ones during reconstruction.

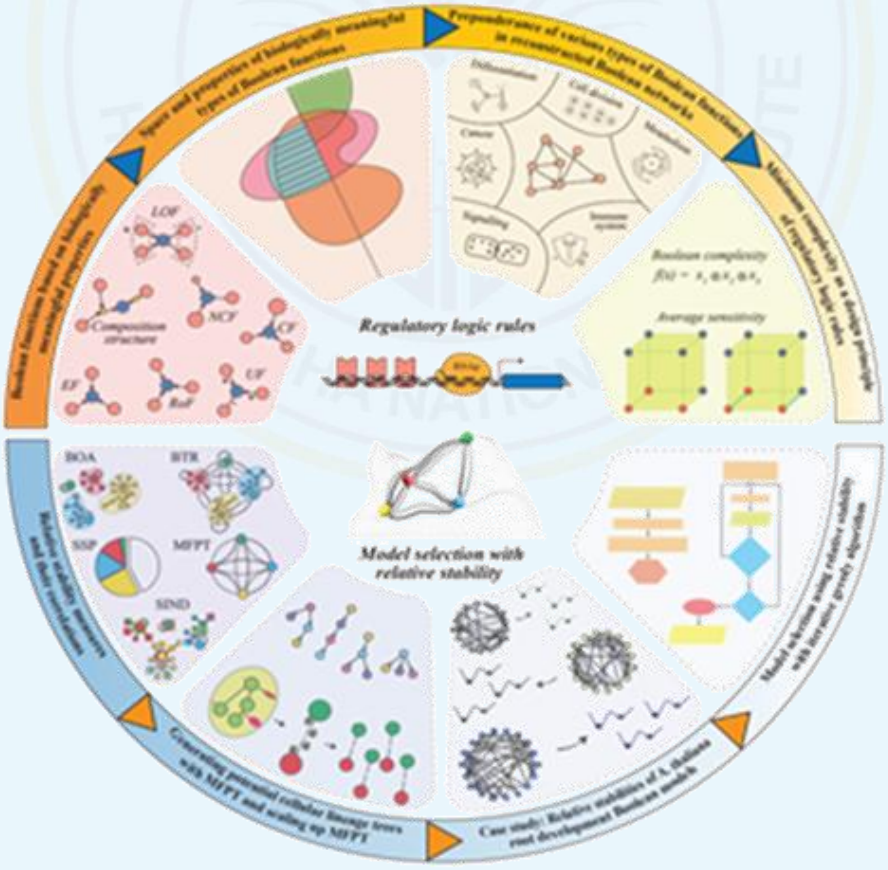

Summary of the research on various types of regulatory logic rules that are biologically meaningful and the methods associated with a model selection framework for Boolean gene regulatory networks using relative stability as a selection criterion

In the thesis, the relative stability of cell states derived from its developmental landscape was leveraged to develop a framework of model selection from an ensemble of models that were otherwise equally plausible in the cell states they recover and in the type of logic rules they employ. It has been demonstrated that the present model selection framework on the root development Boolean GRN of *Arabidopsis thaliana* and could provide several improved models over the original one. Overall, present thesis has elucidated the design principles of regulatory logic in GRNs and leverage those principles to develop methods for realistic reconstruction of Boolean models of biological systems.

4.3 National Institute of Science Education and Research, Bhubaneshwar

4.3.1 Genetic and Epigenetic Regulation of Candidate Genes Associated with Pseudoexfoliation

Pseudoexfoliation (PEX) is a systemic disease manifesting prominently in the eye. It is characterized by deposition of white flaky extracellular material in the tissues and organs. The early stage of deposition termed as pseudoexfoliation syndrome progresses in approximately 50% individuals to the advanced glaucomatous stage leading to irreversible blindness. Pseudoexfoliation accounts for most secondary glaucoma cases worldwide. It is a multifactorial disease with genetic and epigenetic factors implicated in its causation and progression. Destabilized extracellular matrix (ECM) and proteotoxic stress are characteristic features of PEX.

The study identified some regulatory mechanisms that might contribute to PEX pathogenesis, as shown in Figure below. (1) The functional risk variants in fibulin-5 (FBLN5) affect its expression which results in a destabilized ECM. (2) Upregulation of cluster in might contribute to cytotoxicity by getting deposited in the exfoliative material resulting in the unavailability of the chaperone for maintaining proteostasis. Regulatory single nucleotide polymorphisms in cluster in (CLU) and promoter hypomethylation could be responsible for the increased expression of CLU in PEX pathogenesis. Hypomethylation of CLU promoter due to decreased expression of the DNA methyl transferase 1 (DNMT1) results in increased access of Sp1 to CLU promoter triggering its enhanced transcription. (3) Increased cluster in induces the expression of the Wnt antagonist Dickkopf-1 (DKK1), which ultimately produces toxic protein aggregates detrimental to the cell. Increase in DKK1 results in an upregulation of the Rho kinase, ROCK2, which in turn regulates the expression of vimentin. This aberrant expression of these proteins contributes to the formation of exfoliative material. (4) In parallel, decreased expression of GSTP1 in patients results in increased oxidative stress that adds to the impaired cytoprotective mechanisms in PEX pathogenesis.

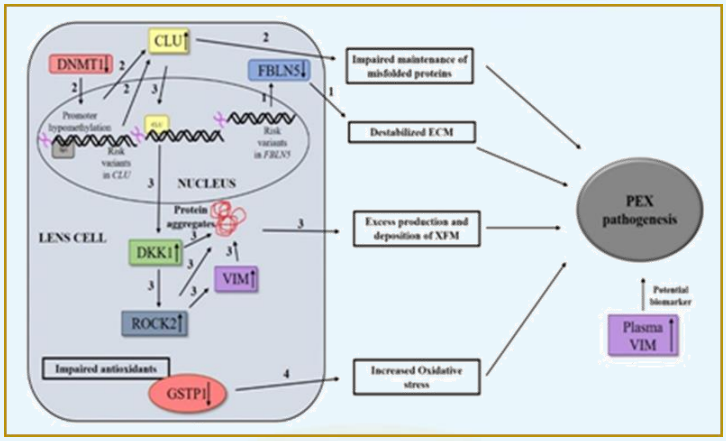

Differential regulation of CLU, FBLN5, VIM and GSTP1 contribute to PEX pathology

4.3.2 Structure-Function-Dynamics of PanPL, a Bacterial Polysaccharide Lyase from PL-5 Family

The research work in the thesis incorporates the detailed characterization of structure-function-dynamics aspects of a bacterial polysaccharide lyase PanPL from PL-5 family found in a nosocomial pathogen *Pandoraea apista.* The biochemical studies of PanPL with alginate and poly mannuronic acid substrates revealed PanPL to be an alginate specific, endolytic, allosteric enzyme ((iii) B-C in schematic). The crystals of PanPL were obtained across the pH spectrum from pH 3.5 to pH 8.5 (i() in schematic). The crystal structures were found to maintain the characteristic pseudo-toroidal fold forming a closed catalytic tunnel covered by a N-terminal loop lid (N-loop-lid) ((iv) in schematic). The substrate bound crystal structure of PanPL with tetra-ManA was determined and the interacting residues in the tunnel were catalogued ((vi) in schematic). The structural flexibility of the N-loop- lid of PanPL characterized by B-factor analysis, ensemble refinement along with the electrostatic surface charge calculation as a function of pH provide the basis of grouping PanPL structures into their active and inactive/low active states. Our B- factor and ensemble refinement analyses on the substrate bound crystal structure revealed substrate induced fluctuation at the N-loop-lid. In addition to that, the presence of hidden conformational states in the crystal structures were revealed by the ensemble refinement analysis. Interestingly, the MD simulation studies showed the presence of a hidden but transiently accessible open state suggesting the inherent flexibility of N-loop-lid ((vii) in schematic)). The research work reported a four residues insertion at N-terminal helix near the N-loop-lid which was suggested to assist PanPL in selecting closed state with fluctuation over open-close state transition ((vii) in schematic)). Further the point mutations were created at the entry and the exit site of the tunnel to rewire the electrostatic network inside the catalytic tunnel which could alter the catalytic and dynamic behaviour of the enzyme ((viii) in schematic)). Additionally, the future aspects of the thesis work were discussed to design engineered enzymes to perform various functionalities and serve the medical and industrial fields.

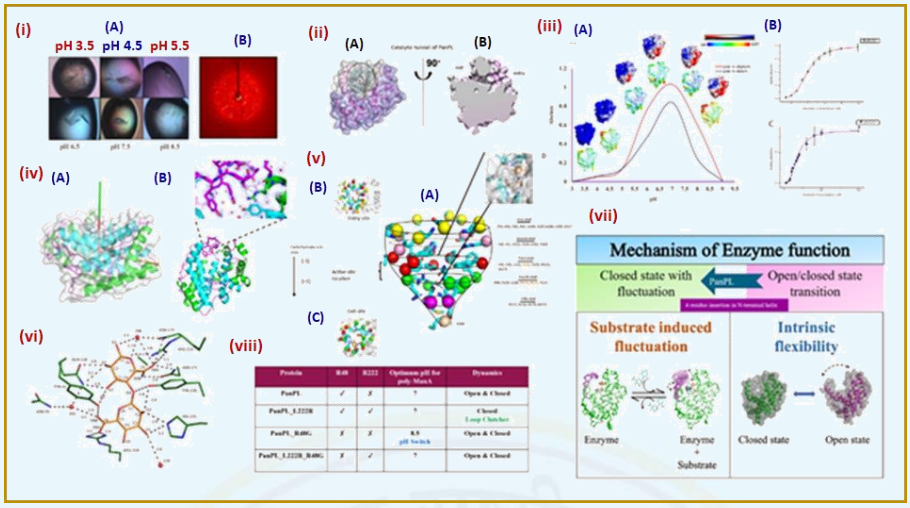

Schematic showing graphical summary of structure, biochemistry and dynamics of PanPL: (i) The crystal images of PanPL at (A) different pH, the diffraction image (B); (ii) The catalytic tunnel of PanPL (A-B); (iii) The pH scan of enzyme activity, B-factor and electrostatic surface charge of PanPL (A), The enzyme kinetics plot of PanPL shows positive cooperativity(B-C); (iv) The pseudo-toroidal fold of PanPL(A), N-loop-lid of PanPL 42-52aa (B); (v) tunnel architecture of PanPL, wine glass architecture (A), entry site(B), exit site(C), active site residues(A). (vi) Enzyme substrate interactions; (vii) Distinct modes of PanPL dynamics showing intrinsic flexibility and substrate induced fluctuations, four residue insertion selects the closed state with fluctuation mechanism. (viii) Effect of flanking Arginine residues in the tunnel on catalysis, dynamics, and mechanism

4.3.3 Development and Characterization of a Drug-Loaded Smart Injectable Hydrogel as a Drug Delivery Systems for the Treatment of Rheumatoid Arthritis

Rheumatoid arthritis (RA) is an autoimmune condition that accompanies chronic inflammation of joints with limited therapeutic options. This disease dramatically affects patients' quality of life, as no single treatment can completely halt the disease's progression. This thesis described the development of polymer systems for delivering hydrophobic drugs for treating joint conditions, such as RA and OA. This approach immensely abrogated the pharmaceutical limitations of the loaded drugs (MTX and PEITC) when prepared as nanoparticles. Further loading these NPs into a hydrogel system enabled co-delivery, sustained release, injectability, and thermo-responsive behaviour. A probable mechanism of combinational hydrogel in treating RA is shown in the schematic below. The DD NP HG, when injected IA into the FCA- induced animals, showed marked amelioration of chronic inflammation and assisted in restoring bone morphology in RA rats.

Further, DD NP HG has been shown to enhance the anti-inflammatory efficacy and reverse cartilage disruption through a synergistic effect between two nano-particulate forms of MTX and PEITC, which can effectively improve the drawbacks of free forms of both drugs. From the thesis work, it has been successfully optimized and thus fabricated a novel smart

hydrogel-based delivery system for poorly soluble drugs to either deliver them singly or in combination to attain greater efficacy. Such nano- delivery systems have significant applications in diseases that require chronic or multi-drug treatment.

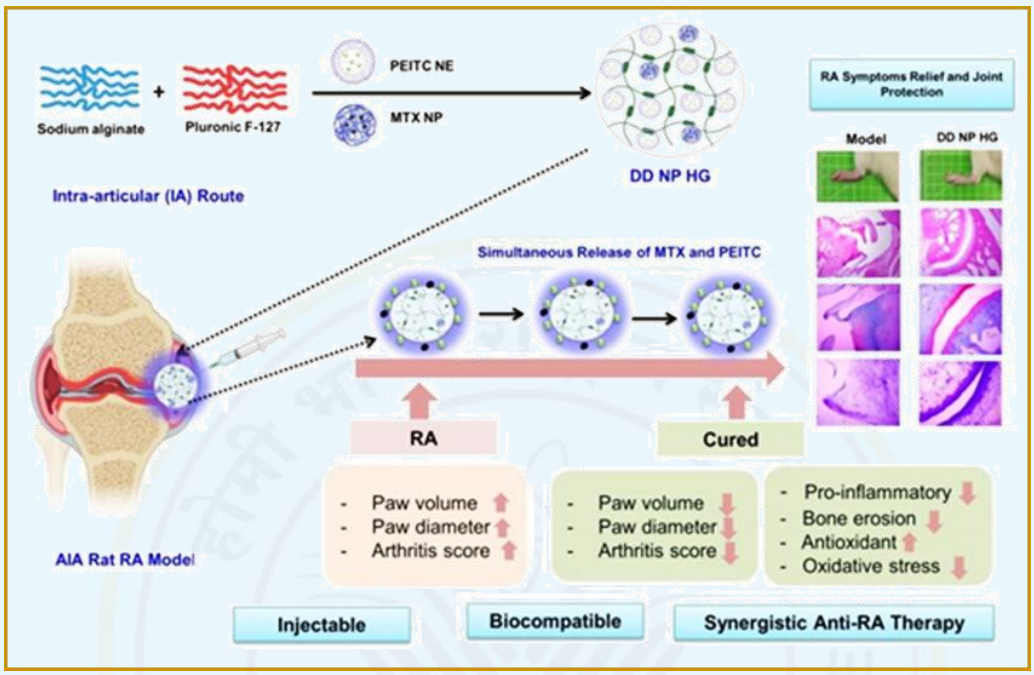

A probable mechanism of combinational hydrogel (DD NP HG) in treating RA

4.3.4 Role of TLR4 in Chikungunya Virus (CHIKV) Infection and Associated Altered Cell Mediated Immune Responses

Starting from its discovery in 1952, the Chikungunya virus (CHIKV), a member of genus: *Alphavirus* and family: *Togaviridiae*, has shown its re-emergence across the globe several times. As it is a mosquito-borne disease (vector is *Aedes sp.*), the densely populated areas with a lack of effective mosquito-control facilities were specifically reported for the repeated CHIKV outbreaks. To date, the lack of available vaccines or specific medications also demonstrates the severity of the disease (1,2). The major initial symptoms of CHIKV-infected patients are high fever, headache, polyarthralgia, and myalgia which may further lead to failure of cardiovascular, neuronal, renal, or respiratory systems in later stages and therefore, permanent physical disability.

The crucial factor of CHIKV pathogenesis is massive pro-inflammatory cytokine burst due to the activation of host immune responses. The reports reveal that the marked upregulation of tumor necrosis factor (TNF), interleukin (IL)- 6, 4, 1β and 12 in mouse as well as human macrophages via p38 and Jun N-terminal protein kinase (JNK)-mitogen-activated protein kinase (MAPK) mediated pathway is associated with polyarthralgia and CHIKV infection mediated fever (CHIKF). However, the initial cellular pathways associated with CHIKV-driven

activation of the host immune system are yet to be explored. Interestingly, the literature reveals that toll like receptor 4 (TLR4), an innate immune system component, regulates pro-inflammatory responses in various cases of microbial infection, cancer, and autoimmunity. Several pro- inflammatory clinical irregularities such as necrotizing enterocolitis (NEC), and inflammatory bowel disease (IBD) are well-reported to be associated with TLR4-directed regulation. Moreover, *in vivo* inflammation models such as mouse sepsis or lung injury model specifically demonstrate the positive regulation of TLR4 towards inflammation and modulation of host immune responses. Furthermore, some of the structural proteins of respiratory syncytial virus (RSV), foot and mouth disease virus (FMDV), and SARS-CoV2 have recently been reported to interact with host TLR4. Therefore, the above-mentioned studies reveal the possibility that TLR4 might play a pivotal role in viral entry as well as disease manifestation in the host.

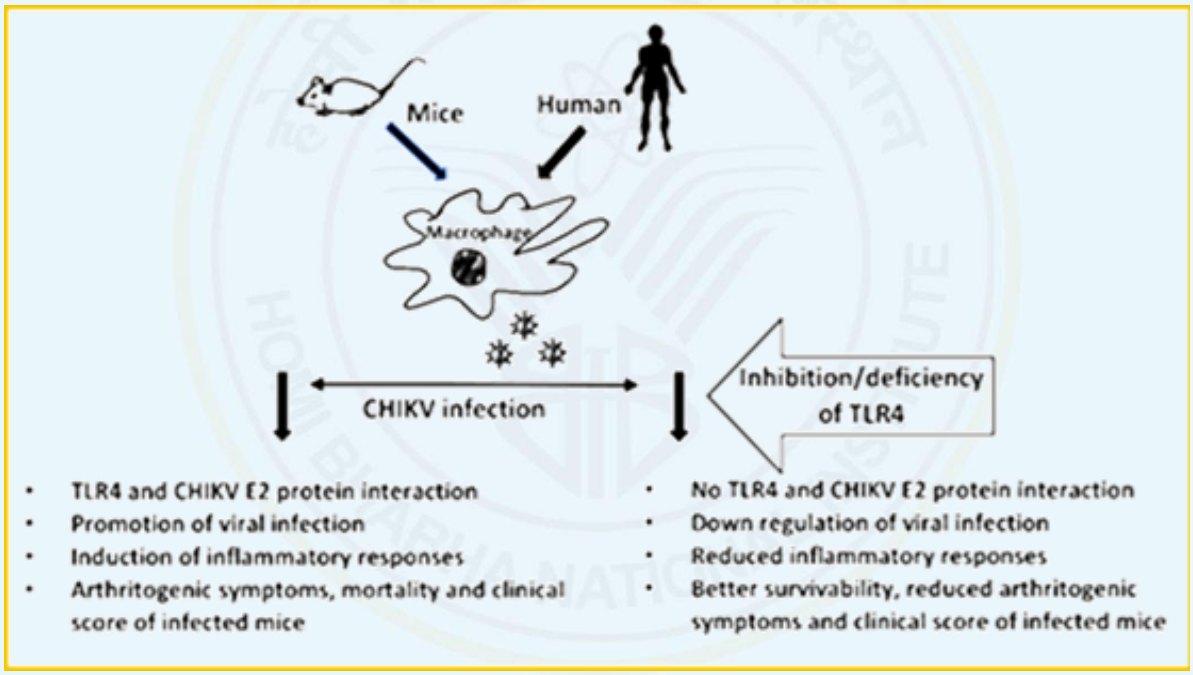

Possible association of TLR4-driven regulation of CHIKV infection, inflammatory responses, and interaction with viral E2 protein

The CHIKV-driven activation of host immune systems and rise in pro-inflammatory cytokines (cytokine storm) via the MAPK pathway has been reported in literature. Since host TLR4 activation is already reported to be associated with MAPK activation and pro-inflammatory cytokine release (such as TNF), the possible connection between CHIKV infection and host TLR4 activation is yet to be explored. Hence, it was hypothesized that host TLR4 might be associated with the regulation of CHIKV infection and subsequent host immune responses. Therefore, the study is designed to explore the possible regulation of TLR4 on CHIKV infection and associated host immune responses using *in vitro* models of different origins, *in silico* as well as *in vivo* mice model.

4.3.5 Role of Intestinal Microbiota on Exogenously Induced Colitis and Associated Physiological Changes: A Comparative Analysis of DSS and Antibiotic Treatment

The balanced gut microbial composition of the host helps to maintain physiological homeostasis and health. A novel paradigm to understand the role of a microbe on host health is to perturb the gut microbial composition (abundance and diversity). The perturbation can be done in a direct or indirect way. Present study uses antibiotics for direct or Dextran sulfate sodium (DSS) for indirect perturbation of the gut microbiota. All kinds of manipulations in this study were done on rodents' model, in C57BL/6 (Th1 biased) and BALB/c (Th2 biased) mice. Results from the current study revealed that antibiotic treatment had a more immediate effect on the alteration of gut microbial composition and diversity. However, the dysbiotic condition was comparatively long-lasting for the DSS-treated group. The impact of immune dysregulation was also more profound on the DSS-treated group than the antibiotic-treated groups. Moreover, the DSS-treated group of both mice strains showed typical diseased symptoms, which resembles the pathophysiology of human colitis. The current study with DSS treatment also helped us establish a new model system for studying colitis. A multi-omics approach and mass spec-based metabolomics approach were utilized in the current study to understand the onset and etiology of colitis. Present study also invented a totally new data analysis methodology for the analysis of the omics data. The results revealed that a) DSS could trigger transient inflammatory responses in both C57BL/6 and BALB/c mice at higher dosage of DSS (5%), b) the Th2- bias of BALB/c mice could alleviate inflammation to restore normalcy at reduced (2.5%) DSS dosage. However, C57BL/6 mice maintained severe inflammation even at the reduced (2.5%) DSS dosage. The differential immune bias of the mice used in this study could be the primary reason for different inflammatory responses. The cause of different responses could be due to differential a) gut barrier function, b) SCFA production, c) psychological stress responses, e.g., anxiety and depressive behavior, and d) an altered gut microbial composition in C57BL/6 and BALB/c mice. Moreover, the multi-omics approach helped us discover a) unique metabolic and microbial markers and b) key metabolic pathways associated with colitis severity. These biomarkers could be used in diagnostics and pathways to intervene and understand disease etiology. The severity of the disease could be controlled by modifying the gut microbial composition of the host. Antibiotic is one of the most widely used approaches to treat the altered gut microbial profile of colitis patients. In this study, it has been tried to understand how an intervention strategy can be suggested by understanding gut microbial dysbiosis for colitis. However, reports also suggested that repeated antibiotic exposure is probably the key reason to enhance colitis disease susceptibility.

The current study concludes that in Th1- biased C57BL/6 mice, antibiotics treatment rescued the DSS treated group from the diseased condition by activating the carbohydrate and nucleotide metabolism pathway, which converted the pro-inflammatory status of the host in an anti-inflammatory condition. On the other hand, early exposure to antibiotics increases

disease susceptibility by activating pro-inflammatory lipid and amino acid metabolism pathways. The scenario was quite different in Th2-biased BALB/c mice. Antibiotic treatment always activated the carbohydrate metabolism pathway, which ultimately provides a therapeutic effect against colitis, whether administered before or after the DSS treatment.

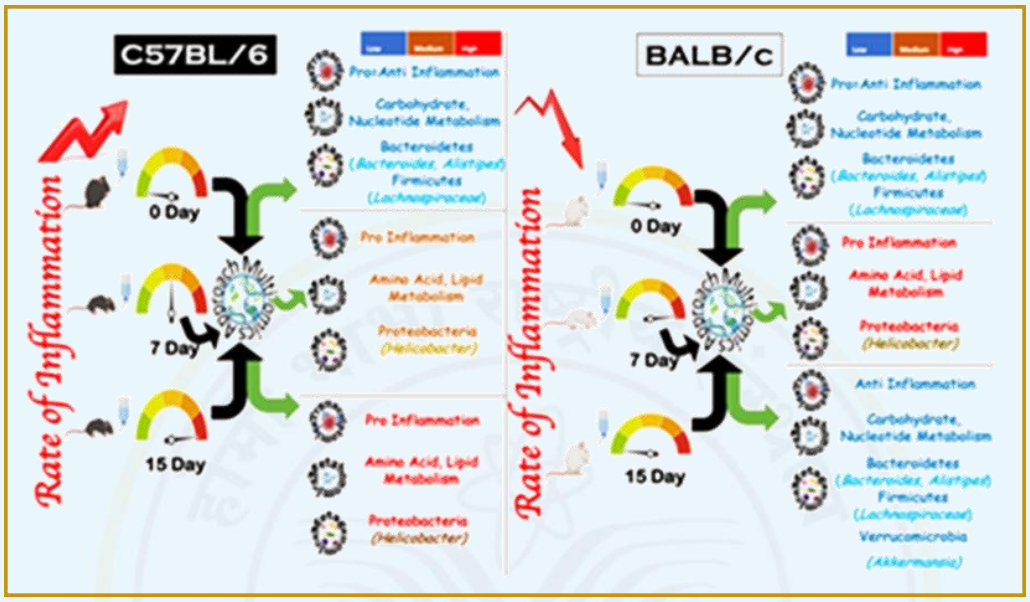

Schematic of the comparative analysis of DSS and antibiotic treatment

4.4 Saha Institute of Nuclear Physics, Kolkata

4.4.1 Lamins and DNA Damage in Context of Gynaecological Cancers

Nuclear lamins act as the major determinant of nuclear mechano-morphological features which are potent regulatory factors for clinical diagnostic approaches to analyse the malignant potential of cancer cells. This thesis sheds light on ovarian cancer where modulation of neoplastic changes has been associated with the extent of alteration in nuclear functions and morphology. The first part unravels the consequences of nuclear morphological alterations regulated by nuclear lamins and its clinical aspects in ovarian cancer and the second part attempts to unravel the regulatory circuitry behind the role of lamin A in DNA damage repair. Ovarian cancer is the eighth most prevalent cancer among women, the seventh most common cancer diagnosed globally, and the third most frequent disease among women in India. A strong connection between lamin proteins and various kinds and subtypes of ovarian cancer has been the subject of several recent investigations. Lamins act as a complex regulatory machine in various cancers but whether its expression alteration is a cause or a consequence of a particular type and stage of cancer calls for deeper investigation. To potentially exploit its function, a better understanding of the pathobiology underlying both mechanical stability and genome protection is of utmost necessity. The journey began with the aim to study the expression and morphometric distribution of nuclear lamin proteins as specific parameters in

ovarian cancer and normal tissues. In a pilot study, exhaustive imaging of ovarian cancer versus normal tissue was performed, and a dual pipeline architecture was developed combining the matrices of nuclear morphometric parameters based on lamin A and B staining with a novel Deep Hybrid Learning model which enabled to differentiate between cancerous and normal samples successfully. In line with this observation, the study further continues to explore the role of lamins in ovarian cancer with emphasis on DNA damage repair. This summarised and collated for the first time the molecular cues behind the role of lamin A in the maintenance of genomic stability, cellular viability, apoptotic evasion, and resistance to DNA damaging agents in the context of high grade ovarian serous carcinoma. This study highlights new avenues unravelling the role of upregulated lamin A in confronting chemically induced genomic instability in the context of high-grade ovarian serous cancer. A simultaneous aim was to explore the mechano-physiological properties of an ovarian cancer nuclei with high lamin A level. Some preliminary observations of this study have been discussed.

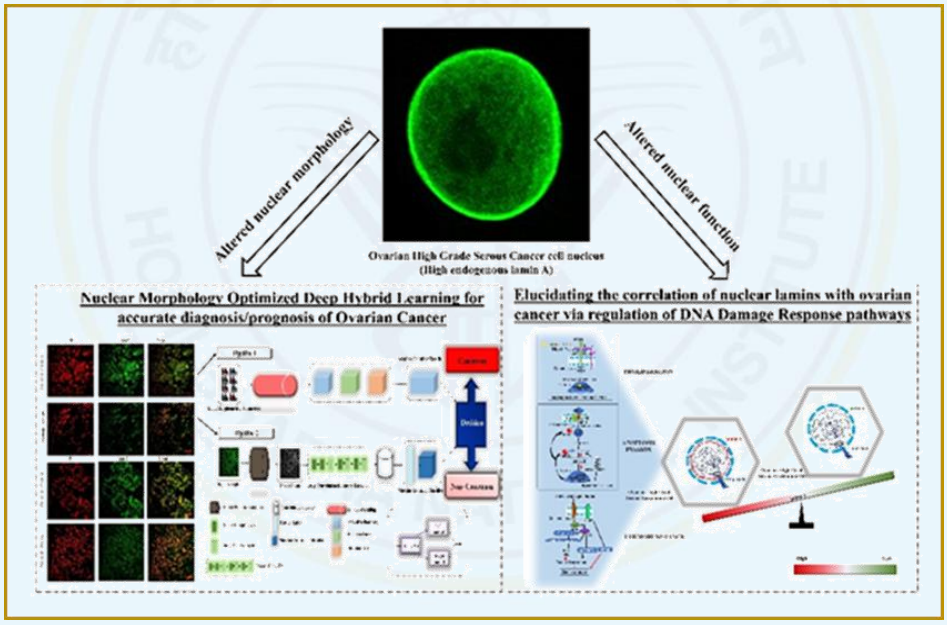

Schematic showing the role of nuclear lamins in restoration of nuclear and cellular homeostasis in ovarian carcinogenesis. Alterations in two major nuclear attributes governed by nuclear lamins and their implications

4.4.2 Role of Lamin A Mutations in Myogenesis

Lamins are nucleoskeletal proteins of mammalian cells that stabilize the structure and maintain the rigidity of the nucleus. These type V intermediate filament proteins provide necessary tensile strength to the nucleus. Single amino acid missense mutations occurring all over the lamin A protein form a cluster of human diseases termed as laminopathies, most of which principally affect the muscle tissues responsible for load bearing functionalities of the body.

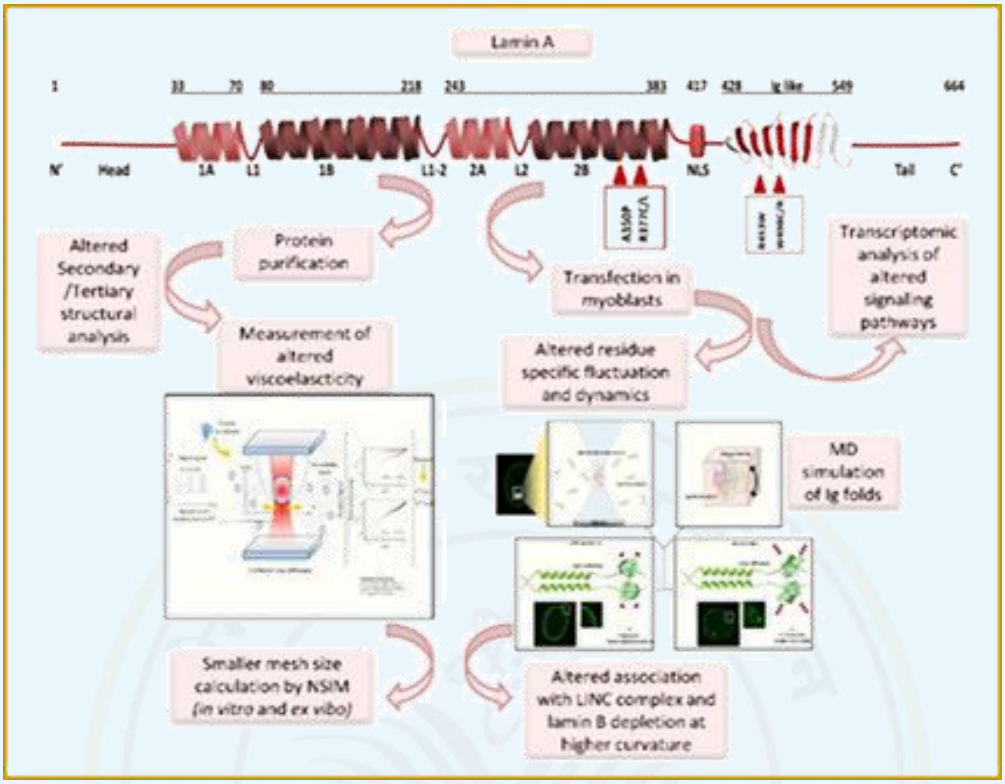

Schematic representing the effect of lamin A and its mutants in the pathogenesis of DCM and EDMD

The research work presented in the thesis elucidates the role of 6 severe lamin A mutations namely, A350P, R377C, R377L, R453W, W498C and W498R in human and mice myoblasts in the development of disease phenotypes. The application of active microrheology was shown to investigate any alterations in the viscoelastic parameters of the mutant A350P protein meshwork in vitro, which might translate into possible changes in nuclear plasticity. Findings were confirmed from this method by imaging both the wild type and mutant lamin A networks using a super resolution microscope, and changes in the mesh size was reported which corroborated our measured changes by OT. The effects of R453W, W498C and W498R were elucidated on the dynamics and flexibility of the Ig-fold domain and its consequence on the full-length lamin A in terms of assembly into lamina by live cell imaging, FCS, and molecular dynamics (MD) simulations. From our experimental observations, the novel and powerful “nanomachine” like activity of the Ig-fold domain was reported, capable of rapid movement which “tugs” the full-length protein through the viscous nucleoplasm to the nuclear periphery in the process of self-association into a giant polymeric laminar structure. The mutants could be demarcated to have an anomalous association mechanism leading to misshapen lamina. The effects of different dilated cardiomyopathic mutations were also investigated on the structural alterations and dynamics of the full-length protein by biophysical characterization. Present thesis has further studied the cellular context by inducing a static compressive force on human skeletal muscle cells and C2C12 cells bearing lamin A mutations and explored the altered signalling pathways therein.

4.5 Tata Memorial Centre, Mumbai

4.5.1 Evaluation of Phytochemicals with Immunomodulatory Activity for Graft-Versus-Host Disease Prophylaxis

Acute graft-versus-host disease (GVHD) is a major cause of non-relapse mortality following allogeneic hematopoietic stem cell transplantation (allo-HSCT). Current prophylactic regimens show limited clinical success and are associated with severe toxicities, the development of steroid-refractory GVHD, increased incidence of infections, and relapse. Furthermore, it is now well established that immunosuppression is not the best strategy for acute GVHD prophylaxis. Thus, the development of novel strategies/pharmacological agents that can modulate the donor immune response in favor of antitumor immunity while suppressing allogeneic immune responses is an unmet need in the field of allo-HSCT. The present study aimed to identify and develop phytopharmaceuticals with immunomodulatory activity for prophylaxis of acute GVHD. Our study identified 5-hydroxy-1,4-naphthoquinone (5NQ) or juglone as the lead molecule after screening a phytochemical library of 136 compounds.

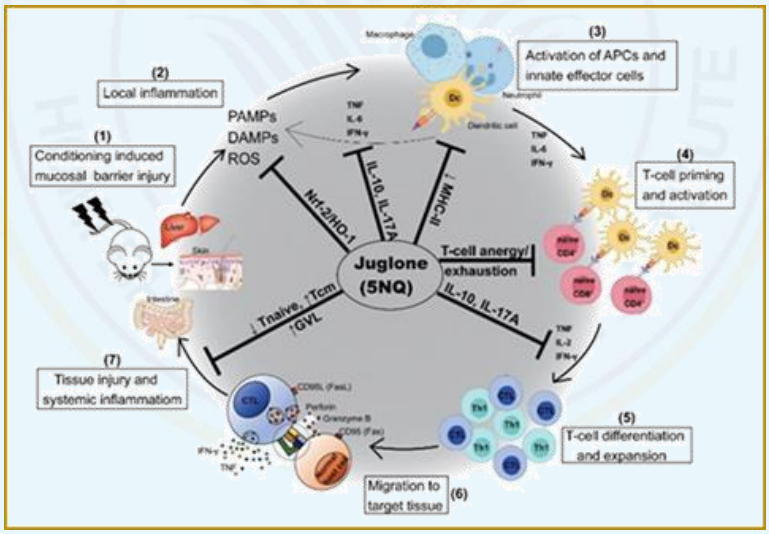

Lead molecule juglone exhibited immunomodulatory activity like upregulating antioxidant response, inhibiting proinflammatory cytokines, promoting anti-inflammatory cytokines, inhibiting activation of dendritic and CD4⁺ T cells, inhibiting lymphocyte proliferation, inducing exhaustion of CD4⁺ T cells, and promoting central memory T cells and thereby preventing GVHD development while preserving GVL activity in murine model of allo-HSCT

The study established the cytotoxic T cells ($CD8^+$ granzyme B^+). Oral administration of 5NQ resulted in a decrease in the number of $CD4^+$and $CD8^+$ naïve T-cells and an increase in $CD4^+$ and $CD8^+$ central memory T cells. Our mechanistic studies revealed that 5NQ upregulated Nrf-2/HO1 antioxidant response signaling in leukocytes by modulating cellular redox status. In addition, our study established the safety prolife of 5NQ which can be used to derive a human equivalent dose of clinical translation.

4.5.2 Imaging Molecular Interaction Dynamics in Drug Resistance Breast Cancer

Understanding the molecular drivers of cancer growth and developing precise therapies for distinct cancer subtypes is of paramount importance. Our research reveals that the mutations within the dimerization domains of HER2 can instigate a shift in receptor interactions and signaling patterns, resulting in the emergence of aggressive, inherently resistant forms of HER2-positive breast cancer. These mutations, namely S305C, G309A, S310F, S310Y, and P523S, were the focus of the present investigation. In the present research work, extensive molecular dynamics simulations have been utilized to study how these mutations affect the structure and interactions of HER2. One of our key findings was that HER2-WT and S305C mutants formed stable HER2:HER2 interactions, while G309A, S310Y, and P523S mutants displayed unstable interactions instead preferred HER3 as its partner. This change in interaction patterns was not just structural; it also had significant downstream consequences. HER2-WT and S305C expressing cells preferred the MAPK signaling pathway, whereas G309A, S310Y, and P523S mutants switched to the PI3K-AKT signaling pathway. Importantly, it has been discovered that these mutants failed to respond to two commonly used breast cancer drugs, trastuzumab and neratinib. This resistance was further validated in mouse models, which validated our *in-vitro* findings. Inhibition of the AKT pathway using AKT-IV proved to be effective against G309A, S310Y, and P523S mutants, while HER2-WT and S305C mutants responded better to inhibition of the ERK pathway using trametinib. Furthermore, our study revealed that tucatinib, a relatively new drug, held promise in limiting the growth and invasiveness of breast cancer cells expressing HER2 mutants. This suggests that tucatinib could be a valuable addition to the arsenal of treatments for HER2-positive breast cancer. Overall, our research provides comprehensive insights into how specific mutations in HER2's dimerization domains can lead to structural and functional changes that render breast cancer cells resistant to standard therapies. These findings pave the way for more targeted and effective treatment strategies for HER2- positive breast cancer patients.

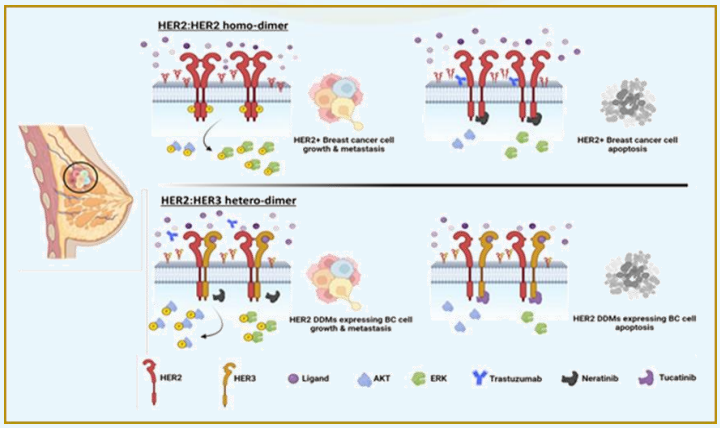

Schematic representation of the receptor switching in HER2 positive BC patients due to HER2 dimerization domain mutations (DDMs). Subsequent downstream signaling switch from MAPK to AKT causes targeted therapy resistance. However, tucatinib can be used to kill HER2-WT and its DDMs expressing cells

4.5.3 Structural and Functional Basis to Evaluate PML-RARA Response to Arsenic Trioxide

The study focuses on the role of mutations in driving resistance to targeted therapies, ATO and ATRA, used against acute promyelocytic leukemia (APL) caused by the PML-RARA fusion protein. The research employs a multidisciplinary approach to investigate the structural and functional consequences of mutations associated with resistance. The findings are: h-PML-RBCC domain characterized as a stable tetramer and its interaction with ATO leads to higher- order oligomerization and aggregation. ATO-resistant mutations C213R, A216V, L217F and L218P destabilized PML-RBCC protein structure and ATO-binding pocket by altering nearby cysteine residues. PML-B2 motif exists in dimeric form in solution and its crystallization was optimized. The successful purification and characterization of PML-B2 mutations were accomplished. RARA-LBD-WT was co- crystallized with ATRA. Q276/W276 mutation led to disruption in electrostatic interaction between RARA-LBD and ATRA. Additionally, S287W and G391E impact the protein stability and conformation. These mutations significantly alter the structure of RARA-LBD and its ATRA binding pocket. The successful purification and identification of the full-length PML-RARA (97kDa) has been achieved. Contribution to Understanding Resistance Mechanisms: These findings offer a deeper understanding of how mutations in crucial domains of PML-RARA contribute to resistance mechanisms against ATO and ATRA therapies. By uncovering the structural and functional consequences of these mutations, the study provides valuable insights into potential avenues for improving the effectiveness of therapies against APL.

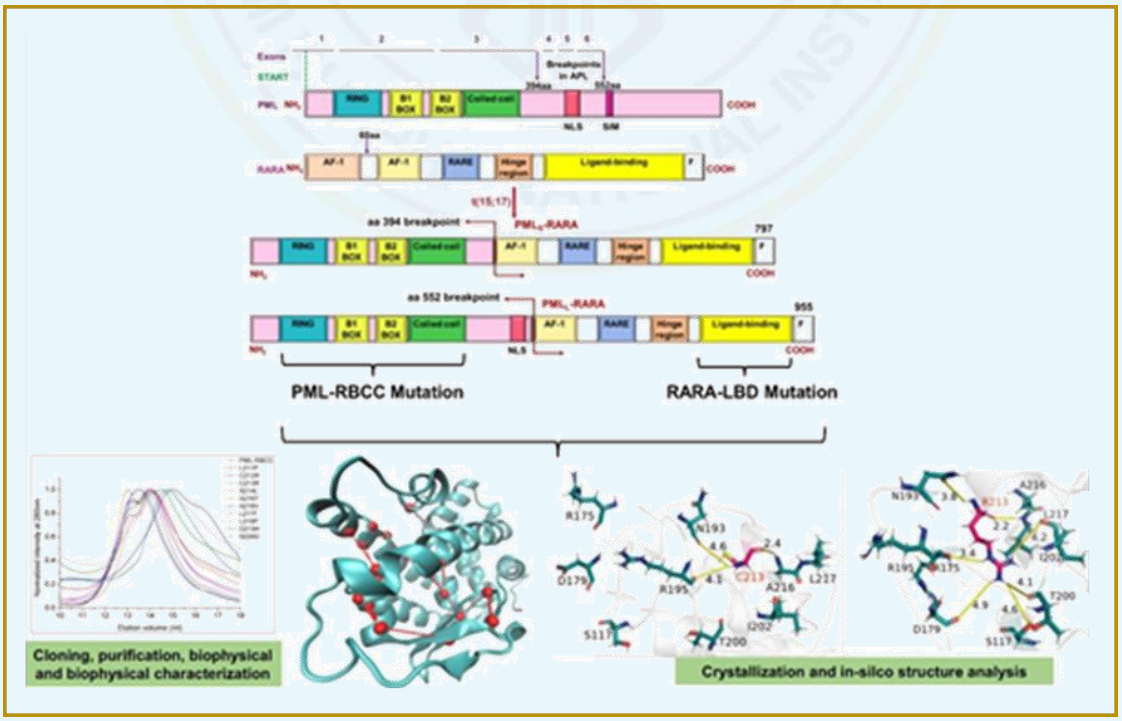

Schematic representation of the domain structure of PML, RARA, and PML-RARA, detailing the multi-modal characterization of clinically identified mutations resistant to ATO and ATRA in APL pathogenesis

4.5.4 Deciphering the Role of Mcl-1 in Stress and Autophagy in Oral Cancers

Mcl-1, distinguished by its distinctive structural attributes, diverges from other members of the Bcl-2 family by engaging in various physiological functions. This study delves into the unconventional role of Mcl-1 concerning radiation-induced DNA damage and autophagy within oral cancer cells. The investigation underscores how ionizing radiation triggers the upregulation of Mcl-1, which subsequently relocates to the cell nucleus, facilitating the activation of ATM and the ensuing downstream signaling within the homologous recombination (HR) pathway. Intriguingly, the study's data concurrently reveals that Mcl-1 expression impedes the autophosphorylation of DNA-PKcs, interfering with the non-homologous end- joining (NHEJ) pathway. Furthermore, the research suggests that neither the BH-1 domain nor the BH-3 domain of Mcl-1 significantly impacts the activation of ATM and the HR pathway. In parallel, the study explores the response of oral squamous cell carcinoma (OSCC) cells to ionizing radiation, uncovering that these cells resort to autophagy as a survival mechanism when faced with radiation-induced stress. Notably, Mcl-1 appears to play a pivotal role in the initiation of autophagy, particularly in clearing damaged mitochondria. In the absence of Mcl-1, the accumulation of damaged mitochondria suggests a potential deficiency in mitophagy, the selective autophagic process responsible for clearing these dysfunctional organelles.

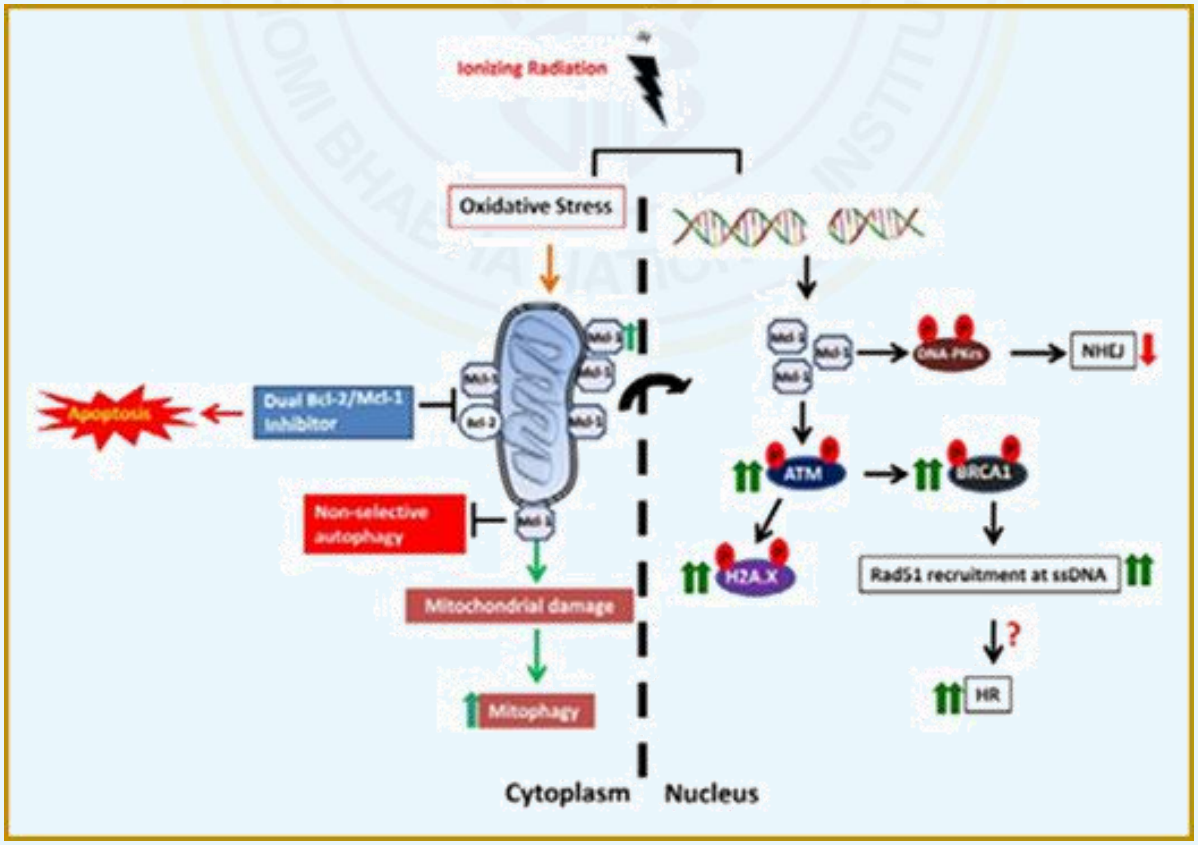

Proposed model for mode of action of novel compounds targeting Bcl-2 and Mcl-1 and role of Mcl-1 in radiation induced autophagy and DNA damage repair

The study further assesses two categories of bicyclic compounds, benzimidazole, and flavonoid, for their anti-proliferative effects on oral cancer cells. Remarkably, two compounds emerge from this screening process, exhibiting not only a strong affinity for Bcl-2/Mcl-1 but also demonstrating the ability to activate the canonical pathway of apoptosis at lower IC50 values compared to single-specific inhibitors targeting Bcl-2 and Mcl-1.In summary, this study demonstrates Mcl-1's multifaceted role in promoting the HR pathway for precise DNA repair while concurrently regulating autophagy to clear damaged mitochondria resulting from exposure to ionizing radiation. Additionally, it highlights the discovery of novel compounds with enhanced inhibitory activity compared to conventional Bcl-2 and Mcl-1 inhibitors, shedding light on potential therapeutic avenues for oral cancer treatment.

4.5.5 Molecular and Functional Characterization of Small Molecule Inhibitors to Evaluate Anti-Tumor Activity in Acute Myeloid Leukemia

Drug resistance is still an issue despite the significant progress that has been achieved in creating new therapies for AML patients. Treatments that address a crucial target to combat leukemic cells are now given to high-risk patients and those who relapse. However, this is a virtually challenging undertaking because of the inherent intricacy of AML blasts. This emphasizes the need to keep looking for novel therapeutics and, more importantly, to create chemosensitizing tactics that can prevent or, at the very least, limit the development of resistance to newer therapy such as Venetoclax or Ara-C, the standard treatment for AML for more than 50 years. Cyclin-dependent kinases (CDKs) are essential for the proliferation of cells, and it is becoming more well-known that they might be used as molecular targets for cancer treatments. It forms a functional CDK-activating kinase (CAK) with cyclin-H and MAT1, phosphorylating other CDKs to regulate the cell cycle. Furthermore, to promote transcriptional initiation and elongation, CDK7 phosphorylates serine 2 (S2), serine 7 (S7), and serine 5 (S5) of RNA polymerase II's carboxy-terminal domain (CTD). Owing to CDK7's crucial function in transcription and the cell cycle, CDK7 inhibitors effectively combat cancers by leveraging the transcriptional receptiveness of oncogenes and cell cycle proteins in a variety of cancer forms.

In the present thesis, the clinical-stage CDK7 inhibitor XL102 has been assessed, which causes the transcriptional suppression and cell cycle arrest leading to the downregulation of c-Myc and upregualtion of p53 mediated apoptotic signaling. Further, the purpose of this study was to ascertain whether a selective and targeted BCL-2 inhibitor (Venetoclax) would synergize with CDK7 inhibition via novel XL102 to eliminate leukemic burden and to decipher the molecular mechanisms underlying this phenomenon using leukemic cell lines, patient samples, and mouse models of AML.

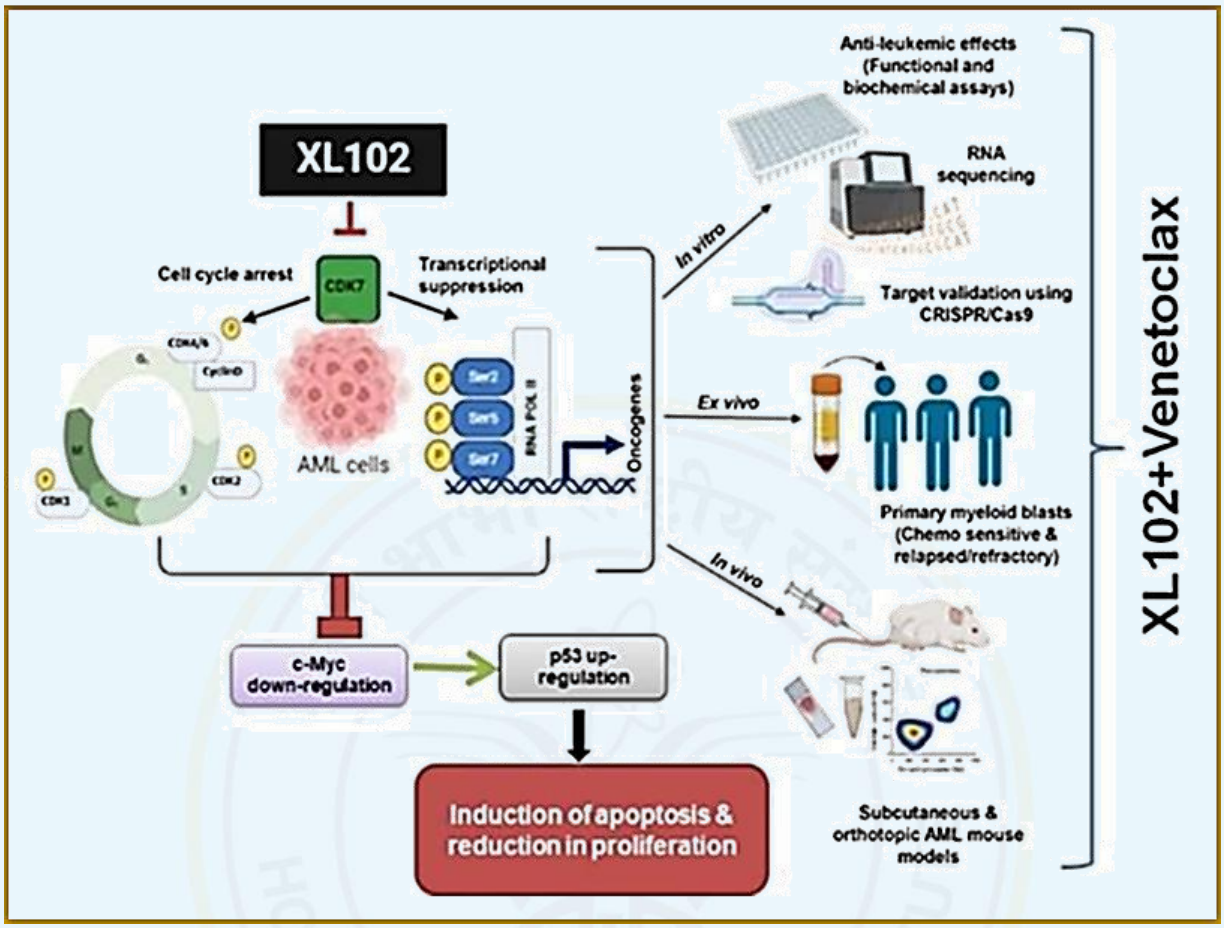

XL102 inhibits cell cycle and suppresses transcription leading to decrease in c-Myc and increase in p53 mediated apoptotic signaling

4.5.6 Identification of Mechanisms Required for Tumor Progression upon LCN2 Overexpression

LCN2 levels are elevated in multiple tumor types such as breast cancer, colon cancer, lung cancer, pancreatic cancer, and ovarian cancer, indicating that LCN2 expression could lead to tumor progression n in multiple tissues. Previous studies from laboratory have shown that inhibiting the expression of LCN2 in HCT116 cells derived PKP3 knockdown clone shpkp3.2 led to a significant decrease in migration, invasion, colony formation in soft agar and tumor formation in immunocompromised mice. In congruence with these findings, it has also been demonstrated that LCN2 expression is necessary and sufficient to increase migration and invasion. In this thesis it has been shown that LCN2 binds with Catechol:Iron complex to export iron out of the cell and reduces intracellular labile iron pool. Reduced labile iron pool in the cells leads to inhibition of ROS generation which inhibits the actin monomers oxidation and thus, actin monomer is available to take part in actin polymerization for filamentous actin formation.

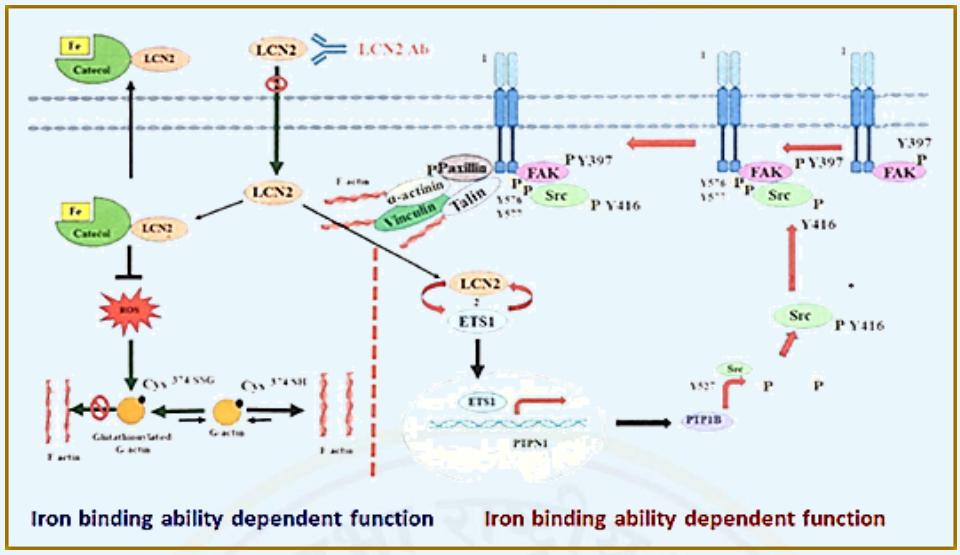

Schematic of the iron binding ability dependent filamentous formation and iron binding ability independent focal adhesion formation of LCN2 required for cell migration and invasion

Inhibiting LCN2 functions with LCN2 antibody increase ROS in the cells leading to actin glutathionylation which impair the actin polymerization. These filamentous actins are the basic cytoskeletal filaments required for focal adhesion assembly and disassembly to increase migration and invasion. In congruence with this fact, present research work also found that the LCN2 increases the focal adhesion formation and inhibits the LCN2 functions with LCN2 antibody (3D12B2). LCN2 promotes focal adhesion formation by increasing expression of ETS1 mediated PTP1B, which leads to the activation of Src. Activated Src binds to FAK to phosphorylate paxillin at Y118 which leads to the initiation of cascade of focal adhesion assembly formation. Notably, it is also observed that LCN2 mediated focal adhesion formation is independent of the binding ability of iron. Therefore, the LCN2 mediated filamentous actin formation and the focal adhesion formation leads to the increased migration and invasion.

4.5.7 Understanding the Molecular Mechanism of Leukemia Resistance using Cellular and Pre-clinical Model of Leukemia Resistance

Anthracyclines have been an integral part of chemotherapeutic regimens for cancer treatment since their first clinical trial in the 1960s. Its beneficial effects through topoisomerase II enzyme inhibition span from hematological malignancies to solid tumors. However, the development of resistance has limited efficacy and remains a clinical challenge, particularly in Acute Myeloid Leukemia (AML). In this thesis, the molecular basis of anthracycline resistance in AML relapse has been investigated by using patient biopsies, primary cultures of AML patient blast cells, and clinically relevant cellular models of anthracycline resistance developed in our laboratory that recapitulate AML-acquired resistance.

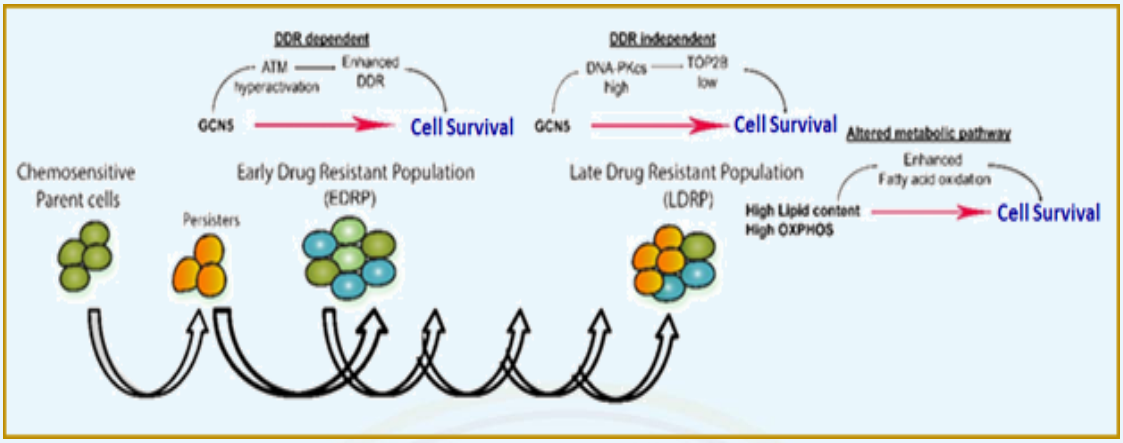

Model for anthracycline resistance mechanism in Acute Myeloid Leukemia (AML)

Using genetic, molecular, and biochemical experiments in patient samples and cellular models, the research work in this thesis has demonstrated that the relapsed resistant cells have multiple deregulated pathways to render resistance and adapt to drug pressure. Resistant cells rewired their cellular energetics to prefer fatty acids, exhibited higher oxidative phosphorylation, and, importantly, histone acetyltransferase (HAT) enzyme GCN5 in resistant relapse cells acts as a transcriptional activator and mediates the transcriptional upregulation of DNA-PKcs expression via its acetyltransferase activity. Notably, overexpressed DNA-PKcs, independent of its DNA damage repair function, acts as a transcriptional repressor of the anthracycline's target TOP2B enzyme by directly binding to its promoter, thereby rendering resistance. Furthermore, TOP2B repression is a function of the DNA-PKcs kinase activity. Accordingly, genetic, or pharmacological inhibition of DNA-PKcs alleviates TOP2B repression, rendering relapsed resistant cells susceptible to anthracycline. Thus, DNA-PKcs inhibition re-sensitizes primary cultures of refractory relapsed AML blast cells and resistant cells from a cellular model to anthracyclines, inducing apoptosis and abrogating their *in vivo* tumorigenic potential. Together, this study identified the GCN5-DNAPKcs-TOP2B transcriptional regulatory axis as the driver of anthracycline resistance.

4.5.8 CD26 and Adenosine Signaling Pathway Molecules as Regulators of Immune Reconstitution in Human Hematopoietic Stem Cell Transplantation

Allogeneic stem cell transplantation (ASCT) is a well-established desired curative mode of treatment for several hematological disorders and malignancies or for those patients with relapse post-chemotherapy. In the present study, G-CSF mobilized donor harvest was used for ASCT in transplant recipient. Complete leukapheresis product was used during transplantation, therefore it was ideal to profile various immune cells, CD26 expression on all immune cell subtypes and soluble markers in transplant donor harvest and evaluate their association with GVHD occurrence, infections, and survival post-transplant in transplant patients.

The three central risk factors that demoralize post-ASCT success are GVHD, infections and leukemia relapse. GVHD is the most unfavorable complication of ASCT. One of the key challenges is to maintain the long-term survival of transplant patients by preventing GVHD. With the use of standard prophylaxis regimens (BMT Unit, ACTREC) grade I (42.3%) and grade II to IV aGVHD (27%) incidences were observed. 34.6% of patients were presented with cGVHD post-ASCT. Regardless of using these immunosuppressive strategies, there are still mortalities detected post transplantation.

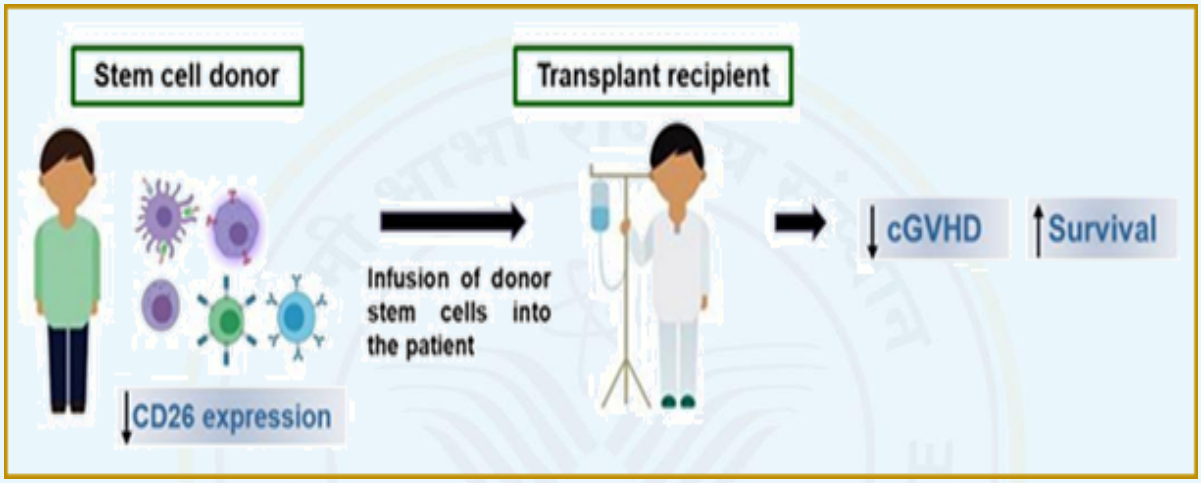

Low CD26 expression on immune cell subtypes of the donor stem cell harvest is associated with reduced risk of GVHD and better survival

CD26 is a multifunctional surface glycoprotein expressed on a wide range of cells. Donor harvest CD26 expression associates positively with risk of cGVHD incidence ($p=0.055$). Amongst the various immune cell subtypes, decreased B cells in harvest showed significant association with aGVHD ($p=0.022$) whereas increased myeloid dendritic cells and CD3+T cells of transplant recipients correlated with cGVHD ($p=0.046$) and aGVHD ($p=0.035$), respectively. Decreased levels of Early NK and Pre-switched memory B cells of donor harvest led to better EFS in transplant recipients at Day100. Donor harvest CD26+ NK/B/Treg cells correlated negatively with patient survival ($p<0.05$). To decipher the role of CD26 in GVHD, WBCs from healthy individuals were stimulated with PHA in the presence or absence of CD26 inhibitor, Sitagliptin and then checked for NF-κB localization and inflammatory cytokines production. CD26 inhibition hampered T cell activation and cytokines secretion via NF-κB pathway. The research work presented in this thesis has implicated that low CD26 expression on immune cell subtypes of the donor stem cell harvest is associated with reduced risk of GVHD and better survival.

5. Mathematical Sciences

During the period of report, HBNI awarded 13 Ph.D. degree in Mathematical Sciences in a variety of research areas such as Lie Algebra, Group Theory, Number theory, and Algebric Geometry. Some of the theses are summarized below.

5.1 The Harish-Chandra Research Institute, Prayagraj

5.1.1 Diophantine m-tuples in Quadratic Number Fields

The present thesis deals with Diophantine *m*-tuples with the property *D(n)* in the set of positive integers, rational numbers, and rings of integers of quadratic number fields. The thesis is divided into fine chapters. Essential tools like elliptic curves and Diophantine approximations which are useful for analyzing Diophantine m-tuples have been introduced in Chapter 1. In Chapter 2, Diophantine m-tuples with the property D(n) are defined and a brief history and some known results of Diophantine m-tuples with the property D(±1), D(±4), and D(n) with an integer n are given. Further, a study on we look at rational Diophantine m-tuples has been done. Chapter 3 begins by extending the definition of a Diophantine *m*-tuple from the set of positive integers to any commutative ring with unity. After that, Diophantine $m = -1$ tuples O_K with the property *D(n)*, and for the case when $n = -1$, are discussed and an upper bound on *m has been determined*, where O_K is the ring of integers of an imaginary quadratic field *K*. Chapter 4 is based on Diophantine *m*-tuples in the ring of integers of a real quadratic number field.

Chapter 5 contains some information about Diophantine *m*-tuples which have the property *D(n)* for more than on *n* and results for Diophantine quadruples and quintuples as well are discussed. It has been proved that for every integer *n*, there exist infinitely many Diophantine triples with the property *D(n)*, which also have the property *D(t)*, where $n \neq t$ and *t* is an integer. It is also demonstrated that there exist infinitely many Diophantine triples in $\mathbb{Z}[i]$ with the property *D(-1)* also having the property *D(n)* for two distinct values of *n*, other than $n = -1$. Also, an example of a Diophantine triple which has the property *D(n)* for four distinct values of *n* simultaneously has been provided.

5.1.2 Tensor t-structure on The Derived Categories of Schemes

Derived categories were introduced by Grothendieck in the 60's. Although widely accepted as the right framework for any kind of derived functors, e.g., cohomology groups, higher direct images, etc., they were usually considered as rather formal objects without much interesting internal structures. However, the situation has changed drastically in the last two decades.

In the thesis, an attempt has been made to shed some light on the structure of the derived categories of Noetherian schemes by classifying various interesting subcategories in terms of the underlying schemes. It has been shown that a compactly generated tensor t-structure on the derived category of a Noetherian scheme is completely determined by Thomason filtrations on the underlying scheme. Using this classification, it has also been described how the weight structures on the derived category of a separated Noetherian scheme arise from Thomason filtrations.

As an application of the results obtained, it has been proved that the tensor telescope conjecture is true for separated Noetherian schemes. In other words, it has been shown that the homotopically smashing tensor t-structures are compactly generated. Finally, to get a better understanding of the general results, various things in the special case of the projective line have been computed. A surprising result has been obtained which says there are no non-trivial tensor weight structures on the bounded derived category of the projective line, which contrasts the fact that there are many tensor t-structures.

5.2 Institute of Mathematical Sciences, Chennai

5.2.1 Exploring Size Complexity and Randomness in the Query Model

Decision trees are among the simplest computational models, where a computational task is performed by adaptively querying the input with the goal of minimizing the number of queries. Despite its simplicity, it remains a puzzle with many unresolved questions. Key complexity measures in this model are the depth complexity (the worst-case number of queries) and the size complexity (the space required to store the query algorithm). While depth complexity is well-studied, size complexity is less explored.

The thesis investigates the relationship between size complexity and other complexity measures across various computational modes: deterministic, randomized, and pseudo-deterministic. We investigate the relationship between deterministic size complexity and Fourier sparsity (an algebraic notion of size), as well as the relationship between deterministic and non-deterministic size complexity. An important class of function is that of composed function, the behaviour of size complexity under function composition has been studied and a size composition theorem in the deterministic setting has been proved.

A recurring theme in the research work is understanding the role of randomness in the query model and its variations. Nisan's classic result (SICOMP '91) established that the deterministic depth complexity of a total Boolean function is at most the cube of its randomized depth complexity. However, the role of randomness on size complexity has not been explored. Adding to Nisan's result, it is shown that the logarithm of the deterministic decision tree size

complexity of any total Boolean function is at most the fourth power of the logarithm of its bounded-error randomized decision tree size complexity, up to a polylogarithmic factor in the input dimension. Drawing an analogy, one can associate the depth of a decision tree with time complexity and its size with space complexity. Consequently, Nisan's result can be viewed as derandomizing time, while our result can be seen as derandomizing space.

Generalized decision tree models such as AND-decision trees (allowing AND queries), (AND, OR)-decision trees (allowing both AND and OR queries), and linear decision trees (allowing linear threshold functions as queries) have been investigated. These variants serve as insightful and natural intermediaries between the ordinary query model and Yao's 2-party communication model. For (AND, OR)-decision trees, it is shown that deterministic complexity is at most the fourth power of its randomized counterpart. For AND-decision trees, it is shown that deterministic complexity is at most the cube of its randomized counterpart. In the linear decision tree model, we explore the relationship between size-restricted LDTs and depth-2 threshold circuits has been explored. The thesis also explores the concept of pseudo-deterministic computation for search problems, a notion introduced by Gat and Goldwasser (ECCC-11). Pseudo-deterministic algorithms are randomized algorithms that almost always provide the same canonical solution for each input, addressing the variability in results typically seen in randomized algorithms. The interplay between determinism, randomness, and pseudo-determinism concerning both depth and size complexity in the ordinary query model and its variants has been investigated.

5.2.2 A Logical Study of the Improvement Graphs formed from Games

The Nash equilibrium for any finite game is known to exist due to Nash's famous theorem on the class of all finite games. The decision and the search problems of the Nash Equilibrium for a given finite game turn out to depend on the representation of the game in question. Multiplayer games in normal form require an exponential (in the number of players) amount of data in order to be described. Also, Nash's existential result does not hold for the decision and the search problems of pure nash equilibria of any finite game. The computational problem is not meaningful is the normal form case where the entire payoff tables for each player is given, because one can simply do an exhaustive search through the entries of the table. Monderer and Shapley in their paper on Potential Games first gives the insights which lay out the foundations for an improvement graph and improvement dynamics associated with it. The ideas get used in the context of social network games by Apt and Simon to establish complexity results for the game properties associated with an improvement graph for social network games. From a logical perspective, the resources required to describe the properties of the improvement graph seems interesting. It would perhaps even help the community establish properties describable within a logic for a class of games. Towards this endeavour, the monadic variant of the least fixed-point logic and the propositional dynamic modal logic are used in the present research work.

Using the research work presented in the thesis, it has been possible to capture the properties of interest in improvement graphs. One needs to be able to capture path and vertex properties of the improvement graph. First order logic can capture interesting vertex properties of a graph, but it is not possible to capture path properties. To add in additional power to First order logic, the least fixed-point operator is introduced. First order logic can capture isomorphic classes of games.

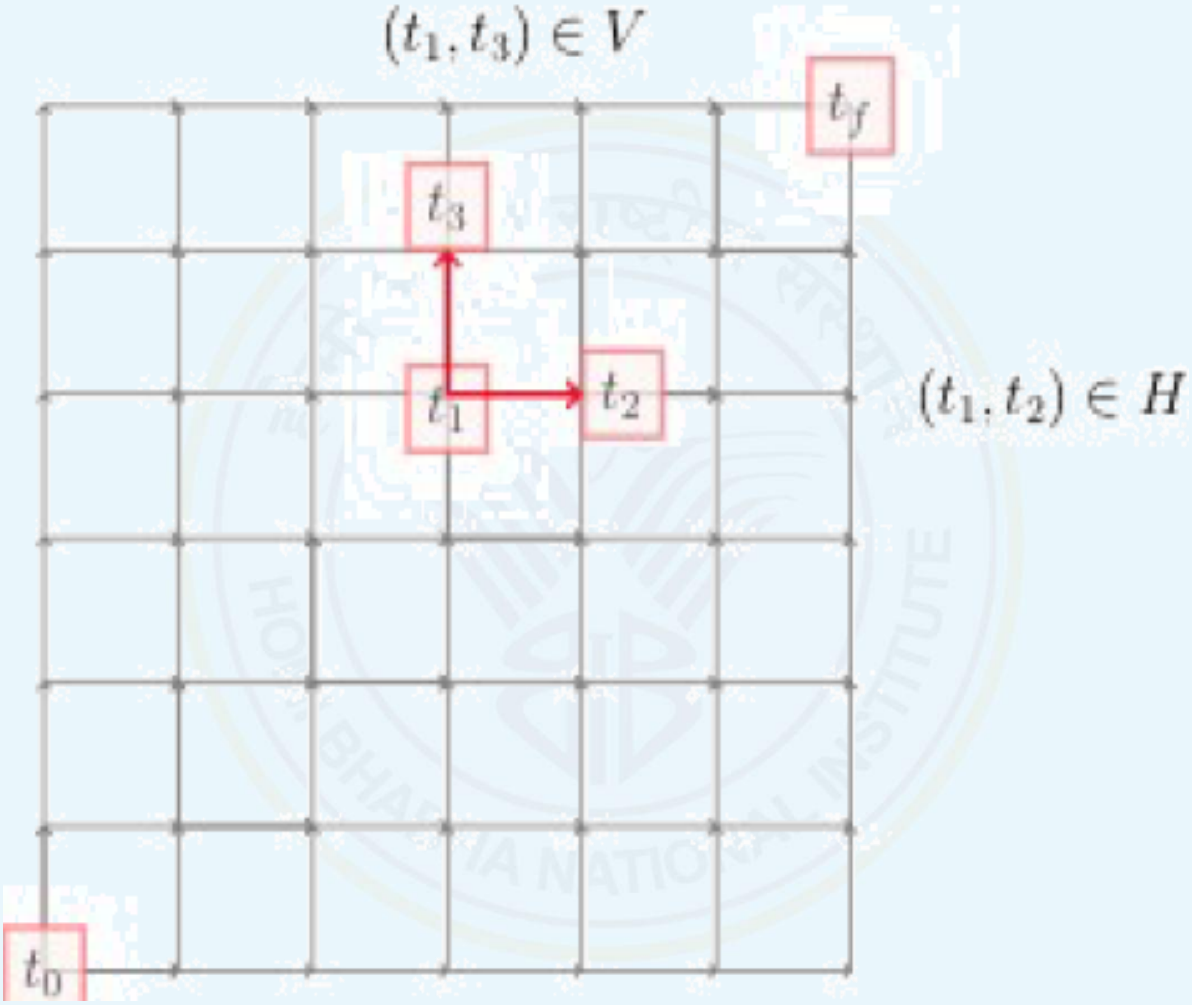

Reduction for undecidability

However, a coarser characterisation of game classes where player behaviour is emphasised on is needed. Towards that, a modal logic with path operators like the diamond star operator is introduced. The improvement graph is turned into a pointed Kripke structure and dynamic modal logics can offer similar expressive powers, subjected to the local view from the starting vertex in question. The additional benefit the utilisation of the coarser relation of bisimilarity to characterise game classes that are based upon player behaviour over the class of finite improvement graphs. The decidability of these modal logic variants has been proved via their respective completeness proofs. An undecidability proof for a second order logic expressing a subclass of Large Games is also provided.

5.3 National Institute of Science Education and Research, Bhubaneswar

5.3.1 Nonvanishing of L-functions and Differential Operators for Jacobi Forms

The nonvanishing property of L-functions holds huge significance, serving s a key point in various analytic results such as the prime number theorem, where, the, the nonvanishing of the Riemann zeta function assumes a pivotal role. The generalized Riemann hypothesis states that all the zeroes of an L-function attached to the Hecke eigenform lie on the critical line. A converse theorem studies the equivalence of modular properties of an automorphic form and the analytic properties of L-functions attached to it. In other words, deriving transformation properties of q-series from the functional equation of L-functions and vice versa. The differential operators on the spaces of modular forms are linear operators and give rise to many interesting identities involving the Fourier coefficients of modular forms.

The thesis deals with the study of L-functions associated with Jacobi forms of integer and matrix index and Jacobi Poincaré series. L-functions attached to Jacobi forms half-integral weight have also been studied. The research work conducted in the thesis also examines the properties of Rankin-Cohen brackets and their relation with the Poincaré series for Jacobi forms. The construction of Jacobi cusp forms involving special values of certain Dirichlet series as their Fourier coefficients has been studied.

6. Physical Sciences

During the period of report, HBNI awarded 142 Ph.D. degree in Physical Sciences in a variety of research areas such as Condensed matter physics, Nanoscience, Surface physics, Material science, Spintronics, X-ray Multilayer, Radiological Physics, Computational Spectroscopy, Density Functional Theory, Quantum information and computation, Nuclear Physics, Neutrino Physics, Plasma Physics and Astroparticle Physics and Cosmology. Some of the theses are summarized below.

6.1 Bhabha Atomic Research Centre, Mumbai

6.1.1 Vibrational and Electronic State Spectroscopy Studies on Carbonate Green Solvents using Synchrotron Radiation

Dimethyl carbonate (DMC), diethyl carbonate (DEC) and ethyl methyl carbonate (EMC) comes under the framework of green chemistry. Much of the work on carbonyl green solvents, till date revolves around their use as electrolyte co-solvent in lithium-ion batteries, as fuel additives and as industrial alkylating reagents. The spectroscopic information available on these molecules is limited to few vibrational studies and even fewer electron impact-based dissociation studies. Accurate experimental and theoretical data pertaining to spectroscopic information on electronic energy levels, vibrational modes, potential energy curves, dissociation mechanisms, etc is vital for understanding the chemical reactions that the molecules undergo.

The VUV photoabsorption spectra of the alkyl carbonates are found to comprise mostly of weak spectral features assigned to *ns*, *np* and *nd* Rydberg series converging to the IPs superimposed on an intense broadband continuum. In DMC, the broad intense features are attributed to the presence of unresolved valence transitions, while those observed in DEC and EMC are due to significant valence-Rydberg interactions between states of same symmetry. Density functional theory (DFT) and time dependent DFT (TDDFT) calculations on these molecules are carried out using GAMESS (US) computational chemistry code with a view to assign and interpret the observed VUV and IR spectral feature. Using mass spectroscopy methods, experiments are carried out to study fragmentation mechanisms consequent to electron induced as well femtosecond laser based multi-photon excitation. Based on detailed comparative analysis, the possible mechanisms involving a combination of direct bond cleavage as well as isomerization and reorganization are proposed to explain the observed dissociation products. Further, photoelectron kinetic energy release distributions measured in coincidence with various fragment ions and compared for all three molecules offers a validation of the proposed mechanisms. In summary, the VUV and IR spectroscopic data on electronic structure, molecular orbitals, vibrational modes, vertical excited energies, nature

of the excited states combined with studies on fragmentation pathways is expected to lead to a better understanding of their photochemistry and reaction mechanisms.

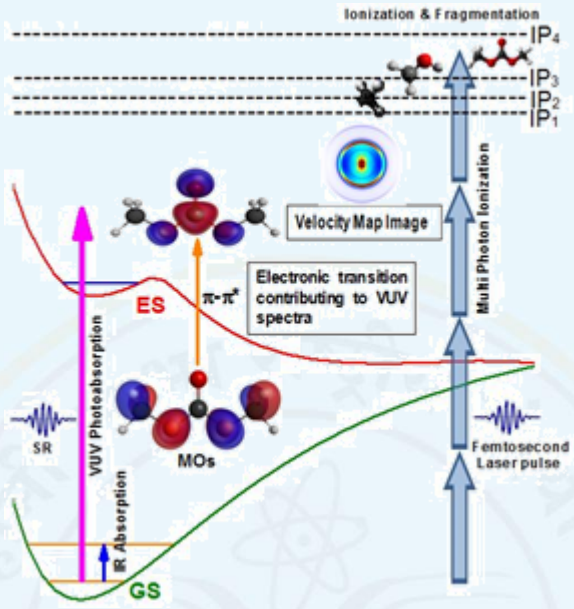

Spectroscopic information obtained from VUV photoabsorption, IR absorption and laser induced multiphoton ionization/ fragmentation

6.1.2 Thermodynamic Properties and Diffusion in Ionic Conductors

The solid ion conductors having high ion conductivity and low activation energy have many scientific and technological importance. Various Na/Li based superionic conductors were discovered as potential candidates of solid electrolytes for solid state batteries. Study of ionic diffusion at atomistic level in these materials becomes very important to design new materials.

The diffusion of the ions in solids depends on availability of sufficient number of vacant sites or interstitial sites, concentration of diffusive ions, and interaction of diffusive ions with surrounded atoms. Generally, highly disordered structure materials, such as, off-stoichiometric compounds, softer lattice, and amorphization, show high ion diffusion coefficient.

To better understand the ion transport property and nature of diffusion at the atomistic level, the study of lattice vibrations is essential. The phonon modes of the crystalline materials correspond to the high amplitude vibrations of atoms and appear in low energy side which may play a crucial role in accelerating the hopping of ions. These phonons are highly anharmonic and may contribute in fast ionic conduction in these materials. The research work in the thesis deals with the study of phonon dynamics in a variety of ionic conductors and their impact on diffusion. Further, the thesis also deals with enhancement

of the migration of ions and reducing the hopping barrier energy via applying strategies such as tunning of stoichiometry/vacancy, and amorphization.

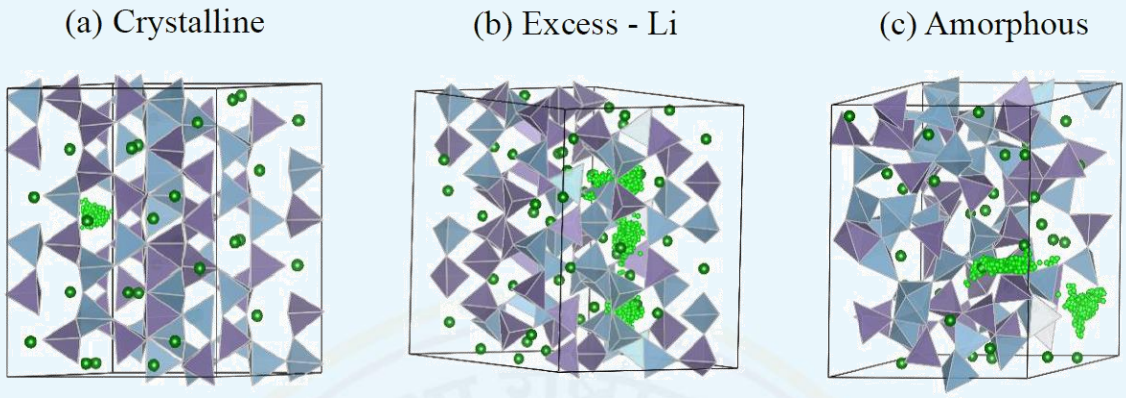

Atomic trajectory of Li atom in three structures of $LiAlGeO_4$ shows the tunning of Li ion diffusion

6.1.3 Non-Markovian and Non-Gaussian Behaviour in Molecular Diffusion within Complex Fluids

The concept of Brownian motion has been fundamental to advancements in numerous fields, including biology, materials science, finance, and environmental science, offering crucial insights into the stochastic processes underpinning diverse phenomena across these disciplines. Central to Brownian motion are the principles of Markovianity and Gaussianity, valued for their broad applicability in real-world systems. However, with the advent of new experimental and simulation methodologies, we can now critically assess the validity of these assumptions. Frequently, it becomes evident that the Brownian motion model falls short, necessitating the development of models that are not constrained by Gaussian/Markovian assumptions. The thesis explores various complex fluids which exhibit strong deviation from tenets of Brownian motion and provides comprehensive theoretical models to describe processing involving non-Gaussian and non-Markovian diffusion mechanisms. The thesis also explores deviations from Brownian diffusion in complex fluids systematically and extends the framework for describing diffusion beyond the Brownian regime.

The lateral diffusion of molecules within self-assembled aggregates has been studied, finding subdiffusive behavior characterized by non-Markovian dynamics and a system-specific memory function. Notably, this lateral diffusion adheres to the Gaussian approximation, with subdiffusion linked to medium-induced viscoelasticity (Flow chart shown below). This behavior is confirmed through quasielastic neutron scattering (QENS) experiments and molecular dynamics (MD) simulations on bilayer and micellar systems. In a separate study on deep eutectic solvents (DESs), QENS experiments reveal non-Gaussian molecular diffusion. MD simulations attribute this to a cage-jump diffusion mechanism, where molecular caging is associated with complex formation (Flow chart shown below). Additionally, how water modifies complexation and dynamics within DESs is also examined systematically.

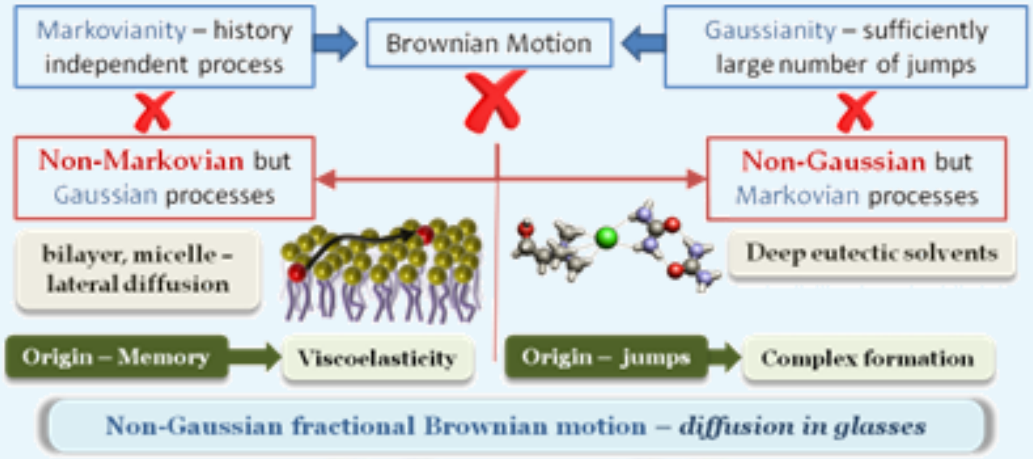

Flow chart describing the emergence of non-Markovian and non-Gaussian diffusion processes in complex fluids. The simultaneous breakdown of Markovian and Gaussian assumptions is observed in molecular diffusion within glass-forming liquids

The phenomenon of sub-diffusion crossover in glass-forming liquids is explored, which involves simultaneous existence of non-Markovian and non-Gaussian dynamics. This process is modeled using non-Gaussian fractional Brownian motion (nGfBm), which successfully explains QENS data for various glass-formers.

6.1.4 Interface Driven Magnetization in Complex Oxide Heterostructures

Interfaces of layered complex oxide heterostructures are an epicentre for many novel properties due to sharp electronic density modulations, symmetry lowering, and strain as a result of lattice mismatch and defects at the interfaces. Moreover, hetero-interfaces made of materials with different types of magnetic ordering give rise to a variety of interfacial phenomena such as emergent ferromagnetism, exchange bias effect, magnetic proximity effect, and alloying, etc. Layered oxide heterostructures having interfaces of ferromagnet (FM)/paramagnet (PM), FM/superconductor (SC) and FM/phase-separated (PS) materials were investigated using polarized neutron reflectivity (PNR) and other relevant techniques of structural, magnetic and morphology characterization and the major highlights of the research are discussed.

The PNR results of FM/PM heterostructures of $La_{0.67}Sr_{0.33}MnO_3$ (LSMO)/$LaNiO_3$ (LNO) indicate the emergence of a ferromagnetic layer in the LNO near the LNO/LSMO interface on MgO substrates, which is antiferromagnetically coupled to the LSMO layer ((a) in schematic shown below). The absence of this interfacial magnetization on STO substrates highlights the critical role of substrate-induced strain in modulating interfacial magnetic properties. The next system comprises of the FM/SC and FM/I/SC heterostructures of LSMO/YBCO in proximity geometry (direct contact) and LSMO/STO/YBCO in the proximity geometry (FM and SC separated by a thin insulator ((b) in schematic shown below).

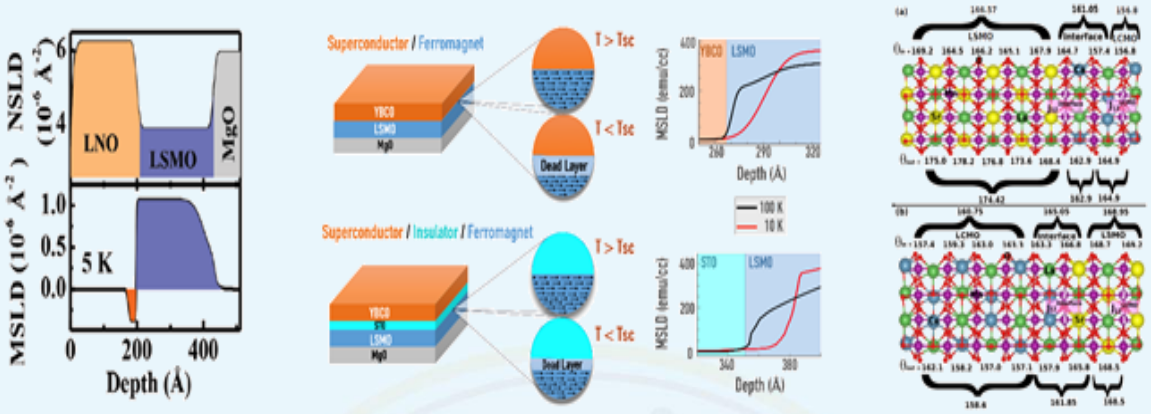

(a) (b) (c)

(a) Emergent interfacial FM in FM/PM, (b) MPE in FM/(I)/SC, (c) Varying rotation angle in FM/PS systems

The study establishes the intrinsic nature of long-range magnetic proximity effect (MPE) in these heterostructures through a series of experiments. The study also explores the impact of layer stacking sequence on MPE strength, emphasizing the critical role of saturation magnetization and T_{sc} of the layers in these interactions. The third system that we have studied is the FM/PS heterostructures comprising LSMO/LCMO and LSMO/LPCMO on LSAT (001) substrate where LPCMO exhibits stronger PS as compared to LCMO. Interface-driven magnetic exchange interactions due to modification in the octahedral rotations at the interfaces of the isovalent LCMO/LSMO heterostructures has been reported by combining PNR and density functional theory. The oxygen octahedral angles for the different layers in LSMO/LCMO and LCMO/LSMO heterostructures was found to be different ((c) in schematic shown below) indicating higher electronic bandwidth and stronger FM behavior of the interface for the former.

6.1.5 Development and Study of Variable FrequencyAPPJ as A Unique Radiation Source for Biomedical Application

Cold atmospheric plasma discharges have been promising sources of active chemical species for a range of applications, from material processing to biomedical applications due to compactness and ability to function at ambient conditions. Although frequencies over a broad range have been investigated in the literature, the deployed frequency mostly remained fixed for a particular study, and the effect of the driving frequency on the produced plasma and associated applications wasnot explored enough. The research work carried out in the thesis focuses on the development and characterization of such a variable frequency source for breast cancer treatment.

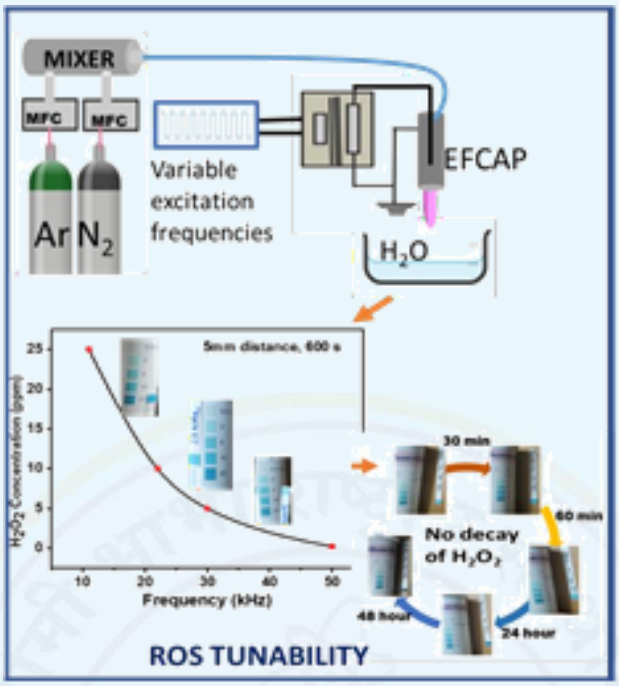

Tunability in frequency with EFCAP

The present work investigates a tunable excitation frequency-controlled cold atmospheric pressure plasma (EFCAP) through experiments and simulation (COMSOL), and emphasises the 'excitation frequency' (11 kHz to 50 kHz) control feature of the discharge. The tunability was observed for electrontemperature, gas temperature, radical generation (pH, EC, NO_3^-, NO_2^-, H_2O_2) and breast cancer cell death.

Just 60 seconds of plasma treatment at 11 kHz demonstrated the selective killing of cancer cells overnormal, healthy breast cells. A comparative study with 13.56 MHz revealed that 11 kHz can better beused for cancer cell treatment as the gas temperature is low and the RONS generated can be tuned. Also, careful nitrogen should be mixed with argon since N_2 leads to a reduction of both electron temperature and number density.

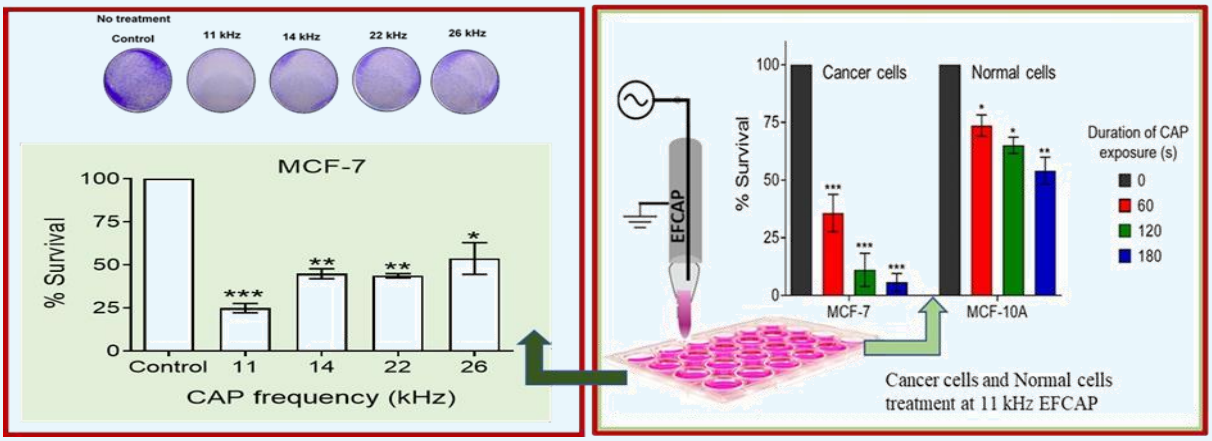

Selective cancer cell death with EFCAP at 11 kHz

6.1.6 Structural, Magnetic, Thermal, And Electronic-Ionic Conduction Properties of Naturally Grown Layered Transition Metal Oxides

Understanding the diverse magnetic properties in two-dimensional (2D) magnetic systems is an emergent field due to their unusual physical properties, arising from quantum fluctuations and/or geometrical spin frustrations. Understanding of such novel magnetic phenomena and the role of underlying magnetic lattice geometry are the motivation of the present thesis work. We have considered the compounds where the magnetic layers are separated by intermediate *A*=Li/Na/K-ions layers. Such layered materials provide high ionic conduction, suitable for applications in battery applications. The present thesis works aim to gain understanding of the microscopic mechanism of ionic conduction and to bring out the important role of the underlying crystal structure on the ionic conduction properties.

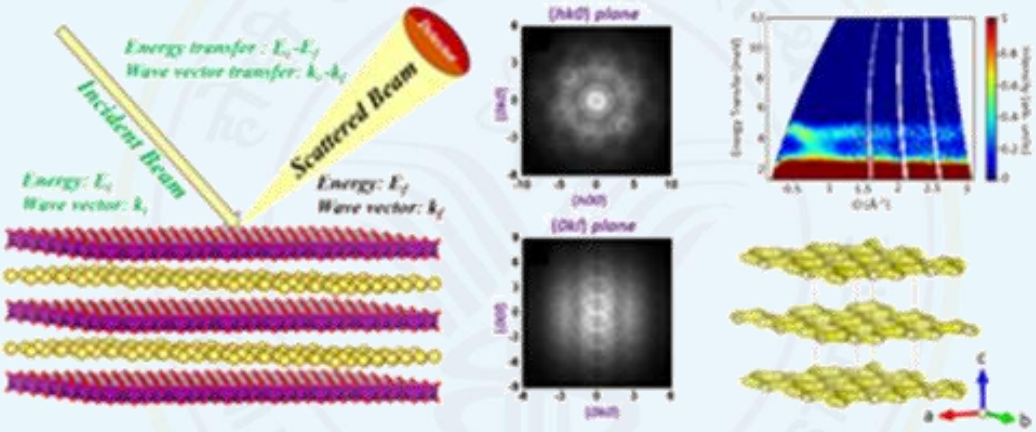

Schematic of the crystal structures of the 2D layered transition metal oxide compounds studied in the present thesis framework, (i) $Na_3Fe(PO_4)_2$ (triangular lattice), (ii) $Na_2Mn_3O_7$ (maple leaf lattice), (iii) $A_2Ni_2TeO_6$ (A = Na/Li) (honeycomb lattice) and (iv) $KNa_3Mn_7(PO_4)_6$ (diamond lattice)

In the present thesis, four layered transition metal oxide compounds comprising of different 2D magnetic lattices (a) triangular lattice [$Na_3Fe(PO_4)_2$], (b) maple leaf lattice [$Na_2Mn_3O_7$], (c) honeycomb lattice [$A_2Ni_2TeO_6$ (*A*=Na/Li)] and (d) diamond lattice [$KNa_3Mn_7(PO_4)_6$] have been considered. The present thesis work provides that the combination of low dimensionality, geometrical spin-frustration, and inherent anisotropies, spin-magnitude, and the underlying lattice geometry has a significant impact on the magnetic ground states. The study on the distorted triangular lattice having two in-plane exchange interactions J_1 and J_2, a collinear magnetic ground state is stabilized, which is different from 120° chiral spin state as expected for isotropic triangular lattice. For a Maple Leaf Lattice, the triangular plaquettes are connected by sharing their edges with two neighbouring triangles, in comparison to the three triangles in the case of a triangular lattice, which leads to the possibility of multiple chiral spin structures. On the other hand, the uniqueness of honeycomb lattice that it shows the coexistence of the commensurate (CM) and incommensurate (ICM) magnetic correlations

with an unusual up-up-down-down periodicity of the commensurate AFM structure. Our study depicts how the periodic removal of lattice points from a regular triangular lattice results into a change in the lattice geometry and consequently, leads to the possibility of multiple spin structures. Thus, as an outlook, the investigations of other possible 2D frustrated lattices based on triangular plaquettes that can be obtained from the triangular lattice would be of immense interest for exploring the novel spin structures as well as their correlations with the underlying lattice geometry.

Further, the work provides a detail investigation on the ionic conduction properties with a specific focus on its potential battery applications. Out of all the studied compounds in the present thesis work, the honeycomb layered transition metal oxide compound $Na_2Ni_2TeO_6$ has been found to have highest ionic conductivity, making it suitable for battery applications. The research work brings out the microscopic origin of the microscopic mechanism of ionic conductivity, such as in their internal structures of the alkali metal ion layers, distance between the alkali metal ions, local crystal structural environment, site occupancy, alkali-ion deficiencies etc. The understanding of the microscopic crystal structure, electrical properties and their inter-correlations obtained from the present thesis work, is expected to be useful for the design/fabrication of highly efficient layered battery materials.

6.1.7 Development of Toxic Gas Sensors (NO_2, H_2S, NH_3, Cl_2, Co etc.) for E-Nose Application

Detecting toxic gases is vital for safety in industries and homes, but conventional methods using expensive equipment limit their widespread use. This thesis centers on creating toxic gas sensors for an electronic nose (EN), providing a cost-effective solution for detecting gas mixtures.

ZnO nanowires (NWs) based e-Nose has been effectively designed and demonstrated to distinguish between H_2 and NO_2 gases. For this, multiple sensors were developed by modifying the ZnO NW's surfaces with sensitizers namely Ni, Au, Cu and MgO. The Principal Component Analysis (PCA) shows good correlation between variable and principal components (PCs) which was useful in achieving the distinct separation between the target gases. Further the effect of sensitizers namely Pt and Pd have been studied for differentiating between multiple gases namely H_2S, H_2, and NO_2. The three gases were distinguished using 3D PCA wherein the first three PC1, PC2 and PC3 have variance percentages of 42.32, 33.26 and 24.20% respectively. Further the effective identification and classification of four gases namely CO_2, H_2S, NH_3 and NO_2 from their mixture has been achieved by a high-performance e-Nose employing MSA consisting of four sensors. On the training and validation sets, the SVM classifier with RBF kernel model shows the greatest accuracy. The confusion matrix indicates a 2.5% test error rate for validation set and a 0% out of box estimate error rate for training data. Finally, the ability to control the morphology of ZnO

has been exploited to achieve the partial specificity towards H_2S, NO and their mixture. Three nanoforms namely nanoflowers, nanogranules and nanowires that were produced using a simple chemical route were used to achieve this. Using SVM, regression analysis it has been demonstrated that a wise selection of combination of sensors can give a very good accuracy on the prediction of target gas mixture.

6.1.8 Effect of nano sized features on the thermoelectric performance of low, medium, and high temperature range thermoelectric materials

In most of industrial processes waste heat is generated over a wide temperature range from 300K to 1273K. Thermoelectric materials can directly convert such waste heat into electricity. The figure-of-merit of thermoelectric materials is temperature dependent therefore for different temperature range separate materials are proposed. In the thesis, an effort has been made to improve figure-of-merit (*ZT*) of thermoelectric materials for three different temperatures range namely low temperature range (300-573K), mid temperature range (573-823K) and high temperature range (823-1273K). An approach of producing coherent nano inclusions in the matrix of thermoelectric materials was implemented in order to improve the performances of selected materials, such as Ag_2Se for low temperature range, SnTe for mid temperature range, and SiGe for high temperature range. In comparison to traditional low temperature bismuth telluride materials, silver selenides display high merit near room temperature with added advantage e.g. tellurium-free and environmentally friendly. In this work an improved thermoelectric performance has been observed in Ag_2Se when doped with Al. The in-situ generated AgAl phase and the emergence of the Se-rich $Ag_2Se_{1.02}$ phase in the $Ag_{1.95}Al_{0.05}Se$ sample were credited with this improvement in grain connectivity. The uni-leg device made with the optimized $Ag_{1.95}Al_{0.05}Se$ material demonstrated conversion efficiency (η) of 3.2% at a temperature difference of 93 K, which is close to the highest value reported for traditional bismuth telluride. For medium temperature range SnTe material was investigated which is one of the best replacements for PbTe. It was observed that the in-situ created Te nanostructures in the $Sn_{0.9}Te$ matrix enhances the *ZT* up to 1.5 at 750 K. Apart from this, in the optimized $(SnTe)_{0.5}(PbTe)_{0.5}$ nanocomposite sample shows a high *ZT* of 1.2 at 750 K due to the presence of n-type PbTe in p-type SnTe matrix creating p-n interfaces at the nano scale range and the hierarchical defects in the SnTe matrix. The uni-leg thermoelectric device made using optimised $(SnTe)_{0.5}(PbTe)_{0.5}$ material showed η ~4.9% at ΔT ~400 K. For High temperature range SiGe alloys was investigated. Both p and n-type of SiGe alloys were prepared by mechanical alloying route and their densification behaviour was studied. A simulation technique (i.e., response surface analysis) was employed to study the effect of milling time and sintering temperature on the thermoelectric properties of SiGe. The thermoelectric performance of p-type SiGe is usually inferior as compared to the n-type SiGe. In this work, by in-situ creation of coherent TiO_2 nanoinclusions and boron rich regions in p-type SiGe a high figure-of-merit of ~1.3 is achieved at 1100 K, which is 29 % higher as compared to pristine p-type SiGe.

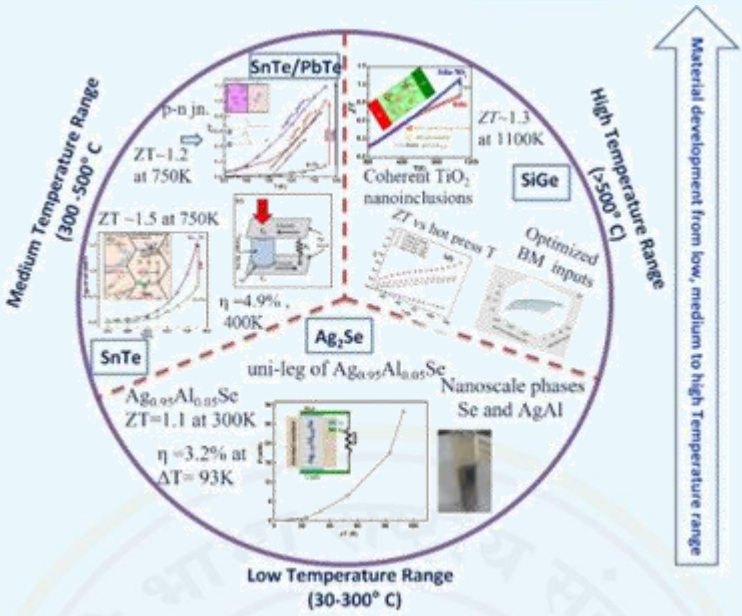

Improvement of thermoelectric performance in the selected materials (Ag_2Se, SnTe and SiGe) for three different temperature range

6.1.9 Toxic Gas Detection Based on Inorganic, Organic Materials, their Composites and Allied Techniques

Gas sensors are essential in both domestic and industrial environments and metal-oxide semiconductors have been the subject of extensive investigations for chemiresistive sensing applications towards various toxic gases. Metal-oxides present excellent sensing performance towards various oxidizing and reducing gases such as H_2S, NO_2, NH_3, CO_2 etc. However, the sensing characteristics of metal oxides can be greatly enhanced using various strategies viz using nanomaterials, modifying metal oxides with other suitable materials. Present research work has been focused on investigating the gas sensing properties and mechanisms of ZnO thin films, ZnO nano belts, NiO nanoparticulate thin films, SnO_2: Pt thin films, SnO_2: NiO thin films and SnO_2: MgPc thin films prepared using various methods.

ZnO thin films exhibited maximum response to NO_2 (SR~250 for 20 ppm) at an operating temperature of 200°C due to the presence of donor defects viz oxygen vacancies and zinc interstitials. ZnO nanobelts have displayed room temperature response towards H_2S and NO. Analysis of effect of operating temperature and the gas concentration on sensor response and recovery time has revealed the dissimilar mechanism towards these two gases. Apart from typical oxidation of H_2S, ZnS formation led to sluggish recovery at higher gas concentrations. Thin films of NiO with different particle sizes showed an anomalous response towards H_2S, which was affected by operating temperature, gas concentration and particle size. Investigation of these films revealed that the response occurred due to the combination of two different sensing mechanisms viz H_2S oxidation and sulphide formation. Better NO_2 response had resulted with SnO_2: Pt thin films at a lower operating temperature (200°C - SR

~24 for 10 ppm) as compared to pristine SnO_2 thin films (300°C and SR ~8 for 10 ppm) due to the catalytic effect of Pt. SnO_2: NiO thin films exhibited excellent response to H_2S (SR ~450 for 10 ppm) at room temperature at sub ppm level owing to p-n heterojunctions. SnO_2: MgPc thin films demonstrated better performance towards NO2 at 175°C (SR ~18.5 for 5 ppm) which is better than their individual counterparts. Enhancement oxygen adsorption sites on the sensor surface and formation of p-n heterojunction at the interface lead to the improved response of modified films. Sensing performance exhibited by all the systems have been shown inf Figure 1. In essence, for H_2S sensing applications, SnO_2: NiO material system can be investigated further. For NO_2 sensing ZnO thin films, SnO_2: Pt and SnO_2: MgPc material systems can be examined furthermore.

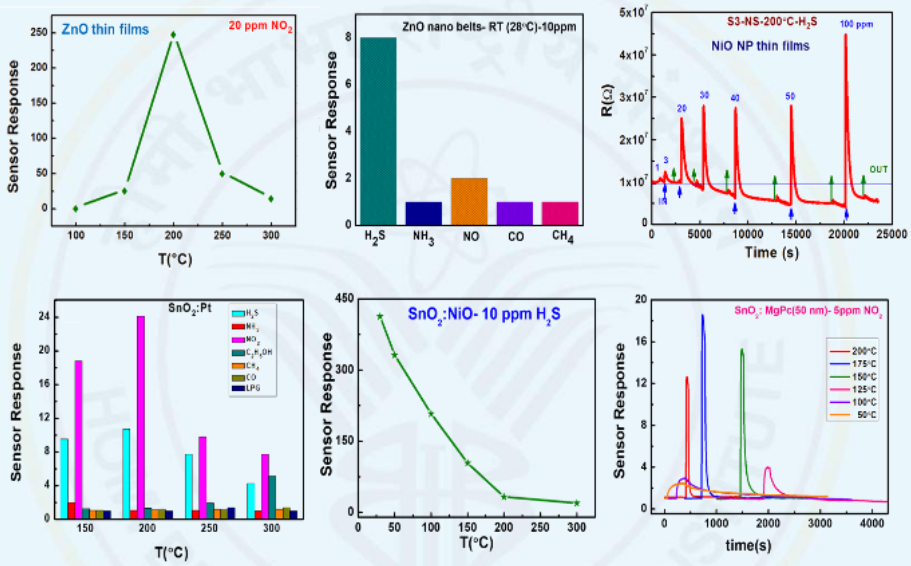

Sensing performance exhibited by ZnO thin films, ZnO nanobelts, NiO NP thin films and thin films of SnO_2: Pt, SnO_2: NiO, SnO_2: MgPc

6.1.10 Neutron Spectrometry and Dosimetry in Diverse Radiation Environments

The thesis focuses on advancing neutron pectrometry and dosimetry techniques for complex radiation environments, including cosmic ray backgrounds, nuclear reactors, and accelerators. The research involves developing novel spectrometry systems, utilizing Monte Carlo simulations, and performing extensive experimental measurements. Key objectives include creating a compact neutron spectrometry system and correlating neutron energy with LET.

The study employs various neutron spectrometers and dosimeters, such as ROSPEC, BSS, and TEPC. Significant results include high- altitude and polar region neutron spectrometric data, the first published in the Indian subcontinent, and detailed characterization of neutron fields in different environments.

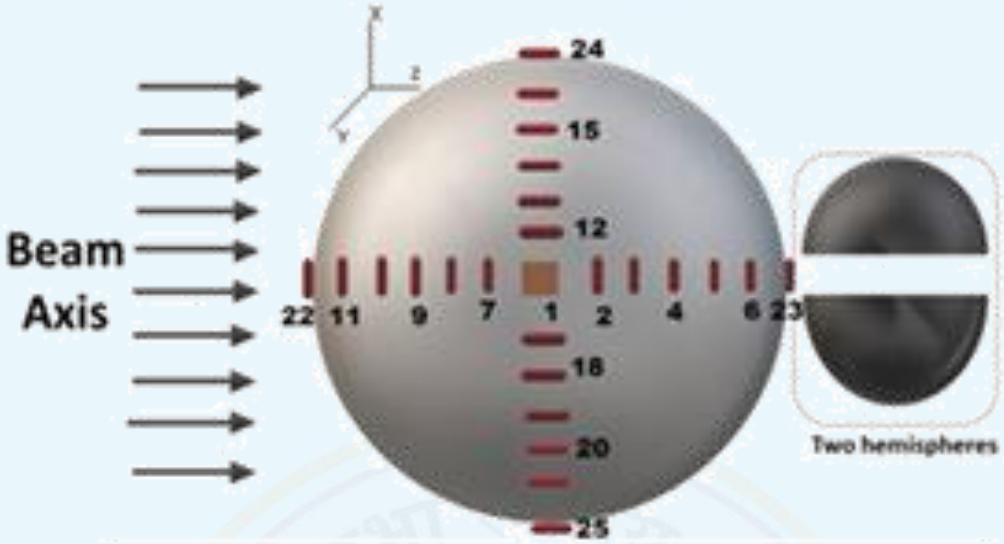

Designed and developed SSMDSS system

In cosmic ray environments, the research presents seasonal variations in neutron spectra and cosmic ray background impacts at Indian Antarctic research stations. In accelerator and reactor settings, it examines neutron production and shielding effectiveness, using BSS and TEPCs. The findings establish correlations between neutron energy spectra, LET spectra, and dosimetry quantities, proving the effectiveness of the developed systems. This work significantly contributes to neutron spectrometry and dosimetry, providing robust tools for accurate radiation measurement across diverse environments, and suggests future research directions in enhancing detector sensitivity and expanding applications.

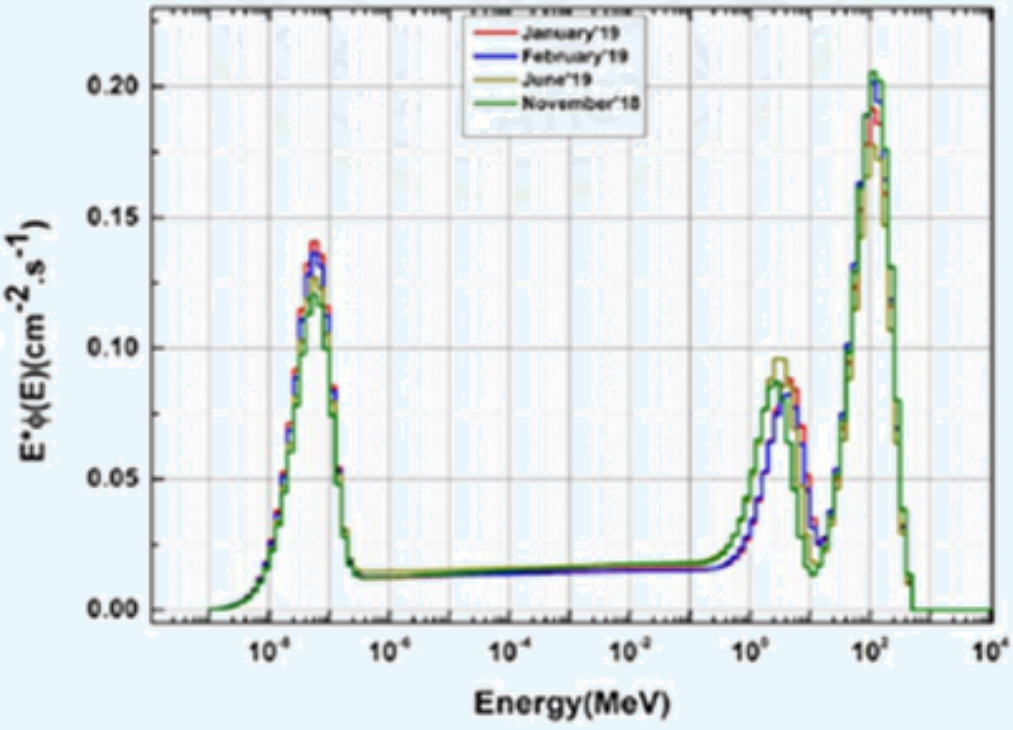

Cosmic ray neutron spectra at Gulmarg

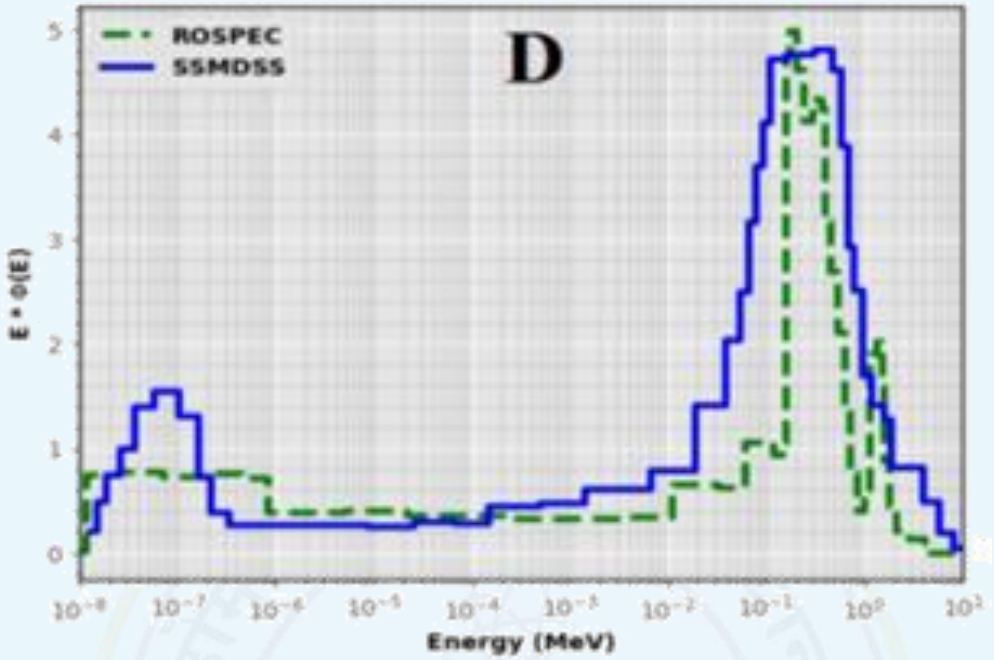

6.1.11 Modelling and Characterization of Emission and Transport from Large Area Field Emitters

Large Area Field Emitter (LAFE) is a promising electron source that has found applications in polymer industry, electron beam machining, miniaturized X-ray source for medical applications, high power microwave generation etc. The thesis focuses on the modelling of large area field emitters (LAFE) having smooth curved endcaps. Due to the computational resource limitations, simulation of LAFE containing thousands of emitter tips is difficult. The thesis work provides an analytical technique that can be utilized to estimate individual emitter currents and eventually the net emission from the LAFE. The analytical methodology can model sharp nano-tips of generic geometrical shape distributed randomly or placed in an array on the cathode patch.

The thesis considers several emitter configurations beginning with the anode at infinity and thousands of hemi-ellipsoidal tips are placed uniformly and randomly on the cathode patch. The consequences of electrostatic shielding are further studied considering the presence of the anode at close proximity of the nano-emitters. To ensure uniform emission throughout the cathode patch, an optimization technique has been demonstrated by tailoring either the positions of the emission sites or alternatively tailoring the individual emitter heights with the positions fixed. A new characterization technique has been demonstrated that captures the emission pattern of a LAFE in terms of an 'emission dimension' which lies between 1 and 2 depending on the degree of uniformity of electron emission. Finally, the thesis deals with the transport of the LAFE emitted electrons in the high field gradient region near the tips using

semi-analytical fields and the interactions of the electrons with neutral atoms in material medium using stochastic Monte-Carlo technique.

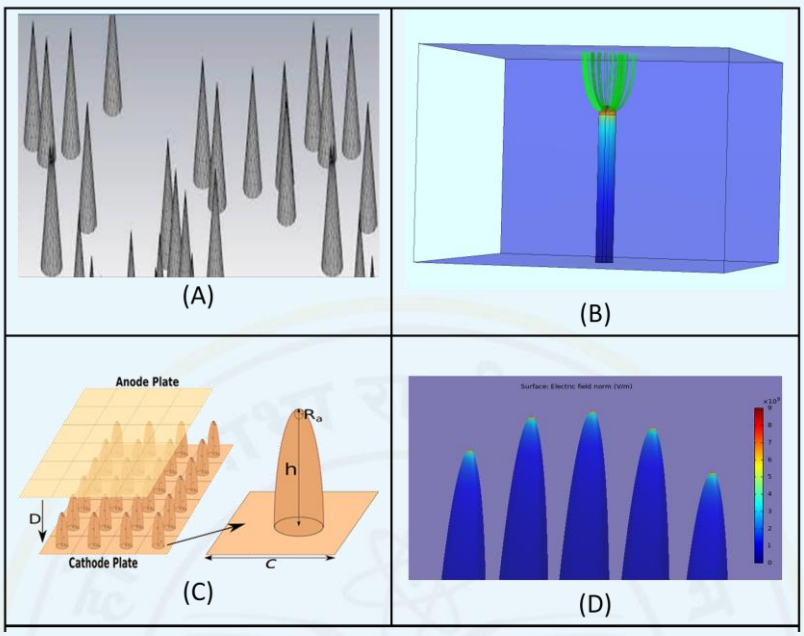

(A) Schematic of a large area field emitter with randomly placed emitter tips. (B) The convergence of the electric field lines on a nano-tip in a planer diode configuration. (C) Schematic of a large area field emitter with anode positioned at close proximity of emitters. (D) The surface electric field profile on central row emitters in a 25-pin height optimized emitter cluster emitting uniformly

6.1.12 Probing Nanoparticle-Surfactant Complexes using Scattering Techniques

Nanoparticles-surfactant complexes come across as promising materials in diverse areas including enhanced oil recovery, froth floatation, waste-water treatment, therapeutics, and synthesis of products such as cosmetics, paints, and lubricants. The complexes of nanoparticle-surfactants are observed to show tunable physicochemical properties such as surface hydrophobicity/hydrophilicity, electronic structure, surface chemistry, mechanical strength, and chemical reactivity, which are being used to enhance material performance in specific applications.

The present thesis has examined the characteristics of nanoparticle-surfactant complexes that are influenced by the interplay of interactions (electrostatic as well as non-electrostatic) between the constituents. According to the head group polarity, the C12E10, SDS, and DTAB surfactants interact with silica nanoparticles in quite different ways. Non-ionic C12E10 micelles tend to adsorb on silica nanoparticle surfaces, forming a decorated micelle shell around the core of nanoparticles. Due to electrostatic repulsion, the similarly charged SDS micelles and nanoparticles coexist without any physical contact, whereas the oppositely charged DTAB micelles strongly adsorb to the nanoparticles, forming aggregates that exhibit

fractal morphology. The characteristics of these nanoparticle-surfactant complexes were tuned by modifying the surfactant concentration, nanoparticle size, solution parameters such as ionic strength and additive, and electrostatic interactions between the constituents. The observed variations in the adsorption and phase behavior of nanoparticle-surfactant complexes are described in terms of changes in the fundamental interactions in the system (nanoparticle-surfactant, nanoparticle-nanoparticle, and surfactant-surfactant) and resulting structures (nanometer to micron size) of the complexes. The findings of the current thesis could be utilized in practical applications such as phase-separation processes, drug delivery, and synthesis of mesoporous functional materials. The future research work can focus on examining the phase behavior of nanoparticle-surfactant under charge reversal of nanoparticles in presence of multivalent salts in continuation with the present understanding of nanoparticle-surfactant solutions as provided in the thesis.

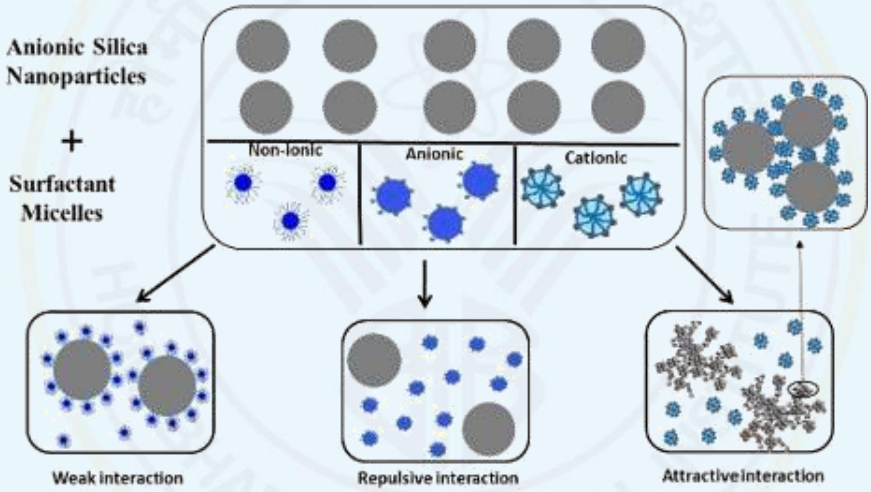

Schematic representation of the microstructures of the interaction of anionic silica nanoparticles with various charged surfactants

6.2 Indira Gandhi Centre for Atomic Research, Chennai

6.2.1 Mössbauer Studies on Some Fe/Bi Based Multifunctional Oxides

The thesis is devoted to understand the ways of improving multiferroic properties of $BiFeO_3$. It addresses few aspects such as size effect, cation substitution and addition of functional magnetic oxides nanoparticles on the magnetic and magneto-electric coupling properties of nano-BiFeO3. The atomic scale understanding of these systems on the observed properties are provided based on detailed Mössbauer spectroscopic studies.

A detailed understanding on multiferroic properties of pristine and doped nano BiFeO3 and its composites have been investigated by extensive Mössbauer spectroscopy along with other bulk characterization techniques. An atomic scale understanding on the formation of phase

pure $BiFeO_3$ have been carried out. The role of defect structure associated with weak ferromagnetic shell of nanoparticles plays an important role in controlling magnetic and coupling properties. MEC in composites are mainly due to the interface magnetic interactions as deduced by Mössbauer spectroscopic results.

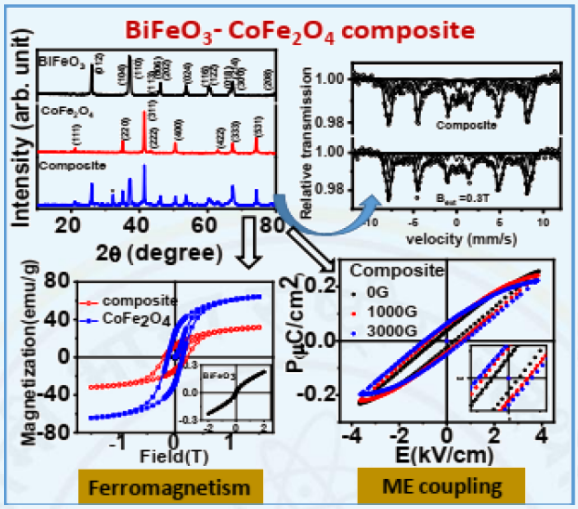

Structural, magnetic and magneto electric coupling properties in $BIFeO_3$-$CoFe_2O_4$ composite are understood based on Mössbauer results. Significance of interface magnetic interactions leading to the appreciable magneto-electric coupling is elucidated in the study

6.2.2 Magnetic and Transport Characteristics of CdTe Nanostructures using ab-initio Techniques

The thesis discusses the magnetic, optical, vibrational, and electronic transport properties of undoped, and transition metal (TM) doped CdTe nanostructures, including clusters, wires, tubes, slabs, and cluster-assembled materials. The significance of this work lies in its demonstration of the ability to tune the properties of CdTe nanostructures for various applications, such as energy harvesting, spintronic devices, and the development of stable surfaces with minimal reconstruction for optoelectronic devices.

Systematic studies of various properties of CdTe nanostructures across the dimensions within the top-down and bottom-up approach have been carried out. The CdTe nanostructures in the 2D and 1D studied within the top-down approach show substantial quantum confinement effects as reflected in the variations in band gap, optical properties, etc., when the size is below the excitonic Bohr radius (Schematic (a)). It is shown show that the self-healing occurs in some of the nanostructures due to surface reconstruction and orbital reorientations. It is shown that Cd_9Te_9 is the smallest stable cage-like cluster (Schematic (b)). It is semiconducting with 1.6 eV energy gap. Passivation with fictitious H atoms leads to substantial changes in structure and properties. The clusters can be tuned to act as metal or halfmetal upon doping by suitable transition metal (TM) atom. The doping causes the clusters to act like electron donor or acceptors, like semiconductors. They also show substantial magnetic moments

which follows the Slater-Pauling behaviour. The electronic transport properties in the tunnel junction devices formed by these clusters and Au electrodes have been studied considering spintronic applications. The I-V characteristics of TM (Ti, V, Cr, Mn, Fe) encapsulated clusters show half-metallic behaviour and spin-filtering effects (Schmatic (c)). Further, the Cd_9Te_9 clusters are used as the building blocks for exploring the self-assembled nanostructures in 1, 2 and 3 dimensions within the bottom-up approach (Schematic (d)). It was found that the 3D self-assemblies arise from 2D stacked self-assembled monolayers. The properties of the 2D stacks and 1D cluster chains are also studied. The most stable assemblies are 3D FCC and 2D hexagonal systems. The effect of quantum confinement is seen in the band gap of self-assemblies across the dimensions. The optical properties of these self-assemblies point to their potential applications in solar cells.

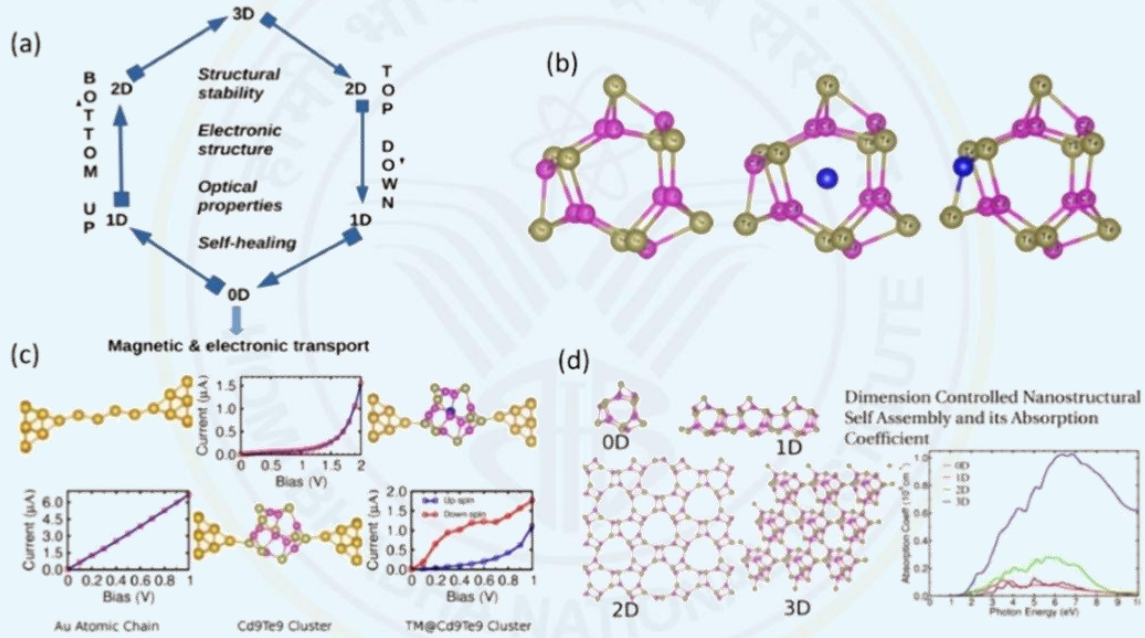

Schematic showing (a) The workflow of the thesis for studying various properties of CdTe nanostructures using top-down and bottom-up approaches; (b) Geometry of bare, endohedrally and substitutionally doped Cd9Te9 cluster; (c) The electronic transport in Au chain, semiconducting and half-metallic Cd9Te9 cluster-based tunnel junction devices; (d) Nanostructures self-assembled from Cd9Te9 cluster and their optical absorption spectrum

6.2.3 Effect of Heat Dissipation on Photoluminescence Quantum Yield in Large- Area Mono-layer MoS_2 and its Applications

Molybdenum disulphide (MoS_2) is an elderly member of the 2D transition metal dichalcogenides family that got an explosive interest in research communities due to its interesting optical, electronic, excitonic, and thermal properties. The monolayer (1L) MoS_2 is an excellent light absorber however, it suffers from the low quantum yield (QY) of the photoluminescence (PL) emission due to various structural defects. Before seeking any

surface treatment, it is important to investigate the impact of local temperature on PL emissions because quasiparticles are very sensitive towards doping, dielectric medium, and temperature.

Different (~30-6000 µm2) sized 1L-MoS_2 flakes grown by modified chemical vapour depositon technique, are used to investigate the mentioned effect. Interestingly, the large area (~6000 µm2) 1L-MoS_2 showed PL QY of ~1.8% because of high heat dissipating capacity and low phonon-assisted exciton scattering (Schematic (a)). Also, the grain boundaries in a large area 1L-MoS_2 act as thermal barriers. Moreover, same effect under variations in the laser excitation energy, which is supported by Raman thermometry results and corroborated with computational simulations. Furthermore, the heat-dissipating area influences the emission of bound excitons in 1L-MoS_2 flakes at low temperatures (>77K). The transferred 1L-MoS_2, useful for fabricating flexible electronics, is inevitably prone to polymer residues. Unfortunately, low thermal conductivity of polymers can restrict cross-plane heat dissipation. Therefore, a film cleaning method was developed and demonstrated to obtain the 'ultra-clean 1L-MoS_2' (Schematic (b)), which showed improved field-effect transistor (FET) key device parameters. The Raman correlative plot analysis further supports the supposition.

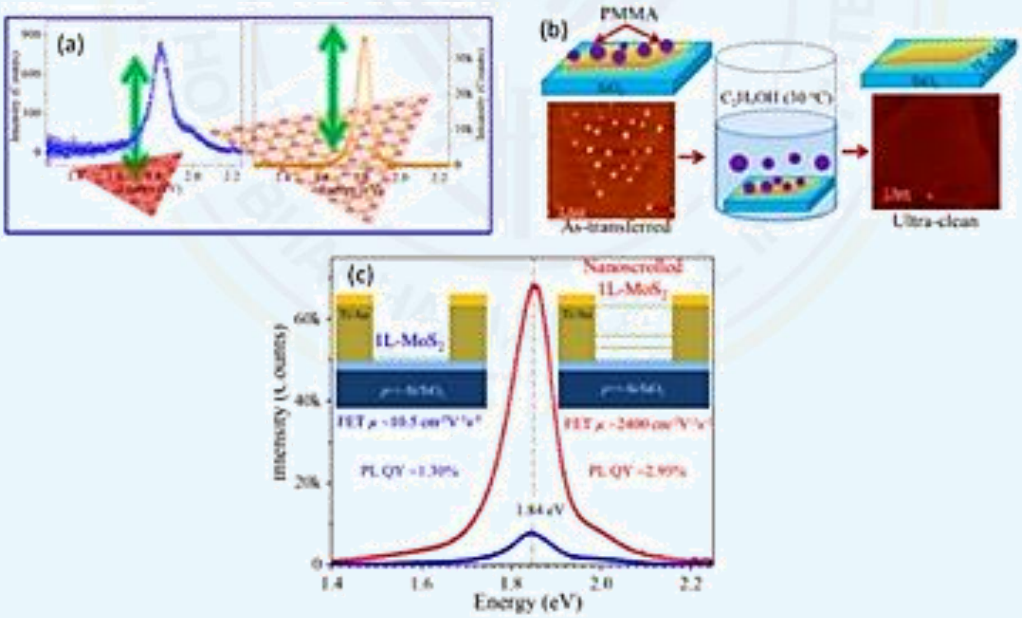

(a) Small-area and large-area 1L-MoS_2 flakes representing different PL QY due to variation of heat dissipating area and phonon-assisted exciton scattering; (b) Cross-plane heat dissipation in transferred 1L-MoS2 film is obtained by treating with hot ethanol treatment for 96 h and ultra-clean film was obtained; (c) Nanoscrolled 1L-MoS_2 is synthesized by evaporation assisted nanoscroll formation which showed enhanced PL QY and superior key device parameters in FET devices.

Thermal management is critical in electronic and optoelectronic devices due to the increasing drive for compact and high-performance electronics by escalating the power density. One of

the critical issues of power density can be nullified by increasing the cross-sectional area of channel material in similar dimensions i.e., by fabricating nanoscrolled 1L-MoS_2. Nanoscrolled 1L-MoS_2 are multilayer in morphology, however, they behave monolayer electronically. Nanoscrolled 1L-MoS_2 exhibit a direct optical gap, and enhanced PL QY (~2.95%) compared to planar 1L-MoS_2 (Schematic (c)). The thermally stable nanoscrolled 1L-MoS_2 demonstrates enhanced photocurrent and superior FET device performances, such as a one-order higher on/off ratio and two-order higher field-effect mobility compared to the device fabricated using planar 1L-MoS_2.

6.2.4 Observational Analysis and Numerical Modeling Studies of Sea Breeze, Convective Thunderstorms and Air Pollution Dispersion along the Southeast Coast of India

Sea and land breezes (SB) are mesoscale circulations which have impact on local weather and air pollution transport. Observational analysis revealed that selection method considering both surface and upper air parameters provide more realistic detection of SB events in the south coastal region. Noah-MP land surface scheme in WRF provided better prediction of SB events. The recirculation effect during onset of SB has led to nearly 30% increase in pollutant concentration/ radioactivity dose during SB onset phase. Simulations revealed that sea breeze convergence initiated intense convective thunderstorms in summer in study region. Development of Horizontal Convective rolls before the onset of SB alters the pollutants concentration by trapping the pollutants. The observational analysis and numerical simulations were conducted to study these phenomena and highlighted in the thesis.

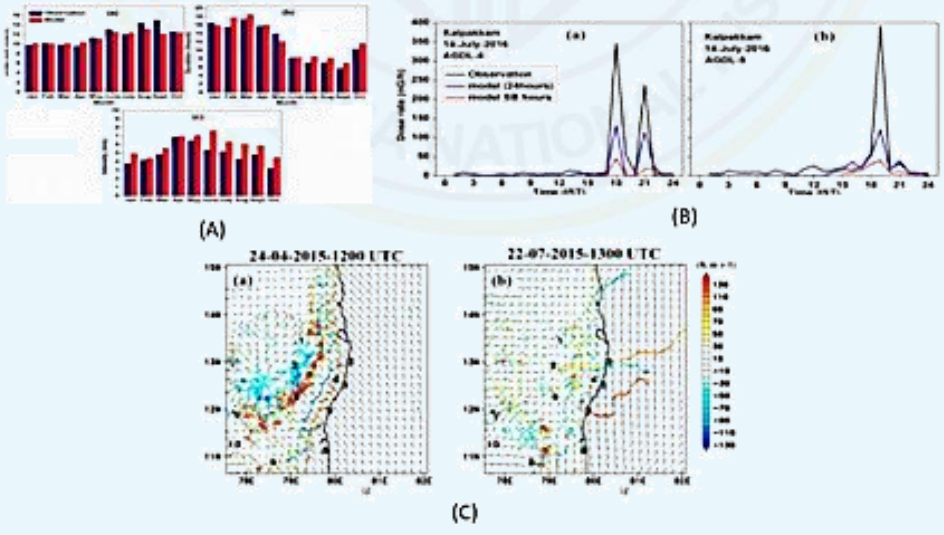

Scheme (A): Comparison of sea breeze onset time (a), duration (b) and Maximum Intensity (c) at Kalpakkam between observations and simulations for selection method identified sea breeze days; Scheme (B): Comparison of observed and model simulated Ar41 dose rate (nGy/h) a) AGDL-4 and b) AGDL-5 on 14 July 2016 at Kalpakkam; Scheme (C): Simulated surface wind flow (at 10 m) and vertically integrated moisture convergence in the layer 1000-300 hPa at a) 1200 UTC/1800 IST on 24 April 2015 for TS1 and b) 1300 UTC/1900 IST on 22 July 2015 for TS2

Sea breeze is predominant along the coastal regions and its detection is important for its influence on the local weather and air quality management. An objective selection method proposed with six meteorological conditions gives more realistic detection of SB days of 129 days compared to 152 days by conventional method, the WRF model simulated SB days by using selection method are 122 days with 77 common days indicating 63% accuracy in detecting SB events. The main influencing parameter for SB was the synoptic winds and the surface wind directional shift. SB was stronger & early with longer duration in summer (Scheme (A)). The sensitivity of SB circulation with different land surface physics with observations shows a better representation SB feature in Noah-MP followed by Noah than 5-layer scheme. The air pollutants released at the time of SB shows an increased (30%) pollutants concentration along the coastal regions at the time of SB onset (Scheme (B)). The convective thunderstorms developed during summer & southwest monsoon shows the presence of strong low level SB convergence is the basic triggering mechanism. The stronger SB convergence during summer associated with high CAPE led to intense storms compared to southwest monsoon storms (Scheme (C)). The sensitivity to cloud microphysics simulation showed that the Morrison & Goddard schemes better predicted the thunderstorm features compared to the Lin and Thompson schemes. The differences in conversion factors of solid hydrometeors in microphysics schemes lead to the better representation thunderstorm features in Morrison followed by Goddard. The HCRs developed before the onset of SB was mainly due to the presence of moderate wind shear shows the presence of thermal instability is the main mechanism of formation. The sensitivity to different land surface models shows a more realistic simulation of rolls by Noah-MP than Noah.

6.3 Institute of Physics, Bhubaneswar

6.3.1 Studies of Metal Oxide and Chalcogenide Thin Film Based Memristors for Memory and Neuromorphic Computing Applications

The limitations of the conventional computing architecture such as von Neumann bottleneck and memory wall impinge serious criticality to the data-centric and power-hungry computations of AI algorithms which restrains its applications in edge devices. In recent years, researchers from academics and industries have been looking forward to novel materials and new device architecture for a novel computer architecture based on the structure and functions of the human brain also known as neuromorphic computing.

The thesis focuses on the resistive switching study of vacancy-engineered TiO_2 memristors and persistent photoconductivity of two-dimensional MoS_2 optoelectronic synapses for memory and neuromorphic computing applications. Digital and analog resistive switching is observed in an Ag/TiO_2/Pt memristive device. Digital resistive switching behaviour is attributed to the formation/rupture of the conducting filament. While the analog resistive switching is due to the modulation of Schottky barrier height due to the accumulation of oxygen vacancies at the TiO_2 and Ag interface. Density functional theory studies show that

during the filament formation (ON state) a conduction path is created between the bottom and top electrode while the path is broken (OFF state) due to the discontinuity in the bandgap. The analog resistive switching behaviour is utilized to demonstrate various synaptic functions such as potentiation, depression, etc. Following that an oxygen vacancy engineered Ag/$TiO_{2-\Delta x}$/Pt memristor is constructed which shows the coexistence of volatile and non-volatile resistive switching. The volatile nature of the resistive switching can be explained using a field induced nucleation model. The conducting filament of the Ag/$TiO_{2-\Delta x}$/Pt memristor can be narrowed down to an atomic level where quantized conductance states are observed. The device exhibits threshold and relaxation dynamics which are used to demonstrate complex neuromorphic functions such as spike time dependent plasticity (STDP), spike rate dependent plasticity (SRDP), long term memory (LTM), short term memory (STM), and nociceptive behaviour such as allodynia, hyperalgesia. Finally, a two-dimensional MoS_2 optoelectronic synapse is constructed for the emulation of logic and arithmetic operation along with synaptic functionality in a single device. The persistent photoconductivity of the device is used as the synaptic weights which can be modified synergistically by optical as well as electrical pulses. An Ag/MoS_2-TiO_2/Pt memristor is fabricated which shows resistive switching behaviour. This thesis work provides an opportunity to emulate various complex forms of learning principles and their possible implementation in neuromorphic computing circuits.

6.3.2 Nanoscale TiO_x-based Memristive Synaptic Devices for Neuromorphic Computing Applications: Role of Defect Engineering

Mimicking biological brain-like functionalities in memristor is the most sought-after attribute leading to the recent development of neuromorphic devices for advanced computing applications. The intrinsic defects in the form of oxygen vacancy (O_V) or metal ions vacancy play a decisive role to decide the resistive switching (RS) property and artificial synaptic functionalities of an oxide-based memristor. For instance, defects across an oxide thin film can be altered by varying the growth parameters, albeit it is difficult to have a precise control over it. In this respect, ion implantation is a versatile and universally used technique which offers a simple way to produce well-controlled defects in oxide layers over a desired region, making it a robust approach for defect engineering in oxide-based devices. On the other hand, the size of a synaptic device has tremendous technological importance because it determines the degree of integration: smaller the device size, higher the memory integration density. One of the convenient ways to realize memristive synapses and acess their performances in such a small scale is the use of conducting atomic force microscopy (cAFM), where the cAFM tip can behave as a movable top electrode generating devices having configuration: cAFM tip /active medium/bottom electrode.

In the present thesis, TiO_x thin film-based two-terminal memristive synapses are investigated by employing cAFM in search of an optimized device in terms of reliability, high scalability, and power efficiency for neuromorphic computing. The defects inside the TiO_x film were altered following two different ways: one is by varying *in-situ* growth parameters using different

physical vapour deposition techniques [i.e., pulsed laser deposition and radio frequency (*rf*) magnetron sputtering] and the other is by employing post-growth ion implantation technique. Here, two parametric phase diagrams are developed to summarise the growth parameter dependent-memristive performances in the TiO_x/p^{++}-Si devices. Following this, also explore ITO substrates to grow TiO_x films by PLD technique, where artificial synaptic behaviour was detected in the films. In contrast, the sputter-grown TiO_x films on p^{++}-Si and ITO-coated glass substrates under RT did not show any RS or synaptic functions within the measurable range of our cAFM setup. This were related to the less O_V within the bulk of the film. In order to improve the O_V concentration on both the PLD and sputter-grown TiO_x films, next we tune the post-growth defect density and consequently the RS behaviour using ion implantation by varying the ion mass (viz. Ar, Ni, and Au). Firstly, 5 keV Ar-ions having different fluences are implanted on both PLD and *rf* sputter-grown TiO_x/p^{++}-Si samples which leads to a fluence-dependent increase in O_V content in case of PLD grown TiO_x, resulting in improved RS and artificial synaptic behaviour. In contrary, sputtered TiO_x films do not show any RS at nanoscale after implantation. This may be due to the high resistivity of these samples. Next, to address this limitation, we increase the mass of the implanted species from Ar (40 amu) to Ni (58 amu). Eventually, 15 keV Ni-ion implantation on sputtered TiO_x/p^{++}-Si sample leads to excellent RS stability at the nanoscale, which has been shown to work as a source of true random number generation. Nevertheless, no synaptic functionalities can be observed in these films. This leads us to further increase the ion mass to Au (196 amu) in order to probe whether any synaptic plasticities could be discernible in the sputter-grown Au implanted TiO_x films. A remarkably improved RS and bio-synaptic behaviour is demonstrated for 60 keV Au-ion implanted memristors. Overall, in the present thesis work, the role of defects (mainly O_V concentration) in TiO_x-based memristors has been investigated by employing local probe techniques and find out the optimized memristor suitable for highly scalable, low power neuromorphic applications.

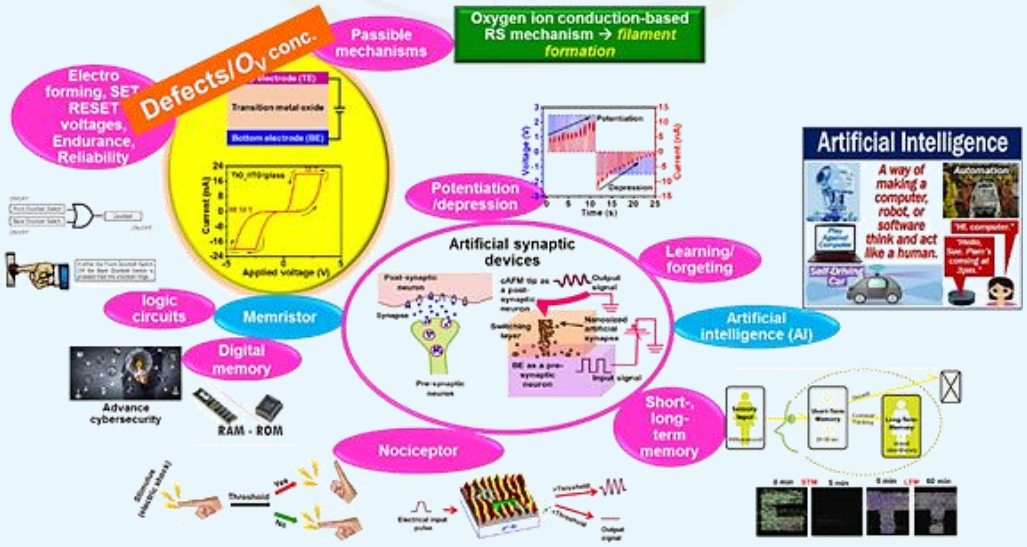

Schematic representation of highlight of the thesis work

6.3.3 Development of Large Scale CVD Grown Two Dimensional Materials for Field-Effect Transistors, Thermally-Driven Neuromorphic Memory, and Spintronics Applications

Two-dimensional (2D) materials have emerged as a captivating class of quantum materials, with transition metal dichalcogenides (TMDCs) at the forefront of research due to their semiconducting properties and potential for diverse applications. This thesis presents a comprehensive exploration into the synthesis, characterization, and application of TMDCs, particularly focusing on MoS_2 and WS_2. Various 2D TMDCs such as monolayer/multilayers of MoS_2 and WS_2 have been synthesized using modified CVD set up and the impact of growth parameters on the structural and optical properties of the materials. Optimization strategies are also explored to enhance the scalability and quality of TMDC synthesis, paving the way for their integration into electronic devices. Field -effect transistors have been fabricated on monolayer MoS_2 using photolithography technique. The optoelectronic response in optimally grown MoS_2 samples is presented to demonstrate tunable electronics properties under wavelength selective illuminations. The achievement of high- performance hysteresis-free field-effect transistors (FETs) and the exploration of their intrinsic transistor behavior lay the foundation for future device applications in memory, logic, and sensor systems.

Further, mem-transistors based on monolayer MoS_2, showcasing their multifunctionality as both high-performance transistors and synaptic memory devices have been explored. The temperature-dependent memory mechanism and the development of a transfer technique for device fabrication are highlighted, offering insights into scalable memory solutions. The potential of WS_2-based mem-transistors for more than 64 storage states and synaptic operations has been demonstrated, catering to the demands of ultra-high-density memory applications. The ion-gating mechanism and stable device functionalities underscore the suitability of WS_2 for advanced memory technologies. The development of dilute magnetic semiconductors (DMS) based on TMDCs, particularly focusing on Co- doped WS_2 and MoS_2 monolayers has been explored. First-principles calculations and micromagnetic simulations reveal the potential of these materials for spintronic applications, highlighting their magnetic properties under strain engineering.

6.3.4 Optoelectronic Optimization of Thin Films Related to the Metal Oxide Contact-Based Photovoltaic Cell

The thesis presents a detailed study on the growth and characterizations of individual layer necessary for constructing heterojunction thin film solar cells and their electrical, optical, structural, and compositional aspects.

Different constituent layers for developing heterojunction thin film solar cells by using pulsed DC/rf magnetron sputtering technique have been studied. Different materials used for different layers of the solar cell include tungsten oxide (WO_3) and Al doped ZnO (AZO) as

metal oxide contact based window layers and Sb_2Se_3 as absorber layers. Pyramidally textured Ge substrates fabricated using metal-assisted chemical etching technique have been used. It has been observed that local work function and resistivity systematically reduce with increasing AZO film thickness. Annealed Sb_2Se_3 films deposited at an angle of 0° and having a thickness of 1000 nm show the optimal optoelectronic properties for its possible use as an absorber layer in PV cells as it exhibits band-gap of 1.14 eV and highest absorption co-efficient (1.40 × 105 cm-1 corresponding to a photon energy of 1.61 eV). The optoelectronic properties of as-deposited and annealed WOx/p-Si heterojunctions (having varying WOx film thickness, growth angle, and partial oxygen pressure) have also been investigated. The research work caried out in the thesis a path of developing Sb_2Se_3-based thin film solar cells having optimized

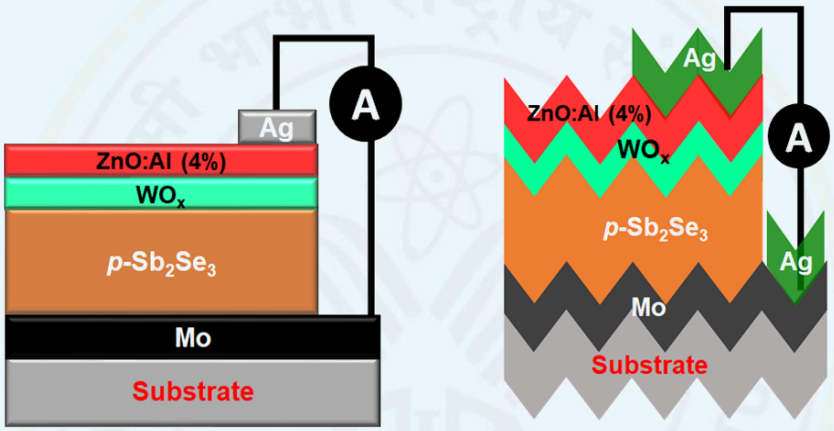

Schematic representation of Sb_2Se_3-based solar cell

6.3.5 Phenomenology of Neutrino Mass Models at Present and Future Collider Experiments

Despite its tremendous success the Standard Model (SM) of particle physics, fails to explain a few major experimental observations. One of such observations is the tiny neutrino masses and their mixings which compels us to invoke beyond the Standard Model (BSM) physics. In this thesis, we explore a certain class of BSM models that can generate neutrino masses and mixings via the "Seesaw Mechanism" has been explored and their detection prospects at the future collider experiments have been analyzed.

The collider potential for detecting Right-Handed Neutrino (RHN) in the $U(1)_{B-L}$ model has been highlighted. The gauge interaction of RHN facilitates its pair production with sizable cross-section at pp colliders, such as HL-LHC and FCC-hh. The dedicated signatures in the inner detector and the muon spectrometer have been analyzed, which are a pair of displaced fat-jets and tracks, respectively. The study reveals significant sensitivity to active-sterile mixing. The FCC-hh shows promise, demonstrating sensitivity consistent with the seesaw relation.

The R_2 Lepto-quark-assisted seesaw model, LQ discovery potential at proposed electron-proton colliders (LHeC and FCC-eh), where resonant LQ production occurs has been presented. The production rate of LQs using both $e^{\pm}$ beam and the effect of polarized $e^{\pm}$ beam on production rate has been studied. The high transverse momentum lepton and jet final state from LQ decay offers promising discovery prospects. Further, this model provides a promising framework to test the presence of RHNs as it predicts a large production rate of RHNs via LQ decay. In this production mode RHNs lighter than $W^{\pm}$ boson, originating from a TeV scale LQ can be boosted and displaced, leading to displaced and collimated decay products. It is proposed to reconstruct such final states as displaced fat-jet and use of two ratio variables, r_N and r_E associated with jets, to reduce background. Performing a comprehensive analysis, RHN with mass $\mathcal{O}(10)$ GeV can be detected at the LHeC with only $\mathcal{L} = 120\ (2)\text{fb}^{-1}$ luminosity with e^- (e^+) beam.

The phenomenological aspects of the Type-II seesaw model, which predicts doubly-charged and singly-charged Higgs with promising collider signatures have also been studied. A detailed discussion on the variation of the branching ratio of the doubly charged Higgs with neutrino oscillation parameters considering the 3σ uncertainties of the oscillation parameters is presented. The observed limit on the mass of the doubly-charged scalar set by the CMS search in same-sign di-lepton final states has been reinterpreted. A weaker limit after including maximal possible branching ratios instead of assuming at 100 % is obtained. In addition, the potential of a future hadron collider, HE-LHC, to probe doubly-charged scalar in the multi-lepton final states has been explored.

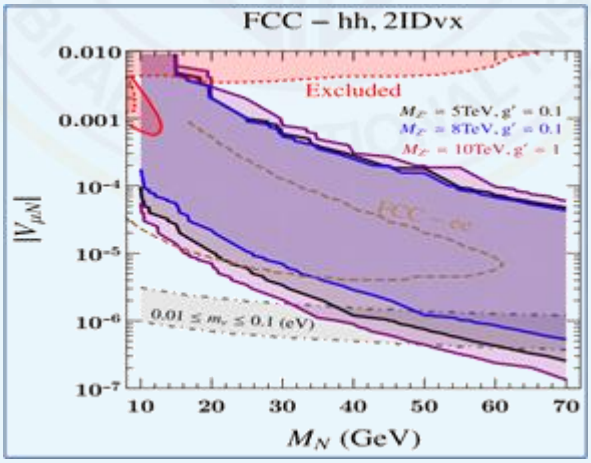

6.3.6 Structural Properties and Thermal Evolution of Neutron Stars through Dense Matter Equation of State with Observational Constraints

The thesis constitutes a comprehensive exploration of the static and dynamic aspects of neutron stars through the application of the relativistic mean field (RMF) formalism. Diverse RMF parameter sets, including NL3, FSUGold, IU-FSU, G3, and IOPB-I, have been meticulously

employed to satisfy experimental and observational constraints, thus enhancing the breadth of analysis. The extension of RMF formalism to finite temperature unveiled critical insights into phase transition temperatures, binding energy, and symmetry energy derivatives for infinite nuclear matter at varying temperatures. Notably, the G3 parameter set demonstrated a higher critical temperature for the liquid-gas phase transition, aligning more closely with experimental observations. A remarkable highlight emerged from the alignment of the G3 parameter set's curvature parameter at saturation density with constraints derived from PSR J0030+0451 and GW170817 observations. The investigation delved into the cooling mechanisms and mass-radius profiles of proto-neutron stars, demonstrating that the G3 parameter set's predictions aligned with observational data, accommodating constraints from PSR J0740+6620 and PSR J1614-2230. The incorporation of neutralino as dark matter candidate within neutron stars revealed a profound interplay between dark matter admixtures and equation of state, leading to shifts in star mass and cooling dynamics. Furthermore, the study uncovered the pivotal role of enhanced neutrino cooling mechanisms, triggered by the direct Urca process, sending cooling waves from core to crust, subsequently influencing the star's surface temperature and internal thermal equilibrium.

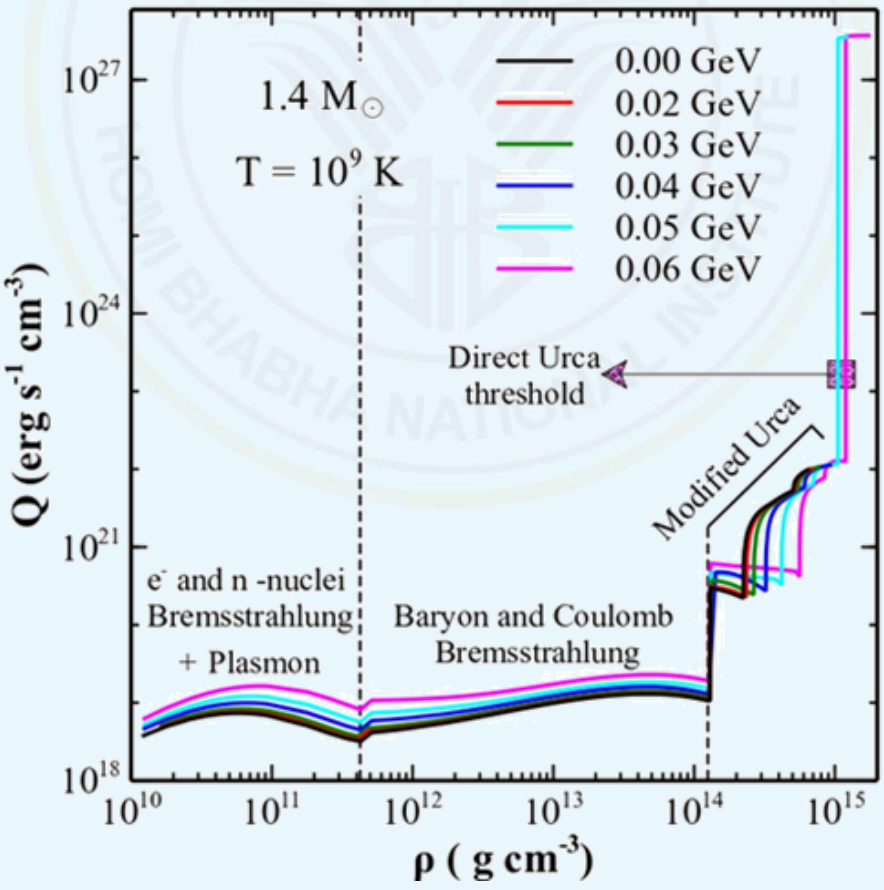

The exploration of quarkyonic matter presented a paradigm-shifting highlight, as the quarkyonic model's predictions converged with the conformal limit for speed of sound. This model accurately predicted the masses of massive neutron stars while accommodating tidal deformability estimates from gravitational wave events. Importantly, the study delved into

post-merger dynamics of binary neutron star mergers, unveiling the quarkyonic equation of state's potential to prevent remnant core collapse into black holes. Additionally, the incorporation of the coherent density fluctuation model (CDFM) within the RMF framework offered novel insights into finite nuclei and neutron stars, bridging the realms of nuclear physics and astrophysics. These collective highlights illuminate the profound implications of RMF formalism across a spectrum of phenomena, providing a richer understanding of ultra-dense matter and astrophysical processes.

6.3.7 Floquet Generation of Higher-Order Topological Systems

Very recently, the idea of bulk boundary correspondence has been generalized in the context of higher-order topological (HOT) systems, giving rise to a new paradigm of topological phases of matter. A *d*-dimensional n^{th} order HOT system is characterized by *(d-n)*-dimensional boundary modes. On the other hand, Floquet engineering allows one to generate the topological phase starting from a topologically trivial system. In this emerging direction of non-equilibrium generation of topological systems, in the present thesis, the possibility of engineering the Floquet HOT systems employing various periodic driving protocols has been investigated.

A semi-metallic system irradiated by circularly polarized light employing the high-frequency limit has been explored. The system exhibits a Floquet HOT insulator (FHOTI), hosting in-gap modes when the discrete four-fold rotational and time-reversal symmetries are broken by adding a Wilson-Dirac (WD) mass. The Floquet generation of the second-order topological superconducting (SOTSC) phase, hosting zero-dimensional (0D) Majorana corner modes (MCMs) has been theoretically investigated employing a quantum spin Hall insulator with proximity-induced superconducting *s*-wave pairing. The dynamical prescription consists of the periodic kick in an in-plane magnetic field and a WD mass term in bulk. Another exciting aspect of Floquet engineering is that one can realize anomalous boundary modes at finite quasienergy, namely π-modes, with concurrent regular 0-modes. Such π-modes does not have any static analog. In this direction, two driving schemes- a two-step drive and mass-kick protocol have been proposed to systematically generate the hierarchy of Floquet topological insulators in two and three dimensions.

A three-step periodic driving scheme to engineer two-dimensional (2D) Floquet quadrupolar superconductors and three-dimensional Floquet octupolar superconductors hosting 0D MCMs has also been proposed, based on unconventional *d*-wave superconducting pairing. To circumvent the subtle issue of characterizing 0- and π-MCMs separately, the periodized evolution operator to construct the dynamical invariants is employed, namely quadrupolar and octupolar motion in two and three dimensions, respectively. However, engineering the step-drive protocol seems to be an extremely challenging experimental task in the context of

real material platforms. Hence, a practically feasible time-periodic sinusoidal drive protocol in onsite mass term is proposed to generate the 2D Floquet SOTSC, hosting both the regular 0- and anomalous π-MCMs while starting from a static 2D topological insulator/*d*-wave superconductor heterostructure setup. Furthermore, the Floquet perturbation theory in the strong driving amplitude limit has been employed to provide analytical insight into the problem.

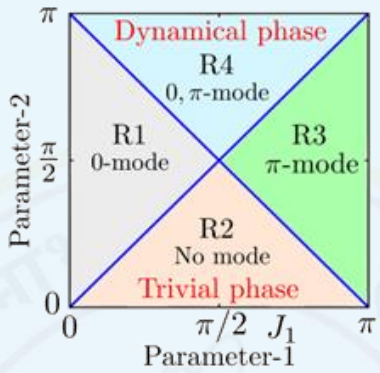

Phase diagram of a Floquet HOT system in the parameter space

6.3.8 Spin-orbit Coupled Electron Transport, Interface Magnetism in Transition Metal Oxide and Heavy Metal Thin Films

The thesis mainly concerns about low temperature mangetotransport effects on a few distinct conducting materials. The interplay of different mechanisms including (1) weak localization/anti-localization, (2) electron-electron interaction, and (3) topolgical effects (chiral anomaly) is carefully analyzed. Main finding of the thesis is that the magnetotransport properties can be utilized as a powerful tool to extract the information of different types of scattering process and their corresponding scattering strength. Highlight of this part includes a procedure to disentangle electron-electron interaction effect from weak localization physics, and the dimensional crossover effect resulting in a metal-insulator transition.

Quantum transport on Pt thin films exploiting multi-band conduction theory of Hikami-Larkin-Nagaoka equations reveals the existence of two independent different types of conduction bandswhich are s and d orbitals. Further, it was realized that effective inelastic scatterings are very different for two conduction bands. The band made of more symmetric orbital (*i.e.,* s orbital) experience lower effective inelasticscattering strength in comparison with less symmetric orbitals.The study on bilayer structure of $SrIrO_3/SrCuO_2$ revealed that antiferromagnetic proximity effect quenches the magnetic impurity scattering and promotes the manifestation of the chiral anomaly effect in a predicted Dirac semimetal $SrIrO_3$.In the final part of the thesis, spontaneously stabilized bilayer system consisting of ferromagnet and antiferromagnet has been discussed, which leads to magnetic exchange bias effect at low temperatures.

6.4 Institute for Plasma Research, Gandhinagar, Gujarat

6.4.1 Experimental Study of a Quasi-Two-Dimensional Complex Plasma

A complex plasma system consists of highly charged dust grains embedded in a pool of electrons, ions, and neutral atoms. The strong coupling in complex plasma leads to the freezing of the system to a crystalline phase, and in the weakly coupled regime, the system acts as a fluid. In this thesis cross-disciplinary phenomena in 2D complex plasma crystals is investigated and critical factors underlying complex observations are identified. Experiments are conducted in the Dusty Plasma Experimental-II device with an asymmetric electrode arrangement to reduce ion streaming and facilitate stable 2D dust crystals in direct-current discharge conditions. Initially, a square lattice is observed through a structural phase transition, achieved by mitigating non-reciprocal forces and mode coupling instability. In a subsequent set of experiments, the effect of initial dust densities on the transition sequences of a 2D dust crystal is explored. At low dust densities, the monolayer crystal transitions to quasi-bilayer square, disordered, and vertically aligned hexagonal layers. Above a density threshold, a “Triple Point" state emerges with square, hexagonal, and liquid regions, driven by localized complex or mixed instability. The effect of varying radial confinement strengths on the 2D dust crystal is then studied. It is observed that monolayer buckles and square lattice formation take place. This state is also characterized by dynamical structural rearrangements occurring due to the heterogeneous cooperative motion of dust particles. Lastly, a self-sustained solid-liquid coexistence state is also achieved by controlling the discharge parameter.

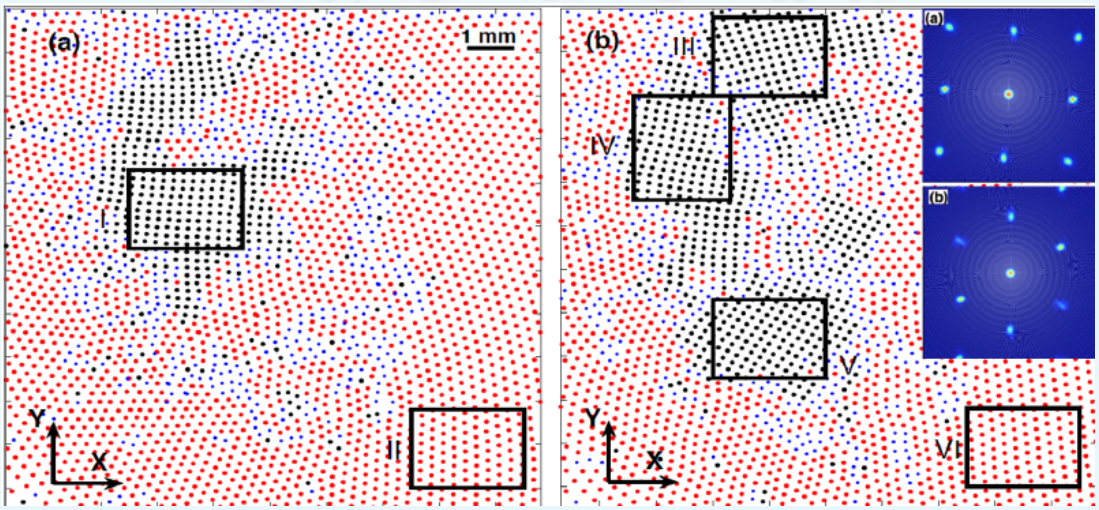

Local structural topology of dust system at (a) V = 400 V, and (b) V = 396 V at a constant pressure of P = 5 Pa. The red particles have hexagonal geometry, the black particles have square geometry and defects are represented by blue. The inset show static structure for region I and II

6.4.2 Control of Edge and Scrape-off Layer Tokomak Plasma Turbulence

The plasma in the edge and scrape-off layer (SOL) regions of a tokamak is highly turbulent mainly due to the excitation of the interchange instability. This instability occurs as the directions of centrifugal force due to the rapid toroidal plasma motion and the density/pressure gradient are in opposing directions. The plasma turbulence gives rise to some coherent nonlinear density structurescalled “blobs” and these blobs are responsible for the anomalous transport of the plasma. Therefore,the control of anomalous transport and these instabilities are necessary for the stable/safe operationof tokamaks. This thesis deals with the control of turbulence from the perspective of the blob birth generation mechanisms, and by applying an external bias (electrode biasing) in the edge region.

A blob formation mechanism in the SOL and far SOL region of a tokamak plasma model has been derived theoretically and validated numerically using three-dimensional (3D) simulation in the SOL region. It is found that the poloidal gradient of the poloidal electric field (PGPEF) plays an importantrole in the formation mechanism that was not considered in the earlier works. The blob formation takes place when the amount of shear exceeds the non-linear growth rate (γ_n) of the basic interchange instability within the radially elongated streamer region. Further, cross-correlation between different shears and γ_n has been examined which indicate that γ_n and these shears are not independent phenomena, they may be connected by a blob formation. It is found that if the contribution of PGPEF is removed, the blob formation criterion does not satisfy or marginally satisfy that indicates the importance of PGPEF in this thesis. It is found that PGPEF is related to the plasma blob rotation during and after the blob formation which is a scope on investigation in future. Edge biasing can control particle recycling, exhausts, confinement time, and heat loads on the limiter/divertor plates.

This thesis deals with the investigation of the above effects theoretically as well as numerically. A linear analysis of a set of model fluid equations has been done after inclusion of terms related to the edge biasing. Non-linear analysis shows that the positive biasing to lead to alarger increment in plasma density and temperature as compared to negative and no (w/o) biasing.Effect of positive and negative biasing has been examined on the cross-correlation between densityand poloidal electric field, plasma density and poloidal electric field fluctuations, cross field transport,power spectra, blob fraction, heat & particle loads. It is found that the heat and particle fluxes in theedge region are seen to increase with the radial electric field shear in the region where a flow reversaltakes place that may be an indication of Kelvin-Helmholtz instability. This will be investigated in future. Instead of direct current (DC) biasing, alternative current (AC) is also the scope of future.

6.4.3 Sheath Effects on the Resonance Hairpin Probe in Negative Ion Diagnostics

This thesis investigates the effects of the sheath formed around the cylindrical limbs of a hairpin probe (HP) for negative ion diagnostics, focusing on both steady-state and dynamic sheath conditions. The HP, which directly estimates the dielectric properties of the medium between its limbs, is employed with both DC-bias and pulse-bias to modify the sheath around its cylindrical limbs. The width of the sheath is experimentally determined, and the valid range of applied bias is identified. These findings allow for the calculation of the electric field at the sheath edge, supporting theoretical predictions.

The dielectric properties of the sheath depend on the presence of thermal electrons within it. The influence of electron parameters, such as density and temperature, on the resonance frequency is examined, revealing that the resonance frequency is primarily a function of electron temperature. Experimental measurements are compared with theoretical model values, enhancing our understanding of plasma-sheath interactions. The study also includes the estimation of plasma potential and the sheath area correction factor, which are then used in the saturation current ratio (SCR) method to deduce plasma electronegativity in oxygen plasma. A brief description of the SCR method is provided, and its application is extended to determine the radial profile of plasma electronegativity in a magnetized plasma. Additionally, the thesis explores the role of time-dependent bias in the HP for negative ion diagnostics, demonstrating the applicability of this approach in both electropositive argon and electronegative oxygen plasma.

6.5 National Institute of Science Education and Research, Bhubaneswar

6.5.1 Probing New Physics through Standard Model Higgs to Diphoton Signature in pp Collisions at $\sqrt{s}$ = 13 TeV

The discovery of the Higgs boson during the Run 1 of LHC has provided the answer to the long-standing puzzle of electroweak symmetry breaking at least within the Standard Model. Recent ATLAS and CMS results strongly indicate the Higgs boson couples with the SM particles as predicted by the SM. Presently, various production mechanisms (ggF, VBF, VH and ttH) and decay modes of the Higgs boson (at the LHC) are being explored to achieve further precision on the existing measurements, while looking for any deviation from the SM predictions. H→γγ decay is an interesting final state signature due to the involvement of a virtual top quark loop and thus any beyond the Standard Model (BSM) physics involving Higgs boson production would lead to an excess in the diphoton invariant mass spectrum (from Higgs). Furthermore, during the Run 2 of LHC, an additional Higgs boson production mode associated with a single top quark (tH) is explored for the first time in this thesis to improve the sensitivity further for the H→ γγ analysis and to explore associated possibilities beyond the SM.

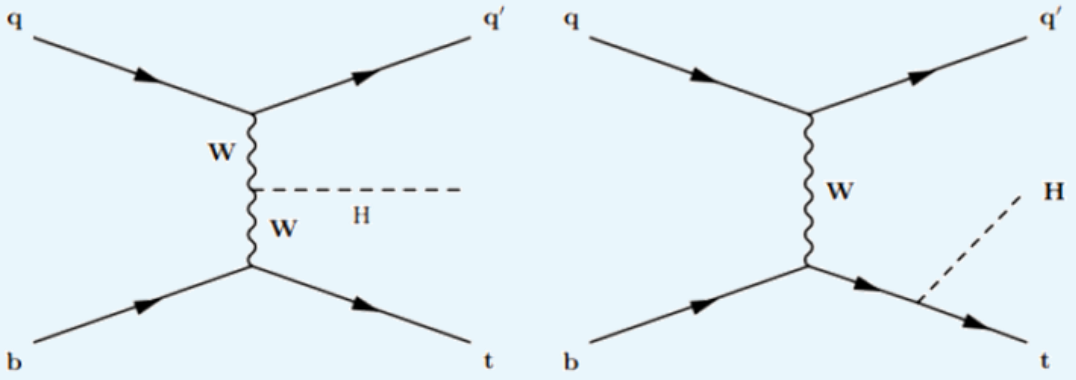

The associated production of the Higgs boson with one top quark in a hadron collider

After the discovery of the Higgs boson, the SM is complete as a low-energy effective theory describing all known fundamental particles and their interactions. However, several problems remain unanswered including why the quantum correction of the Higgs boson mass diverges to the Plank scale. In many models and extensions of the standard model, inclusion of a new type of fourth generation particles, called vector-like quarks, T' and B', provides a feasible solution. A dedicated analysis is performed to search for production of the T' vector-like quark in proton-proton collisions at a center-of-mass energy of 13 TeV using data corresponding to an integrated luminosity of 137 fb^{-1} collected by the CMS detector during the 2016-2018 LHC run. This analysis presents the asymptotic upper limit of the T' production signal strength (μ = σ_{obs}/σ_{SM}) over the T' mass range of 600 GeV to 1200 GeV. This search is the first T' search to exploit the decay of the Higgs boson in the diphoton channel.

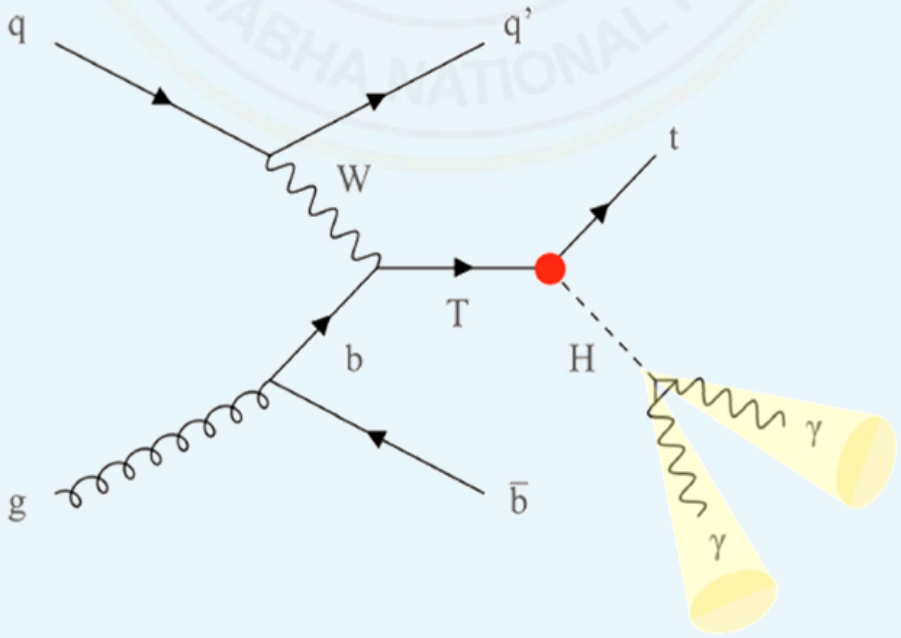

An example of Single T' production in LH

6.5.2 Characterization of Non-Trivial Spin Texture and Anomalous Electronic Transport Properties in Mn-Based Heusler Systems

This thesis investigates the characterization and stability of the antiskyrmion phase, along with the anomalous electronic transport properties, in Mn-based Heusler compounds. In the first part, the antiskyrmion phase is identified through thermomagnetic responses such as Magnetocaloric effect and AC susceptibility study. The positive magnetic entropy changes during the helical-to-antiskyrmion phase transition and the anomalies present in field-dependent AC susceptibility are utilized to construct the antiskyrmions phase diagram. Following this, the stability and phase evolution of antiskyrmions are explored in micron-sized single crystalline devices. A distinct topological Hall signature is observed in the out-of-plane direction, confirming the presence of the antiskyrmion phase. Further, the stability and phase evolution of antiskyrmion phase is studied by applying an oblique magnetic field relative to the c-axis. The topological Hall effect diminishes as the inclination angle increases and eventually vanishes at a higher tilt angle. The experimental observation is well supported by micromagnetic simulations, which show that applying a tilted field annihilates the antiskyrmions, leading to a reduction in the topological Hall effect. In the final part, the manipulation of electrical transport properties in MnPt(Ir)Sn is studied. It is found that the anomalous Hall effect (AHE) increases with increasing Ir doping in place of Pt, while the total magnetization decreases significantly. Scaling analysis of AHE reveals that the scattering-independent intrinsic mechanism increases with Ir concentration while the scattering-dependent extrinsic contribution decreases. The study presents a crossover from an extrinsic to an intrinsic mechanism of the anomalous Hall effect with increasing Ir doping, highlighting the evolution of various contributions to the AHE.

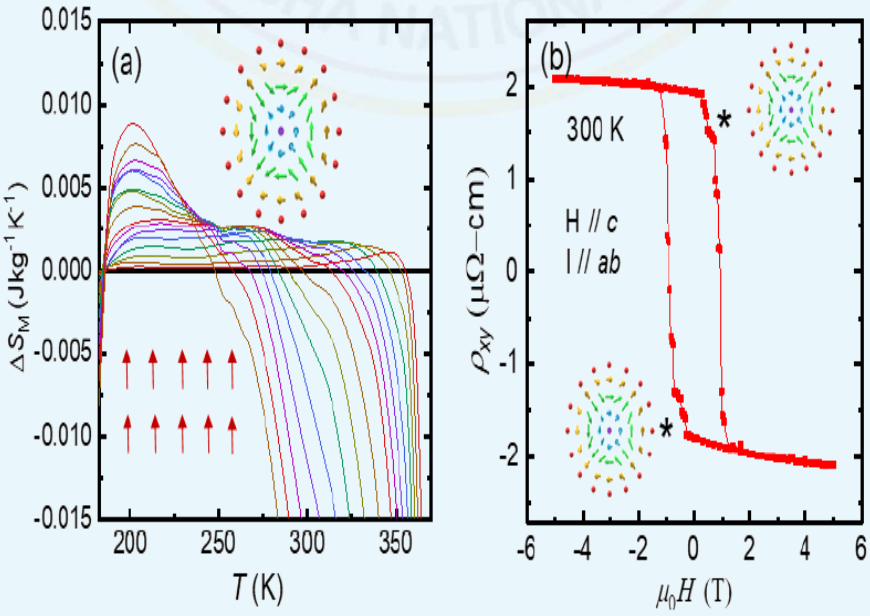

Identification of antiskyrmion phase utilizing (a) Magnetoentropic signature and (b) Topological Hall effect

6.5.3 Defect Induced Tunable Charge Density Wave Ordering and Optical Properties In 2D -Tise$_2$ TMDs Materials

This work is devoted to synthesizing the two-dimensional transition metal based TMD $TiSe_2$ thin films grown on the Si substrate using chemical vapour deposition (CVD) technique. This material has drawn tremendous interest for their charge density waves (CDWs), thermoelectric, and spintronic applications. CDW is a type of periodic oscillation of charge density, due to lattice distortion, that arises in crystalline materials below certain critical temperature (T_{CDW} ~ 200K). T_{CDW} can be tailored to operate in both low and high temperatures above 200 K via doping, intercalation, and external stimuli for CDW-based optoelectronic device applications. Here the addition of impurities was done under low energy ion implantation or surface passivation for the enhancement of optical, thermoelectric, photocatalytic, and ferromagnetic properties.

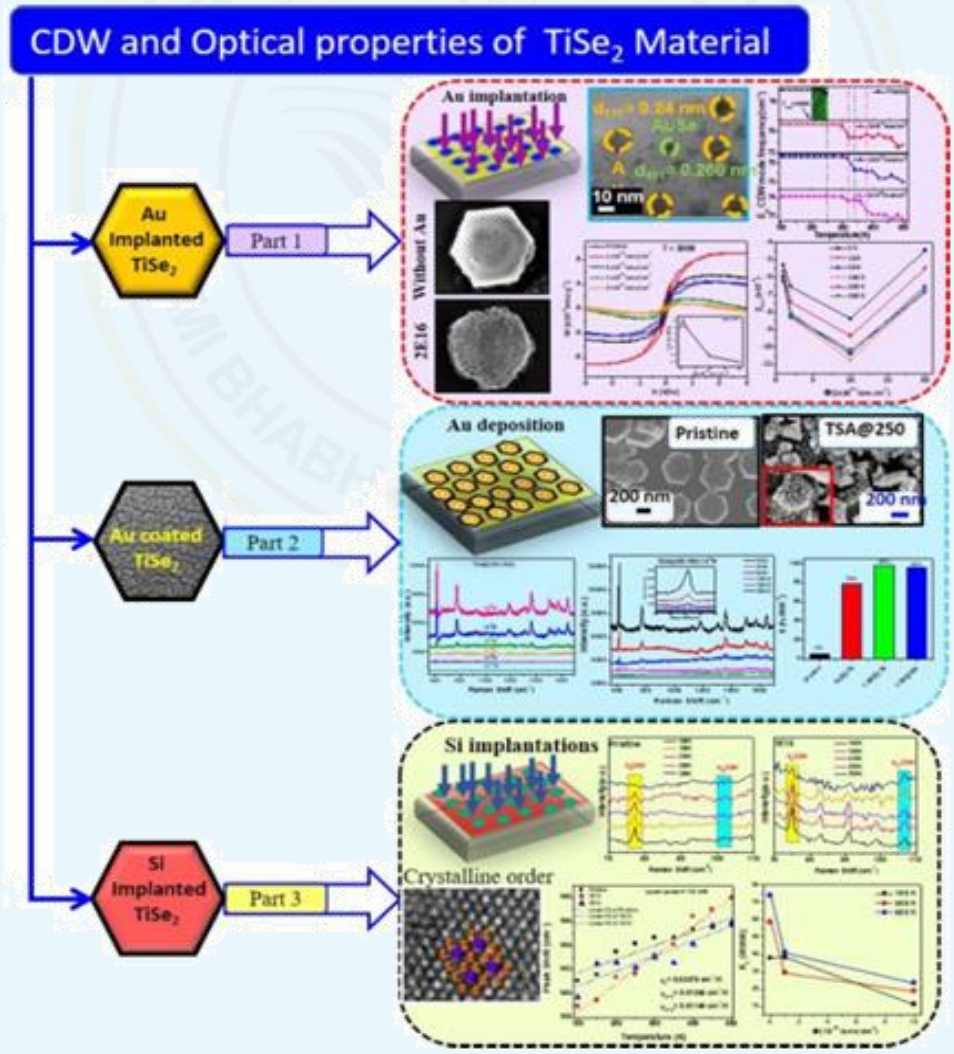

Pictorial summary of the thesis

20 keV Au ions were implanted in $TiSe_2$ nanocrystals at different fluence ranges of $\phi = 5 \times 10^{14}$, 1×10^{15}, 2×10^{15}, 1×10^{16}, and 2×10^{16} ions cm^{-2} and demonstrated the T_{CDW} above room temperature up to 500 K. The CDW ordering at higher temperatures was observed but, the underlying mechanism is still unclear, which need more theoretical investigations. The work also includes the investigation of the magnetic response of Au-implanted $TiSe_2$ nanocrystals due to the formation of Au nanoparticles and the increase in Se vacancies. The work carried out on Au nanoparticle decorated $TiSe_2$ nanocrystals illustrates enhanced surface-enhanced Raman spectroscopy and better photocatalytic activity. Raman spectroscopy has been used to study SERS and coherent laser light induced photocatalytic activity. The selective deposition of Au on the top of the hexagonal $TiSe_2$ surface creates many hotspots and tunable surface Plasmon resonance, resulting in a better SERS signal and improved photocatalytic degradation of R6G dye. The (30 keV) low energy Si ions were implanted to demonstrate the tunable CDW and lattice thermal conductivity of $TiSe_2$ nanocrystals. During CDW formation, electron-phonon coupling disrupts the lattice translational symmetry that contribute to the thermal conductivity of the sample. In conclusion, defects play a crucial role in tuning the CDW, magnetism, and optical properties of $TiSe_2$, making it a viable 2D material for spintronic, environmental pollution, and magnetic sensing device applications.

6.6 Raja Ramanna Centre for Advanced Technology, Indore

6.6.1 Studies on $La_{0.7}A_{0.3}MnO_3$ (A=Ba, Sr and Pb) Embedded P(VDF-TrFE) Nanocomposite films for Room Temperature Magnetoelectric Coupling Applications

High magnetoelectric (ME) coefficient at room temperature in nanocomposites (NCs), (which consists of piezoelectric and magnetostrictive phases) is required for device application. The magnetostrictive phase in NCs should have high magnetostriction and it should require low magnetic bias field. Ferromagnetic metals and metal alloys have good magnetostriction but they have high fabrication cost, high eddy current loss and problems of chemical stability with temperature. Colossal magnetoresistance CMR based magnetostrictive $La_{0.7}Ba_{0.3}MnO_3$(LBMO), $La_{0.7}Sr_{0.3}MnO_3$(LSMO) & $La_{0.7}Pb_{0.3}MnO_3$(LPMO) nanoparticles (NPs) show high Curie temperature, high saturation magnetization, high volume magnetostriction, CMR property and low coercivity. Hence, they can be a good choice of magnetostrictive phase in the ME composites. However, there is no study on CMR based NCs for ME applicatins. The effect of structural and magnetic properties of the LBMO, LSMO and LPMO NPs on the ME effect in NCs are unexplored. The multiferroic and ME properties of the CMR based polymer NCs are unfamiliar and the ME effect based applications using these NCs are still to be explored. A new kind of flexible, uniform (0-3) nanocomposite (NC) films were prepared embedding LBMO, LSMO and LPMO NPs in P(VDF-TrFE) matrix by solution casting method. It is shown that these NC films show room temperature multiferroic properties up to 2 vol.% of NPs. These films exhibit strong strain mediated ME coupling.

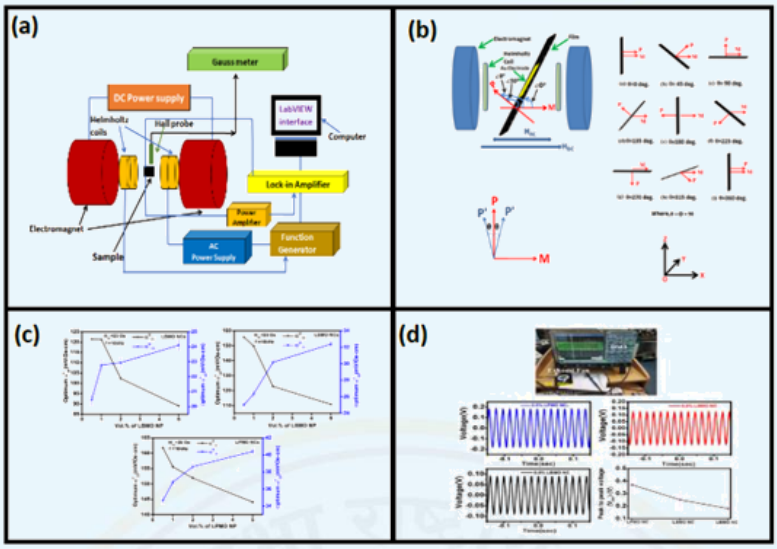

Schematic of the magnetoelectric (ME) coefficient measurement setup with Lock-in technique. (b) Effect of angular variation between polarization (P) and magnetization (M) on ME coefficient of 0.5vol% LBMO/P(VDF-TrFE) NCs. (c) Variation of ME coefficient with NP's vol.% in 31 and 33 mode of LBMO/P(VDF-TrFE) NCs, LSMO/P(VDF-TrFE) NCs and LPMO/P(VDF-TrFE) NCs. (d) ME effect-based energy harvesting application from stary magnetic field of 0.5 vol.% LBMO/P(VDF-TrFE) NCs, 0.5 vol.% LSMO/P(VDF-TrFE) NCs and 0.5 vol.% LPMO/P(VDF-TrFE) NCs

It is observed that these NC films show maximum ME coupling effect in the 31-mode. As the ME coefficients of these NC films are high, they are used in ME based device applications. The magnetic noise energy harvesting from stray magnetic field have been demonstrated using these NC films. In summary, LBMO, LSMO and LPMO-P(VDF-TrFE) based NC films show good multiferroic properties at room temperature. The strong interfacial connectivity between the NPs and polymer phase display high ME effect, they are good source of energy harvesting using the electromagnetic noises. In future, these CMR based NC films can be used in AC magnetic field sensor and in spintronics applications.

6.6.2 Studies on Resistive Switching in TiO_2 Thin Films for Non-Volatile Memory Applications

The resistive random-access memory (RRAM) has emerged as the promising alternative to existing flash memories. Titanium dioxide (TiO_2) has been widely used; however, TiO_2-based RRAM devices face challenges in switching time, power consumption, and an established physical mechanism. In the present thesis, the TiO_2 thin films-based RRAM devices were fabricated with different electrode materials and geometries, to improve switching parameters and elucidate mechanisms. Reliable unipolar switching was observed using inert electrode Au in Au/TiO_2/Pt configuration, showing good endurance and retention. The reset process was significantly slower (~252µs) than the set process (~180ns), however it decreased to ~400 ns as amplitude of reset voltage pulse increased from 0.8 to 1.8V. The power consumption (~10s of mW) was high in Au/TiO_2/Pt devices. Active metal Cu was used in place of Au to form Cu/TiO_2/Pt devices, which showed bipolar switching with lower switching

voltages (<1V) and currents (~10s μA), resulting in reduced switching power (~μW) and fast switching times (~250ns) led to low energy (~pJ) operation. Compliance current (I_C) controlled 3-bit multilevel switching was also achieved by creating distinct low resistance states, enhancing integration density. Cu/TiO_2/Pt devices were also fabricated in 8×8 crossbar geometry, demonstrating excellent yield and switching variability (σ/μ~20%). It showed half-integral quantised conductance, where increase in I_C caused enhanced number of quantised states, promising higher-order multibit switching. The switching mechanism was explained by conducting filament (CF) model. Unipolar switching was attributed to oxygen vacancy-based self-accelerated thermal dissolution, while bipolar switching to Cu CF based electrochemical metallisation (ECM). Theoretical calculations revealed increase in CF diameter with I_C caused multibit switching and higher quantised states. The impedance spectroscopy studies established the source of resistive and capacitive contribution to memory states. Similarity in switching behaviour of RF sputtered TiN thin films and Pt-based RRAM devices established TiN as potent substitute for the noble metal Pt. In summary, the findings of the thesis offer insights into switching mechanisms and methods to improve switching parameters crucial for non-volatile memories and neuromorphic computing applications.

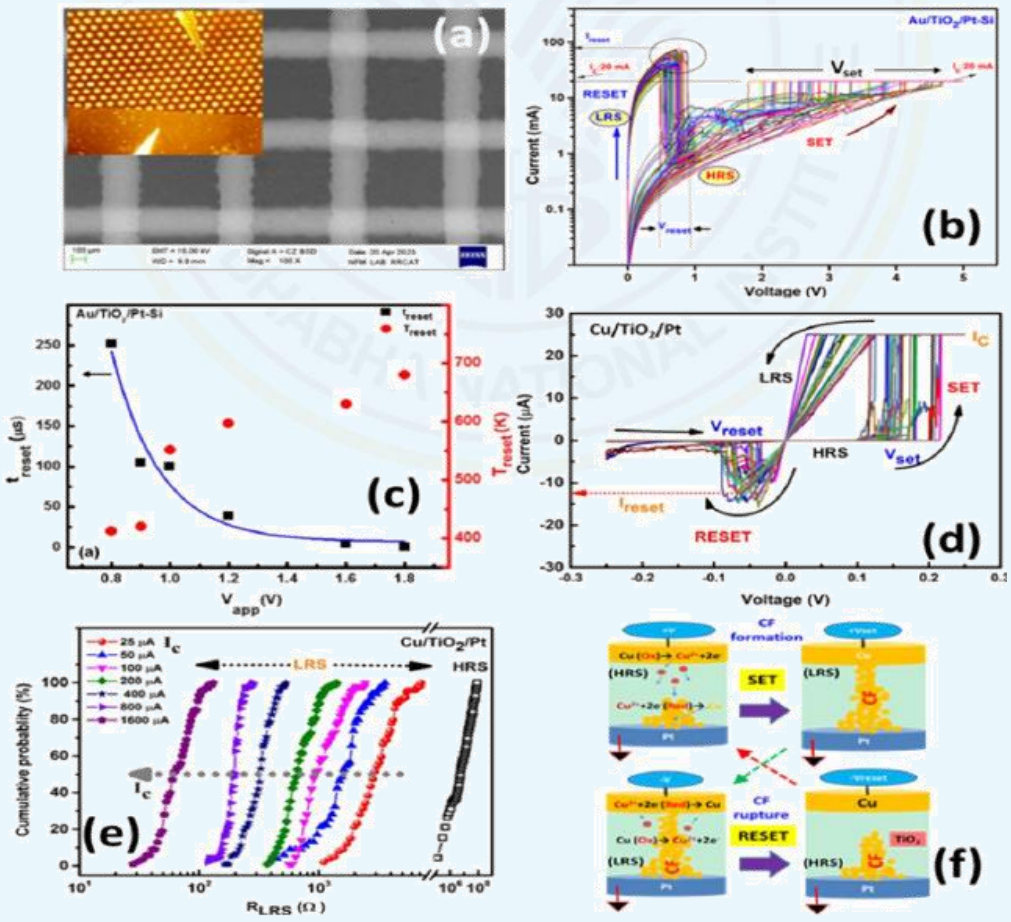

(a) Device structure crossbar and common bottom electrode (Inset), (b) Unipolar resistive switching in Au/TiO_2/Pt, (c) Reset switching time vs voltage, (d) Bipolar switching in Cu/TiO_2/Pt, (e) 3-bit multilevel switching, and (f) ECM switching mechanism

6.6.3 Application of Synchrotron Based Spectroscopy Methods for Study of Ion Implanted Materials

The investigation of precise depth distribution of implanted ions in a crystalline and non-crystalline material has become increasingly important as they find widespread applications in various fields of science and technology. In addition, it is also equally important to understand the stopping mechanism of energetic ions as well as damage caused by them in a target material. Particularly, transition metal ion (Au, Ni, etc.) implanted silicon substrates offer unique advantages because of their modified band gap and spectral response in the field of semiconductor technology. Implantation of a transition metal ion produces an intermediate band in the forbidden band gap region in the silicon material. Applicability of the intermediate band materials in the fabrication of infrared detector and high efficiency solar cell have rapidly driven the growth of this field in last few years. The performance of an implanted silicon-based device greatly depends on the depth distribution, chemical state, local structure of implanted ion species, as well as damage caused by the implanted ions in the Si material.

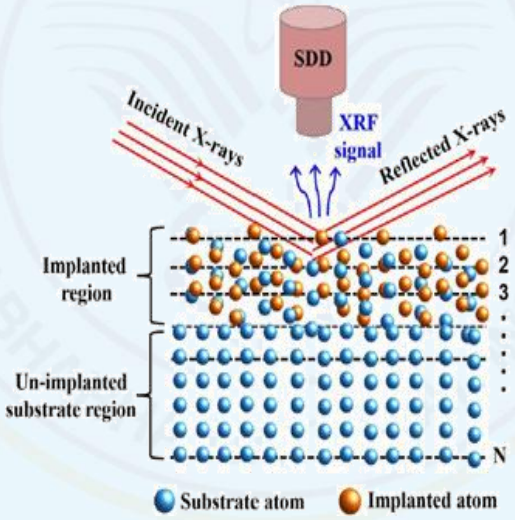

Schematic representation for the GIXRF and XAS measurements to study the ion implanted materials

In the present thesis, depth distribution, structural properties and local co-ordination of the gold and nickel ion implanted in a silicon <100> substrate have been studied using different X-ray based techniques. It has been shown that the XSW assisted GIXRF analysis in combination with the XRR measurement allows non-destructive determination of micro-structural parameters of ion implanted materials with a depth resolution of 5Å. The most significant advantage of the simultaneous XRR and GIXRF analysis is that it reduces the uncertainties of the individual techniques thereby improving the reliability of the estimated parameters of ion implanted regions. Structural and mechanical properties of gold thin layers deposited on a silicon <100> substrate have also been investigated in detail in order to explore their potential applications as X-ray optics in synchrotron beamlines. In addition, using the

conventional EDXRF excitation geometry, a new XRF measurement scheme has been proposed to obtain improved detection sensitivities for the various elements present in an analyte. The proposed method benefits from all the advantages of the TXRF method. It is expected that the proposed XRF measurement scheme would be highly useful for the depth profile analysis of an ion implanted substrate that utilize a controlled sequential chemical etching procedure.

6.7 Saha Institute of Nuclear Physics, Kolkata

6.7.1 Exploring Leptogenesis and Pre-BBN Universe with Primordial Gravitational Waves and their Spectral Features

The thesis focuses on the long-standing question of why there is more matter than antimatter in the universe. Leptogenesis deals with this by simultaneously explaining light neutrino masses via the seesaw mechanism. Such mechanisms are very difficult to probe due to the very high scale (M) associated with it. To overcome this challenge, the use of high-amplitude Gravitational Waves (GW) from cosmic strings and the modification of the spectral shape of inflationary GWs as potential sources to investigate these mechanisms has been explored.

The work on Radiatively induced gravitational leptogenesis (RIGL) and its GW complementarity reveals that the gravitational coupling of right-handed (RH) neutrinos with the curved background might be responsible for generating a non-zero lepton asymmetry even in equilibrium. The study focused on the flavor effects in RIGL, which has been shown to successfully explain leptogenesis with the lightest RH neutrino mass scale below the Davidson-Ibarra bound. Taking RIGL as the primary source of lepton asymmetry, the GW complementarity between the NANOGrav Pulsar Timing Arrays (PTA) 12.5 years data and future neutrino less double beta decay (0νββ) experiments has been analyzed. Finally, since kination domination has shown as a natural requirement for efficient lepton asymmetry production from RIGL, which in turn produces an upward-going GW spectral break, a study on Neutrino-Gravitational Wave Complementarity (NGWC) has been carried out.

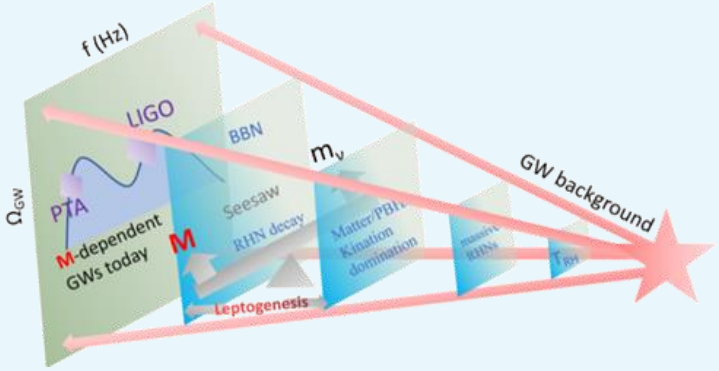

Graphical representation of PhD thesis

Further, leptogenesis from ultralight PBH evaporation has been investigated, where massive RH neutrinos are emitted by the PBHs and subsequently decay in a CP-asymmetric manner to generate a lepton asymmetry, with strong constraints on RH neutrino and PBH masses for the correct baryon asymmetry. The focus has been on the PBH-dominated case, where the baryon asymmetry is independent of PBH density at formation. It was found that a GW spectral break might occur at much higher frequencies for a successful leptogenesis scenario. The consequences of a high-scale (B - L) gauge symmetry breaking on low-scale leptogenesis, which may have led to a scalar-dominated epoch have been addressed. The GW signatures of this intermediate scalar epoch in primordial inflationary blue-tilted GWs have been explored explaining NANOGrav12.5-year data. The study also highlights how the cosmic string complementarity makes the scenario unique compared to any other intermediate matter domination.

6.7.2 Morphology and Electronic Structures of Organic Semiconducting Thin Films

Electronic structures and energy level alignment (ELA) at the metal/organic interfaces play a pivotal role in the performance of organic semiconductor (OSC)-based electronic and optoelectronic devices. Efficient charge injection across the metal/organic interface depends on these electronic structures and ELA. Any energy barriers at the interface can hinder the charge injection and limit the device efficiency. Wettability is another major issue at these metal/organic interfaces which can be improved for optimal device performance. The interfacial electronic structures at metal/organic interfaces are heavily influenced by factors such as interfacial interactions, molecular orientation, and wettability. Thus, refining such important interfacial parameters becomes imperative in gaining a comprehensive understanding of the ELA at these metal/organic interfaces.

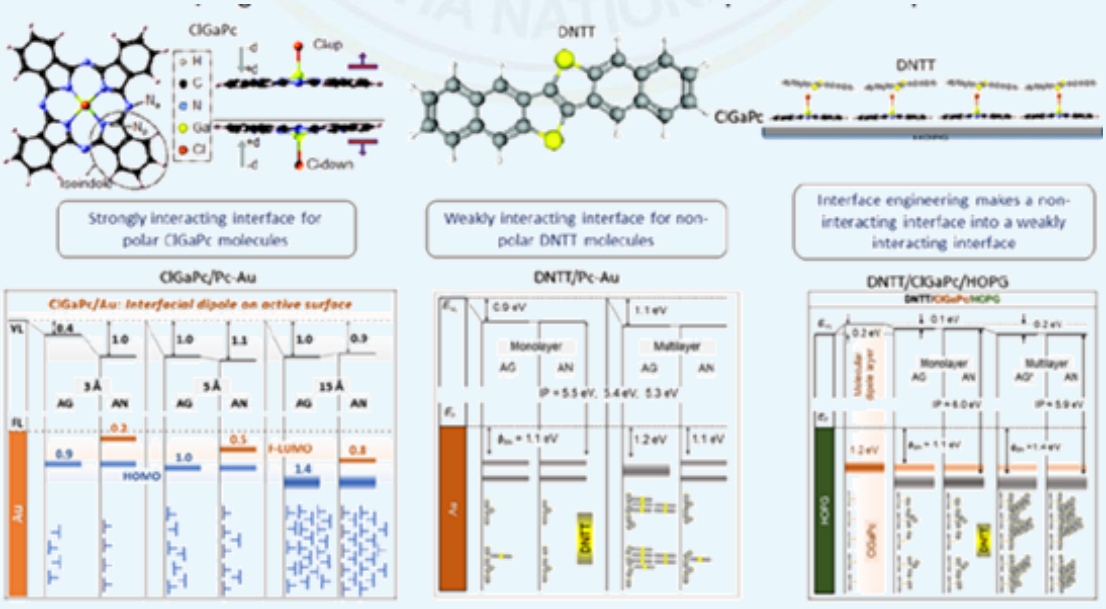

Graphical representation of PhD thesis

In this context, the energy level structures of polar chlorogallium-phthalocyanine (ClGaPc) and non-polar dinaphthothienothiophene (DNTT) molecules were examined on active polycrystalline-Au (pc-Au) and relatively inert highly oriented pyrolytic graphite (HOPG) surfaces in the present thesis.

The goal was to comprehend the ELA at these interfaces through photoelectron spectroscopy. Notably, a site-specific interaction was identified at the ClGaPc/pc-Au interface, resulting in the formation of an interface state known as the former lowest unoccupied molecular orbital (F-LUMO) state, as shown in left side of the schematic. Additionally, a remarkable band dispersion of the highest occupied molecular orbital (HOMO) level was observed at the DNTT/pc-Au interface, prompting an investigation into the distinctive structure of the DNTT molecular seed layer on pc-Au surfaces, as illustrated in middle of the schematic. Following these pivotal inquiries, modifications were made to the ELA and interfacial molecular coverage of DNTT. This was achieved by introducing an interfacial molecular dipole layer and altering the molecular conformation. The results demonstrated the capability of the interfacial molecular dipole layer to adjust the charge injection barrier and enhance wettability, which is demonstrated in the right of the schematic. This finding holds significance in achieving an improved ELA for this promising DNTT molecule, which, in turn, can contribute to enhance the device performance.

6.7.3 Statistical Physics Perspectives on Driven Systems

This thesis is based on the studies of the statistical properties of the steady states in a class of systems driven out of equilibrium. The absence of detailed balance makes nonequilibrium phases and phase transitions much richer and complex, allowing for the existence of orders having no equilibrium analogues. Lack of any general framework to study the statistical properties of nonequilibrium systems has often prompted to construct and study simple conceptual models that are easily tractable, both analytically and numerically such that questions of basic principles can be answered in straight forward manner within well-controlled approximations. The study here is for advancement of this direction by exploring collective behaviour of large collections, as well as it is focussed on one and higher dimensional systems. The problems include asymmetric exclusion processes, surface growth phenomena, effects of quenched disorders, active XY models, hydrodynamic models for active membranes with or without couplings to another active species. A principal focus of the research has been to find the long wavelength universal scaling behaviour and the associated properties of nonequilibrium steady states in the above-mentioned systems. Standard techniques including hydrodynamic modeling, field theoretic calculations, perturbative renormalisation group (RG) methods and Monte-Carlo simulation have been used. The thesis presents a spectrum of work ranging from microscopic model to hydrodynamic theory of the nonequilibrium systems and active matter with their novel results. The findings in this thesis will assist significant insights and fundamental understanding for future progression in this direction.

6.7.4 Tuning Structural Ordering of π-conjugated Homopolymer and Donor-Acceptor Copolymer Thin Films

In the past few decades, π-conjugated semiconducting polymers have garnered significant attention in printable electronics due to their remarkable electrical and optical properties, cost-effectiveness, and ease of fabrication. In thin films, these conjugated polymers are semicrystalline in nature, where the crystalline aggregates are interspersed with disordered regions. The charge carrier mobility (μ) of these polymers in organic thin-film transistors (OTFTs) critically relies on the quality, quantity, and orientation of the crystallites within the thin films. High-quality films are characterized by a high backbone planarity (BP) along the polymer chains. On the other hand, the orientation of these crystallites is pivotal in controlling the movement of charge carriers in OTFTs.

Films with edge-on oriented (EO) crystallites are preferable to those with face-on oriented (FO) crystallites for optimizing charge carrier transport. The present thesis primarily focuses on investigating the structural ordering of π- conjugated homopolymers and donor-acceptor (D-A) type copolymers thin films prepared through various deposition techniques, to understand the quality, quantity, and orientation of the crystallites, particularly near the film-substrate interface to get better device properties.

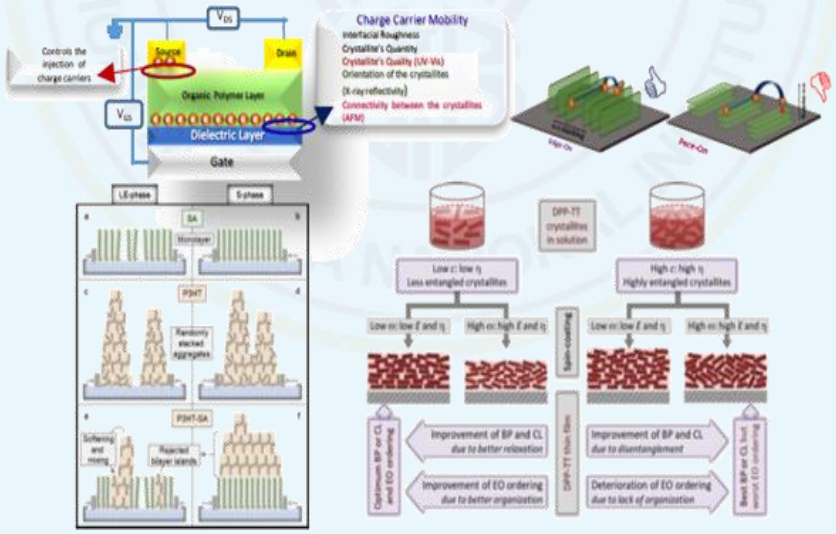

Graphical representation of PhD thesis

6.7.5 Exploring Half-Metallic Ferromagnetism and Magnetic Frustration in Some Structurally Disordered Novel Quaternary Heusler Alloy

In the realm of spintronics, understanding the effect of structural disorder on half-metallicity and the phenomenon of magnetic frustration in Heusler alloys is of paramount importance. Quaternary Heusler alloys are known for their unique electronic and magnetic properties, making them promising candidates for spintronic applications. This thesis explores the

intricate interplay between structural disorder and the attainment of half-metallicity, revealing the surprising resilience of high spin-polarization in disordered environments. Additionally, the occurrence of magnetic frustration within Heusler alloys, exemplified by reentrant spin-glass states, adds complexity to their magnetic behavior. This research contributes vital insights for advancing the development of spintronic materials within a concise framework.

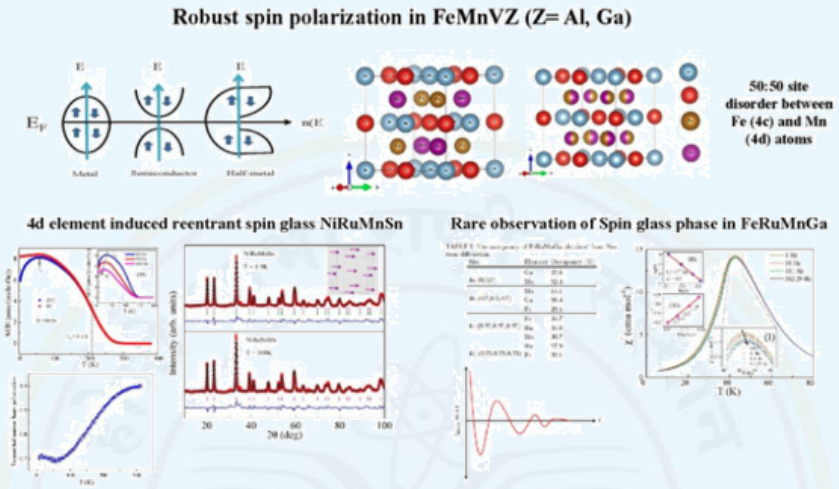

Visual representation of the thesis work

The thesis extensively explores quaternary Heusler alloys, focusing on their significance in spintronics and the intriguing concept of half-metallicity. It begins by examining FeMnVZ (Z = Al, Ga) compounds, where despite their disordered crystalline structures, theoretical calculations predict a robust half-metallic ferromagnetic ground state. This discovery underscores the resilience of high spin-polarization in disordered conditions, setting these compounds apart from other Heusler alloys. Additionally, CoMnCrGa, another captivating quaternary Heusler alloy, exhibits a half-metallic ferromagnetic ground state, even amidst structural disorder, positioning it as a promising candidate for room-temperature spintronics due to its high Curie temperature (TC) and spin-polarization. The investigation also encompasses CoFeVAl, initially predicted to possess a half-metallic ferromagnetic ground state but crystallizing differently, shedding light on the intricate interplay between structural disorder and half-metallicity, with profound implications for spintronic material design. Furthermore, NiRuMnSn reveals a partially disordered structure and a rare reentrant spin-glass state, impacting the magnetic moment and enhancing our understanding of spin-glass behavior in equiatomic quaternary Heusler alloys. Lastly, the highly disordered and equiatomic structure of FeRuMnGa surprisingly exhibits a pure spin-glass state, a rarity in quaternary Heusler compounds, with disorder affecting electron transport properties, resulting in semi-metallic behavior and an anomalous Hall effect at low temperatures. This underscores the role of structural disorder in shaping electronic and magnetic properties. In conclusion, this research provides crucial insights into quaternary Heusler alloys, their relevance to spintronics, and the impact of structural disorder on magnetic and electronic properties.

6.7.6 Investigation of Cosmic-Ray Muon Flux Variation with Overburden and Study of Nuclear Physics Inputs to Astrophysics

The thesis combines experimental measurements, theoretical modeling, and computational simulations to address challenges in low count-rate experiments and advance our understanding of nuclear astrophysical phenomena, providing valuable insights for various scientific applications.

In the realm of experimental work, this thesis addresses the challenges posed by background interference in low count-rate experiments, focusing particularly on the impact of cosmic muons. Through a series of muon flux measurements at the UCIL underground laboratory in Jaduguda, India, the study elucidates strategies for mitigating interference.

The investigation extends on the theoretical front to the computation of reaction cross-sections and astrophysical reaction rates, crucial for understanding nuclear astrophysical phenomena and advancing reactor technology. By employing realistic nuclear level densities obtained through the spectral distribution method, the thesis provides insights into nuclear processes of astrophysical significance, including radiative neutron capture and heavy-ion fusion reactions. Notably, the research demonstrates the importance of considering collective excitations and cross-shell effects in NLDs, and sheds light on key parameters (The density dependence of nuclear symmetry energy, etc.) influencing astrophysical S-factors for asymmetric nuclei.

6.8 The Harish-Chandra Research Institute, Prayagraj

6.8.1 Scattering Amplitudes in Bi-Adjoint Scalar and Massive Theories

One of the important aspects of the S-matrix program is to develop efficient techniques for calculating scattering amplitudes. In the eighties, Parke and Taylor observed that the maximally helicity violating (MHV) gluon amplitudes, which in the conventional Lagrangian formulation require computation of numerous Feynman diagrams, can be expressed in a nice compact form. In the last couple of decades, there has been huge progress in evaluating scattering amplitudes using on-shell techniques. Britto, Cachazo, Feng, Svrcek, and Witten have shown how to compute higher point amplitudes recursively from lower point ones. Massless supersymmetric, and non-supersymmetric amplitudes can be computed using these on-shell recursions without the Lagrangian description of the theory. Witten's seminal work on twistor string theory led to the formulation of integral representations of the S-matrix for N=4 super-Yang-Mills theory (SYM). Higher loop amplitudes are also calculated using twistor formalism and the generalised unitarity cut method. Inspired by string theory, worldsheet formalisms for S-matrix computations, *e.g.,* the Cachazo-He-Yuan (CHY) formalism and ambitwistor string models, are of interest as they offer novel insights into quantum field

theories. The Arkani-Hamed, Bai, He, and Yan (ABHY) construction based on positive geometry are notable developments in the contemporary S-matrix program. Cachazo, Early, Guevera, and Mizera (CEGM) generalised the usual CHY formalism to (k-1)-dimensional complex projective spaces. These n-point CEGM amplitudes for generalised bi-adjoint scalar theory have a relation with Grassmannian Gr(k,n) cluster algebras. In this thesis, the double soft factorisation of generalised (k,n) amplitudes has been calculated. We have also shown how our double soft factor for (3,6) amplitude mapped to the facet of the one-loop D_4 cluster polytope. Using recently developed massive spinor-helicity variables and on-shell massive supersymmetry, we compute tree-level scattering amplitudes in N=2* theory and higher loop amplitudes in the Coulomb branch of N=4 SYM theory.

6.9 The Institute of Mathematical Sciences, Chennai

6.9.1 A Primordial Solution to The Tensions in Cosmology

Acoustic peaks in the Cosmic Microwave Background (CMB) temperature spectrum as observed by the Planck satellite appear to be smoother than our expectation from the standard model lensing effect. This anomalous effect can be also mimicked by a spatially closed Universe with a very low value of Hubble constant that consequently aggravates the already existing discordance between cosmological observations. This thesis identifies a novel solution that removes these anomalies along with improved fit to Planck 2018 data compared to the standard model and at the same time alleviates/subsides existing tensions between different datasets in the estimation of cosmological parameters such as H0 and S8.

A signature from the early Universe is reconstructed, a particular form of oscillation in the primordial spectrum of quantum fluctuations as shown in the schematic, that solves or substantially reduces all these anomalies. The results are further supported theoretically by identifying examples of single field inflationary trajectories beyond the slow-roll regime. A damped oscillation in the first Hubble flow function - or equivalently a feature in the potential - and the corresponding localised oscillations in the primordial power spectrum, this model can lead simultaneously to larger value of H_0 and a smaller value of S_8. The model also provides unique signature in polarisation angular power spectrum which could act as litmus test for the model using future CMB data.

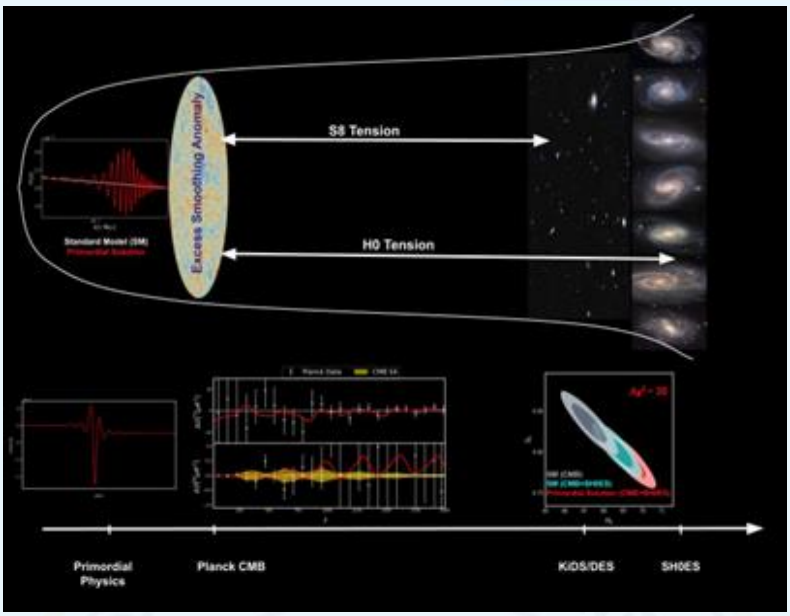

The primordial solution accounts for excess smoothing in Planck CMB data and removes the S_8 tension and substantially reduces the Hubble tension with a good improvement in fit to the data

6.10 Variable Energy Cyclotron Centre, Kolkata

6.10.1 Growth and Properties of Nano-Dot and Wire Structures Developed by Ion- Implantation on Pre-Fabricated Nano-Templates

The study presents the formation of isolated silver and carbon nano-dots on a pre-fabricated nano- template. To achieve this, a silver (Ag) ion-beam was developed using Electron Cyclotron Resonance (ECR) plasma sputtering, where silver atoms are introduced into the argon plasma via sputtering a biased silver plate within the ECR chamber. The resulting Ag^+ ions are then extracted, mass-separated, and transported to a UHV target chamber for implantation. The research investigates the flux variation of the Ag^+ ion beam by manipulating parameters such as applied bias voltage, microwave power, argon gas pressure, and the position of the silver plate relative to the ECR plasma center. It observes that the sputtering rate of Ag and the resulting Ag beam current strongly correlate with the applied bias voltage and plate position. Furthermore, the study explores the effects of microwave power and gas pressure on beam intensity, attributing variations to ionization processes and the mean free path of ionized atoms. Ultimately, 6 keV Ag^+ ions are implanted onto pre-patterned silicon nitride nano-pyramidal templates, leveraging the templates' geometrical shape and the ion beam's directionality to form an array of Ag nano dots on the nano-pattern. Through atomic force microscopy and surface chemical analysis, it is confirmed that well-defined pyramidal structures can be formed under specific ion bombardment conditions, as shown schematically in Figure 1. The presence of isolated silver dots enhances the Raman signal and alters significant light reflectance on the surface. Similarly, green to red emissive carbon dots are formed on silicon-nitride nano-templates

through successive implantation of nitrogen and carbon ion beams. Raman spectroscopy and X-ray photoelectron spectroscopy confirm the presence of amorphous carbon dots including SiC and graphitic nitrogen. Photoluminescence study shows emission spectra toward the deep red region, which is actually very difficult to achieve as normally C-dots show emission spectra in comparatively higher energy region, i.e., in the blue region. Excitation wavelength-dependent photoemission is observed, and the phenomena is shown due to the defect formation as well as graphitic nitrogen formation into the C-dots. Additionally, the growth of nano- patterns on a smooth silicon surface during carbon ion as well as nitrogen ion bombardment was explored. It reveals the transformation of ripple structures into triangular nano-pyramidal structures at higher ion fluences, attributed to silicon carbide or silicon nitride formation and differential sputtering effects. The variation in structural characteristics is explained based on existing continuum theory, with the transformation into three-dimensional pyramids attributed to local ion impact angles and consequent effects.

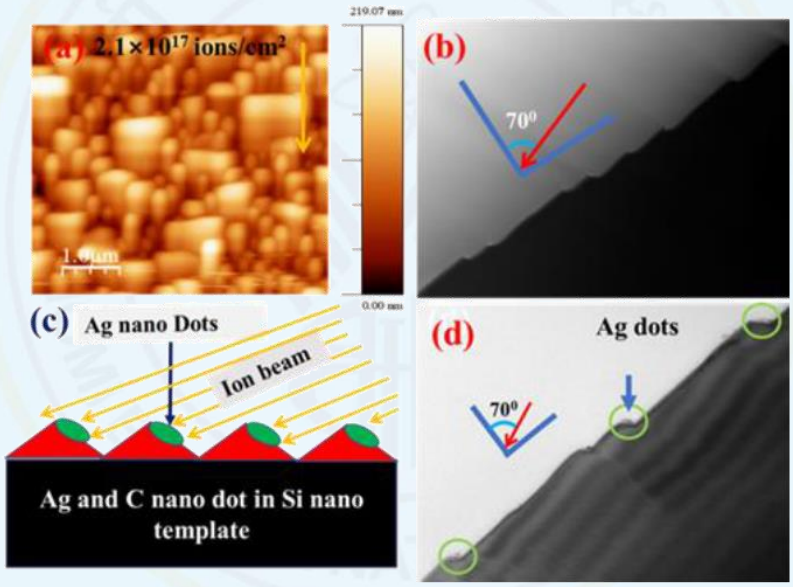

Formation of Ag and C nano-dot by successive ion implantation

6.10.2 Theoretical and Experimental Studies of Organic Inorganic Hybrid Perovskite Material implantation on pre-fabricated nano-templates

Room temperature ferromagnetic semiconductor is an essential requirement in spintronics due to its potential applications in non-volatile memory for computers, magneto-optic devices, Quantum computing and so on. The large impedance mismatch between ferromagnetic-semiconductor junctions largely reduces the spin-transport efficiency. Therefore, introducing magnetism in non-magnetic direct band gap semiconductors will ensure the transport of spin polarized electrons efficiently. Hybrid organic inorganic perovskite materials are direct band gap semiconductors which are mainly used for photovoltaic applications due to its fascinating optoelectronics properties such as, tunable direct band gap, large absorption coefficient, low excitation binding energy, long carrier

diffusion length etc. The thesis reports an extensive theoretical as well as experimental study on electronic and magnetic properties in hybrid halide perovskite materials i.e., $CH_3NH_3PbX_3$ (X=I, Br, Cl). The ab-initio calculation of magnetic properties in hybrid perovskite material has been performed in the frame work of density functional theory with MedeA-VASP software. The defect characterization of hybrid perovskite material has been carried out using positron anhilliation spectroscopy (PAS). Atomic vacancy or doping of two identical 3d transition metal ions at the Pb-site of $MAPbX_3$ can induce significant amount of magnetic moment. It has been found that only lead vacancy can induce magnetic moments in the system. But, methylammonium vacancy or bromine vacancy cannot generate any magnetic moment in the host. In case of doping, the asymmetric density of states calculation suggests that the 3d orbital electrons are the primary source of magnetism in these doped systems. The magnetic ordering has been enhanced significantly by doping of two molybdenum (Mo) atoms at Pb-site of $MAPbX_3$. Additionally, Mo doped systems shows half-metallic behavior. Electrical measurements and in-situ PAS studies reveal that the formation of lattice defect in $MAPbI_3$ is reversible up to 1.2 V applied bias and beyond this it becomes permanent. The temperature-dependent 'S' parameter measurement from PAS analysis directly correlates the structural phase transition of $MAPbBr_3$ from tetragonal to cubic at 260 K. The PAS studies show the presence of significant amount of iodine vacancy in ball-mill ground $MAPbI_3$. SQUID measurement also shows room temperature ferromagnetism in ball-mill ground $MAPbI_3$.In summary, the detail theoretical and experimental study reveals that defects i.e., atomic vacancy or doping of transition metal ions can induce significant magnetic moment in non-magnetic hybrid perovskite along with n/p type semiconducting behavior. Ferromagnetism along with semiconducting behavior makes it a viable for spintronics applications.

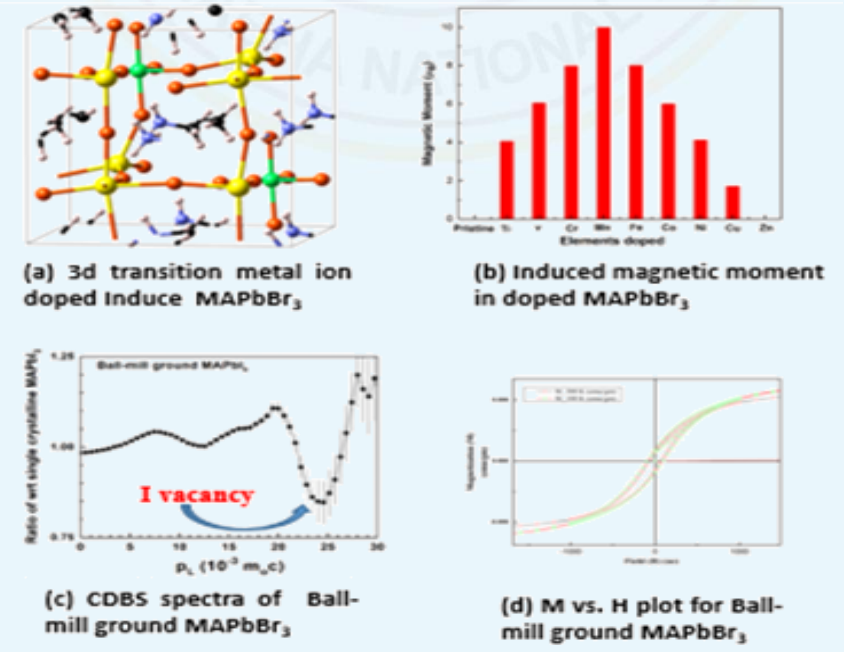

(a) 3d transition metal ion doped Induce $MAPbBr_3$

(b) Induced magnetic moment in doped $MAPbBr_3$

(c) CDBS spectra of Ball-mill ground $MAPbBr_3$

(d) M vs. H plot for Ball-mill ground $MAPbBr_3$

(a) Doped $MAPbBr_3$ (b) Induced magnetic moment (c) CDBS spectra of BM grind $MAPbI_3$ and (d) M-H curve of BM ground $MAPbI_3$

Section III

(List of students who have completed Ph.D. during the period August 1, 2023-July 31, 2024)

Discipline: Applied Systems Analysis

S. No.	Name of the Student	CI/OCC	Enrollment No	Title of the Thesis
1	Dasarathi Padhan	NISER	APSA11201704002	Integrated Economic and Environmental Accounting of Mineral Resources in India
2	Prachi Parimita Rout	NISER	APSA11201704004	Sociological Aspects of Sex Reassignment Surgery: An Empirical Study of Lived Experiences of Transgender People in Odisha
3	Biswajit Apat	NISER	APSA11201704005	A Sociological Study of Early Career Teachers of Government Elementary Schools in Odisha
4	Isha Bihari	NISER	APSA11201804001	A Systemic Inquiry into the New Normative Practice in Operational Working Hours
5	Swatiprava Rath		APSA11201804002	Social Contexts of Solid Waste in Urban Households: Uncovering the Practices of Waste Segregation and Littering in Bhubaneswar
6	Debasish Mishra	NISER	APSA11201904001	The Quest for a Home in the Jesus Trilogy of J. M. Coetzee
7	Maheshwar Kumar	NISER	APSA11201904003	Performance as Cultural Text: Defamiliarizing the Performing Art Tradition of Purulia Chhau

Discipline: Chemical Sciences

S. No.	Name of the Student	CI/OCC	Enrolment No.	Title of the Thesis
1	Soumen Das	BARC	CHEM01201704005	Clinical Scale Formulation and Evaluation of Novel Diagnostic Agents based on ^{99m}Tc and ^{68}Ga
2	Ashutosh Srivastava	BARC	CHEM01201704008	Redox and Molecular Speciation of Actinyl Ions in Aqueous and Deep Eutectic Solvent Media
3	Shiny Suresh kumar	BARC	CHEM01201704010	Task Specific Separation Procedures for Plutonium Recovery
4	Kartik Dutta	BARC	CHEM01201704011	Design, Synthesis and Biological Evaluation of Small Heterocyclic Molecules
5	Manjeet Singh	BARC	CHEM01201804002	Laser Induced Breakdown Spectroscopy (LIBS) for Direct Analysis of Nuclear Fuels and Waste Glasses

6	Rahul Agarwal	BARC	CHEM01201804003	Electrochemical Determination and Recovery of Uranium and Plutonium in Aqueous Medium
7	Bijaideep Dutta	BARC	CHEM01201804004	Physico-chemical and Biological Evaluation of Organic–inorganic Nano-structures for Cancer Therapy
8	Ram Pada Das	BARC	CHEM01201804006	Preparation, Characterization, and Efficacy Evaluation of Protein Nano-carrier/Gel-based Drug Delivery Systems for Therapeutic Applications
9	Ram Karan	BARC	CHEM01201804009	Studies on Leaching of Rare Earth Values from Primary and Secondary Resources using Deep Eutectic Solvents
10	Amit Kumar Sharma	BARC	CHEM01201804015	Development of Radiolabelled Peptides and Peptide-drug Conjugates for Diagnostic Imaging and Targeted Radiotherapy of Cancerous Lesions
11	Akalesh Girdhari Yadav	BARC	CHEM01201904002	Studies on the Extraction Chromatography of Lanthanides and Actinides from Acidic feeds using Diglycolamides
12	Gourab Karmakar	BARC	CHEM01201904003	Design, Synthesis and Characterization of Molecular Precursors for Metal Chalcogenide Materials and their Energy Applications
13	Sudeshna Saha	BARC	CHEM01201904008	Studies on Advanced Materials for e-waste Management
14	Piyali Banerjee	BARC	CHEM01201904013	Studies On the Extraction Chromatography of Actinides Using Resins Containing Aza-Crown Based Diglycolamide Ligands
15	Ananda Karak	BARC	CHEM01201904017	Studies on the Extraction and Liquid Membrane transport of Actinides from Lean Effluents using Tripodal Amide Ligands
16	Naveen Kumar	BARC	CHEM01202004007	Exploring the Potential of Novel Radiolabelled Biomolecules and Biomolecule - drug Conjugates for Imaging and Therapy of Cancers
17	Namrata Upadhyay	IGCAR	CHEM02201504013	Electrochemical Noise Studies to Evaluate Localized Corrosion in Structural Materials of Future Fast Breeder Reactors

18	Suvendu Kumar Barik	IGCAR	CHEM02201604004	Development of Sodium Aluminium Phosphate Glass, as a Host Matrix for Immobilization of Minor Actinides - A Simulation Study with Lanthanides (Ce, Pr, Nd and Gd) as Surrogates
19	Nibedita Samanta	IGCAR	CHEM02201604012	$AlCl_3$ Assisted Conversion of Uranium and Lanthanide (Sm, Nd, Pr, Ce AND La) Oxides to their Corresponding Chlorides in Molten LiCl-KCl Eutectic for Pyrochemical Reprocessing
20	Dasarath Maji	IGCAR	CHEM02201604015	Gel Based Methods for the Synthesis of Nanocrystalline TiO_2 and $(U_{1-y}Ce_y)O_{2\pm x}$ and their Characterization
21	Anwesha Mukherjee	IGCAR	CHEM02201704001	Studies Pertaining to Direct Electrochemical De-oxidation of Solid Metal Oxides in Molten $CaCl_2$
22	Biswajit Pada Samanta	IGCAR	CHEM02201704004	Experimental Investigation of Phase Equilibria, Phase Stability and Thermo-physical Properties of Zr & U-based Alloys
23	Ramakrishna Reddy Sareddy	IGCAR	CHEM02201704006	Some Studies on Platinum Supported Silica Catalyst for Preparation of U(IV) Towards Reprocessing Application
24	Namitha Janardhanan	IGCAR	CHEM02201704008	Application of Laser-Induced Breakdown Spectroscopy and Mass Spectrometry Based Techniques Towards Chemical Characterization of Nuclear Materials
25	Puchakayala Rajani	IGCAR	CHEM02201804001	Experimental and Theoretical Studies on the Extraction of Actinides by Organo-phosphorus Compounds
26	Vaddanam Venkata Sravani	IGCAR	CHEM02201804002	Synthesis and Evaluation of Novel Functionalized Metal-organic Frameworks for the Recovery of Metal Ions, Sensing, Luminescence and Hydrogen Storage Applications
27	Subhashree K	IGCAR	CHEM02201804003	A Study on Tris(2-methylbutyl) Phosphate as an Extractant for the Processing of Nuclear Materials
28	Rini Kumari Vishwakarma	IGCAR	CHEM02201804004	Surface Modified, N-Functionalized and Composite Graphene Oxide Membranes for Efficient Separation of Strontium from Aqueous Solutions

29	Swaroop Chandra	IGCAR	CHEM02201804006	σ and π Hole Driven Pnicogen Bonding involving Phosphorus and Nitrogen: Exploration through Matrix Isolation Infrared Spectroscopy and Quantum Chemical Methodology
30	Rama Krishna Pagoti	IGCAR	CHEM02201804008	Luminescence Properties of Lanthanides and Uranium Doped Borophosphate Glasses
31	Sanjit Kumar Parida	IGCAR	CHEM02201804009	Rational Design of Non-Precious Metal and Carbon Based Electrocatalysts for Oxygen Reduction Reaction
32	Sachin Aditya Ramesh	IGCAR	CHEM02201904003	Electronic Structure and Complexation Behavior of Phosphine Oxide Ligands with Lanthanides and Actinides
33	Rupayan Biswas	NISER	CHEM11201604025	Machine Learning Representation of Potential Energy Surfaces and Energy Transfer in Gas-Surface Scattering
34	Sagarika Meher	NISER	CHEM11201604026	Syntheses and Biochemical Assessments of Modified Nucleosides, Nucleic Acids and Peptides Containing Tropolone Surrogates
35	Namrata Prusty	NISER	CHEM11201704003	Synthesis and Functionalization of N-Heterocycles via Bismuth catalyzed S_EAr Reaction and Nickel Catalyzed C-H/C-N bond Activation
36	Sandip Pattanaik	NISER	CHEM11201704005	Catalysis Based on Cobalt Pincer Complexes
37	Anwesha Bhattacharya	NISER	CHEM11201704009	Selective C–N, C–S & C–C Bond Formation of Substituted Thioamides & Nitriles
38	Kiran Devi Tulsiyan	NISER	CHEM11201704016	Storage, Stability, and Activity of ctDNA, tRNA, Hemoglobin and Cytochrome c in Choline-based Ionic Liquids
39	Manish Kumar Gupta	NISER	CHEM11201704019	Synthesis and Conformational Analyses of Unnatural Amino Acids and their Hybrid Peptides
40	Murali A C	NISER	CHEM11201704020	Thioketone and Pyrazole based Luminescent Boron Compounds: Synthesis, Characterization and Photophysical Properties of Poly(indazaboles)
41	Rajata Kumar Sahoo	NISER	CHEM11201704023	Molecular Zinc(I) Dimers, Zinc (II) Hydrides, and Cations: Synthesis,

				and Catalytic Applications with Mechanistic Insights
42	Abhisek Padhy	NISER	CHEM11201804001	Metal Phosphate and Oxide based Electroactive Material for Energy Conversion and Storage Application
43	Sahadev Barik	NISER	CHEM11201804005	Studies on the Structural Organizations and Dynamics of Some Deep Eutectic Solvents and Room Temperature Ionic Liquids in the Absence and Presence of Electrolyte and Biomolecule by Various Spectroscopic Methods
44	Tanmoy Pain	NISER	CHEM11201804008	Design, Modification, and Diverse Applications of Tetrapyrrolic Macrocycles: Exploring both Free-Base and Metallated Variations
45	Amit Akhuli	NISER	CHEM11201804010	Understanding the Interactions of Luminescent Coinage Metal Nanoclusters with Target Analytes using Various Spectroscopic and Microscopic Techniques
46	Amita Mahapatra	NISER	CHEM11201804011	Understanding the Inter-molecular Interaction and Structural Organization in Some Imidazolium and Pyrrolidinium-Based Ionic Liquids: Implications in Biological and Electrochemical Applications
47	Nachiketa Sahu	NISER	CHEM11201804016	MOF-derived Metal Chalcogenide Nanostructured Materials as Electrocatalysts for Water Splitting in Electrochemical Energy Conversion
48	Prajnashree Panda	NISER	CHEM11201804018	Fabrication of Hybrid Nanostructured Materials and Porous Carbon for Energy Storage and Gas Adsorption Applications
49	Rahul Ghosh	NISER	CHEM11201804019	Development of Ruthenium and Iron Complexes for Catalytic Applications in Sustainable Oxidations and Reductions
50	Rakesh Ranajn Behera	NISER	CHEM11201804020	Development of Low-valent Manganese Complexes for the Catalytic Applications in Hydrosilylation Reactions
51	Sonali Panigrahy	NISER	CHEM11201804021	Carbon Supported Nano-materials for Electrochemical Energy Applications

52	Subrat Sethi	NISER	CHEM11201804024	Synthesis and Characterization of Copper Complexes with Tridentate NNO and NNS Ligands and their Catalytic Applications in Oxidation and Cycloaddition Reactions
53	Surajit Panda	NISER	CHEM11201804025	Development of Iridium Catalyst for A-Alkylation using Alcohol as Alkylating Partner and Utilization of Cobalt Catalyst for Hydrosilylative Reduction
54	Unmesh Dutta Chowdhury	NISER	CHEM11201804028	Investigating the Aggregation of Neurodegenerative Protein using Molecular Dynamics Simulations: Implications for Tau Pathogenesis
55	Ashis Mathuri	NISER	CHEM11201904005	Sustainable Approaches in the Synthesis of Organosulfur Compounds

Discipline: Engineering Sciences

S. No.	Name of the Student	CI/OCC	Enrolment No.	Title of the Thesis
1	Bhupendra Patidar	BARC	ENGG01200904047	Design and Modelling and Experimental Validation of Induction Heating Process by using Single and Multistrand Copper Coils
2	Mohandas Karamchand Pradhan	BARC	ENGG01201304042	Study on Response of Group of Piles in Cohesionless Soil under Dynamic Loads
3	Satendra Kumar	BARC	ENGG01201304047	Experimental Study and Optimization of Process Parameters in Electro-Magnetic Welding of Tubular Geometries
4	Vinay Kumar	BARC	ENGG01201404007	Cartesian Grid-Based Navier-Stokes (NS), Direct Simulation Monte Carlo (DSMC), and Hybrid NS-DSMC Methods for Continuum and/or Rarefied Gas Flows Around Complex Geometries
5	Sushil Kumar Bahuguna	BARC	ENGG01201404009	Compressed Sensing Distributed Artificial Neural Network for Core Flux Distribution Monitoring in Nuclear Reactors
6	Bhase Swapnil Shashikant	BARC	ENGG01201504012	State Estimation and Parameter Estimation of Differential-Algebraic Equa-tion (DAE) Systems
7	Pavanraj H R	BARC	ENGG01201504013	Development of Moving Window Based State and Parameter

				Estimation Schemes under Bayesian Frameworks
8	Lokesh Goel	BARC	ENGG01201504015	Irradiation - Induced Evolution of Second Phase Precipitates in Zr-Nb based Alloys
9	Sudhanshu Sharma	BARC	ENGG01201504017	Investigation of Deformation & Fracture Behaviour of Pressure Vessel Steel at High Strain Rate Loading
10	Subhankar Bhandari	BARC	ENGG01201504023	Development and Characterization of Plasma Sprayed YPO_4 Coatings on Graphite
11	Keskar Nachiket Avinash	BARC	ENGG01201504025	A Study on the Discontinuous Precipitation of α-Cr in Ni-Cr Alloys
12	R Rakesh Radhakrishnan	BARC	ENGG01201504026	Phase Transformation and Oxidation Behaviour of Uranium-Molybdenum based Ternary Alloys
13	Abhishak Kumar Srivastava	BARC	ENGG01201604007	Investigation on Natural Circulation Behaviour of Molten Salt Coolants for Molten Salt Reactor
14	Satendra Pal Chauhan	BARC	ENGG01201604014	Thermal Management of Passive Decay Heat Removal System under Seismic Conditions
15	Kumar Sourabh	BARC	ENGG01201604019	Dynamic Strain Aging & Creep Behaviour of Alloy 690
16	Suranjit Kumar	BARC	ENGG01201704005	Development of Damage Models for Porous Ductile Material Subjected to Wide Range of Stress Triaxialities
17	Kewlani Hitesh Mohanlal	BARC	ENGG01201704007	Characterization of ECR Plasma and Ion Beam in Continuous and Pulse Modes
18	Hari Prasad Kolla	BARC	ENGG01201704008	Evolution and Implementation of Precision Time Interval Measurement Techniques in ASIC and FPGA Technologies
19	Peddireddy M S Reddy	BARC	ENGG01201804004	Model Reference Adaptive Control for Power Control of Nuclear Reactors
20	Samyak Sanjay Munot	BARC	ENGG01201804005	Experimental and CFD Simulations of Coolability and Ablation Behaviour of Sacrificial Material by Molten Corium in the Core Catcher of an Advanced Nuclear Reactor
21	Saurabh Srivastava	BARC	ENGG01201804011	Study and Optimization of Silicon Photomultiplier – Scintillator Detector based Instrumentation for Radiation Monitoring Applications
22	Kaushal Jha	BARC	ENGG01201804012	Friction Stir Welding of Cu-Cr-Zr Alloy

23	Vanya Goel	BARC	ENGG01201804022	Study and Characterization of 60 kW Indirectly Heated Cathode-based Strip Electron Gun
24	Nandyala Pavan Kumar	BARC	ENGG01201804025	Study, Simulation and Experimentation for Ultrasonic Imaging and Gauging of Thin-Walled Tubes and Pipes
25	Deeksha Gupta	BARC	ENGG01201804026	Development of Advanced Electroluminescence System for Solar Cell Application
26	Sujeesh S	BARC	ENGG01201904003	Catalytic Decomposition of Sulphuric Acid in Integrated Reactor: Experimental Study, Modeling & Optimization
27	Dheeraj Kumar Singh	BARC	ENGG01201904010	Study of High Voltage Discharge and Optimization of Electrical Parameters in Copper Vapor Laser
28	Sutanwi Lahiri	BARC	ENGG01201904018	A Study on Sonochemical Decontamination of Graphite Substrate
29	Mukesh Kumar Sharma	BARC	ENGG01201718001	Design, Optimisation and Performance Evaluation of Portable Triple to Double Coincidence Ratio (TDCR) System as an Absolute Standard for Radioactivity Measurement
30	Keyurkumar C. Pancholi	BARC	ENGG01201518009	Study of Plasma-assisted Pyrolysis for Application in Radioactive Waste Management
31	Perumalsamy G	IGCAR	ENGG02201304004	Investigation of Motion Planning and Control of Robotic Arm, and Reliable Eddy Current Probe Design for Inspection of Steam Generator Tubes
32	Mabin Joseph Puthiakulangara	IGCAR	ENGG02201404006	Analysis of (Lightweight) Symmetric-Key Algorithms and their Software Implementations
33	Ajay Kumar Keshri	IGCAR	ENGG02201504010	Investigations towards the Development of Sensor Array and Instrumentation for Multiple Analytes
34	Sachin Tom	IGCAR	ENGG02201604003	Numerical Analysis of Sodium Flow Boiling in Narrow Channels Related to SFR Safety
35	Anoop K Unni	IGCAR	ENGG02201604015	Numerical Simulation and Experimental Validation of Fusion Welding of 316LN Stainless Steel
36	Kalvala Rajakrishna	IGCAR	ENGG02201604016	Novel Thin Film Coated Polystyrene or Epoxy based Plastic Scintillators Loaded with Microparticles of Inorganic Compounds

37	Bala Sundaram G	IGCAR	ENGG02201405010	Development of Thermal Hydraulic Models for In-Vessel Core Catcher of Future Indian Fast Reactors
38	Kumar S	IGCAR	ENGG02201405011	Phased Array Ultrasonic Testing of Dissimilar Weld Joints – Modelling and Experiments
39	C. Teena Mouni	IGCAR	ENGG02201405013	Effect of Prior Deformation Above Md Temperature on the Tensile Behaviour of Type 304 Metastable Austenitic Stainless Steel
40	Paulson Varghese	IGCAR	ENGG02201605005	Development of Ceramic Coatings for FBR Applications Involving High Temperature Sodium Environment
41	Arnab Jyoti Deka	IPR	ENGG06201504010	Design, Development and Characterization of Doppler Shifted Spectroscopic Diagnostic System for Negative Hydrogen Ion Beam in Fusion Application
42	Vala Sudhirsinh Jivubhai	IPR	ENGG06201504011	Development of a Rotating Tritium Target-based D-T Neutron Generator System for Fusion Neutronics Studies
43	Sebin Augustine	IPR	ENGG06201804002	Development of SERS Substrates based on Self-Organized Nanoparticles for Molecular Sensing Applications
44	Priyanka Tiwari	IPR	ENGG06201804004	Analysis, Design and Characterization of Metasurfaces for RCS Reduction
45	Ajay Kumar Pandey	IPR	ENGG06201804006	Guided and Leaky Modes Characteristics of Dielectric Loaded Helix Structure
46	Bharatsingh Bhupendrasingh Rawat	IPR	ENGG06201804007	Studies on Extraction of an Ion Beam and its Transport from a Multi-cusp Gridded Ion Source
47	Ram Krushna Mohanta	IPR	ENGG06201804008	Investigation of Thermal Plasma Jet for Low – Pressure Plasma Spraying
48	Milaan Vijaybhai Patel	IPR	ENGG06201804009	Development of Pulsed Supersonic Beam System for Tokamak Edge Diagnostics and Other Applications
49	Sumit	RRCAT	ENGG03201704002	Investigation on Shape Control Methodologies of Piezoactuator-based X-ray Deformable Mirror, its Fabrication and Character-ization for Adaptive Optics
50	Trijit Kumar Maiti	VECC	ENGG04201504001	Experimental Evaluation of the Thermodynamic Processes for Helium Liquefaction / Refrigeration Systems Operated in Mixed Mode

Discipline: Life Sciences

S. No.	Name of the Student	CI/OCC	Enrolment No.	Title of the Thesis
1	Totade Sumit Prakashrao	BARC	LIFE01201604003	Molecular Mapping of Resistance Gene to Bacterial Leaf Pustule in Soybean
2	Prashant Kumar Mishra	BARC	LIFE01201704003	Enhancement of Post-harvest Quality of Fishery Products through Hurdle Technologies
3	Rahul Singh	BARC	LIFE01201704006	Molecular Investigations into the Process of Plasmodial Protein-Mediated Hemozoin Production and its Inhibition by Chloroquine
4	Lokesh Kishore Mishra	BARC	LIFE01201704008	Molecular Mechanisms Involved in Starvation Physiology of *Salmonella enterica* serovar Typhimurium
5	Krupa Thankam Philip	BARC	LIFE01201704010	Functional Role of RECQL5 Helicase in Regulating Replication Stress Response in Cancer
6	Reshma	IMSc	LIFE10201504001	Modeling Active Transport in Axons
7	Ajay Subbaroyan	IMSc	LIFE10201904001	Elucidating and Leveraging Design Principles towards Realistic Reconstruction of Boolean Models of Gene Regulatory Networks
8	Farhina Mozaffer	IMSc	LIFE10201718001	Studies in Disease Dynamics
9	Kundharapu Satyamurthy	NISER	LIFE11201504006	Dengue Virus Non-structural Protein Complexes in Genome Replication: Structural and Functional Characterization
10	Rojalin Pradhan	NISER	LIFE11201504008	Cytoskeletal Phenomena Associated with Novel Lateral E-cadherin Junctions during Organ Degeneration in the Respiratory System of Drosophila melanogaster
11	Chandan Mahish	NISER	LIFE11201604005	Role of TLR4 in Chikungunya Virus (CHIKV) Infection and Associated Altered Cell Mediated Immune Responses
12	Ram Prasad Sahu	NISER	LIFE11201604006	Importance of TRPV3 in the Regulation of Sub-cellular Organelles Functions: Implications in Health Disorders
13	Saptarsi Mitra	NISER	LIFE11201604007	Neuropeptidergic Regulation of Dopaminergic Pathways in the Brain
14	Vinay J	NISER	LIFE11201604010	Genetic Predisposition and Molecular Mechanistic Studies of Matrix Metalloproteinases in Gallbladder Carcinogenesis

15	Prerana Dash	NISER	LIFE11201604011	Structure-Function-Dynamics of PanPL, a Bacterial Polysaccharide lyase from PL-5 Family
16	Ajay Kumar Sharma	NISER	LIFE11201604012	Assembly and Dynamics of Escherichia coli FtsZ Mutants L68W and T127A & Validation of FtsZ Inhibitors using Fission Yeast as a Heterologous Host
17	Bratati Mukherjee	NISER	LIFE11201604013	Mechanistic Insights Towards Understanding FRG1 Mediated Regulation of Breast Tumorigenesis and Angiogenesis in Different Molecular Subtypes
18	Kapuganti Ramani Shyam	NISER	LIFE11201604014	Genetic and Epigenetic Regulation of Candidate Genes Associated with Pseudo exfoliation
19	Dhyanendra Singh	NISER	LIFE11201704002	The Impact of Altered Light-dark Cycle on Gut Microbiota in Mouse Model
20	Prakash Haloi	NISER	LIFE11201704003	Development and Characterization of a Drug-loaded Smart Injectable Hydrogel as a Drug Delivery Systems for the Treatment of Rheumatoid Arthritis
21	Sohini Mukhopadhyay	NISER	LIFE11201704005	Role of Intestinal Microbiota on Exogenously Induced Colitis and Associated Physiological Changes: A Comparative Analysis of DSS and Antibiotic Treatment
22	Uday Pandey	NISER	LIFE11201704012	Gut Microbial Regulation of Intestinal Epithelial Development in Mice and Organoid Models- A Postnatal Temporal Study
23	Alena Patnaik	NISER	LIFE11201804022	Correlating Light Signaling and GIGANTEA with Auxin in Patterning the Root and Shoot Development in Plants
24	Priyadarshini Suchismita Sethy	SINP	LIFE05201604007	Role of Untranslated Region in Regulation of Human δ-tubulin Expression at Post-transcriptional Level
25	Chandrayee Mukherjee	SINP	LIFE05201704004	Role of Lamin a Mutations in Myogenesis
26	Duhita Sengupta	SINP	LIFE05201704005	Lamins and DNA Damage in context of Gynaecological Cancers
27	Anuradha Roy	SINP	LIFE05201804005	Exploring Clinical Prospects of Noble Metal-Based Investigation of Dengue Virus Infection and Its Mechanical Profiling
28	Mulla Saim Wasi	TMC	LIFE09201404010	Proteasomal Chaperones and the Cross-Talk with NF-κB Signaling- An

				Integrated Network and Experimental approach
29	Christie Joel Parsottam	TMC	LIFE09201504002	Quantitative Proteomic approach to Characterize the Functions and the Regulatory role of Proteasomal Assembly Chaperones
30	Inchanalkar Mayuri Bhimrao	TMC	LIFE09201504003	Genomewide DNA Methylation in Leukoplakia and Oral Cancers
31	Rashmi Puja	TMC	LIFE09201504007	Understanding the Role of VRK2A in Regulation of Apoptosis and Cancer
32	Suchita Dubey	TMC	LIFE09201504008	Structural and Functional Basis to Evaluate PML-RARA Response to Arsenic Trioxide
33	Abhay Ramaji Uthale	TMC	LIFE09201504011	Deciphering the Role of Mcl-1 in stress and Autophagy in Oral Cancers
34	Acharekar Anagha Anil	TMC	LIFE09201504020	Understanding the Role of Radiation Induced Cell-cell Fusion in Glioblastoma
35	Souvik Mukherjee	TMC	LIFE09201604001	Consequence of Differential Activation of Notch Signaling in Ovarian Cancer Progression and Chemoresistance
36	Swapnil Sudhir Oak	TMC	LIFE09201604002	Exploring Mutant p53-Associated Functions and Pathways that Promote Tumorigenesis
37	Bhasker D	TMC	LIFE09201604004	Characterizing Genome-wide Aberrations that Underlie Oral Cancer
38	Tripti Verma	TMC	LIFE09201604005	Stem Loop Binding Protein (SLBP), a Key Factor in the Control of Histone Gene Expression and its Implication in Cancer Progression
39	Bhagya Shree Choudhary	TMC	LIFE09201604006	Identification of Mechanisms Required for Tumor Progression upon LCN2 Overexpression
40	Neelima	TMC	LIFE09201604008	Characterization of Long Non-coding RNAs in Human Breast Cancer
41	Sukanya	TMC	LIFE09201604011	Delineating the Hypoxic Microenvironment Induced Changes in Cancer Epigenome
42	Barua Siddhartha Anup	TMC	LIFE09201604013	A Structure-based Approach to Elucidate Protein-Protein Interactions of BRCT Repeats
43	Dievya Dilip Gohil	TMC	LIFE09201604014	Evaluation of Phytochemicals with Immunomodulatory Activity for Graft-versus-Host Disease Prophylaxis

44	Saket Vatsa Mishra	TMC	LIFE09201604017	Understanding the Molecular Mechanism of Leukemia Resistance using Cellular and Preclinical Model of Leukemia Resistance
45	Natu Abhiram Girish	TMC	LIFE09201604020	Understanding the Role of Epigenetic Alterations in Acquirement of Chemoresistance in Cancer
46	Shruti Sham Kandekar	TMC	LIFE09201604021	CD26 and Adenosine Signaling Pathway Molecules as Regulators of Immune Reconstitution in Human Hematopoietic Stem Cell Transplantation
47	Pranay Dey	TMC	LIFE09201704001	Imaging Molecular Interaction Dynamics in Drug Resistance Breast Cancer
48	Mujawar Aaiyas Abdulhamid	TMC	LIFE09201704004	Developing In Vivo Bio-Imaging Methods using Fungal Luciferase
49	Megha Garg	TMC	LIFE09201704007	Investigating the Molecular Basis of Altered Pharmacokinetics and Toxicity of Anticancer Drugs under Conditions of Malnutrition
50	Tarang Gaur	TMC	LIFE09201704020	Molecular and Functional Characterization of Small Molecule Inhibitors to Evaluate Anti-Tumor Activity in Acute Myeloid Leukemia
51	Saurabh Kumar Gupta	TMC	LIFE09201904009	Evaluation of Oral Withaferin-A for Prophylaxis against Acute Graft versus Host Disease in Murine Model of Allogeneic Hematopoietic Stem Cell Transplantation

Discipline: Mathematical Sciences

S. No	Name of the Student	CI/OCC	Enrollment No	Title of the Thesis
1	Arup Kumar Maiti	HRI	MATH08201604001	On Fourier and Weyl Multipliers
2	Gopinath Sahoo	HRI	MATH08201604002	Tensor T-Structures on the Derived Categories of Schemes
3	Santanu Tantubay	HRI	MATH08201804004	On Simple Modules of Some Infinite Dimensional Lie Algebras
4	Shubham Gupta	HRI	MATH08201804003	Diophantine m-Tuples in Quadratic Number Fields
5	Aritra Bhattacharya	IMSc	MATH10201804008	Haglund's Conjecture and Clebsch-Gordan Rule for Macdonald Polynomials
6	Ramit Das	IMSc	MATH10201604001	A Logical Study of the Improvement Graphs Formed from Games

7	Rashi Sanjay Lunia	IMSc	MATH10201904003	Arithmetic and Analytic Aspects of Values of L-Functions
8	V. Sathish Kumar	IMSc	MATH10201804009	On Factorization Results for Tensor Products and Twisted Characters
9	Yogesh Dahiya	IMSc	MATH10201804010	Exploring Size Complexity and Randomness in the Query Model View
10	Diptesh Kumar Saha	NISER	MATH11201704004	On-Commutative Neveu Decomposition and Associated Ergodic Theorems
11	Gorekh Prasad Sena	NISER	MATH11201704005	Lehmer's Problems and Algebraic Points of Weierstrass Sigma Functions
12	Mrityunjoy Charan	NISER	MATH11201804002	Some Problems on Nearly Holomorphic Modular Forms
13	Shivansh Pandey	NISER	MATH11201904008	Nonvanishing of L-Functions and Differential Operators for Jacobi Forms

Discipline: Physical Sciences

S. No.	Name of the Student	CI/OCC	Enrolment No.	Title of the thesis
1	Alok Kumar	BARC	PHYS01201404015	Thermal hydraulic Coupling with Neutron Kinetics in 540 MWe PHWR at TAPS - 3 and 4
2	Rupali Pal	BARC	PHYS01201504016	Development of a Combination Neutron Detector System for Dosimetry in Reactor and Accelerator Environment
3	Rita Behera Sahoo	BARC	PHYS01201604006	Studies on Quantum Interference Effects in Atomic Ensemble
4	Amod Kishore Mallick	BARC	PHYS01201604008	Studies on the Efficient Fission Source Convergence in Monte Carlo Neutron Transport for Criticality and Source Mode Simulations
5	Tanay Dey	BARC	PHYS01201604020	Development of a RPC System with Detailed Performance Simulation
6	Vijay Karki	BARC	PHYS01201604023	Compositional Variation and Depth Distribution in D.C./R.F. Sputter Deposited Ni-Ti Alloy Thin Films
7	R Thiru Senthil	BARC	PHYS01201604028	Tau Neutrino Studies at the Proposed ICAL Detector in INO
8	Meghraj Singh	BARC	PHYS01201704001	Development of a Computational Framework for Estimation of Gamma Dose Absorbed in Product Irradiated in Gamma Irradiator

9	Shefali Shukla	BARC	PHYS01201704003	Evaluation of Hydrogen Diffusion Parameters for Zr-2.5%Nb Alloy Pressure Tube Material using Neutron Imaging Technique
10	Kailasa Ganapathi S	BARC	PHYS01201704004	Toxic Gas Detection based on Inorganic, Organic Materials, their Composites and Allied Techniques
11	Siba Prasad Sahoo	BARC	PHYS01201704005	Development and Characterization of Widely Tunable Solid-state Laser
12	Mangla Nand	BARC	PHYS01201704006	Development of an UHV-PPLD System and Studies on PLD Deposited Y Doped HfO_2 Thin Films
13	Devesh Raj	BARC	PHYS01201704008	Investigation of Light Water Lattices for Thorium Utilisation
14	Sougata Rakshit	BARC	PHYS01201704009	Development and Establishment of a Transfer Standard Ionization Chamber for Use in Dosimetry of Beta Radiation
15	Yogesh Kumar	BARC	PHYS01201704010	Electronic, Structural, and Vibrational Properties of Monazite and Zircon Host Materials for Nuclear Waste
16	Honey	BARC	PHYS01201704017	Magnetic Field Studies and Physics Implications for ICAL at INO
17	Vishal Vatsa	BARC	PHYS01201704019	Study and Mitigation of Noise in Low Temperature Bolometer Detectors
18	Mamta Jangra	BARC	PHYS01201704020	Cosmic Muon Veto Detector at Mini-ICAL
19	Roni Dey	BARC	PHYS01201704021	Measurement of Anti-neutrino by ISMRAN at Dhruva Research Reactor
20	Asim Kumar Das	BARC	PHYS01201704022	Vibrational and Electronic State Spectroscopy Studies on Carbonate Green Solvents using Synchrotron Radiation
21	Hariom Sogarwal	BARC	PHYS01201804002	Study of Atmospheric Muons and Muon-neutrinos and their Interactions
22	Gaurav Singh	BARC	PHYS01201804003	Modeling Space Charge Affected Electron Emission from the Curved Surface using Particle-in-Cell Technique
23	V B Jayakrishnan	BARC	PHYS01201804004	Crystal Structure and Electrical Properties of Lead-Free Ferroelectric Materials
24	Sangeeta Ashok Anupama Dhuri	BARC	PHYS01201804006	Probing Shell Effects in Fission of Nuclei with A ≈ 200

25	Telagasetti Santhosh	BARC	PHYS01201804008	Measurement of Nuclear Level Density through Fast Neutron Spectroscopy
26	Sinjumol K Rajan	BARC	PHYS01201804009	Development of Toxic Gas Sensors (NO_2, H_2S, NH_3, Cl_2, CO etc.) for E-Nose Application
27	Sajid Ahmad	BARC	PHYS01201804010	Effect of Nano Sized Features on the Thermoelectric Performance of Low, Medium, and High Temperature Range Thermoelectric Materials
28	Vandana Chaturvedi Misra	BARC	PHYS01201804013	Development and Study of Variable Frequency APPJ as A Unique Radiation Source for Biomedical Application
29	Avijit Das	BARC	PHYS01201804021	Study of Neutron-Gamma Coupled Methodologies for Effective Shield Design
30	Himanshi Singh	BARC	PHYS01201804023	Probing Nanoparticle-Surfactant Complexes using Scattering techniques
31	Sajan Kumar	BARC	PHYS01201804024	Thermodynamic Properties and Diffusion in Ionic Conductors
32	Bikash Chandra Saha	BARC	PHYS01201804025	Structural, Magnetic, Thermal, and Electronic-Ionic Conduction Properties of Naturally Grown Layered Transition Metal Oxides
33	Rashbihari Rudra	BARC	PHYS01201904005	Modelling and Characterization of Emission and Transport from Large Area Field Emitters
34	Arghya Chattaraj	BARC	PHYS01201904006	Studies on Stochastic Distributions of Energy Deposition at Cellular and Sub-cellular Levels in Neutral and Charged Particles Environment
35	Sandipan Dawn	BARC	PHYS01201904007	Neutron Spectrometry and Dosimetry in Diverse Radiation Environments
36	Harsh Bhatt	BARC	PHYS01201904010	Interface Driven Magnetization in Complex Oxide Heterostructures
37	Harish Srinivasan	BARC	PHYS01201904011	Non-Markovian and Non-Gaussian Behaviour in Molecular Diffusion within Complex Fluids
38	Rajasree R	BARC	PHYS01201904013	Curvature Effects on Electron Emission
39	Komal Kumari	BARC	PHYS01202004005	Towards Controlled and Tunable Superconducting Qubits: Theoretical Design and Development
40	Ramandeep Gandhi	BARC	PHYS01202004019	Surrogate Reactions Relevant for Fission and Fusion Reactors

41	Ms Faruk Abdulla	HRI	PHYS08201704001	Weyl Semimetals and their Surface States in Magnetic Fields
42	Subhojit Roy	HRI	PHYS08201704003	Some Cosmological and Collider Implications of the NMSSM
43	Ahana Ghoshal	HRI	PHYS08201804002	Towards a Local Version of the Second Law of Thermodynamics and its Utility in Quantum Thermal Devices
44	Kajal Singh	HRI	PHYS08201804006	Unveiling The Statistical Correlation Between the Cosmological Constant and Susy Breaking Scale in Flux Vacua
45	Kornikar Sen	HRI	PHYS08201804008	Energy Extraction from Quantum Batteries
46	Md Abhishek	HRI	PHYS08201804009	Scattering Amplitudes in Bi-Adjoint Scalar and Massive Theories
47	Srijon Ghosh	HRI	PHYS08201804015	Designing Quantum Thermal Machines in Many Body Quantum Systems
48	Vivek Pandey	HRI	PHYS08201804019	Measurement of Entanglement and Limitations on its Production
49	Sohail	HRI	PHYS08201505004	Nonseparability and Channel-state Duality in Quantum Information
50	Suman Jyoti De	HRI	PHYS08201505005	Study of Topological Phases in Presence of Magnetic Fields
51	Alphy George	IGCAR	PHYS02201504005	Origin of Diffuse Arcs in ω Forming β Ti-Mo alloy
52	Parvathy N S	IGCAR	PHYS02201604008	Mössbauer Studies on Some Fe/Bi based Multifunctional Oxides
53	Chavan Kashinath Tukaram	IGCAR	PHYS02201604010	Magnetic and Transport Characteristics of CdTe Nanostructures using ab-initio Techniques
54	Parvathy Harikumar	IGCAR	PHYS02201604012	Empirical and Semi-empirical Modeling of Electron Transport in Disordered Magnetic Tunnel Junctions
55	B. Revanth Reddy	IGCAR	PHYS02201704006	Observational Analysis and Numerical Modeling Studies of Sea Breeze, Convective Thunderstorms and Air Pollution Dispersion along the Southeast Coast of India
56	Choudhury Abinash Bhuyan	IGCAR	PHYS02201804003	Effect of Heat Dissipation on Photoluminescence Quantum Yield in Large-area Monolayer MoS_2 and its Applications

57	Arpan Kundu	IMSc	PHYS10201504004	On the Asymptotic Symmetry Algebra of Classical and Quantum Gravity
58	Shivam Gola	IMSc	PHYS10201704001	A Phenomenological Study of WIMP Models
59	Amir Suhail	IMSc	PHYS10201704002	Dissipation and Recovery in Collagen Fibrils: Modelling and Simulations
60	Umang Ashwin Dattani	IMSc	PHYS10201704004	Cavitation Instabilities in Amorphous Solid: An Athermal Study
61	Surabhi Tiwari	IMSc	PHYS10201704008	Next-to-Soft Virtual Resumed Corrections to Processes at the LHC
62	Apurba Atul Kumar Biswas	IMSc	PHYS10201804003	Mpemba Effect in Granular and Langevin Systems
63	Toshali Mitra	IMSc	PHYS10201804004	Studies of Ultra-relativistic Phenomena Including Real Time Correlations
64	Prateek Inderjeet Kaur Chawla	IMSc	PHYS10201804006	Quantum Walks on Networks – A paradigm for Quantum Simulation and Computation
65	Nishant Gupta	IMSc	PHYS10201804009	Aspects of Chiral Symmetries in Holography
66	Raghvendra Singh	IMSc	PHYS10201605003	The Role of Spacetime Curvature in Quantum Phenomena at Various Length Scales
67	Akhil Antony	IMSc	PHYS10201705001	A Primordial Solution to the Tensions in Cosmology
68	Alapan Dutta	IoP	PHYS07201504006	Optoelectronic Optimization of Thin Films Related to the Metal Oxide Contact-based Photovoltaic Cell
69	Dilruba Hasina	IoP	PHYS07201504010	Nanoscale TiO_x-based Memristive Synaptic Devices for Neuromorphic Computing Applications: Role of Defect Engineering
70	Subhadip Jana	IoP	PHYS07201604004	Spin-orbit Coupled Electron Transport, Interface Magnetism in Transition Metal Oxide and Heavy Metal Thin Films
71	Sudarshan Saha	IoP	PHYS07201604009	Studies on Topological Aspects of Generalized Haldane Model in Two and Three Dimensions
72	Vinaya Krishnan M B	IoP	PHYS07201604010	Study on CP-nature of the Higgs Interaction with τ Lepton at CMS Experiment and Invariant Mass Reconstruction of Heavy Gauge Bosons using Machine Learning Techniques

73	Avnish	IoP	PHYS07201604011	Exploring Neutrino Mass and Dark Matter Motivated TeV Scale Scenarios at the Collider Experiments
74	Bibhabasu De	IoP	PHYS07201704001	Exploring Signatures of Supersymmetric and Non-Supersymmetric Models through Colliders, Cosmological and Precision Data of Observables
75	Rojalin Padhan	IoP	PHYS07201704007	Phenomenology of Neutrino Mass Models at Present and Future Collider Experiments
76	Arnob Kumar Ghosh	IoP	PHYS07201804004	Floquet Generation of Higher-Order Topological Systems
77	Mousam Charan Sahu	IoP	PHYS07201804008	Studies of Metal Oxide and Chalcogenide Thin Film based Memristors for Memory and Neuromorphic Computing Applications
78	Ankit Kumar	IoP	PHYS07201804009	Structural Properties and Thermal Evolution of Neutron Stars through Dense Matter Equation of State with Observational Constraints
79	Sameer Kumar Mallik	IoP	PHYS07201804016	Development of Largescale CVD Grown Two Dimensional Materials for Field-effect Transistors, Thermally-driven Neuromorphic Memory, and Spintronics Applications
80	Sanjeev Kumar Pandey	IPR	PHYS06201604005	Linear and Nonlinear Waves in Spatially Nonuniform 1D Vlasov-Poisson Plasmas
81	Prince Kumar	IPR	PHYS06201704002	Study on Rotating Dusty Plasma Equilibria and their Excitations in Strongly Coupled Quasi-Localized Regime
82	Jagannath Mahapatra	IPR	PHYS06201704003	Magnetohydrodynamic Study of Magnetic Island Coalescence - Role of Shear Flows
83	Pawandeep Singh	IPR	PHYS06201804001	Sheath Effects on the Resonance Hairpin Probe in Negative Ion Diagnostics
84	Vijay Shankar	IPR	PHYS06201804003	Control of Edge and Scrape-Off Layer Tokamak Plasma Turbulence
85	Krishan Kumar	IPR	PHYS06201804004	Excitation of Non-linear Waves and Instabilities in a Flowing Dusty Plasma
86	Swarnima Singh	IPR	PHYS06201804005	Experimental Study of a Quasi Two-dimensional Complex Plasma

87	Shrish Raj	IPR	PHYS06201804011	Effect of Impurity Gas Seeding in the Boundary Region of a Tokamak
88	Anshika Chugh	IPR	PHYS06201804015	Ratchet Effects and Collective Dynamics in Passive and Active Systems
89	Swati	IPR	PHYS06201804016	Studies on Magnetic Field Effects in a Capacitive Coupled Cylindrical Radio Frequency Plasma
90	Sukriti Hans	IPR	PHYS06201804017	Nanopatterns Formation by Low-Energy Ions: Experiment and Simulation
91	Joydev De	NISER	PHYS11201504003	Construction of Optimally Directed Localized Basis for arbitrary Bond-angles, and Correlated Real Time Dynamics in the Proposed Directed Basis for Accurate Estimation of Optical Properties of Large Systems
92	Dipika Dash	NISER	PHYS11201704002	Relativistic Dissipative Hydrodynamics with Extended Relaxation time Approximation
93	Laxmipriya Nanda	NISER	PHYS11201704003	Fabrication of $NiBi_3$ Nanostructures and Studies of Quantum Transport in the Resistive state of $NiBi_3$ Nanowires
94	Bidyadhar Das	NISER	PHYS11201704009	Impact of Impurities and Synthesis Techniques on Superconducting and Magnetic Properties of $NiBi_3$ Thin Films
95	Brindaban Ojha	NISER	PHYS11201704011	Domain Wall and Skyrmion Dynamics in Perpendicular Magnetic Anisotropic Thin Films
96	Dola Chakrabartty	NISER	PHYS11201704012	Stabilization of Magnetic Skyrmion Bubbles and Anomalous Magneto-Transport Properties in Centrosymmetric Hexagonal Magnets
97	Esita Pandey	NISER	PHYS11201704013	Strain-Driven Tuning of Properties in Magnetic Thin Films: Towards Flexible Spintronics
98	Gurupada Ghorai	NISER	PHYS11201704014	Plasmonic Excitations in 1D and Spin-interactions in 2D Cr-based Nanostructures
99	Jobin Sebastian	NISER	PHYS11201704015	Anisotropic Aspects of Heavy Quarkonium Potential in Thermal QCD Medium
100	Prafulla Saha	NISER	PHYS11201704020	Probing New Physics through Standard Model Higgs to Diphoton Signature in pp Collisions at $\sqrt{s}$ = 13 TeV

101	Pushpendra Gupta	NISER	PHYS11201704021	Study of Spin Pumping and Inverse Spin Hall Effect on Manganite based Thin Films
102	Tribeni Mishra	NISER	PHYS11201704026	Searches for SUSY and HCal Performance Studies with CMS Run 2 Data
103	SK Jamaluddin	NISER	PHYS11201804003	Characterization of Nontrivial Spin Texture and Anomalous Electronic Transport Properties in Mn-based Heusler Systems
104	Utkalika Priyadarsini Sahoo	NISER	PHYS11201804012	Defect Induced Charge Density Wave Ordering and Optical Properties in 2D-$TiSe_2$ TMDs Material
105	Subhashree Sahoo	NISER	PHYS11201804013	Bandgap Engineering in Phase Selective TiO_2 Microflowers for Photonic Applications
106	Milan Patra	NISER	PHYS11201605003	The Fluid-Membrane-Gravity Duality
107	Sourav Bhakta	NISER	PHYS11201705005	Ion Beam-Induced Defect Phenomena in Rock-Salt Crystals (MgO, NiO) for Optical and Electronic Device Applications
108	Nitish Paul	RRCAT	PHYS03201604001	Studies on Dissipative Soliton Pulse Shaping in Mode-locked Fiber Laser and Amplifier
109	Vikas Kumar Sahu	RRCAT	PHYS03201604007	Studies on Resistive Switching in TiO_2 Thin Films for Non-volatile Memory Applications
110	Deepak Daiya	RRCAT	PHYS03201704004	Studies on Tiled Grating Pulse Compression along with Diagnostics for Alignment and Spatio-temporal Characterization of Ultra-short Laser Pulses
111	Sougata Koner	RRCAT	PHYS03201704009	Studies on $La_{0.7}A_{0.3}MnO_3$ (A=Ba, Sr and Pb) Embedded P(VDF-TrFE) Nanocomposite Films for Room Temperature Magnetoelectric Coupling Applications
112	Rajeev Dutt	RRCAT	PHYS03201704012	First-principles Calculations to Study Effects of Substitution on Thermoelectric and Spintronic Properties of Heusler Alloys
113	MD Akhlak Alam	RRCAT	PHYS03201804007	Application of Synchrotron based Spectroscopy Methods for Study of Ion Implanted Materials
114	Amrita Datta	SINP	PHYS05201604014	Magnetic Properties of Co-Cr-Al Based Heusler Compounds
115	Smruti Ranjan Mohanty	SINP	PHYS05201604015	Spectromicroscopy Studies of Surfaces and Ultrathin Films using LEEM-PEEM Methods

116	Pritam Nanda	SINP	PHYS05201704002	A Study on the Symmetry of Quasilocal Horizon and Hawking Radiation
117	Dipali Basak	SINP	PHYS05201704003	Study via Statistical and Optical Model of the Measured Low Energy Reaction and Scattering Cross-sections Involving p-Nuclei
118	Pritam Palit	SINP	PHYS05201704004	Search for Higgs Boson Pair Production HH → bbZZ →bb4l Final State using CMS data at $\sqrt{s}$ = 13 TeV at the LHC
119	Astik Haldar	SINP	PHYS05201704007	Statistical Physics Perspectives on Driven Systems
120	Suchanda Mondal	SINP	PHYS05201704017	Studying Magnetic Properties of Layered van der Waals Single Crystals
121	Tanmoy Bar	SINP	PHYS05201704019	High Current Ion Beam Reaction Studies and Heat Generation in Targets
122	Pooja Agarwal	SINP	PHYS05201704022	Correlations Effects in Two Dimensional Systems
123	Satyabrata Datta	SINP	PHYS05201804001	Exploring Leptogenesis and Pre-BBN Universe with Primordial Gravitational Waves and their Spectral Features
124	Tanmoy Ghosh	SINP	PHYS05201804004	Investigation of Cosmic-Ray Muon Flux Variation with Overburden and Study of Nuclear Physics Inputs to Astrophysics
125	Shuvankar Gupta	SINP	PHYS05201804006	Exploring Half-metallic Ferromagnetism and Magnetic Frustration in Some Structurally Disordered Novel Quaternary Heusler Alloy
126	Subhendu Das	SINP	PHYS05201804011	Particle Tracking with Gaseous Detectors and Development of Related Readouts
127	Subhankar Mandal	SINP	PHYS05201804013	Morphology and Electronic Structures of Organic Semiconducting Thin Films
128	Smruti Medha Mishra	SINP	PHYS05201804014	Fabrication of Different Nanostructures for Photovoltaic Applications and their Correlation with Structural Properties
129	Saugata Roy	SINP	PHYS05201804020	Tuning Structural Ordering of π-conjugated Homopolymer and Donor-acceptor Copolymer Thin Films
130	Priyabrata Das	SINP	PHYS05201804021	Study of Exotic Decay Near Proton Drip Line

131	Sudip Chakraborty	SINP	PHYS05201804024	Novel Magnetic Ground-States of Ternary Intermetallic R_2IrSi_3-Series (R = Gd-Ho) and Heusler Alloys
132	Subhash Ghosh	VECC	PHYS04201404001	Study and Use of Ion Induce Emission Phenomena
133	Md Zamal Abdul Naser	VECC	PHYS04201504005	Development and Characterization of Electron Gun and Low Energy Beam Transport Line for Superconducting Electron Linac of ANURIB facility at VECC
134	Jayanta Debnath	VECC	PHYS04201504006	Correction of Magnetic Field and Study of Orbit Stability in K500 Superconducting Cyclotron
135	Dipen Paul	VECC	PHYS04201604004	Experimental Study of Quasi-Fission and Shell Effects in Fission of Heavy Nuclei
136	Ekata Nandy	VECC	PHYS04201704002	Exploring High Density Nuclear Matter with Dimuons & Hadrons at FAIR Energies
137	Shabir Ahmad Dar	VECC	PHYS04201704006	Nuclear Structure Studies of Sb (Z=51) Isotopes
138	Argha Dutta	VECC	PHYS04201804001	Microstructural Characterization of Ion Irradiated Niobium and Its Alloy using X-Ray Diffraction Line Profile Analysis and Electron Back Scattered Diffraction Technique
139	Sudipta Moshat	VECC	PHYS04201904001	Theoretical and Experimental Studies of Organic Inorganic Hybrid Perovskite Material
140	Sneha Das	VECC	PHYS04201904002	Single Particle and Collective Excitations above Z=82
141	Sudip Bhowmick	VECC	PHYS04201904007	Growth and Properties of Nanodot and Wire Structures Developed by Ion-implantation on Pre-fabricated Nano-templates
142	Sujan Kumar Roy	VECC	PHYS04201904011	Study of Compact Stars and their Properties

Section IV

(List of students who have completed M.Tech. and M.Sc. (Engg.) during August 1, 2023-July 31, 2024)

M.Tech.

S. No.	Name of the Student /Enrolment No.	CI/OCC	Discipline	Title of the Thesis
1	Dipesh Kumar Gupta (ENGG01201801022)	BARC	Electrical Engineering	Design, Implementation of Innovative Speed Controller for Induction Motor Simulating Coast-down Characteristics of PHT Pump for Thermal Hydraulic Studies
2	Gaurav Vashishtha (ENGG01201801023)	BARC	Electrical Engineering	Design, Simulation and Hardware Implementation of Cascaded H-bridge Multilevel Inverter with Reduced Number of Switches for Power Quality Improvement
3	Moncy Prasannajith (ENGG01201801027)	BARC	Electrical Engineering	Design and Optimization Methodologies of High Uniformity Solenoid Magnets for Magnetic Resonance Imaging (MRI) Application
4	Varun Kumar Pandey (ENGG01201801032)	BARC	Electrical Engineering	Modelling and Simulation of Two-Phase Induction Motor for Optimal Operation with Two-Phase Inverter Drive
5	Ankit Bangar (ENGG01201801039)	BARC	Mechanical Engineering	Study of the Effect of Single-Phase Flow Conditions on FAC for Various Feeder Bend Geometries of Pressurized Heavy Water Reactor (PHWR)
6	Deep Gupta (ENGG01201801041)	BARC	Mechanical Engineering	Study of Evolution and Distribution of Defects and Change in Mechanical Properties of Alloy 690 in Molten Corrosive Glass Environment
7	Ankan Basak (ENGG01201901006)	BARC	Electronics Engineering	Development of 200 kV, 4 kA, 5 ns Tesla Transformer with Open Magnetic Core
8	Rohit Tyagi (ENGG01201901015)	BARC	Instrumentation Engineering	Simulation of Induction Heating System and Implementation of Control Algorithms for Induction Furnace Temperature Control
9	Abhishek Lanje (ENGG01201901020)	BARC	Electrical Engineering	Design, Parametric Analysis, Modeling & Performance Demonstration of Transients in 11 KV High Tension Substation for Typical Nuclear Facility
10	Abhishek Deep (ENGG01201901035)	BARC	Mechanical Engineering	The Role of Strength Mismatch in Ductile Fracture of Dissimilar Metal Welds

11	Lukka Veera Venkata Naga Satish (ENGG01201901044)	BARC	Chemical Engineering	Modeling and Performance Evaluation of Control Systems for High Precision Temperature-controlled Cooling Water System
12	Bollapragada Seshasaikumar (ENGG01201901069)	BARC	Mechanical Engineering	Development of an Empirical Relation to Estimate the Natural Frequency of Interacting Pipe Assembly
13	Sonu Singh (ENGG01201901070)	BARC	Mechanical Engineering	Development of Modified Bree Diagram for Intersecting Cylinder Type Geometries to Predict the Thermal Ratchet Condition Engineering Sciences
14	Gaurang Agrawal (ENGG01202101004)	BARC	Electrical Engineering	Design and Simulation of Closed Loop System for Beam Control at Pelletron Accelerator
15	Janagam Naveen (ENGG01202101008)	BARC	Electrical Engineering	Development of Phase Angle Controller for Six Pulse High Current Thyristor Rectifier with IPT for Thermal-hydraulic Transient Simulation
16	D. Dhrumitkumar Ghanshyambhai (ENGG01202101009)	BARC	Electrical Engineering	A Comprehensive Study on Optimization of Maximum Power Point Tracking Methods in Solar Photovoltaic Systems and Implementation of Prototype System for Research Reactor
17	Kuldeep (ENGG01202101010)	BARC	Electrical Engineering	Design, Simulation and Hardware Implementation of Compact IGBT based Active Rectifier replacing Conventional Multi-pulse Thyristor Rectifier Powering Plasma Incinerator at RSMS, BARC
18	Arunabha Chatterjee (ENGG01202101012)	BARC	Electrical Engineering	Optimal Design and Simulation of Large Format Outrunner Motor for Light Traction Applications
19	Apaar Parashar (ENGG01202101020)	BARC	Electronics Engineering	Development of Time Delay Estimation Algorithm for Identification of Intrusion location in FO-PIDS System
20	Santhosh Chittimalla (ENGG01202101022)	BARC	Electronics Engineering	Design and Development of Fast Protection System for High Intensity Proton LINAC
21	Sandeep Kumar Yadav (ENGG01202101023)	BARC	Electronics Engineering	Study and Development of Digital Wideband Waveform for Point-to-Point Radio Communication

22	Roshan Rabinarayan Sahu (ENGG01202101025)	BARC	Computer Engineering	Development of Signal Processing Algorithm using Ultrasonic Signal for Corrosion Defect Detection and 3D River Bottom Profile Generation
23	Nitin Kumar Radke (ENGG01202101027)	BARC	Computer Engineering	To Study and Build an Intrusion Detection System (IDS) for Identification of Infected Malicious Connections using Machine Learning (ML)
24	Dileep Kumar Chaudhary (ENGG01202101034)	BARC	Mechanical Engineering	Study of Load Vs Deflection Characteristics of Inconel-718 Tubes under Compressive Loading
25	Manoj Kumar Jangid (ENGG01202101037)	BARC	Mechanical Engineering	Effects of Electron Beam Welding Parameters on Weld Area and Penetration in Thick Stainless Steel Pipe Weld Joint: Experiments and Numerical Analysis
26	Mayank Gaur (ENGG01202101044)	BARC	Mechanical Engineering	Development of Forming Limit Diagram for Anisotropic Zr1Nb Thin-walled Tubes and Its Use in Improvement of End-forming Process
27	Ashin Uthaman P (ENGG01202101045)	BARC	Mechanical Engineering	FE Analysis of Residual Stresses in Rolled Joints of Dhruva Reactor and its Experimental Validation
28	Pranav S (ENGG01202101046)	BARC	Mechanical Engineering	A Simplified Methodology to Generate Floor Response Spectra using complex Frequency Transfer Functions for a Structure with Variation in Base Input Motion
29	Ahmad Faraz Hasan (ENGG01202101050)	BARC	Chemical Engineering	Numerical Simulation and Parametric Study of Hairpin Type Steam Generator for 220 MWe PHWRs
30	Yashwanth Panuganti (ENGG01202101057)	BARC	Civil Engineering	Frequency Dependent Dynamic Impedances for a Rigid Circular Foundation with Applicability to Irregular Shapes on Layered Isotropic Soil
31	Kamleshwar Bhattacharjee (ENGG01202201002)	BARC	Electrical Engineering	Development of Algorithm based on Common Midpoint Cross Correlation Method for Generating High Resolution Surface Wave Dispersion Curve

32	Rakesh R Kamath (ENGG01202201003)	BARC	Electrical Engineering	Optimisation and Development of Single Axis Double Saddle Coil for Linear Gradient Magnetic Field Generation
33	Syed Nabeeluddin (ENGG01202201006)	BARC	Electrical Engineering	Development of Visual-Inertial State Estimation System for Mobile Robot Navigation
34	Rutuja Satish Bhave (ENGG01202201016)	BARC	Electronics Engineering	Analysis and Classification of Multiple Intrusion Events Occurring Concurrently in FO-PIDS System
35	Bharat Jeswani (ENGG01202201019)	BARC	Electronics Engineering	Reliability Analysis of Network Topologies in Hierarchal Network Architectures
36	Prateek Kamal Gyanchandani (ENGG01202201020)	BARC	Electronics Engineering	Development of Localization Algorithm and its Software Implementation for Compton Camera based Gamma Imaging for Hot Cell Application
37	Divyank Mittal (ENGG01202201021)	BARC	Electronics Engineering	Development of Source Coding Technique for Efficient Wireless Voice and Data Communication for SDR Application
38	Prashant Kumar Sharma (ENGG01202201022)	BARC	Electronics Engineering	Design and Development of Portable and Compact OSL Reader System for Space Dosimetry
39	Sweta Agarwal (ENGG01202201023)	BARC	Electronics Engineering	Design of RF System for Vertical Test Stand
40	Jeevika Tiwari (ENGG01202201024)	BARC	Electronics Engineering	Coverage Driven Test-case Generation for HDL Designs
41	Namrata Joshi (ENGG01202201026)	BARC	Computer Engineering	Comparative Study of Channel Access and PV Access under Different Network Topology with Varying Loads
42	Sreekanth T M (ENGG01202201027)	BARC	Computer Engineering	Technical Expertise Identification Model Using Machine Learning
43	Ayush Pandey (ENGG01202201029)	BARC	Computer Engineering	Analysis and Development of Multi-level QOS Environment in Cloud Systems
44	Neelam Singh (ENGG01202201031)	BARC	Computer Engineering	C2 and Phishing Domains Detection using DNS Analysis
45	Sharath S Nair (ENGG01202201035)	BARC	Mechanical Engineering	Risk Analysis of Battery Systems and Mitigating Hydrogen Risk in Submarines
46	Vineeth N V (ENGG01202201039)	BARC	Mechanical Engineering	Development of Iron-Aluminide-Alumina Coating on Reduced Activation Ferritic Martensitic Steel

47	Gundubogula Sri Krishna Kalyan (ENGG01202201042)	BARC	Mechanical Engineering	Thermal Analysis of a Vertical Concentric Annulus to Improve its Performance as a Thermal Barrier
48	Pragyanand (ENGG01202201050)	BARC	Mechanical Engineering	Investigations of Failed Thermosiphon Evaporator and Thermal Hydraulic Performance Evaluation under Different Degraded Operating Conditions
49	Twinkle Jangid (ENGG01202201054)	BARC	Chemical Engineering	Generation of Phase Diagram of Solvent - PAN co-polymer – Coagulant System and Study of Coagulation Process During Fibre Spinning
50	Ankit Ojha (ENGG01202201055)	BARC	Chemical Engineering	Experimental Studies on Multiphase Flow in an Air Lift Contactor
51	Sandeep Singh Tomar (ENGG01202201056)	BARC	Chemical Engineering	Dissolution of Washed and Dried Frit Powder in Nitric Acid to Produce Clear Zirconium Nitrate Solution
52	Seepana Sriharsha (ENGG01202201061)	BARC	Metallurgical Engineering	Study the Effect of Lateral and Transverse Inversion on Clad Thinning during Roll Bonding for Dispersion based Plate Fuel Elements
53	B Vinith (ENGG01202201062)	BARC	Metallurgical Engineering	Studies on a Novel Process for Recovery of Uranium from Tummalapalle Leach Liquor
54	Ajay Kumar (ENGG01202201063)	BARC	Metallurgical Engineering	Characterisation of U-Ti Alloys for Wear Application
55	Nigudage Ganesh Mahadev (ENGG01202201065)	BARC	Metallurgical Engineering	Studies on Effect of Accelerated Thermal Ageing on Reactor Pressure Vessel Steel using Small Punch Test Technique
56	Siddhant Gupta (ENGG01202201066)	BARC	Metallurgical Engineering	Effect of Heat Treatment on Microstructural Evolution and Properties of Additively Manufactured SS316L
57	Poreddy Sai Krishna Reddy (ENGG01202201075)	BARC	Radiological Safety Engineering	Dosimetric Characterization of Four-element OSLD Badge for its Application in Personnel Monitoring using Badge Reader
58	Swapnil Jain (ENGG01202201078)	BARC	Mechanical Engineering	Plant Specific Model Development, Simulation, and Response Analysis for PHWR based NPPSs under Anticipated Operational Occurrences

59	Nandan Boral (ENGG1G202101001)	BARCTS (AMD), Hyderabad	Exploration Geosciences	Study on Petromineralogical Characteristics and Depositional Environment of Dharamshala Group of Rocks w.r.t. Uranium Mineralisation in TileliChah Ka Dora Area, Mandi District, Himachal Pradesh
60	Aman Tiwari (ENGG1G202101002)	BARCTS (AMD), Hyderabad	Exploration Geosciences	Sub-surface Litho-Facies Analysis with Emphasis on Depositional Environment of Kurnool Group of Rocks in Sarangapallibhatrupa Lem Area, Guntur District, Andhra Pradesh
61	Ashish Kumar Rai (ENGG1G202101003)	BARCTS (AMD), Hyderabad	Exploration Geosciences	Petromineralogical and Geochemical Characterisation of Granitoids and Pegmatites for Assessing their Rare Metal and Rare Earth (RM & RE) Potential in and around Kanahalli, Mangalur and Hal Ammapur, Shorapur taluk, Yadgir dist, Karnataka
62	Rishabh Namdeo (ENGG1G202101004)	BARCTS (AMD), Hyderabad	Exploration Geosciences	Geochemical, Petrological and Sedimentological Studies of Mineralised and Non-mineralised impure Phosphatic Dolostone and the Relationship of Zr, K_2O, Al_2O_3, SiO_2, P_2O_5, REE and other elements associated with clastic detritus in the uranium mineralisation of Tummalapalle uranium deposit
63	Ashish Dahayat (ENGG1G202101005)	BARCTS (AMD), Hyderabad	Exploration Geosciences	Geological, Geochemical, and Mineral Chemistry Characterisation of Mineralised and Non-Mineralised Migmatites and Pegmatites of Chundi and Karke Areas, Garhwa district, Jharkhand
64	Owishi Sarkar (ENGG1G202101006)	BARCTS (AMD), Hyderabad	Exploration Geosciences	Lithological and Structural Studies of Granites- Albitities for Deciphering Tectono-magnetic Evolu-tion and Implications on Uranium Mineralization in Geratiyon ki Dhani, Sikar District
65	Priyam Garg (ENGG1G202101007)	BARCTS (AMD), Hyderabad	Exploration Geosciences	Origin of Biotite in Schistose Rock, Soda Granite and Feldspathic Schist and its Bearing on Uranium Mineralization in Bagjata and Pathargora Area, East Singhbhum District, Jharkhand
66	Krishna Chandra Das (ENGG1G202101008)	BARCTS (AMD), Hyderabad	Exploration Geosciences	Characterisation of Different Types of Granitoids South of Kurlagere-Gogi Fault around Gogi-Shahapur-Doranahalli Sector: An Integrated Study to Ascertain

				its Potential as Source Rock for Gogi, Kanchankayi and Hulkal Uranium Deposits, Yadgir District, Karnataka
67	Shivam Yadav (ENGG1G202101009)	BARCTS (AMD), Hyderabad	Exploration Geosciences	Characterization of Sulphides and Carbonaceous Matter in Motur Sandstone of Satpura Gondwana Basin and its Implication on Uranium Mineralization in Dharangmau-Kachhar-Kalapani-Jhapri Areas, Betul District, Madhya Pradesh
68	Sambit Kumar Nayak (ENGG1G202101010)	BARCTS (AMD), Hyderabad	Exploration Geosciences	Petromineralogical and Geochemical Characterisation of Micaceous Quartzite and Carbonaceous Phyllites and their Implication on U-Mo-REE-Au Mineralization around Ampuli Area, Papum Pare District, Arunachal Pradesh
69	Bijay Kanti Biswas (ENGG1G202101011)	BARCTS (AMD), Hyderabad	Exploration Geosciences	Petro-mineralogical and Geochemical Characterization of the Volcano-sedimentary Sequence of Western Part of Khairagarh Basin for Deciphering Basin Evolution and Tectonic Set-up to Develop Uranium Exploration Model for Bijepar-Dongargaon-Lohara Areas, Central India
70	Pranjit Kalita (ENGG1G202101012)	BARCTS (AMD), Hyderabad	Exploration Geosciences	Characterization of Acid Volcanic Rocks Around Magreshwar Area, Barmer District, Rajasthan, and the Role of Peralkalinity in Rare Earth Elements (REE) and Uranium Mineralization
71	Sayan Mondal (ENGG1G202101013)	BARCTS (AMD), Hyderabad	Exploration Geosciences	Structural Mapping and Fracture Array Geometry Analysis of Banded Gneissic Complex (BGC) and Giyangarh-Asind Acidic Intrusive to Characterise Polymetallic Mineralisation in Chhota Udaipur-Kachariya Area, Ajmer Disrict, Rajasthan
72	Sujith M S (ENGG1G202101014)	BARCTS (AMD), Hyderabad	Exploration Geosciences	Petro-Mineralogy, Geo-chemistry, and Genesis of REE Mineralisation in Apatite-Magnetite Veins and Chlorite Biotite Schist in and Around Kanyaluka Area, East Singhbhum District, Jharkhand
73	Suraj Premji Vichhi (ENGG1G202101015)	BARCTS (AMD), Hyderabad	Exploration Geosciences	Geological, Petromineralogical and Heat Flow Studies to Characterize the Bakreshwar- Tantloi Geothermal Province in Parts of Birbhum District, W. B. and Dumka District, Jharkhand

74	C. V. Reddy (ENGG1G202101016)	BARCTS (AMD), Hyderabad	Exploration Geosciences	Petro-Mineralogy and Mineral Chemistry Study and Characterization of Biotite and Garnet in Uranium Braring Migmatities of Chhota Nagpur Granite Gneiss Complx (CGGC), Sonbhadra District, Uttar Pradesh, India
75	Mandlik Shrikant Ramesh (ENGG1A201901007)	BARCTS (NFC), Hyderabad	Mechanical Engineering	Improvement in Stainless Steel Shielded Metal Arc Weld Joint to Enhance Fatigue Life using Different Consumables
76	Tanmay Saha (ENGG1A201901013)	BARCTS (NFC), Hyderabad	Electrical Engineering	Design, Simulation and Hardware Implementation of MOSFET based Switched Mode Converter for Research Applications
77	Ravi Pratap Singh (ENGG1A202101001)	BARCTS (NFC), Hyderabad	Mechanical Engineering	Study of Ultrasonic Test Sensitivity on Zr-2.5% Nb Pressure Tubes with Different Type of Notches and Test Parameters
78	Aniruddha Subhash Tondare (ENGG1A202101004)	BARCTS (NFC), Hyderabad	Mechanical Engineering	Study on Fracture Behaviour and Tearing Crack Growth Analysis in Zr-2.5%Nb Pressure Tube Material
79	Purvesh Shrivastav (ENGG1A202101011)	BARCTS (NFC), Hyderabad	Mechanical Engineering	Defect Characterization in Thin-walled Tubes and Parameters Optimization for Immersion and Contact Ultrasonic Testing
80	Shruti Jain (ENGG1A202101014)	BARCTS (NFC), Hyderabad	Chemical Engineering	Study the Effect of Process Parameters in Uranyl Nitrate Raffinate (UNR) Treatment for Improving the Filterability of Slurry and Reduce Generation of Active Waste
81	Mohd Zahid Hussain (ENGG1A202201012)	BARCTS (NFC), Hyderabad	Mechanical Engineering	Establishing the Oxidation Behaviour of Ti-Al-Zr Alloy in Supercritical Water
82	Aiswarya K V (ENGG02201901005)	IGCAR	Chemical Engineering	Design of Passive Decay Heat Removal System for HLW Tank for FRP
83	Srishti Priya (ENGG02202101015)	IGCAR	Chemical Engineering	Hydrodynamics of a Rotating Solid-Liquid Feed Clarification System
84	Monika Rana (ENGG03201901008)	RRCAT	Engineering Physics	Numerical Simulation of 20 keV/100 mA DC Thermionic Electron Gun for Testing Photon Absorbers of Synchrotron Radiation Source
85	Manish Kumar Singh (ENGG03201901009)	RRCAT	Engineering Physics	Deposition and Characterization of Titanium Nitride Thin Films on Stainless Steel Substrates for Possible Applications in UHV Chambers

86	Bhumika Sharma (ENGG03201901011)	RRCAT	Engineering Physics	A Study on Infrared Stimulated Visible Emission in Strontium Sulphate ($SrSO_4$) Phosphor for IR Beam Visualization Application
87	Shruti Gupta (ENGG03201901012)	RRCAT	Engineering Physics	Studies on Growth Characteristics of Reactive Ion Beam Deposited Ruthenium Oxide Thin Films
88	Saurabh (ENGG03202101009)	RRCAT	Electronics Engineering	Development of FPGA Based VME Bus-Compatible Location Monitor Module
89	Sumit Lalan Kushwaha (ENGG03202101013)	RRCAT	Electronics Engineering	Study and Performance Analysis of OCR Technology on Metallic Objects

M.Sc. (Engg.)

S. No	Name of the Student	CI/OCC	Discipline	Title of the Thesis
1	Subhra Prakash Dey (ENGG01201905001)	BARC	Engineering Sciences	Evaluation of Pressure Profile Inside Complex High Vacuum System
2	Naushad Ali (ENGG01201905004)	BARC	Engineering Sciences	Magnetic Pulse Welding for Application in Electric Power System by Optimizing the Electrical Parameters
3	Balbir Kumar Singh (ENGG02201805004)	BARC	Engineering Sciences	High Temperature Creep Deformation and Viscoplastic Constitutive Modelling of 304L Stainless Steel

Section V

(List of students who completed D.M., M.Ch. and M.D. degrees during August 1, 2023-July 31, 2024)

D.M. Degree

S. No	Name of the Student	CI/OCC	Academic Programme	Enrollment No
1	Dr. Kapu Venkatesh	TMC	D.M. – Medical Oncology	HLTH09202010001
2	Dr. Vora Deep Nareshbhai	TMC	D.M. – Medical Oncology	HLTH09202010002
3	Dr. Rup Jyoti Sarma	TMC	D.M. – Medical Oncology	HLTH09202010003
4	Dr. Keshav Garg	TMC	D.M. – Medical Oncology	HLTH09202010004
5	Dr. Atul Tiwari	TMC	D.M. – Medical Oncology	HLTH09202010005
6	Dr. Tongaonkar Arnav Hemant	TMC	D.M. – Medical Oncology	HLTH09202010006
7	Dr. Sayak Dey	TMC	D.M. – Medical Oncology	HLTH09202010007
8	Dr. Harsh Sahu	TMC	D.M. – Medical Oncology	HLTH09202010008
9	Dr. Laboni Sarkar	TMC	D.M. – Medical Oncology	HLTH09202010009
10	Dr. George John	TMC	D.M. – Medical Oncology	HLTH09202010010
11	Dr. Sobin V Jacob	TMC	D.M. – Medical Oncology	HLTH09202010011
12	Dr. Jatin Choudhary	TMC	D.M. – Medical Oncology	HLTH09202010012
13	Dr. Yallala Mounika	TMC	D.M. – Medical Oncology	HLTH09202010013
14	Dr. Shah Devashee Bhupendrabhai	TMC	D.M. – Medical Oncology	HLTH09202010014
15	Dr. Laxma Reddy Mekala	TMC	D.M. – Medical Oncology	HLTH09202010015
16	Dr. Ramjas Prajapati	TMC	D.M. – Medical Oncology	HLTH09202010016
17	Dr. Meshach M Dhas	TMC	D.M. – Critical Care Medicine	HLTH09202010017
18	Dr. Rakesh Mohanty	TMC	D.M. – Critical Care Medicine	HLTH09202010018
19	Dr. Gondal Gautam Ashish	TMC	D.M. – Critical Care Medicine	HLTH09202010019
20	Dr. Jerubandi Shiva Kumar	TMC	D.M. – Pediatric Oncology	HLTH09202010020
21	Dr. Poonam Khemani	TMC	D.M. – Pediatric Oncology	HLTH09202010022
22	Dr. Mane Kiran Vilasrao	TMC	D.M. – Gastroenterology	HLTH09202010023
23	Dr. Rishabh Bhatia	TMC	D.M. – Interventional Radiology	HLTH09202010025
24	Dr. Nishtha Batra	TMC	D.M. – Onco-Pathology	HLTH09202010028
25	Dr. Priyadarsani S	TMC	D.M. – Onco-Pathology	HLTH09202010029

M.Ch. Degree

S. No	Name of the Student	CI/OCC	Academic Programme	Enrollment No
1	Dr. Mohit Satish Parakh	TMC	M.Ch. – Plastic & Reconstructive Surgery	HLTH09201910004
2	Dr. Arul Kumar A	TMC	M.Ch. – Surgical Oncology	HLTH09202010030
3	Dr. Kovvuru Bhaskar Reddy	TMC	M.Ch. – Surgical Oncology	HLTH09202010031
4	Dr. Harshit Subhashbhai Patel	TMC	M.Ch. – Surgical Oncology	HLTH09202010032
5	Dr. Kaderi Abdeali Saif Arif	TMC	M.Ch. – Surgical Oncology	HLTH09202010034
6	Dr. Subha Sampath	TMC	M.Ch. – Surgical Oncology	HLTH09202010035
7	Dr. Kapadia Raj Dhanesh	TMC	M.Ch. – Surgical Oncology	HLTH09202010036
8	Dr. Divakar Jain	TMC	M.Ch. – Surgical Oncology	HLTH09202010037

9	Dr. Vipin T	TMC	M.Ch. – Surgical Oncology	HLTH09202010038
10	Dr. Vipul Gupta	TMC	M.Ch. – Surgical Oncology	HLTH09202010039
11	Dr. Tale Avinash Shaligram	TMC	M.Ch. – Surgical Oncology	HLTH09202010040
12	Dr. Sadasivudu Vasireddy	TMC	M.Ch. – Surgical Oncology	HLTH09202010041
13	Dr. Varuna S	TMC	M.Ch. – Surgical Oncology	HLTH09202010042
14	Dr. Karthik V	TMC	M.Ch. – Surgical Oncology	HLTH09202010043
15	Dr. Faisal Abdul Mujeeb	TMC	M.Ch. – Surgical Oncology	HLTH09202010044
16	Dr. Kale Ajinkya Shantaram	TMC	M.Ch. – Surgical Oncology	HLTH09202010045
17	Dr. M Vikram Reddy	TMC	M.Ch. – Surgical Oncology	HLTH09202010046
18	Dr. D Bhaskaran	TMC	M.Ch. – Surgical Oncology	HLTH09202010047
19	Dr. Vishnu S Menon	TMC	M.Ch. – Surgical Oncology	HLTH09202010049
20	Dr. Harsh Karun	TMC	M.Ch. – Surgical Oncology	HLTH09202010050
21	Dr. Shah Dhwani Amit	TMC	M.Ch. – Surgical Oncology	HLTH09202010051
22	Dr. Reshma R Balachandran	TMC	M.Ch. – Surgical Oncology	HLTH09202010052
23	Dr. Karthik Prakash	TMC	M.Ch. – Surgical Oncology	HLTH09202010053
24	Dr. Shalu Kumari	TMC	M.Ch. – Gynaecological Oncology	HLTH09202010054
25	Dr. Aishwarya S	TMC	M.Ch. – Gynaecological Oncology	HLTH09202010055
26	Dr. Menon Abhishek Vijay	TMC	M.Ch. – Head & Neck Surgery	HLTH09202010056
27	Dr. Mukesh Kumar Sah	TMC	M.Ch. – Head & Neck Surgery	HLTH09202010057
28	Dr. Anuj Bipinkumar Shah	TMC	M.Ch. – Head & Neck Surgery	HLTH09202010058
29	Dr. Jitendra Kumar Sharma	TMC	M.Ch. – Head & Neck Surgery	HLTH09202010059
30	Dr. Prajyoth Reddy V	TMC	M.Ch. – Plastic & Reconstructive Surgery	HLTH09202010060
31	Dr. Samreen Jaffar	TMC	M.Ch. – Plastic & Reconstructive Surgery	HLTH09202010063

M.D. Degree

S. No	Name of the Student	CI/OCC	Academic Programme	Enrollment No
1	Dr. Newaskar Aditi Anand	TMC	M.D. – Anaesthesiology	HLTH09202009029
2	Dr. Pimpre Kshitija Rajaram	TMC	M.D. – Anaesthesiology	HLTH09202009030
3	Dr. Tupkar Shital Bharatrao	TMC	M.D. – Anaesthesiology	HLTH09202009031
4	Dr. E Ramya	TMC	M.D. – Radiation Oncology	HLTH09202009038
5	Dr. Shaikh Zeba Tarannum Shaikh Gazi Miya	TMC	M.D. – Radiation Oncology	HLTH09202009052
6	Dr. Mahesh Patel	TMC	M.D. – Pathology	HLTH09202009082
7	Dr. Gangawane Sanchi Arun	TMC	M.D. – Pathology	HLTH09202009087

HBNI Ranked 15 in research institutions category

HBNI ranked 17 in university category

HBNI ranked 30 in overall category

CORE VALUES OF HBNI

Key Officials of HBNI

CHANCELLOR		
Prof. Anil Kakodkar	kakodkar@barc.gov.in	022-25505210
VICE CHANCELLOR		
Prof. U. Kamachi Mudali	vicechancellor@hbni.ac.in	022-25597638
Vice Chancellor's Office	vcoff@hbni.ac.in	022-25597621
DEAN		
Prof. A. K. Tyagi	deanhbni@hbni.ac.in	022-25595330
REGISTRAR		
Prof. P. C. Selvin	registrar@hbni.ac.in	022-25597625
Registrar`s Office	registraroff@hbni.ac.in	022-25597569
ASSOCIATE DEANS		
Prof. D. K. Maity	asso_dean@hbni.ac.in	022-25597623
Prof. Naveen Kumar	nkumar@hbni.ac.in	022-25597629
Prof. Dipanwita Dutta	ddutta08@hbni.ac.in	022-25592041
Prof. Haridas Pal	hpal59@hbni.ac.in	022-25597554
Prof. B. K. Nayak	bknayak@hbni.ac.in	022-25507624
ASSISTANT DEAN		
Dr. (Smt.) Anshu Singhal	asinghal@hbni.ac.in	022-25597616
DEPUTY REGISTRAR		
Shri Suresh Nair	dy.registrar@hbni.ac.in	022-25597637

Bhabha Atomic Research Centre
(BARC)

Indira Gandhi Centre for Atomic
Research (IGCAR)

Raja Ramanna Centre for
Advanced Technology (RRCAT)

Variable Energy Cyclotron Centre
(VECC)

Saha Institute of Nuclear Physics
(SINP)

होमी भाभा राष्ट्रीय संस्थान
HOMI BHABHA NATIONAL INSTITUTE

(An aided Institute of the Department of Atomic Energy and
a Deemed to be University u/s 3 of UGC Act 1956)
www.hbni.ac.in

Institute of Mathematical Sciences
(IMSc)

Institute of Physics
(IoP)

Institute for Plasma Research
(IPR)

Harish-Chandra Research Institute
(HRI)

Tata Memorial Centre
(TMC)

Mahamana Pandit Madan Mohan Malaviya
Cancer Centre & Homi Bhabha Cancer
Hospital (MPMMCC & HBCH)

National Institute of Science
Education and Research (NISER)

होमी भाभा राष्ट्रीय संस्थान

Homi Bhabha National Institute

ट्रेनिंग स्कूल परिसर /Training School Complex

अणुशक्तिनगर, मुंबई, (भारत) / Anushaktinagar, Mumbai (India)- 400094

www.hbni.ac.in / Phone No: 022-25597699, 022-25597625